European
Commission

Fire design of steel members with welded ot hot-rolled class 4 cross-section

(FIDESC4)

Research Fund for Coal and Steel

Fire design of steel members with welded ot hot-rolled class 4 cross-section (FIDESC4)

Bin ZHAO

Centre Technique Industriel de la Construction Métallique (CTICM)

Espace Technologique, L'orme des merisiers, Immeuble Apollo, F 91193 Saint-Aubin, France

René OLY

LINDAB SA (LINDAB)

Route d'Ettelbruck, LU 9230, Diekirch, Luxembourg

Fernando MORENTE

Fundacion TECNALIA Research & Innovation (TECNALIA)

Calle Geldo edificio 700 Parque tecnologico de Bizkala, ES 48160 Derio, Spain

Paulo VILA REAL

Universidade de Aveiro (UAVR)

Campo Universitario de Santiago, PT 3810 193 Aveiro/Eixo, Portugal

František WALD

České vysoké učení technické v Praze (CTU)

Zikova 4, CZ 16636 Praha 6, Czech Republic

Jean-Marc FRANSSEN

Université de Liège (Ulg)

Place du 20 août, BE 4000 Liège, Belgium

Petr VELDA

DESMO AS (DESMO)

Radlicka 103/2485, CZ 15000 Praha 5, Czech Republic

Final report

Directorate-General for Research and Innovation

2014   EUR 27820 EN

***Europe Direct is a service to help you find answers
to your questions about the European Union***

Freephone number (*):
00 800 6 7 8 9 10 11

(*) Certain mobile telephone operators do not allow access to 00 800 numbers or these calls may be billed.

Printed in Luxembourg

PRINTED ON WHITE CHLORINE-FREE PAPER

Table of contents

1   Final summary

1.1   Introduction

Owing to their lightness resulted from optimized material utilization, the class 4 cross-section steel members, according to Eurocode 3 definition, are widely used by the steel industry in construction. More precisely, H or I shape class 4 cross-section steel members are commonly used to build the primary framing of steel portal frames.

Unlike the steel members with lower classes of cross-sections (1, 2 and 3), the failure of class 4 cross-section steel members is often the consequence of local instabilities in the web and the flanges.

Despite a heavy use of this type of steel members, the current simple design rules of the fire part of Eurocode 3, i.e. EN1993-1-2, were identified as very approximate in a lot of cases. It was also demonstrated that these rules were too conservative [2]. In fact, EN1993-1-2 recommends in an informative annex to extrapolate the simple calculation methods relative to classes 1, 2 and 3 cross-section steel members to the class 4 cross-section steel members, based on the assumption that the design yield strength of steel is taken as the 0.2 percent proof strength instead of the effective strength at 2% total strain value which is commonly used for lower class cross-section steel members. It has been found that this method is not only unsatisfactory but also leads to an uneconomical result, which penalizes significantly the fire resistance design of steel structures comprising class 4 cross-section steel members. Another possibility is also proposed in the EN 1993-1-2: the use of a fixed critical temperature of 350 °C to avoid any additional accurate calculation. This last possibility is even more conservative. In consequence, more accurate simple design rules have to be established in order to increase the competitiveness of steel industry.

Another concern is related to tapered class 4 cross-section steel members. In fact, such type of steel members is very largely adopted in steel constructions (stores, industrial halls, airports, etc.). But unfortunately, no specific design rules for this type of members in fire situation are defined in EN1993-1-2. Though some research work is already performed for the development of simple calculation method at room temperature, no deep scientific investigation for fire design is made yet.

1.2   Project objectives and conducted tasks

The principal objectives of the project are described in the technical annex of the project (see Appendix 1). However, in order to provide a clear idea about the research works performed in the scope of this project, it is necessary to summarise these objectives as well as the accomplished associated research works.

The first aim of this project is to have a common design of the fire tests, to define the parameters to be taken into account in different numerical parametric studies and to conduct a specific benchmark study in order to have a consistent numerical approach for used computer codes. To achieve these goals, the following tasks have been performed:

- Detailed analysis of the application domain of class 4 cross-section steel members in buildings and of the risk analysis of fire in such type of buildings, leading finally to the proposal of possible real fire scenarios
- Global and consistent design of all the fire tests planned in WP2 to WP5
- Conduct of a numerical benchmark investigation so that the consistency of all the numerical models developed under different computer codes is checked
- Global definition of the appropriate parameters to be used in the numerical parametric studies foreseen in the scope of WP2 to WP5

The second goal of the project is to investigate experimentally and numerically the fire behaviour of steel members with welded or hot-rolled class 4 cross-sections under simple bending and to develop the simple design rules of such type of steel members under above loading condition. The corresponding tasks conducted in the scope of the project to achieve these objectives are as follows:

- Conduct of fire tests of class 4 cross-section steel members subjected to simple bending: two different cross-sections were tested and each of these two cross-sections was tested at both 450 °C and 650 °C
- Validation of numerical models developed with help of shell finite element against above experimental data

- Conduct of a large number of numerical simulations with specifically defined parameters allowing the reliability evaluation of current simple design rules of EN1993-1-2
- Development of new simple design rules on the basis of both experimental and numerical results derived respectively from fire tests and numerical parametric studies
- Correlation investigation of proposed simple design rules so that their accuracy be checked carefully

The third purpose of the project is the investigation on the lateral torsional buckling behaviour of fire exposed steel members with welded or hot-rolled class 4 cross-sections submitted to bending and the development of corresponding simple design rules. The realisation of the above goal is based on the following tasks:

- Conduct of fire tests and creation of a complete set of experimental data concerning the lateral torsional buckling behaviour of class 4 cross-section steel beams
- Validation of previously developed numerical models based on shell finite elements
- Extension of fire behaviour investigation with help of validated numerical models of class 4 cross-section steel beams subject to lateral torsional buckling through a full range numerical parametric study taking account of all relevant parameters identified in one of the first tasks of the project
- Development of specific simple design rules for fire resistance assessment of class 4 cross-section steel beams subject to lateral torsional buckling
- Correlation investigation of proposed simple design rules so that their accuracy be checked carefully

The fourth objective of the current project concerned the fire behaviour investigation of class 4 cross-section steel columns subjected to global buckling under axial compression as well as the development of corresponding simple design rules. The following tasks have been carried out to achieve the goal:

- Conduct of four column tests at elevated temperatures which have provided experimental data on the fire behaviour of slender class 4 cross-section steel columns under axial compressive load
- Validation of previously developed numerical models taking account of local and global buckling on the basis of shell finite element
- Extended investigation, with the help of numerical simulations, of the fire behaviour of slender class 4 cross-section steel columns under axial compression on the basis of previously validated numerical models
- Finally, development of simple design rules for fire resistance assessment of slender class 4 cross-section steel columns based on both experimental and numerical results derived respectively from fire tests and numerical parametric studies
- Correlation investigation of proposed simple design rules so that their accuracy be checked carefully

The fifth target of the project aims at the improvement of the current knowledge about the fire behaviour of class 4 cross-section steel members subjected to combined bending and compression as well as the development of corresponding simple design rules. Once again, the adopted research methodology and the conducted tasks are similar to those already used to achieve previous objectives of the project, namely:

- Conduct of several tests at elevated temperatures leading to the acquirement of precious experimental results about the fire behaviour of class 4 cross-section steel members under combined bending and compression
- Validation of corresponding numerical models using shell finite elements so that the local buckling of class 4 cross-section steel members can be taken into account
- Conduct of full range of numerical investigation of the fire behaviour of class 4 cross-section steel members (constant and tapered) under combined bending and compression on the basis of extended numerical parametric study shared between two computer codes

Another specific objective of current project is to provide a cost-effective application tool relative to the fire resistance assessment of class 4 cross-section steel members which is much more complex due to the necessity of taking account of local buckling of such type of steel members. It comes out that the best way to achieve this goal is the development of a user-friendly design software. At the end of this project, a specific graphical user interface based on VB.NET environment has been developed for this design software in order to apply very efficiently the simple design rules for class 4 cross-section steel members under various loading conditions. In fact, with the finished software, not only the new simple design rules developed during the current project but also the existing design rules of EN1993-1-2 have been implemented.

The last goal of this project concerns the development of a relevant numerical modelling approach so that the global structural analysis of steel structures comprising class 4 cross-section steel members can be carried out cost-effectively in fire safety engineering projects and the establishment of a corresponding numerical modelling guidance providing the necessary recommendations to all engineers intending to do such type of applications in their construction projects. To achieve this goal, an innovative numerical approach has been investigated which consists of introducing a specific material model to represent the possible local buckling behaviour of class 4 cross-section steel members so that the global structural analysis of steel structures comprising class 4 steel members can be carried out with ordinary beam-column elements. The development of above numerical approach has been relied upon the outcomes of the following works:

- Establishment of a specific material model of steel capable of taking into the local buckling behaviour of different steel walls of a class 4 cross-section steel member at elevated temperatures and on the basis of the slenderness of these walls
- Conduct of parametric studies on fire behaviour of single class 4 cross-section steel members with both shell finite element and beam-column finite element with implemented specific material model on the basis of two heating conditions (uniform and variable along the length)
- Conduct of parametric studies on fire behaviour of portal frames made of class 4 cross-section steel members with both shell finite element and beam-column finite element with implemented specific material model on the basis of two heating conditions (uniform and variable under real fire)
- Development of numerical modelling guidance providing relevant recommendations with respect to global structural analysis of steel structures comprising class 4 cross-section steel members in fire situation with help of the approach based on specific material model

All the technical tasks summarized above have led to an important amount of results which will be described in next paragraphs of this report.

The management of the main research activities of the project as well as their interactions to achieve the objectives of the project are illustrated in the scheme given below:
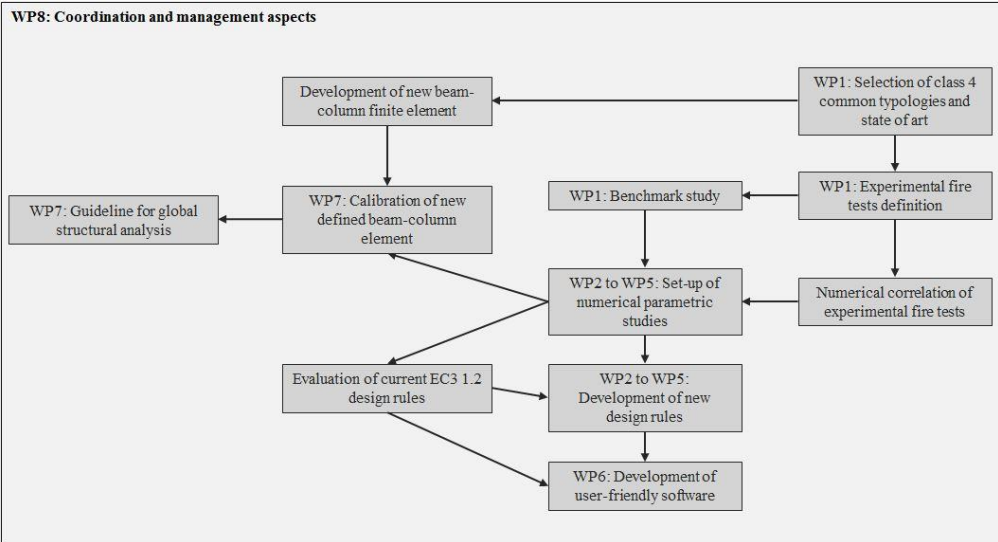

Figure 1: General flow chart of research works of the project

1.3   Obtained results

The outcomes derived from the current project are numerous and can be divided into six families:

- Experimental database relative to the fire behaviour of class 4 cross-section steel members
- Accurate numerical models under three computer codes validated against above experimental results and a specific benchmark study
- Extended database containing not only the information relative to experimental investigation but also all the detailed information of the numerical analysis conducted in various numerical parametric studies
- New or improved simple fire resistance design rules of class 4 cross-section steel members under different loading conditions
- User-friendly software with which cost-effective fire resistance design of class 4 cross-section steel members can be made
- Modelling guidance for global structural analysis of steel structures containing class 4 cross-section steel members

The above outcomes of the project will be summarised hereafter.

The first family of the results obtained from the works of the project concerns the experimental data with respect to the fire behaviour of class 4 cross-section steel members which were established through sixteen tests conducted at elevated temperatures. These tests have provided a large range of experimental evidence about the fire resistance of such type of steel members under the following four loading conditions:

- beams under simple bending (lateral torsional restrained)
- beams subject to bending and lateral torsional buckling
- slender columns under axial compression
- slender members under combined bending and compression

It is necessary to point out here that these results constitute the first experimental database in the world about the fire behaviour of hot-rolled and welded class 4 cross-section steel members. These experimental results have become the essential technical background for all other scientific tasks of the project, such as the development of relevant numerical models for the conduct of numerical parametric studies, the establishment of simple design rules for fire resistance assessment of class 4 cross-section steel members.

As one can find in Figure 2, during the conducted four tests at elevated temperatures with beams under simple bending, an important local buckling of the upper flange was observed and the local buckling on the upper part of web was also noticed. In consequence, the numerical models have to be capable of reproducing this mechanical behaviour in accurate way so that the load-bearing capacity of class 4 cross-section steel members under simple bending can be predicted confidently. The following pictures illustrate for one of these beam tests the failure mode shape from both experimental test and numerical simulation:

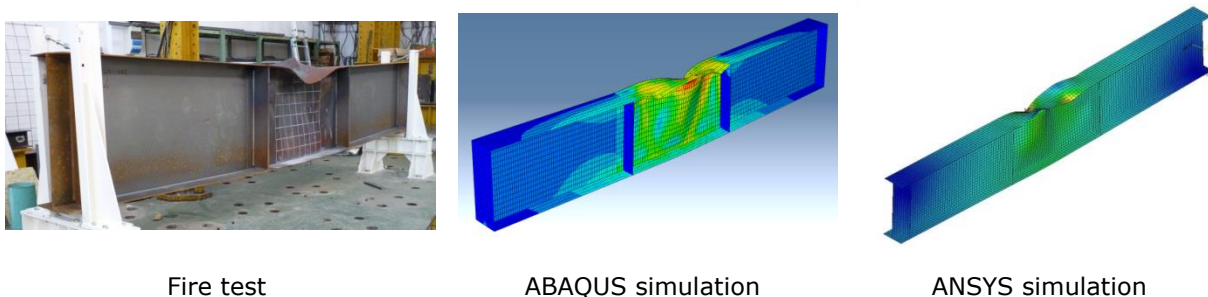| Fire test | ABAQUS simulation | ANSYS simulation |

Figure 2: Failure mode shape of the fourth test of simple bending – 650 °C

At each temperature level, it is always noticed that the beam with bigger cross-section failed at a lower deflection value than the beam with smaller cross-section. Two reasons can explain this phenomenon, firstly, the beam with bigger cross-section has higher stiffness leading to lower deflection and secondly, the bigger cross-section has slender walls: flange width-to-thickness ratio of 37.5 against 20.8 for smaller cross-section, so the local buckling occurred earlier. This behaviour is clearly illustrated in the Figure 3.

Local buckling for flange 250 mm x 12 mm   Local buckling for flange 300 mm x 8 mm

Figure 3: "Intensity" of the local buckling of upper flange according to its width-to-thickness ratio

As far as the numerical models developed in the scope of this project for this loading condition, the numerical simulations conducted with two computer codes (ABAQUS and ANSYS) provided very satisfying correlation with four fire tests. In fact, the maximum difference in terms of load bearing capacity between simulations and tests is about 5%, whereas the average difference of eight cases is only 2.4%. Furthermore, for the linear part of the applied load vs. vertical deflection curves of each test, the numerical and experimental results give very close slope.

The behaviour of four tests conducted to investigate the lateral torsional buckling behaviour of class 4 cross-section steel beams led to the following conclusion: all laterally unrestrained beams failed with lateral torsional buckling combined with local failure of the upper compressive flange. The pictures below (Figure 4) illustrate for one of these beam tests the failure mode obtained respectively from experimental test and numerical simulation.

However, as the lateral torsional buckling is a much more complex behaviour compared with simple bending, the correlations in terms of ultimate load capacity between the numerical analysis and the fire tests are less satisfying. In fact, the maximum gap, for the first test, between finite element analysis and experiment, is about 25% and the average difference is about 13.6%. These quite important differences were explained by the fact that the lateral torsional buckling is very sensitive to applied boundary conditions in the test equipment which could provide some unexpected restraints compared to ideal boundary conditions used in numerical models.
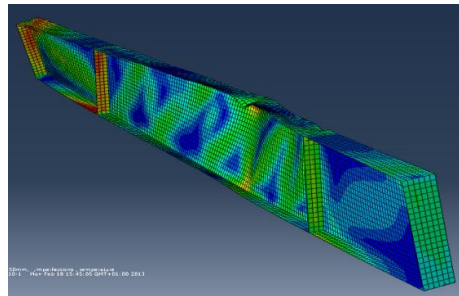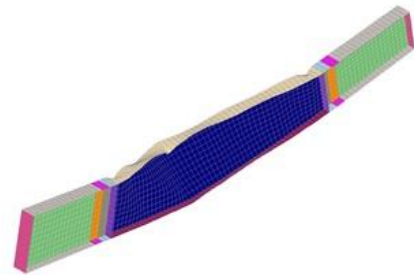
Fire test   ABAQUS simulation   SAFIR simulation

Figure 4: Failure mode shape of the fourth test for LTB – 650 °C

Nevertheless, it appeared that the numerical simulations could predict with accuracy the failure mode obtained in the fire tests. The linear part of the applied force in function of deflection curve from numerical simulations correlates also quite well with that measured in the tests.

It was observed that the local buckling of the flanges occurred in all four class 4 cross-section steel columns subjected to axial compression. However, the hot-rolled IPE240A column shows an important global buckling along the weak axis whereas the local buckling of flanges is less pronounced. The 450x4+150x5 welded column showed an important global buckling along weak axis too and the local buckling of flanges was much more developed. This behaviour can be explained by a higher width-to-thickness ratio for the welded column compared to the hot-rolled one. The failure shapes of the column in the fourth test, which is with a tapered welded cross-section and the results of corresponding simulations are illustrated in Figure 5.

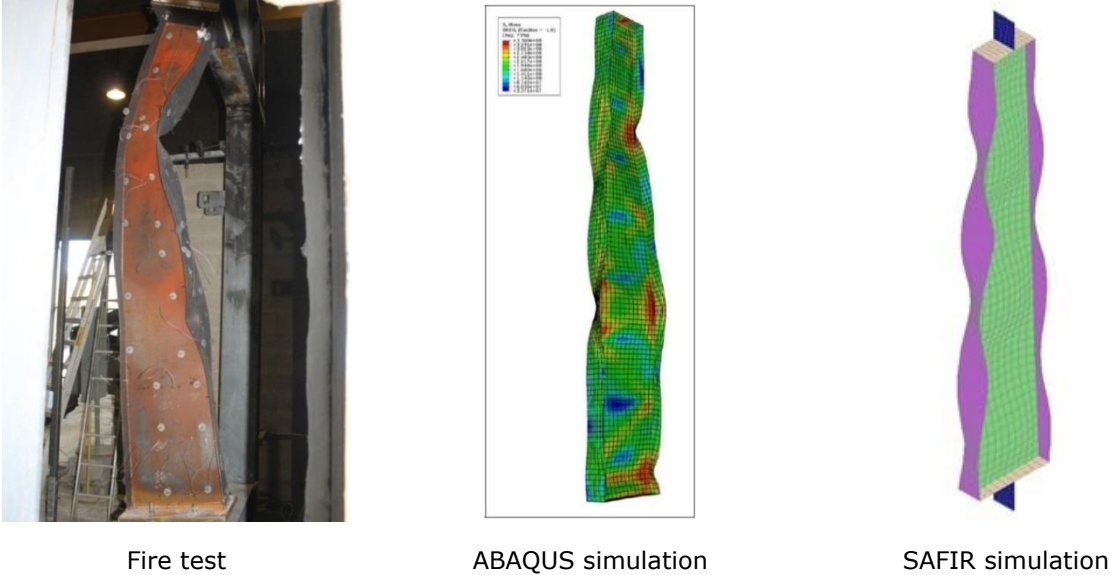| Fire test | ABAQUS simulation | SAFIR simulation |

Figure 5: Failure mode shape of the fourth test for axially loaded column

As shown in the Figure 6, the tapered column failed due to the local buckling near the location of the lowest web height. This is probably due to the lower inertia of the small cross-section at this location compared to other cross-sections of the column. As for the welded cross-sections of tests 2 and 3, the flanges are rather slender and their local buckling is well developed, which complies with the mechanism of local buckling behaviour.

Figure 6: illustration of the global buckling of the tapered column (small cross-section at top)

The correlation between the numerical results (obtained with the computer codes ABAQUS and SAFIR) and the fire tests is satisfactory. In fact, the maximum gap between experimental and numerical results for the failure temperatures was about 6% and the mean difference was about 2.5%. In addition, the displacements (axial and transversal) as a function of temperature are very close between numerical and experimental results.

Furthermore, it was observed that the buckling mode shapes of the columns were predicted with great efficiency in the numerical simulations (see Figure 5). For example, the conducted simulations of the first tested column show a global buckling along the weak axis without any local failure of flanges. This behaviour is very close to the one observed in the test. A great correlation is also noticeable for test 2 where both global failure along weak axis and local buckling of flanges occur; see Figure 7 for illustration.

Failure after the fire test   Predicted failure in the numerical simulations
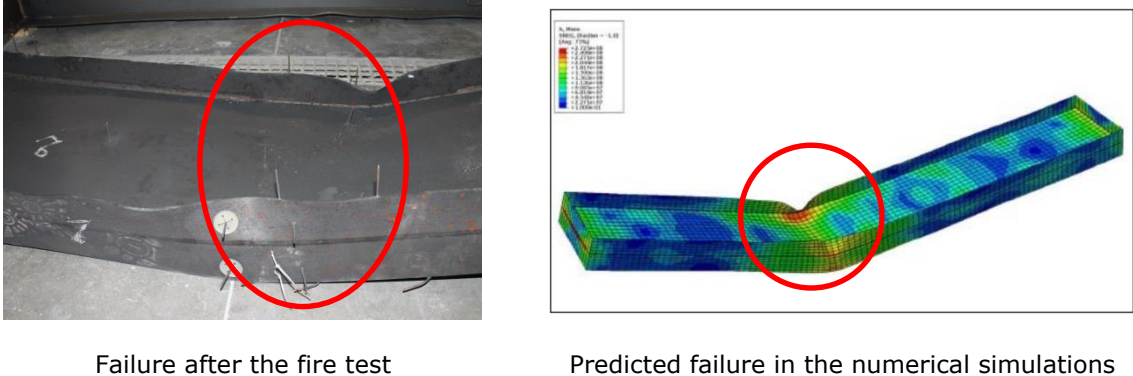
Figure 7: Failure of test 2 for both numerical simulations and experimentation

Therefore, it is concluded that the validity of the numerical models used for this loading condition is fully demonstrated.

Finally, the analysis of last four tests with class 4 cross-section columns subjected to both compressive load and bending at elevated temperatures has shown that unlike the axially loaded columns, the failure modes were all marked by important local buckling of flanges. Figure 8 shows the failure shapes of one of tested columns obtained from both fire test and corresponding numerical simulations.

Fire test   SAFIR simulation   ANSYS simulation
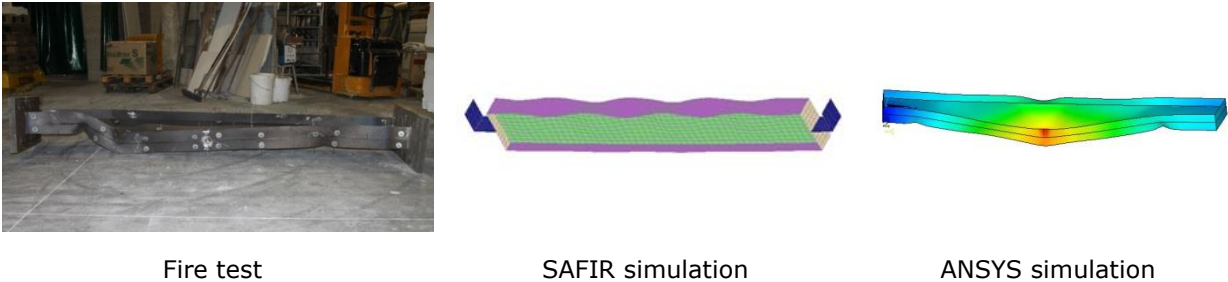
Figure 8: Failure mode shape of the sixth tested beam-column

As for all previous fire tests, the correlation analysis between the numerical simulations and the experimental results in terms of both failure modes and failure temperature has provided clear evidence about the validity of the numerical models developed respectively under the computer codes ANSYS and SAFIR. Similar to axially loaded columns, the maximum gap between numerical and experimental results in terms of critical temperature is about 6% and the average difference is about 2.3% which is fully acceptable. Failure modes were also predicted with sufficient accuracy in the numerical simulations when compared with the experimental results.

As a conclusion, the systematic correlation of the numerical models combined with all the assumptions against the fire tests has validated the numerical models in terms of critical load/temperature and failure mode.

The specific numerical benchmark study conducted in the scope of this project has led to a consistent numerical approach among all used numerical models developed under three computer codes, namely ABAQUS, ANSYS and SAFIR.

For the first example of above benchmark study, which deals with a beam under simple bending, all the numerical simulations under different computer codes have predicted the local buckling of the flange in compression accompanied by a local failure of the upper part of web which is also subjected to compression. The linear slope of load vs. deflection curve was identical between all three computer codes and the maximum difference in terms of ultimate load-bearing capacity was about 6.5%.

The second example of the benchmark covered a class 4 cross-section steel beam subjected to lateral torsional buckling. All the numerical results have predicted successfully the lateral torsional buckling behaviour at mid-length of the beam with a local buckling of the upper flange at the location of the maximal lateral displacement. Similar to the first example, the difference between all computer codes are satisfactory.

The third example of the benchmark study was relative to a tapered class 4 cross-section beam subjected to lateral torsional buckling. Once again, the predictions of all the computer codes are very close in terms of failure mode, with a lateral displacement at mid-length and a local buckling of the upper flange which is in compression. In addition, the linear slope of load as a function of vertical displacement is identical between all the numerical models. For this case, the maximum difference between investigated numerical models in terms of ultimate load-bearing capacity was about 6.4%.

The fourth example of the benchmark study concerned a column subjected either to axial compression or to eccentric compressive load. All the computer codes predicted a lateral failure at mid-height of the column in the direction of the weak axis with the local buckling of the flange. The predicted linear slope of load vs. horizontal displacement was very close between all investigated numerical models and the maximum difference of failure load was about 11.8% which is nevertheless considered as acceptable.

The last investigated single member was a tapered column subjected either to axial compression or to eccentric compressive load. In this example, a local failure of both web and flange was obtained at the bottom basis, where the applied moment was the greatest, in all the numerical simulations. As always, the linear behaviour is almost the same between all the numerical results. The maximum difference between used computer codes in terms of loadbearing capacity is about 8%.

The sixth example of the benchmark study was related to an entire portal frame uniformly heated. For low temperature levels, the linear slope was quite close between all the numerical results. However, when local buckling occurs, some discrepancies are noticeable. However, despite these discrepancies, the maximum difference between the critical temperatures given by the computer codes is only about 4%, which is very low considering so complex case.

Finally, a consistent numerical approach has been achieved in the scope of this project, which has allowed the conduct of all numerical parametric studies with confidence.

Among various numerical parametric studies of the project, the first numerical investigation concerned the cross-sectional resistance of class 4 cross-section steel members subjected to simple bending. In consequence, the parameter under investigation is the moment resistance as a function of the slenderness of both web and flanges. A total of 2260 simulations were conducted in this parametric study which has permitted to cover the following parameters:

- Sizes of cross-section
- Slenderness of walls
- Steel grades
- Account of initial residual stresses or not
- Heating levels

The other modelling parameters were chosen in accordance with the ones used to simulate the fire tests, except the initial geometric imperfections. In fact, for all the numerical parametric studies, the imperfection shapes are based on linear buckling analyses whereas the amplitude was chosen in accordance with the recommendation of EN 1993-1-5 and as a function of the fabrication tolerance given in the execution norm EN 1090-2:2008.

The first conclusion of this parametric study was that the initial residual stresses do not influence the final cross-sectional resistance of the beam at elevated temperatures. Figure 9 illustrates clearly this conclusion.
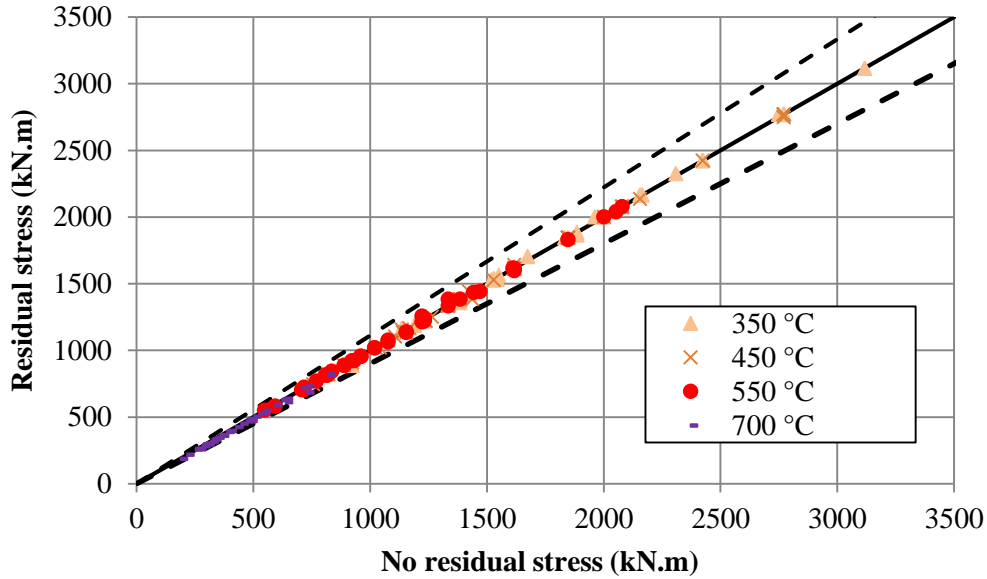
Figure 9: Influence of the residual stress on the cross-section resistance at elevated temperatures

As far as the simple design rules to assess the fire resistance of class 4 cross-section steel members are concerned, important discrepancies were found between the numerical results and the current design rules of EN1993-1-2. For an important part of the simulated cases it was observed that the EN1993-1-2 proposed very conservative fire design but it was also noticed that for a small part of cases, the EN1993-1-2 could lead to an unsafe design of the member. Moreover, an important non-physical jump of the cross-sectional resistance given by EN1993-1-2 is observed at certain value of wall slenderness. This tendency was present regardless of the temperature level and the steel grade. The details of this investigation are given in 2.2.2.3.

In order to remove the current inconsistencies of the current design rules, a new definition of the calculation of the effective part of both web and flanges was proposed following the Winter's formulation. The new equations are illustrated below and compared with current EN1993-1-5 equations:

Wall	EN1993-1-2	New effective width equations
Web	$\rho = \dfrac{\bar{\lambda}_p - 0.055(3+\psi)}{\bar{\lambda}_p^2}$ for $\bar{\lambda}_p > 0.5 + \sqrt{0.085 - 0.055\psi}$	$\rho = \dfrac{\left(\bar{\lambda}_p + 0.9 - \dfrac{0.26}{\varepsilon}\right)^{1.5} - 0.055(3+\psi)}{\left(\bar{\lambda}_p + 0.9 - \dfrac{0.26}{\varepsilon}\right)^{3}}$
Flanges	$\rho = \dfrac{\bar{\lambda}_p - 0.188}{\bar{\lambda}_p^2}$ for $\bar{\lambda}_p > 0.748$	$\rho = \dfrac{\left(\bar{\lambda}_p + 1.1 - \dfrac{0.52}{\varepsilon}\right)^{1.2} - 0.188}{\left(\bar{\lambda}_p + 1.1 - \dfrac{0.52}{\varepsilon}\right)^{2.4}}$

Table 1: Effective length calculation methods

The key points of this new design rules are the following:

- The design strength of steel at elevated temperatures is $f_{y,\theta}$
- The effective cross-section of thin wall steel members is determined on the basis of the wall slenderness

The limit between class 3 and class 4 cross-sections at elevated temperatures is now abandoned so that a continuous behaviour of the resistance of the cross-section can be obtained as a function of the slenderness. The details of this new design rules are available in 2.2.2.4.

The final equations to calculate the cross-section resistance are given below:

EN1993-1-2	New effective width equations
$M_{fi,Rd} = k_{0.2p,\theta} \times W_{eff,EC3\ 1.5} \times f_y$	$M_{fi,Rd} = k_{y,\theta} \times W_{eff,NEW} \times f_y$

Table 2: Equations for the cross-sectional resistance

With this new simple design rule, the gaps between the numerical simulations and the simplified calculation always remain lower than 10%. Moreover, unsafe cases represent less than 20% out of the conducted cases. Finally, the average value of the comparisons is situated on the safe side.

The second numerical parametric study was the investigation on the behaviour of laterally unrestrained slender beams with class 4 cross-sections. The analysis procedure adopted for this parametric study has allowed the evolution of the reduction factor for lateral torsional buckling as a function of the slenderness of the beam (the investigated range of slenderness varied between 0 and 2.5) to be analysed in detail with help of following different parameters:

- Slenderness of walls (web and flanges)
- Steel grades
- Temperature levels
- Simply supported beams or beams with warping prevented
- The initial residual stresses were always taken into account
- Several bending diagrams
- Constant cross-sections and tapered beams

Other modelling parameters are identical to the ones used for the parametric study on the cross-sectional resistance. The results of about 4000 simulations conducted in this parametric study have led to the creation of a solid basis for the development of new simple design rules. If more attention is paid to the simple design rules (Figure 10), one can find that the current rules of EN1993-1-2 are not only very approximate but also too conservative (uneconomic design) though they provide safe side fire resistance assessment of class 4 cross-section beams subjected to lateral torsional buckling.

As far as the new design rules are concerned, they take account of the influence of cross-section slenderness and at the same time the influence of the steel grade with the use of new imperfection factor depending on the effective section factor. In fact, the new design rules (see Table 4) are based on the same principles of those already adopted for cross-section resistance of which all the details are given in 2.2.3.4.

LTB curve	EN 1993-1-2	New design equations
$\theta_{LT,\theta}$	$0.5 \times \left[1 + \alpha \times \bar{\lambda}_{LT,\theta} + (\bar{\lambda}_{LT,\theta})^2\right]$	$0.5 \times \left(1 + \alpha_{LT}(\bar{\lambda}_{LT,\theta} - 0.2) + \bar{\lambda}_{LT,\theta}^2\right)$
Flanges	$\alpha_{LT} = 0.65 \times \sqrt{235/f_y}$	$\dfrac{W_{eff,y}}{W_{el,y}} > 0.9 \rightarrow \alpha_{LT} = 1.25\varepsilon$ $0.8 < \dfrac{W_{eff,y}}{W_{el,y}} \le 0.9 \rightarrow \alpha_{LT} = 1.00\varepsilon$ $\dfrac{W_{eff,y}}{W_{el,y}} \le 0.9 \rightarrow \alpha_{LT} = 0.75\varepsilon$

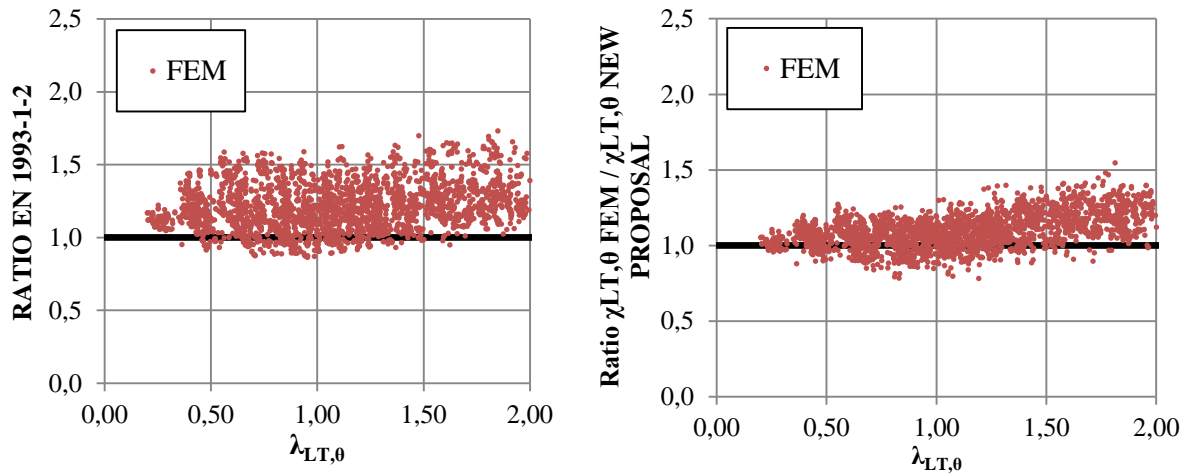Table 3: Conducted modifications for the LTB curves

Figure 10: Correlation of simple design rules against numerical analysis in case of beams subject to lateral torsional buckling

The correlation analysis of new simple design rules developed in the scope of this project has shown that they are much more accurate (see Figure 10). On one hand they helped to bring closer the simple calculation results to the numerical results. On the other hand, they have reduced the number of very conservative cases from about 50% to about 25%, which is a significant economic gain for fire resistance design of steel structures.

The third numerical parametric study concerned the investigation on the behaviour of axially loaded class 4 cross-section columns (without eccentricity). The conducted simulations (a total of about 5500 simulations) together with the experimental results have led to the creation of an important database for fire resistance of axially loaded class 4 cross-section columns and covering the influence of several parameters such as:

- Welded and hot-rolled columns
- Buckling axis (strong and weak)
- Steel grades
- Heating levels
- Simply supported beams or beams with warping prevented
- The initial residual stresses were always taken into account

Other finite element modelling parameters are identical to those used for other parametric studies.

As far as simple design rules are concerned, the current design rules of EN1993-1-2 have proven to be on the safe side and can be improved in terms of cost-effectiveness. The detailed analysis of current simple design rules is provided in 2.2.4.3.

The proposed new design rule of the project is based on the new calculation of the effective area of the cross-section. Furthermore, for the sake of consistency, the use of the temperature reduction factor $k_{0.2p,\theta}$ was replaced by $k_{y,\theta}$. The changes in the equations are listed in Table 4:

Axial compression	EN 1993-1-2	New design equations
λ_θ	$\lambda \times \sqrt{\dfrac{k_{0.2p,\theta}}{k_{E,\theta}}}$	$\lambda \times \sqrt{\dfrac{k_{y,\theta}}{k_{E,\theta}}}$
$N_{b,fi,Rd}$	$\chi_{fi} \times A_{eff,EC3\ 1.5} \times k_{0.2p,\theta} \times f_y$	$\chi_{fi} \times A_{eff,NEW} \times k_{y,\theta} \times f_y$

Table 4: Changes in simple design rules for class 4 cross-section columns

The slight changes introduced in these design rules have led to more competitive simple design rules in terms of buckling resistance of class 4 cross-section columns and moreover the number of unsafe cases remains lower than 12%. The details of the correlation analysis are shown in 2.2.4.4.

The last numerical parametric study conducted within this project for fire resistance of single class 4 cross-section steel members aimed at the study of the behaviour of columns subjected to combined axial compression and bending. The large amount of numerical simulations (a total of about 5000) has allowed the impact of following key parameters to be analysed in detail:

- In-plane and out-of-plane buckling
- Global slenderness
- Wall slenderness (web and flanges)
- Heating levels
- Several bending moment diagram
- Load ratio (compression versus bending)

Once again, the correlation analysis of current simple design rules of EN1993-1-2 has indicated that the interaction curves were not consistent and not cost-effective, especially when lateral torsional buckling is permitted. Moreover, some cases appear to be not safe enough. However, the reasons for these issues are not the same for both directions. The improvement of buckling reduction factor for columns did not improve significantly the in-plane behaviour. In fact, it is found that the corresponding interaction curve was not convenient. In consequence, modifications have been proposed, allowing the increase of the safety level of the simple design rules. Table 5 illustrates the related changes:

In-plane interaction curve	
EN1993-1-2	$\mu_y = \left(2\beta_{M,y} - 5\right)\bar{\lambda}_{y,\theta} + 0.44\beta_{M,y} + 0.29 \leq 0.8 \; but \; \bar{\lambda}_{y,20\,^\circ\,C} \leq 1.1$
Proposal	$\mu_y = \left(2\beta_{M,y1} - 5\right)\bar{\lambda}_{y,\theta} + 0.44\beta_{M,y2} + 0.7 \leq 0.6 \; but \; \bar{\lambda}_{y,20\,^\circ\,C} \leq 1.1$

Table 5: Change for in-plane interaction curve

Out-of-plane interaction curve	
EN1993-1-2	$\mu_{LT} = 0.15\bar{\lambda}_{z,\theta}\beta_{M,LT} - 0.15 \leq 0.9$
Proposal	$\mu_{LT} = 0.45\bar{\lambda}_{z,\theta}\beta_{M,LT} + 0.2 \leq 0.9$

Table 6: Change for out-of-plane interaction curve

These modifications let obtain a far more economic and optimal design for the resistance of class 4 beam-columns. In accordance with the previous exposed new interaction curves, it is equally proposed to update the relations for fire resistance assessment of beam-column class 4 cross-section members:

$$\frac{N_{fi,Ed}}{\chi_{min,fi}\,A_{eff}\,k_{y,\theta}\,\dfrac{f_y}{\gamma_{M,fi}}} + \frac{k_y\,M_{y,fi,Ed}}{W_{eff,y,min}\,k_{y,\theta}\,\dfrac{f_y}{\gamma_{M,fi}}} + \frac{k_z\,M_{z,fi,Ed}}{W_{eff,z,min}\,k_{y,\theta}\,\dfrac{f_y}{\gamma_{M,fi}}} \leq 1$$

$$\frac{N_{fi,Ed}}{\chi_{z,fi}\,A_{eff}\,k_{y,\theta}\,\dfrac{f_y}{\gamma_{M,fi}}} + \frac{k_{LT}\,M_{y,fi,Ed}}{\chi_{LT,fi}\,W_{eff,y,min}\,k_{y,\theta}\,\dfrac{f_y}{\gamma_{M,fi}}} + \frac{k_z\,M_{z,fi,Ed}}{W_{eff,z,min}\,k_{y,\theta}\,\dfrac{f_y}{\gamma_{M,fi}}} \leq 1$$

All above described numerical parametric studies have been assembled together with experimental data inside a common database in ASCII format. The format of the database and symbols are explained in a text document provided together with the database files so that any other researcher can easily take advantage of the results of current project in the future investigation.

The user-friendly FIDESC4 software allowing cost-effective application of the simple design rules for fire resistance assessment of class 4 cross-section steel members has been developed with Visual Basic standards. Moreover, the developed software allows the design calculation of steel members according to both the current design rules of EN1993-1-2 and new simple design rules proposed in the scope of this research project.

Two design possibilities are offered to the user (see Figure 11a):

- Evaluation of the critical temperature
- Fire resistance of a steel element at any fixed heating level

Furthermore, two different modules are available in the software and are illustrated in the Figure 11b:

- Fire resistance of the cross-section
- Fire resistance of members
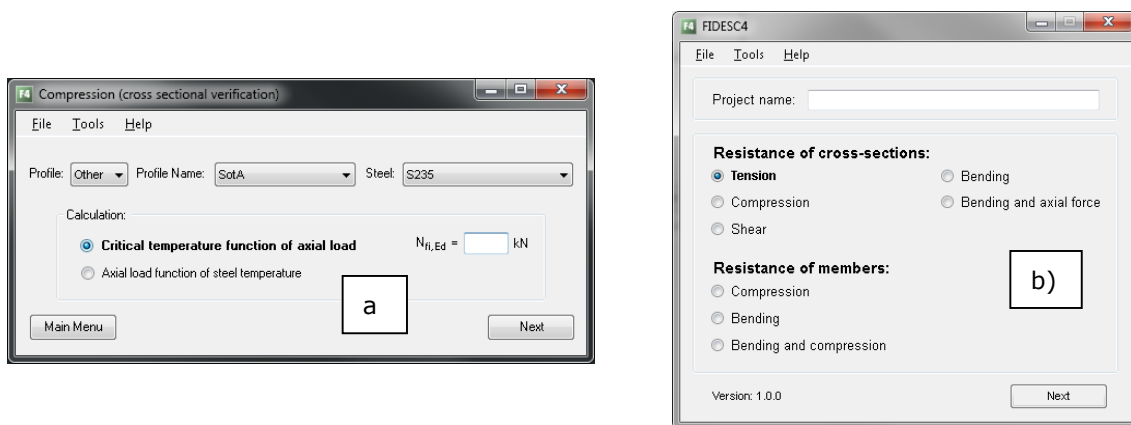
Figure 11: Available modules for "FIDESC4" software

The software, as well as its application manual, is available freely through the following three websites:

- https://www.cticm.com/content/logiciels
- http://www.ua.pt/risco/PageText.aspx?id=18840
- http://fire.fsv.cvut.cz/fidesc4/index.htm

All details are available in the deliverable n°6 which describes the software capabilities and provides an application example.

A numerical guidance relative to global structural analysis in fire situation of steel structures comprising class 4 cross-section members has been established in the scope of this research. It accurately describes the methodology to follow in order to conduct cost-effective fire safety engineering on entire steel structures on the basis of beam-column finite element approach. In fact, in the proposal of the project were anticipated two possibilities for this approach which are:

- Reduced cross-section based on effective width method
- Specific material model based on effective stress method

The analysis of the pros and cons of above potential solutions has led to the findings that the reduced cross-section on the basis of effective width method has more shortcomings than the use of a specific material model taking account of local buckling of wall in compression. In fact, with reduced cross-section based on effective width method, the inertia and the strength of steel structures are heavily underestimated because not all the steel parts in compression will be subject to local buckling. Another difficulty is that in a global structural analysis, it is not known upstream of the analysis the accurate stress distribution on the steel cross-section in order to define the appropriate effective cross-section. That is the reason why the solution using a specific material model based on effective stress method was adopted.

The relevance of the developed material model for this purpose has been investigated with help of either the results of parametric studies presented previously or new cases of portal frames exposed to real fire conditions between the results of shell modelling and the beam element modelling using this material model, from which following conclusions are derived:

- Beam-column finite element using the specific material model is capable of predicting with a quite good accuracy the failure mode of a single element or an entire frame
- The results obtained with this beam-column finite element approach are always situated on the safe side when compared to the shell elements results
- Concerning class 4 cross-section steel beams (pure bending or lateral torsional buckling), the beam-column finite element approach agrees well with the shell finite element models and the calibration ratios are equal or greater than 0.9
- In case of columns, the results obtained with the adopted beam-column finite element approach are largely on the safe side.
- In case of low load ratio for example 0.3, which is a common one for class 4 cross-section steel members, the adopted beam-column finite element approach provides always satisfactory results

This approach developed in the scope of this project has proven to be promising which has provided a very constructive insight for further development in this field.

2   Scientific and technical progress

2.1   Introduction

The simple calculation methods have been incorporated into the latest EN version of Eurocode 3 part 1.2 for fire resistance assessment of steel members with thin wall class 4 cross-sections (cold formed, welded or hot rolled). However, according to the numerical investigations conducted during the establishment of some National Annexes of EN1993-1-2, these simple calculation methods with respect to steel members with thin wall class 4 cross-sections (H and I shape) have proved to be not only very approximate but also too conservative in quite a lot of cases (see Figure 12). In consequence, the fire resistance design based on these calculation rules could penalise significantly the competitiveness of steel structures with such type of steel members of which the major advantage is their lightness and long span capacity.
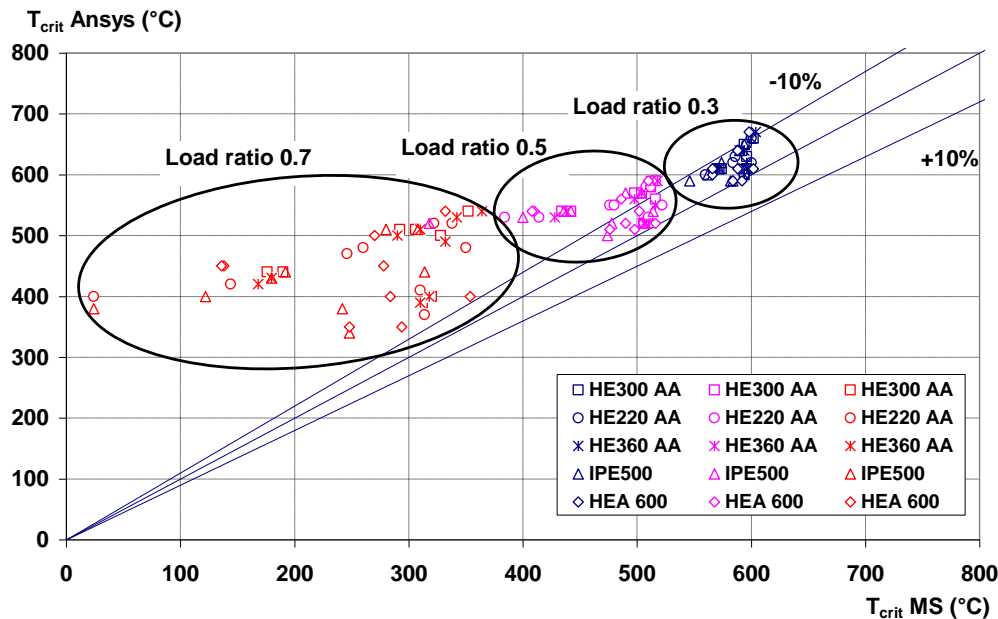
Figure 12: Comparison of critical temperatures between simple calculation method (T_{crit} MS) and advanced numerical model (T_{crit} ANSYS)

On the basis of above background, this project was undertaken with the main objective of developing simple design rules and tools in accordance with the requirements of CEN/TC250 relative to the next revision of Eurocodes, through the improvement of the scientific knowledge on the fire behaviour of class 4 cross-section steel members. More precisely, the primary targets of the project are the followings:

- The first aim is to obtain a full range of experimental data concerning the fire behaviour of steel members with class 4 cross-sections which are either welded cross-sections or hot-rolled cross-sections. Sixteen different fire tests have been predicted to get this experimental data. These tests should also enable to validate the finite element numerical models used for extensive parametric studies to develop the simple calculation rules in the end;
- The second key task is the improvement of current simple design rules of EN1993-1-2. As it is already explained, the current simple design rules of EN 1993-1-2 are not accurate enough when dealing with the fire resistance assessment of class 4 cross-section steel members and in addition are quite often very conservative. In consequence, it is necessary to develop new design rules based on both experimental investigation and a series of extensive numerical parametric studies foreseen in this project;
- As it is well known, the design of class 4 cross-section steel members is much more complex than that of other types of steel members. In order to allow structural engineers to have cost-effective fire resistance design of steel structures with class 4 cross-sections, so to improve the competitiveness of steel industry, it is very helpful to develop user-friendly design tools. In consequence, a specific important task of the project is the development of such type of design software under the VB.NET environment;

- The last expectation of this project is the establishment of a modelling guidance for modern fire structural engineering dealing with the global structural analysis in fire situation of steel structures composed of class 4 class 4 cross-section steel members. The aim is to provide a cost-effective numerical approach to all design engineers to conduct their advanced fire safety engineering projects.

Seven separated work-packages were established in order to reach the objectives listed above:
- WP1: Design of fire tests, benchmark study and definition of numerical parametric studies (see 2.2.1)
- WP2: Fire behaviour of steel members with welded or hot-rolled class 4 cross-sections under simple bending (see 2.2.2)
- WP3: Lateral torsional behaviour of fire exposed steel members with welded or hot-rolled class 4 cross-sections under bending (see 2.2.3)
- WP4: Fire behaviour of steel members with class 4 cross-sections under axial compression (see 2.2.4)
- WP5: Combined bending and buckling behaviour of class 4 steel members subjected to fire (see 2.2.5)
- WP6: Development of user-friendly software to apply simple design rules (see 2.2.6)
- WP7: Global structural analysis using beam column finite element with class 4 steel members (see 2.2.7)

The work conducted in the context of these seven work packages is well explained in following chapters of this report. Further details are available in the corresponding deliverables.

2.2 Description of conducted activities and corresponding outcomes

2.2.1 WP1 - State of art, application domain, limitation of current design rules, design of experimental fire tests and benchmark study

2.2.1.1 Application domain of class 4 cross-section steel members

The following paragraphs aim at defining the application range of steel structures made of welded tapered steel elements with variable class 4 sections in view of defining the parameters for the FIDESC4 research project. They correspond to deliverables from tasks 1.1 and 1.2 of the Technical Annex. In particular, this type of structural elements from the common building system is explained prior to the description of the characteristics of class 4 cross-sections.

A common class 4 cross-section structure is an industrially manufactured steel building structure that is made of pre-designed and pre-fabricated components which represent essentially the load bearing structure of the building, including all stabilization elements and all internal connections, connections to the envelope, and the connections to the substructure (foundations). The building structure can include mezzanine structures, floor beams and crane rail beams made of steel. Those structures are called "primary framing" which by their function are directly fixed to and transferring the loads to the foundations, thus including the wind bracing systems, crane rail beams and mezzanine structures or floor beams. "Secondary framing" encloses all those structural parts which are themselves fixed to the primary structure and support the envelope of the building, including all required stabilization elements and spacer systems or built-up systems. For some structures the envelope is directly fixed to the primary framing (without secondary framing).

Figure 13 : Typical example of class 4 cross-section portal frame

The overall dimensions of a building are defined within each individual building project. The dimensional variations of the steel frames and the members are within a predefined range which however is very large. The final cross section dimensions of the primary framing are defined for each individual case according to the requirements resulting from the static design verification. The portal frames are generally erected on parallel axes, with a defined spacing. For each manufacturer, several typical frame configurations can be pre-defined according to the following list, but other types are possible on request:

- Clear span building with tapered columns: the rafters are either completely or partially tapered and the span of such type of buildings is in general up to 60 m
- Modular building having of 2, 3 or 4 modules respectively: the exterior columns are tapered whereas the interior columns may be pipes or welded beams (H profile). The rafters are usually tapered or partially parallel. The span is in general up to 50 m by bay
- Buildings with a large clear span, a slope of 20% and having tapered columns and rafters: the span is in general up to 90 m
- Clear span buildings with parallel flange columns: the rafters are usually tapered and the span is in general up to 40 m
- Clear span single slope buildings with parallel flange columns: the rafters are usually parallel but can be tapered and the span is in general up to 30 m
- Wing units which can, in principle, be attached to all other types of buildings: the columns are generally parallel flanged. The rafters are usually parallel but can be tapered or "fish-belly". The span is in general up to 25 m
- Tennis buildings with a single or double pitched roof and broken frames: the columns have parallel flanges. The rafters are usually tapered by section. Span in general up to 70 m

The structural members have very commonly either I-shaped or double-T-shaped cross sections. They are welded built-up sections, made from individual flat plates welded together, of steel quality S355 according EN 10025-2:2004. In general, manufacturers for steel structures made of class 4 members do not use other steel grade for the welded elements commercialized in the EU. In general, the welded built-up cross sections are made from plates from the following dimension ranges:

- Flanges: thickness from 5 to 24 mm, exceptionally up to 40 mm and width from 150 to 250 mm, exceptionally up to 420 mm
- Web: thickness from 4 to 12 mm, exceptionally up to 20 mm and depth from 178 to 2000 mm, exceptionally up to 2400 mm

Not every plate size combination is however possible, mainly for manufacturing reasons. The dimensions of steel frames made of class 4 members need to be defined on the basis of the steel profiles available from both manufacturers.
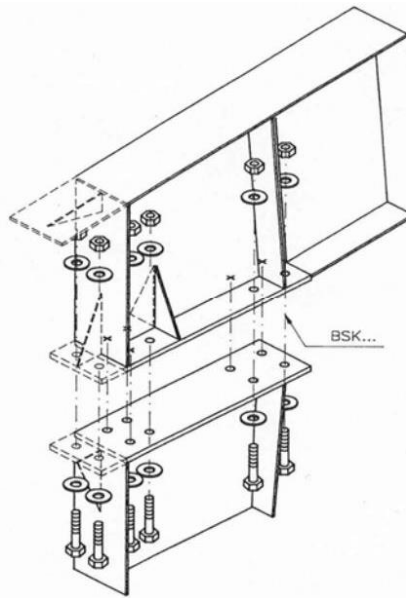
Figure 14 : Typical knee connection

The cross sections of the connections with help of end-plates have the following dimension ranges: thickness from 5 to 24 mm, exceptionally up to 40 mm and width from 150 to 250 mm, exceptionally up to 420 mm.

The welds are defined for their layout and thicknesses in basic welding shapes called "standard welds", which are executed as constructive minimum. In general, the web-to-flanges welds of the primary framing as well as the welds in the connection area are single sided fillet welds according to the standard welds rules. Several welds in the connection area are however double fillet welds sided. Also for web thickness equal to or bigger than 9 mm, the web-to-flange welds are double. If required, the design engineer will adjust the weld thicknesses as well as the type and layout of the welds according to the relevant design verification.

The class 4 steel structured buildings cover mainly:

- single storey industrial buildings (production and warehouse)
- sport halls
- roof structures of museums
- roof structures of railway stations and sometimes airport

2.2.1.2 Limitation of current simple design rules of EN1993-1-2

Steel members with H or I shape class 4 cross-sections, due to their advantages regarding their lightness and efficiency, are widely used in steel constructions. However, the fire design rules of EN1993-1-2 [1] have proven to be not only very approximate but also too conservative [2].

Additionally in the case of tapered steel members it is not clear if normal temperature design rules can be straightforward adapted for fire design. EN1993 gives simple calculation methods for fire design of class 1, 2 and 3 cross-section steel members in its Part 1-2 [1] and recommends the same methods to be used with class 4 cross sections in an informative annex, suggesting that the design yield strength of steel should be taken as the 0.2% proof strength instead of the stress at 2% total strain used on the other classes of cross-sections. However, it has been demonstrated through numerical investigations [2], that this methodology is conservative and leads to uneconomical results.

Another possibility presented in EN1993-1-2, is the use a very low critical temperature of 350 ºC if no calculation is performed to check the fire resistance of a class 4 steel members, which is even more conservative. That is why more realistic formulae should be developed. On the other hand, for tapered steel members, due to the non-uniform cross section along the member length, the corresponding flexural, axial and torsional stiffness also varies making the stability analysis of tapered members much more complicated than that of uniform members.

No specific rules are defined in EN1993 for this kind of elements in fire situation, although they are commonly used. At normal temperature some works have been performed on the calculation of their ultimate load bearing capacity [3], [4] or on the determination of the elastic critical loads of such members [5], [6], [7] and [8] that can be, in theory, adapted for fire situation. Since the stiffness of these non-uniform members varies, clauses 6.3.1 to 6.3.3 of Part 1-1 of EN1993 [9], regarding the stability check of steel members do not apply and the stability check should be performed either by a cross sectional verification based on second-order internal forces or by using the "General Method" as given in clause 6.3.4 of Part 1-1 of EN1993 [9]. However, it should to be noted that the "General Method" is not widely validated [10] and there is no specific guidance on how to proceed at elevated temperature.

To take into account the effect of local buckling that can occur in slender plates or plated structures subjected to compressive in-plane loading, Part 1-5 of EN1993 [11] presents two different calculation methods: the effective width method and the reduced stress method. The former is strongly efficient for standard geometries [12], being the resistance of plated members determined using the effective areas of plate elements in compression for class 4 sections using cross sectional data (Aeff, I eff, Weff) for cross sectional verifications and member verifications for column buckling and lateral torsional buckling according to EN 1993-1-1 [9]. However, the effective width method is not applicable for non-uniform geometries and certain types of loading [12]. On the contrary, the reduced stress method can be applied to almost any geometry and loading due to the generic concept that takes into account the full stress field and its interaction, as mentioned in section 10 of EN 1993-1-5 [11].

Although some studies have been done previously within the scope of one research project [13] for welded or hot-rolled class 4 steel members this type of study is very limited and cover only, for example the buckling of class 4 steel columns [13], [14], [15] and [16] or are related to other types of steel, for example stainless steels [17] which constitutive law are different from carbon steel. In [16] a stain-based approach to local buckling of steel sections in fire is proposed. In this approach, a strain based effective width method is developed and a strength curve is derived from points of intersection between temperature-dependent second-order elastic theory and the yield line theory, for unstiffened elements. With the method proposed, the classification of cross-sections can be avoided and so it can be used for all kinds of cross-sections in fire design. However, a procedure for cross-sections composed of stiffened and unstiffened elements based on this approach is still missing [16].

2.2.1.3 Design of experimental fire tests

Sixteen fire tests were designed in order to improve the experimental knowledge on the failure behaviour of class 4 cross-sections. All the tested beams were made of welded S355 steel grade plates and are class 4 cross-sections (class 4 web, class 3 flanges for beams no.1 and 2 and class 4 flanges for beams no. 3 and 4). The eight beams were 5 m span and were subjected to four-point bending. Both simple bending and lateral torsional buckling were considered. The columns were 2.7 m high and were hot-rolled (two out of eight) or welded cross-sections (six out of eight). The steel grade of columns was S355 too. The compressive loads applied on the columns were either axial or eccentric about the major axis. In order to appropriately initiate the failure buckling mode of the axially loaded columns, an eccentricity of 5 mm was applied about the minor axis or the major axis. On one hand, seven beams out of eight were constant cross-section. On the other hand, six columns out of eight were constant cross-sections. Stiffeners were welded to the beams at two different locations to prevent any local undesired instability: "inner" stiffeners were used at the load applications points and "outer" ones at the supports. Two different means were used to obtain the failure of the tested specimens. The beams were steady-state fire tested. The mechanical load was increased until failure while a given temperature was applied to the part of the beam between the "inner" stiffeners. The columns were progressively heated up until failure. To achieve that goal, a compression load was chosen as a fraction of the cold failure load. The details of the test set-up for beams are shown in 2.2.2.1 and 2.2.3.1. The details of the test set-up for columns are shown in 2.2.4.1 and 2.2.5.1.

The type, size and loading conditions (heating or mechanical) of all the fire tests of the project are provided in Table 7 to Table 10.

Test number	Profile	Temperature (°C)
Beam no. 1	Welded: 650×4+250×12	450
Beam no. 2	Welded: 650×4+250×12	650
Beam no. 3	Welded: 835×5+300×12	450
Beam no. 4	Welded: 835×5+300×12	650

Table 7 - Cross-section and temperature of the beams under simple bending (WP2)

Test number	Profile	Temperature (°C)
Beam no. 5	Welded: 450×4+150×5	450
Beam no. 6	Welded: 450×4+150×5	650
Beam no. 7	Welded: 450×4+150×7	450
Beam no. 8	Welded, tapered: 450/610×4+150×5	650

Table 8 - Cross-section and temperature of the beams under lateral torsional buckling (WP3)

Test number	Profile	Compressive load / eccentricity
Column no. 1	Hot-rolled: IPE 240 A	144.5 kN / 5 mm about minor axis
Column no. 2	Welded: 440×4+150×5	122.4 kN / 5 mm about minor axis
Column no. 3	Welded: 440×4+150×5	204 kN / 5 mm about minor axis
Column no. 4	Welded, tapered: 290/490×4.5+150×5	348 kN / 5 mm about major axis

Table 9 - Cross-section and load of columns under axial compression (WP4)

Test number	Profile	Compressive load / eccentricity
Column no. 5	Welded: 350×4+150×5	231.25 kN / 71 mm about minor axis
Column no. 6	Welded: 350×4+150×5	166.4 kN / 177.5 mm about major axis
Column no. 7	Hot-rolled: HE 340 AA	760.8 kN / 100 mm about major axis
Column no. 8	Welded: 440/340×4+150×5	219 kN / 150 mm about major axis

Table 10 - Cross-section and load of columns under combined bending and compression (WP5)

The set-up of the sixteen fire tests is not representative of the reality of the construction configuration even if the used cross-sections are common. In fact, the real purpose of these tests was to establish an experimental database from which it was possible to calibrate the numerical investigations before extending some parameters of the numerical models to investigate properly the fire behaviour of class 4 beams and columns. The objective was to ensure that the numerical models were able to take account of class 4 particularities as local buckling of plates. That is the reason why the tested elements were all class 4 in fire conditions. These numerical simulations were led with three different finite element computer codes: ABAQUS, ANSYS and SAFIR. The particularity of class 4 cross-section which is local buckling failure mode necessarily led to the use of shell elements. In addition to that, the defined models took account of both geometric and material nonlinearities.

2.2.1.4 Numerical benchmark investigation

In order to develop various numerical parametric studies for fire resistance assessment of steel structures with welded or hot-rolled class 4 steel members with three different computer codes (ABAQUS, ANSYS and SAFIR), it is necessary to ensure the result consistency among these different codes. With this aim, a numerical benchmark investigation is carried out, in which all important parameters are settled for the parametric study of the project.

In this section are simply described all the examples that are developed by the modelling group of the project in order to ensure that the numerical simulations carried out with different computer codes have the same input parameters which should lead to similar results in terms of failure load vs. temperature. Steel S355 based on EN 1993-1-2 definition is used in all examples. Regarding the shell elements to be used, 1st order shell elements (four corner nodes) are proposed.

2.2.1.4.1 1st example: beam under pure bending

For the first example the investigated beam has a constant cross-section. The web and the flanges are class 4. The beam is subjected to 4-point bending and stiffeners are present at both load points and supports. Lateral restraints are applied at the stiffeners locations. The beam is heated at a stabilized temperature of 450 °C along its middle 1.5 m length. The following picture illustrates these conditions and dimensions:
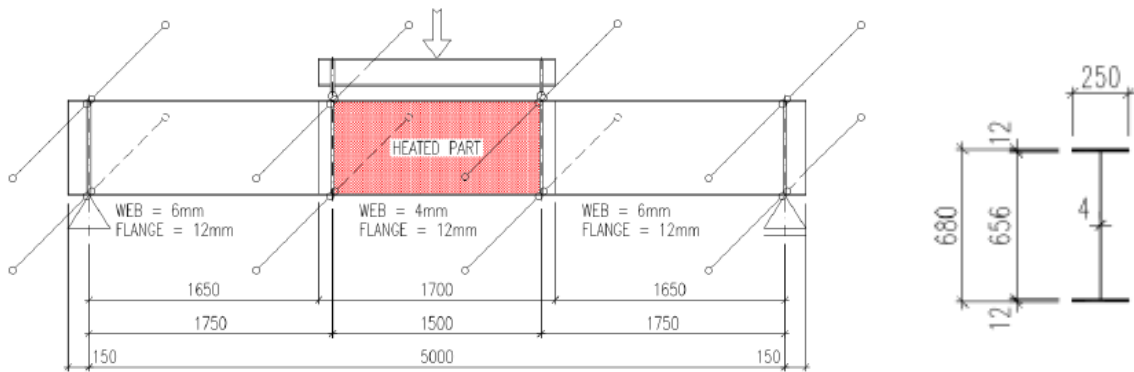
Figure 15 : 1st example of benchmark study

Table 11, Figure 16 and Figure 17 illustrate the failure load, ultimate bending moment and load deflection curve obtained by all partners for the 1st example of the benchmark study under the three different computer codes:

FAILURE LOAD (kN)				
CTICM (ANSYS)	CTU (ABAQUS)	TECNALIA (ABAQUS)	UAVR (SAFIR)	ULG (SAFIR)
306.19	284.98	307.03	284.22	286.91
ULTIMATE BENDING MOMENT (kN.m)				
CTICM (ANSYS)	CTU (ABAQUS)	TECNALIA (ABAQUS)	UAVR (SAFIR)	ULG (SAFIR)
535.84	498.72	537.30	497.38	502.10

Table 11: Failure load and ultimate bending moment for 1st example
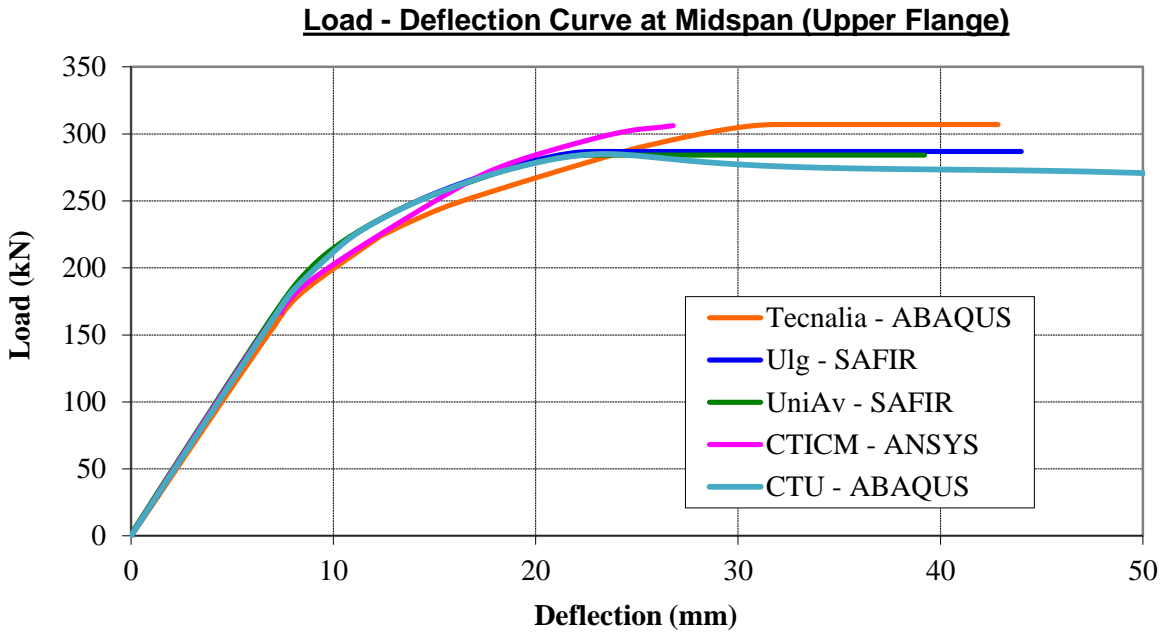
Figure 16: Load-deflection curve at mid-span (upper flange) for 1st example

The failure modes of the beam obtained with the different computer codes are shown in Figure 17:
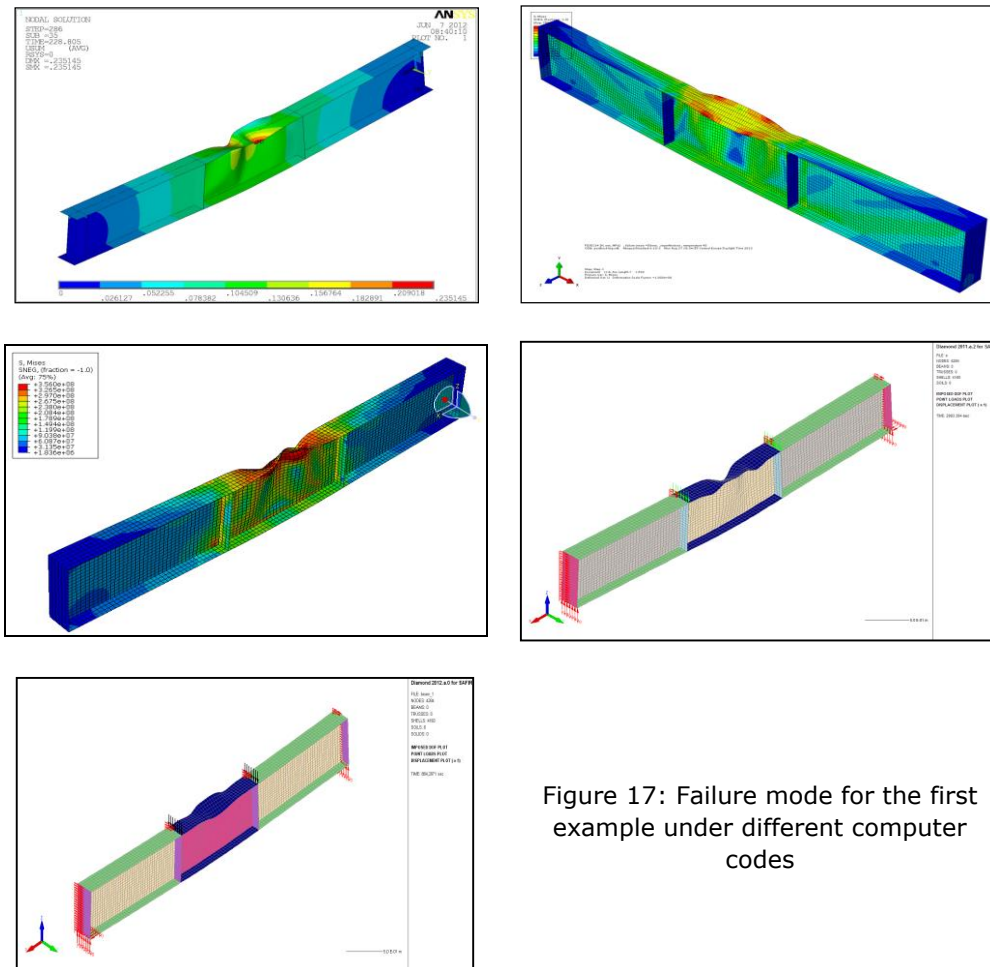
Figure 17: Failure mode for the first example under different computer codes

2.2.1.4.2   2nd and 3rd examples: beams under lateral torsional buckling

The beam with constant cross-section shown in Figure 18 consists of a class 4 web and class 4 flanges. The beam is subjected to 4-point bending, with stiffeners at both load points and supports. Lateral restraints are applied at the four stiffeners location. The beam is to be loaded at a stabilized temperature of 450 °C, which is constant over the middle 2.8 m length, as shown in the following figure:
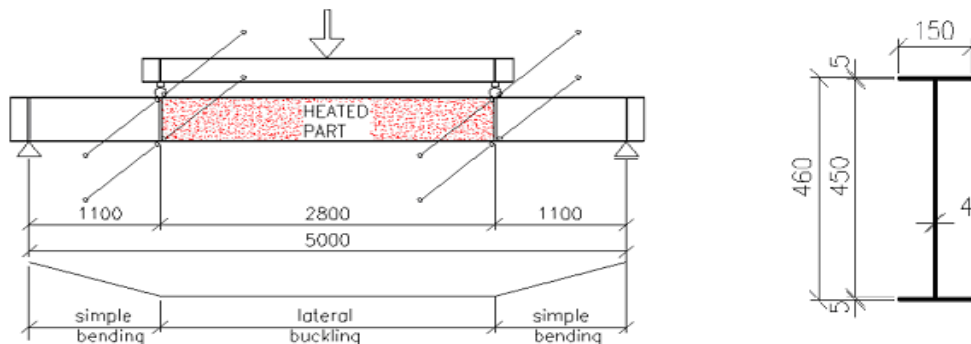
Figure 18: 2nd example for benchmark study

The beam shown in Figure 19 consists of a variable class 4 cross-section. The beam is subjected to 4-point bending, with stiffeners at both load points and supports. Lateral restraints are applied at the four stiffeners locations. The beam is to be loaded at a stabilized temperature of 650 °C, which is constant over the middle 2.8 m length, as shown in Figure 19:
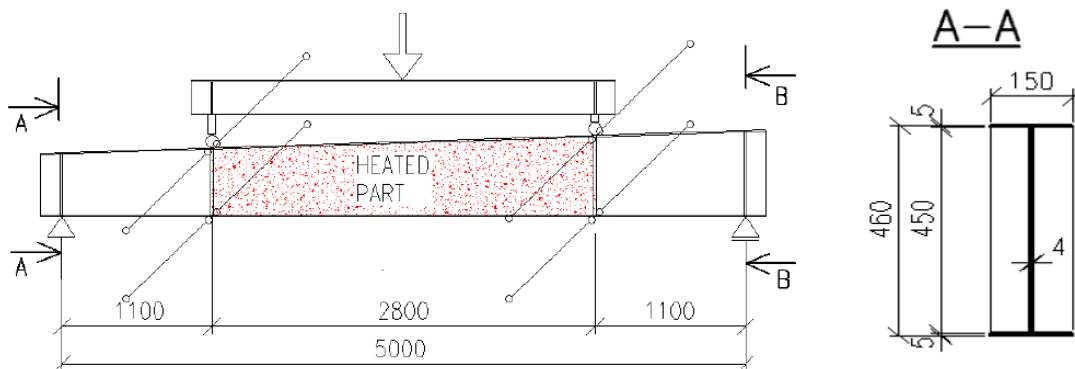
Figure 19: 3rd example for benchmark study

Table 12, Table 13 and figures from 20 to 23 illustrate the failure load, ultimate bending moment and load deflection curve obtained by all partners for the 2nd and 3rd examples of the benchmark study under the three different computer codes:

FAILURE LOAD (kN)				
CTICM (ANSYS)	CTU (ABAQUS)	TECNALIA (ABAQUS)	UAVR (SAFIR)	ULG (SAFIR)
56.10	52.11	55.10	52.07	61.16
ULTIMATE BENDING MOMENT (kN.m)				
CTICM (ANSYS)	CTU (ABAQUS)	TECNALIA (ABAQUS)	UAVR (SAFIR)	ULG (SAFIR)
61.70	57.32	60.61	57.28	67.28

Table 12: Failure load and ultimate bending moment for 2nd example (constant cross-section)

FAILURE LOAD (kN)				
CTICM (ANSYS)	CTU (ABAQUS)	TECNALIA (ABAQUS)	UAVR (SAFIR)	ULG (SAFIR)
30.13	29.89	29.19	22.74	31.19
ULTIMATE BENDING MOMENT (kN.m)				
CTICM (ANSYS)	CTU (ABAQUS)	TECNALIA (ABAQUS)	UAVR (SAFIR)	ULG (SAFIR)
33.14	32.88	32.11	25.02	34.31

Table 13: Failure load and ultimate bending moment for 3rd example (tapered beam)

Load - Vertical displacement at Midspan (Upper Flange)
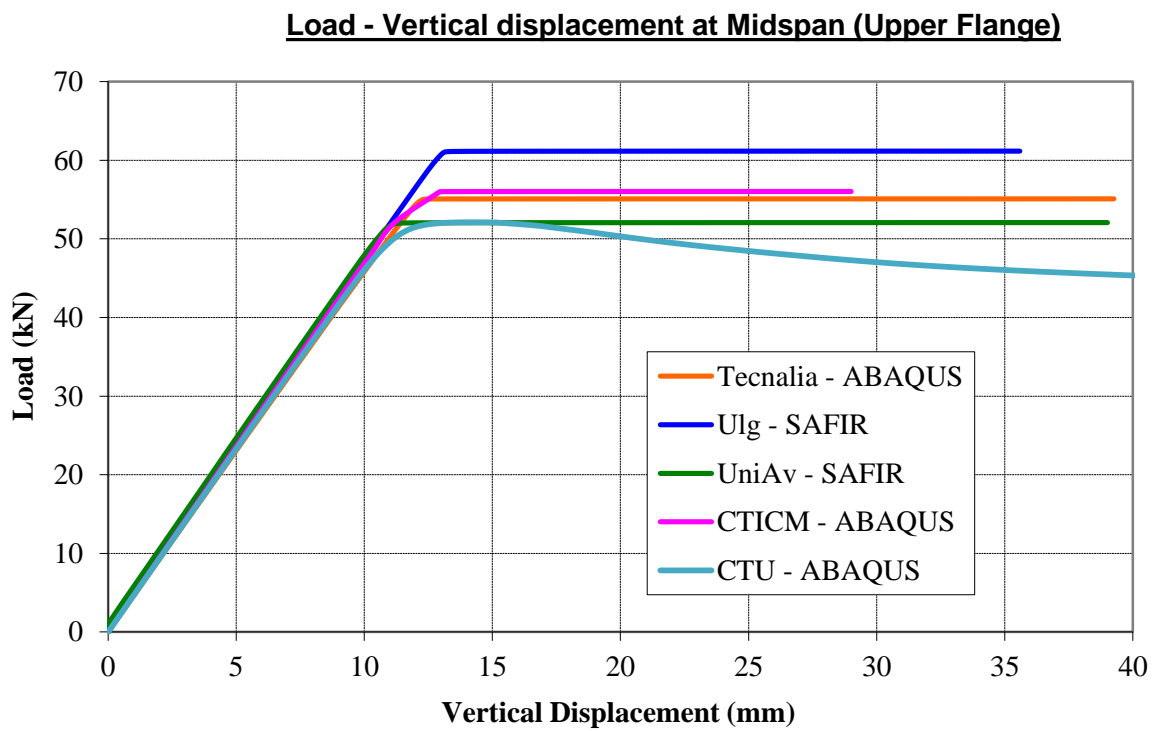
Figure 20: Load-deflection curve at mid-span (upper flange) for 2nd example

28

Load - Vertical displacement at Midspan (Upper Flange)
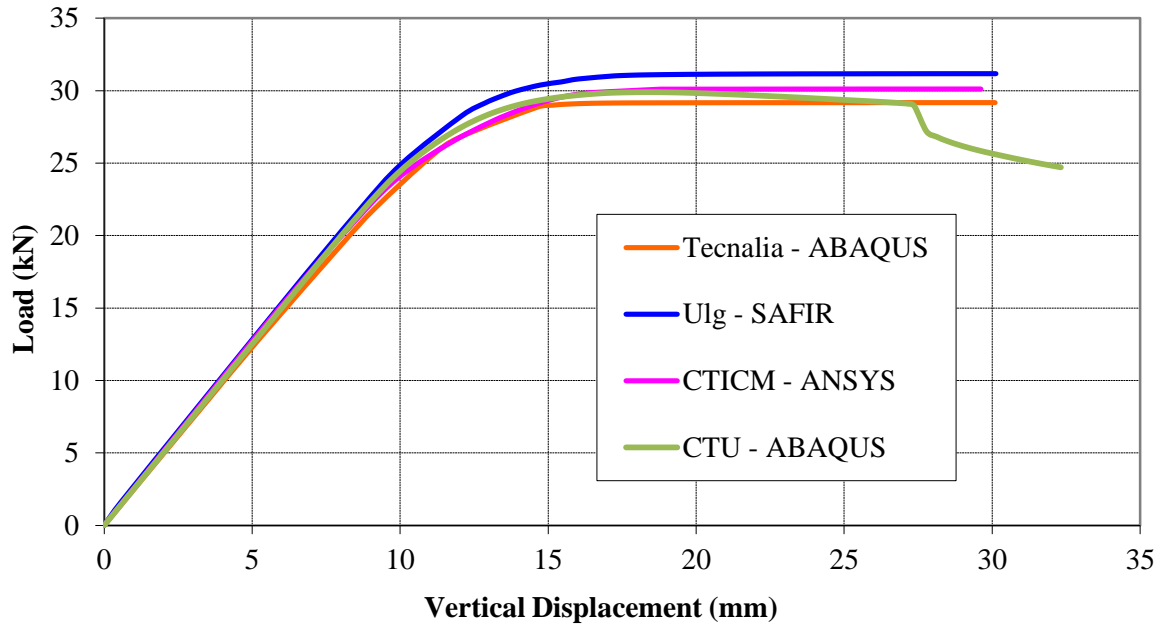
Figure 21: Load-deflection curve at mid-span (upper flange) for 3rd example

The failure modes of the beams of example 2 and example 3, obtained with the different softwares, are shown in Figure 22 and Figure 23:
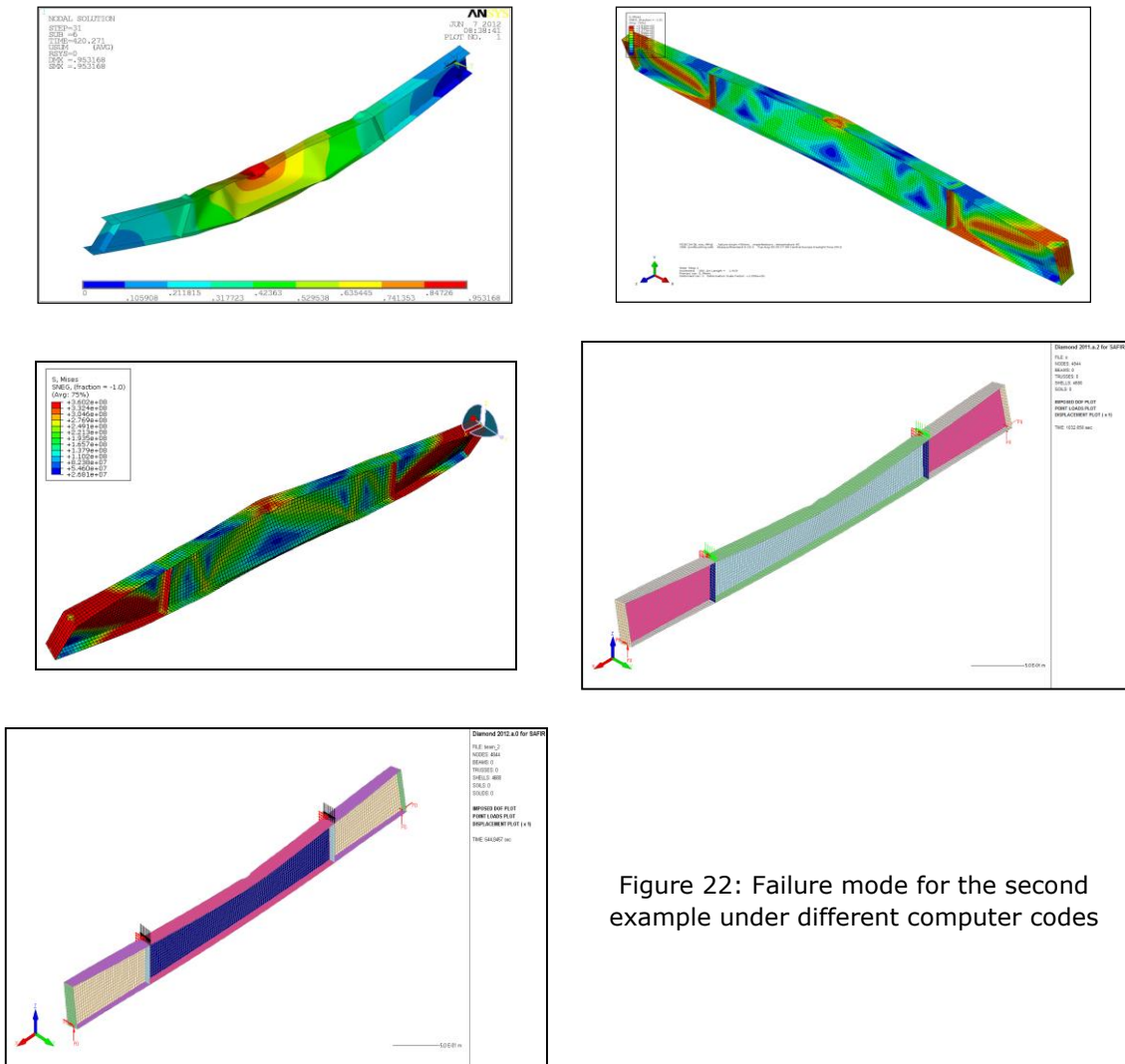
Figure 22: Failure mode for the second example under different computer codes

Figure 23: Failure mode for the third example under different computer codes

2.2.1.4.3 4th and 5th examples: columns under axial compression and eccentric load

The column with constant cross-section shown in the Figure 24 consists of a class 4 web and class 4 flanges. An eccentric axial load about the major axis is applied on the column. The column is heated along its whole length, after reaching a mechanical load ratio:
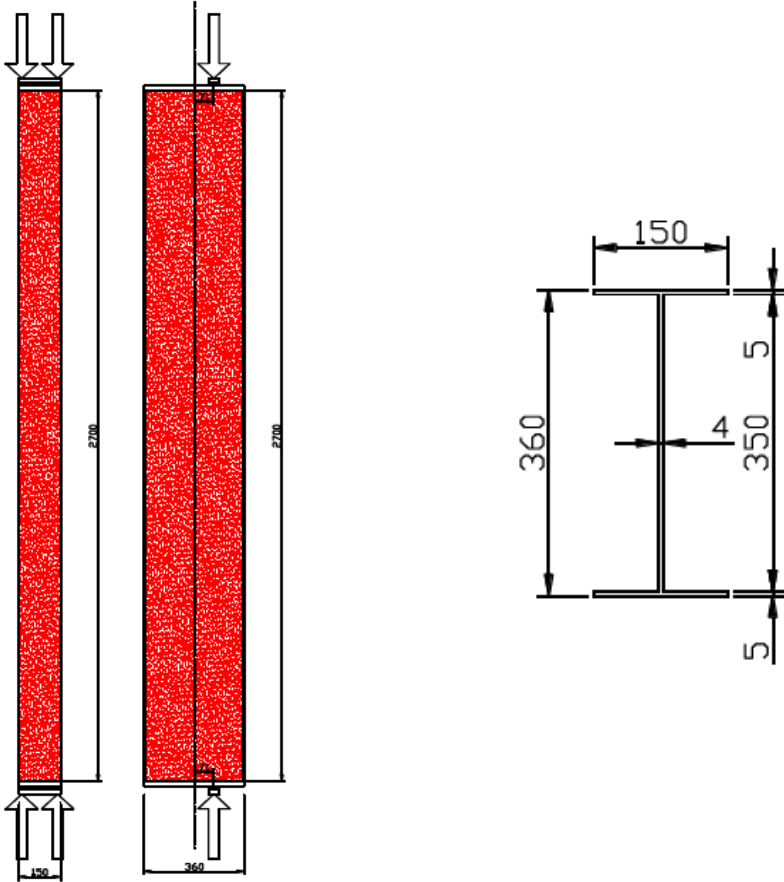
Figure 24: 4th example for benchmark study

The column with variable cross-section shown in the Figure 25 consists of a class 4 web and class 4 flanges. An eccentric axial load about the major axis is applied on the column. The column is heated along its whole length, after reaching a mechanical load ratio:
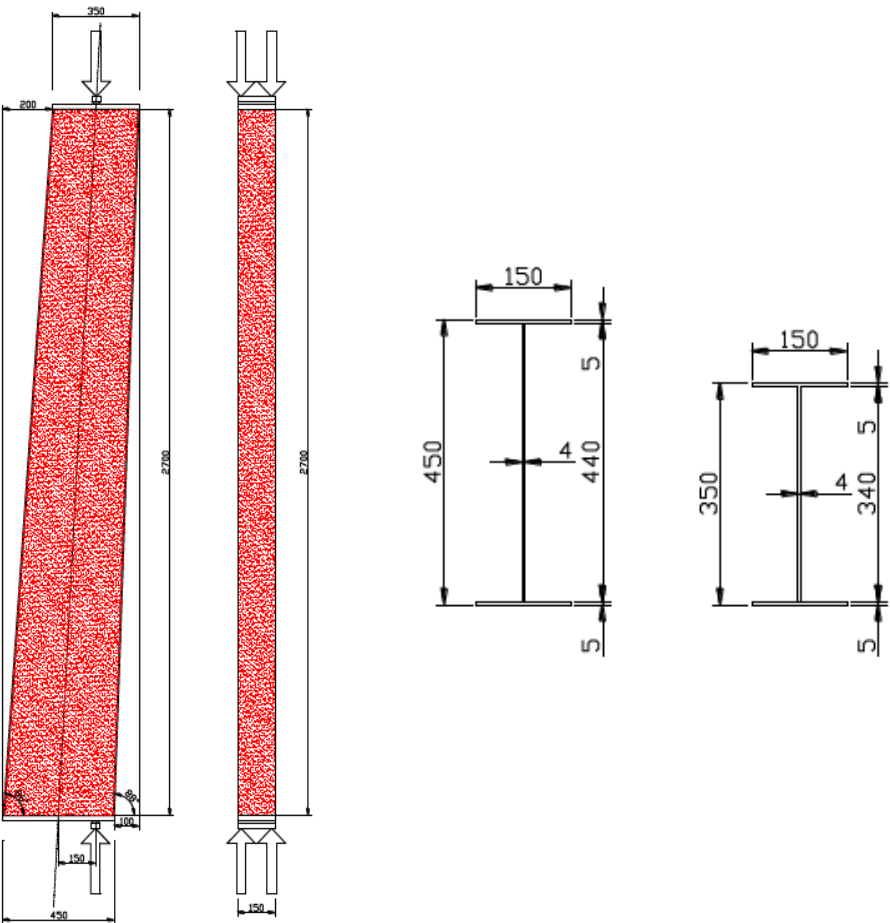
Figure 25: 5th example for benchmark study

The following tables 17 and 18 and figures from 26 to 29 illustrate the failure load and the evolution of the load in function of the horizontal displacement in the strong axis obtained by the partners for the 4th and 5th examples of the benchmark study under the three different computer codes:

FAILURE LOAD (kN) at 500 ºC				
CTICM (ANSYS)	CTU (ABAQUS)	TECNALIA (ABAQUS)	UAVR (SAFIR)	ULG (SAFIR)
235.50	232.71	221.98	207.70	226.56

Table 14: Failure load of column from 4th example

FAILURE LOAD (kN) at 500 ºC				
CTICM (ANSYS)	CTU (ABAQUS)	TECNALIA (ABAQUS)	UAVR (SAFIR)	ULG (SAFIR)
230.30	235.20	216.15	230.12	227.94

Table 15: Failure load of column from 5th example
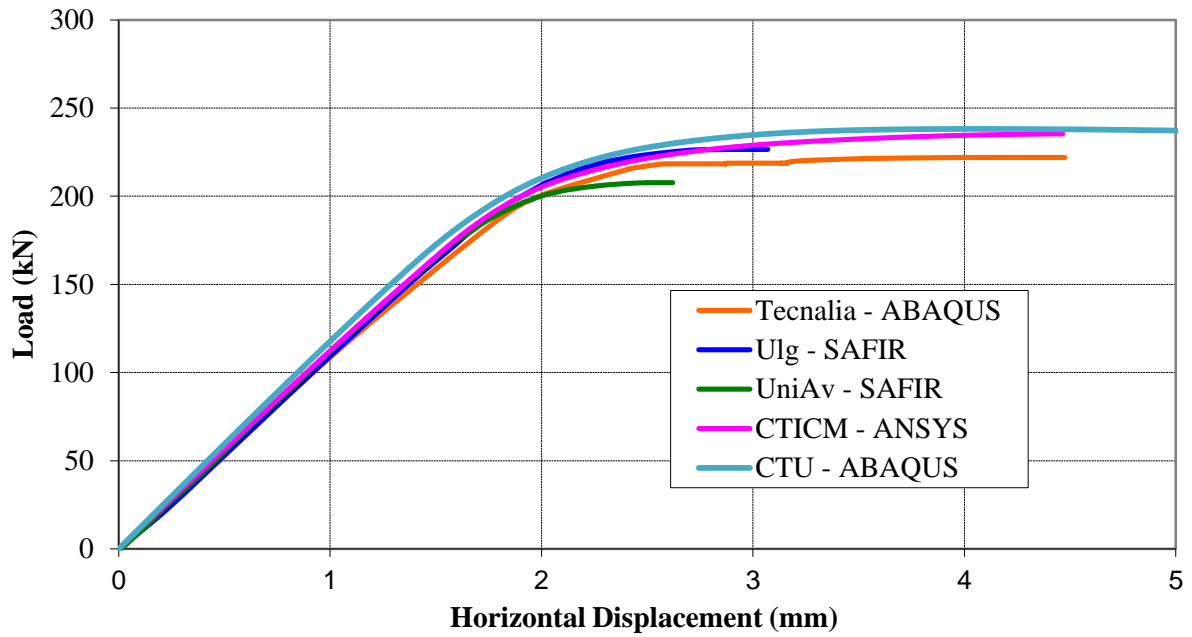
Figure 26: Load – horizontal displacement at middle section in the strong axis for 4th example
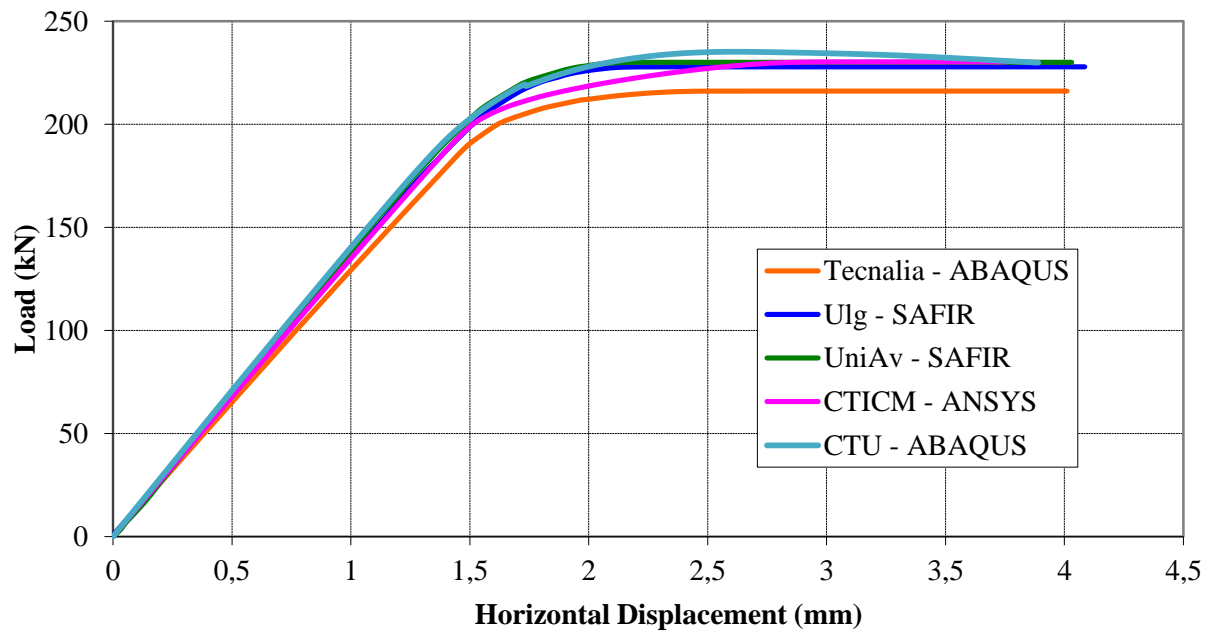
Figure 27: Load – horizontal displacement at middle section in the strong axis for 5th example

The failure modes of the columns of example 4 and example 5, obtained with the different softwares, are shown hereafter:
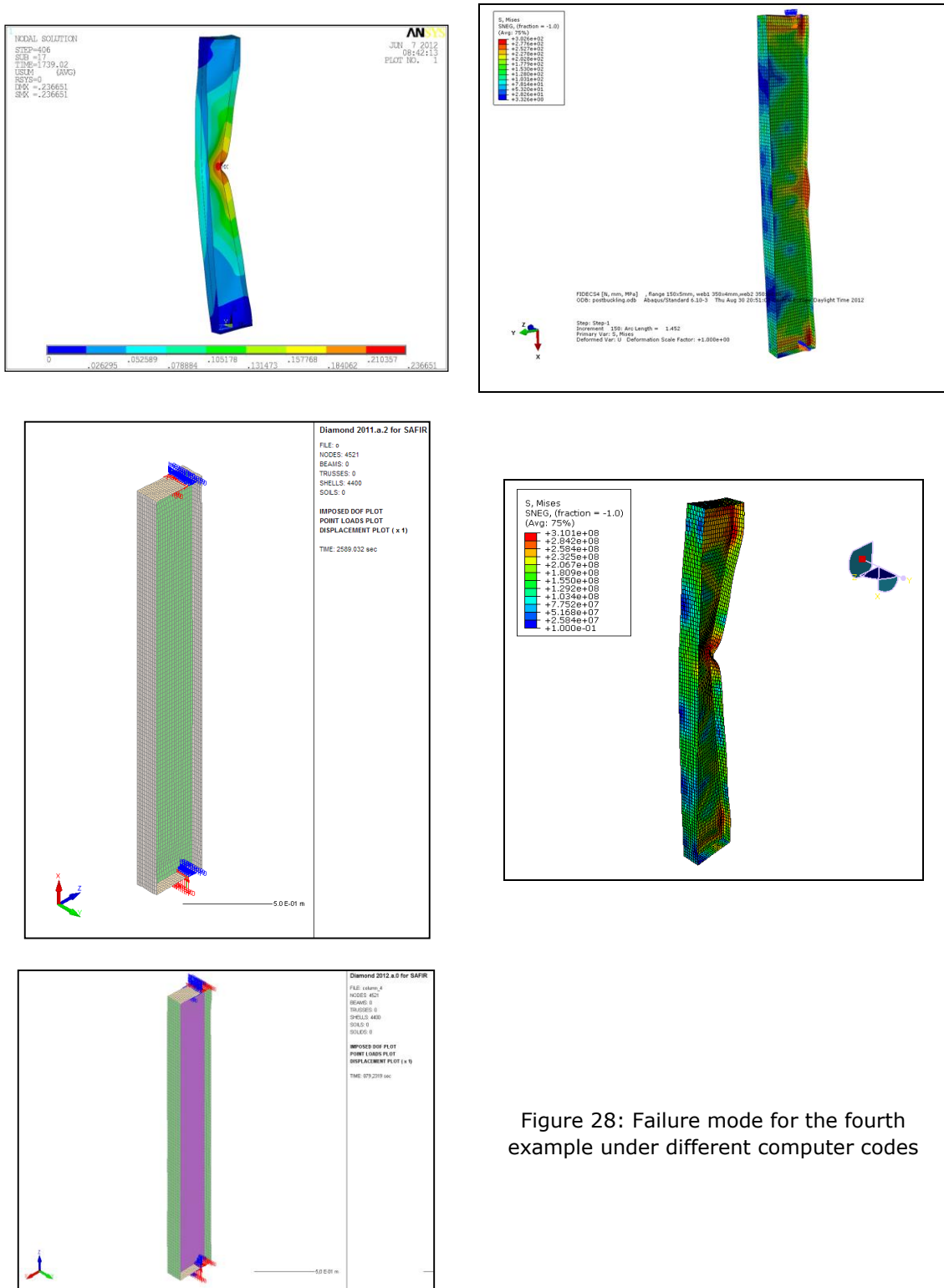
Figure 28: Failure mode for the fourth example under different computer codes
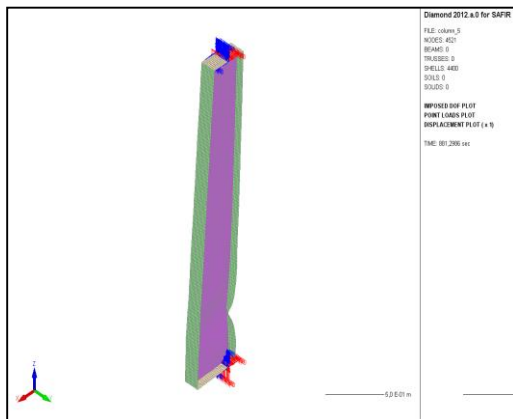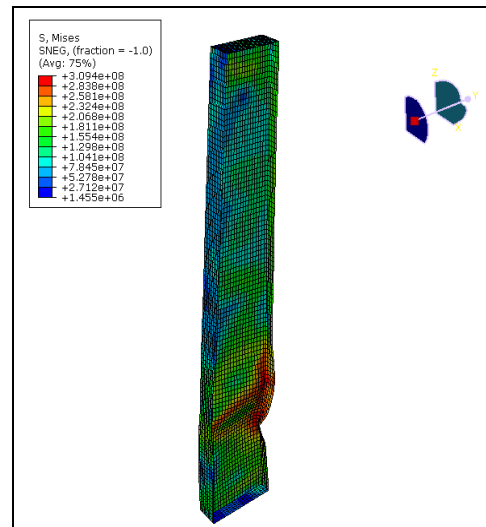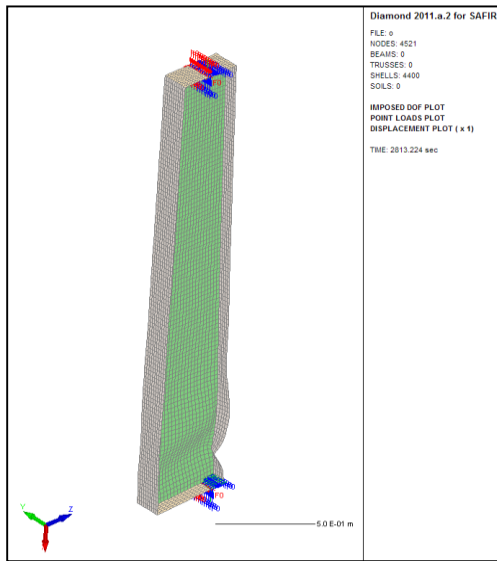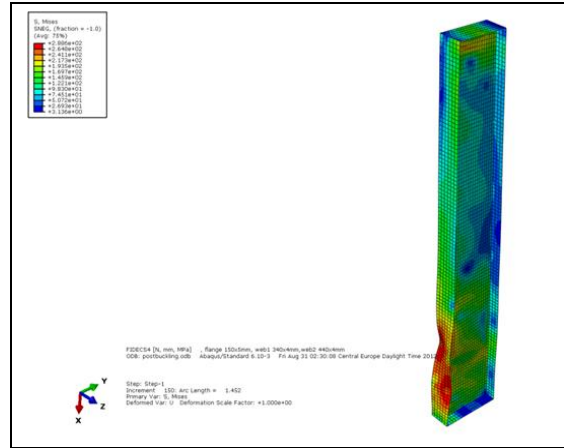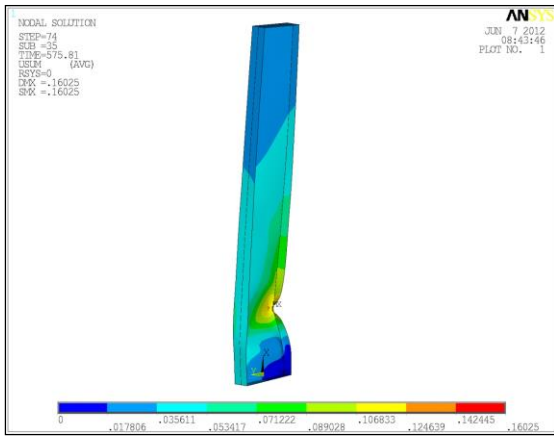
Figure 29: Failure mode for the fifth example under different computer codes

2.2.1.4.4 6th example: single span frame

The single portal frame investigated for the sixth example is shown in the Figure 30. At both supports, deformations in all directions are prevented. At the nodes where purlins and girts are located, displacements are also restrained in the perpendicular direction of the frame. The entire portal frame is heated up until failure. At the locations of the purlins a load of 3.5 kN is applied on all nodes of the upper flange. Self-weight of the structure is also considered.
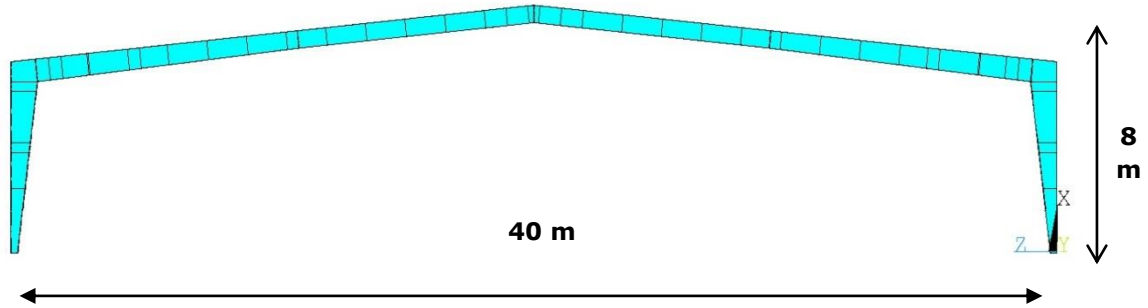
Figure 30: 6th example for benchmark study

Table 16 illustrates the results obtained by the partners using the three different softwares in terms of failure temperature:

FAILURE TEMPERATURE (ºC)				
CTICM (ANSYS)	CTU (ABAQUS)	TECNALIA (ABAQUS)	UAVR (SAFIR)	ULG (SAFIR)
577.80	***	569.98	593.70	595.19

Table 16: Failure temperature of the single frame

The Figure 31 illustrates the results obtained by the partners using the three different softwares in terms of evolution of the temperature in function of the vertical displacement:
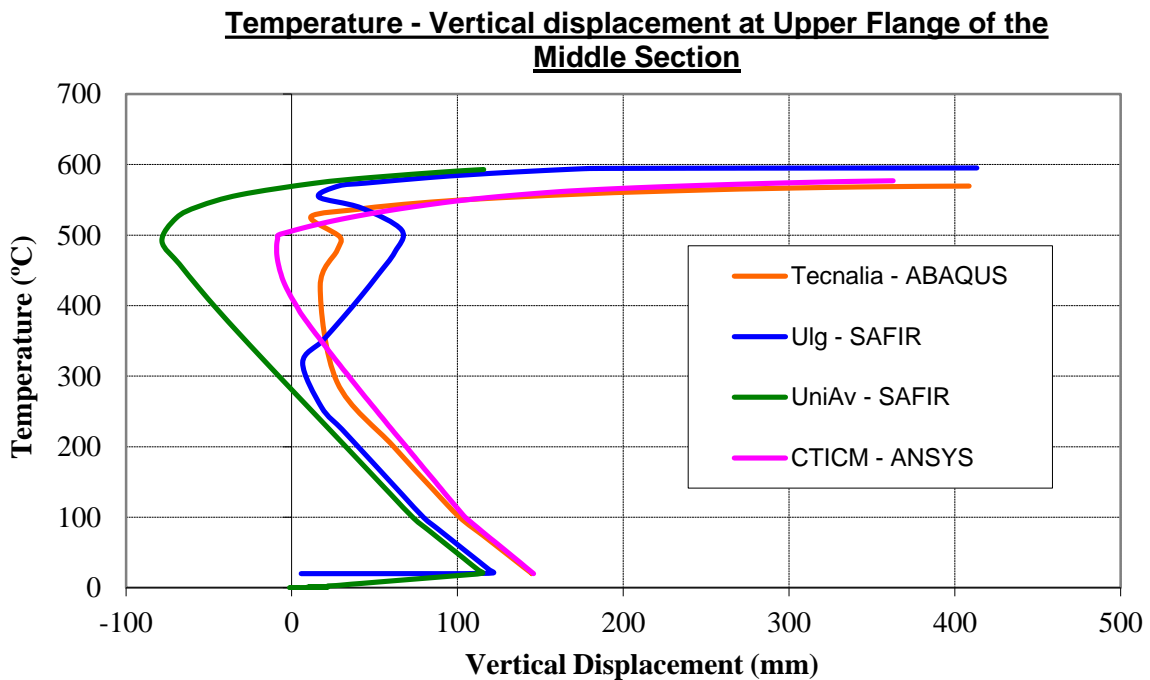
Figure 31: Temperature – vertical displacement at upper flange of the middle section of the frame

The failure mode of the portal frame from the results of all computer codes is illustrated in the Figure 32:
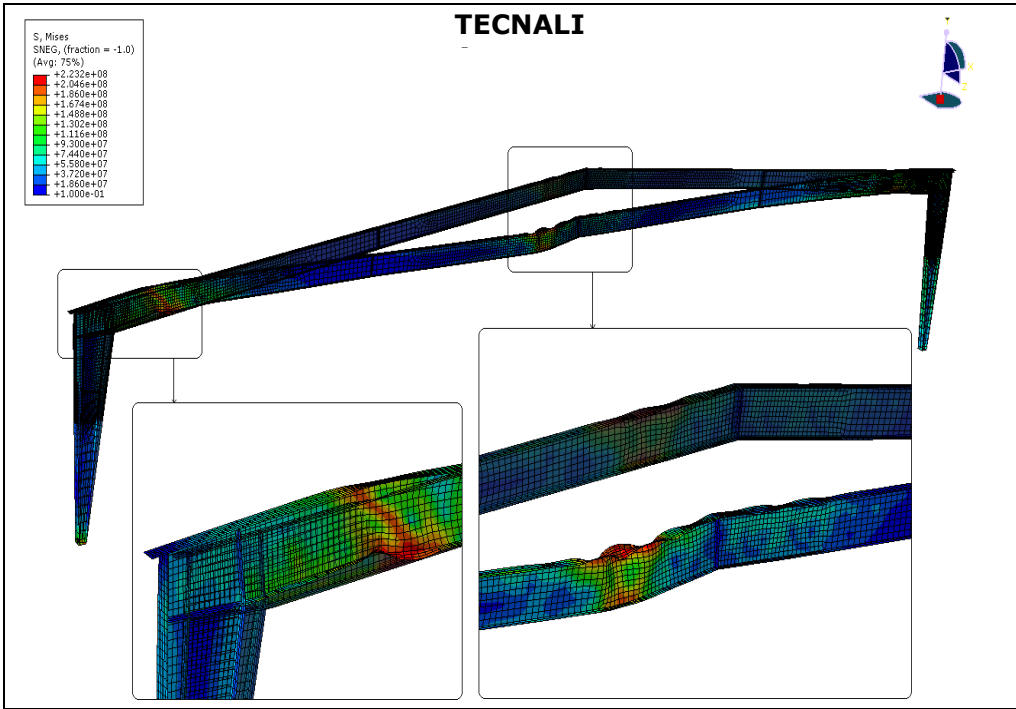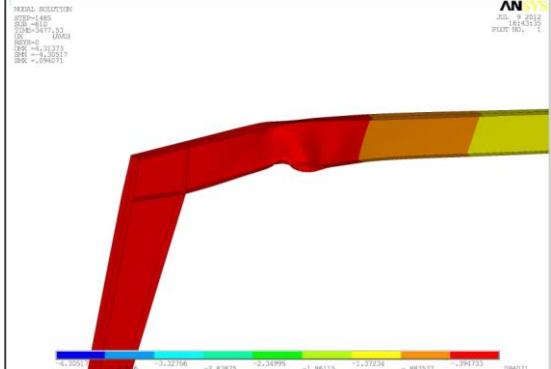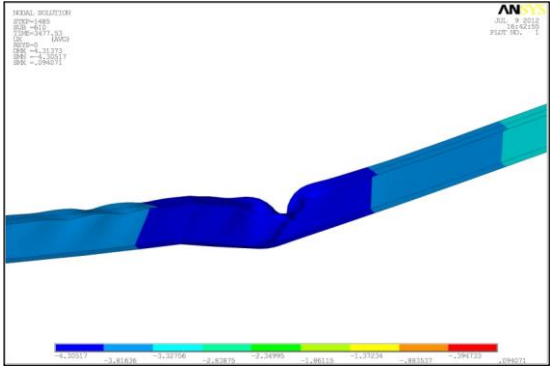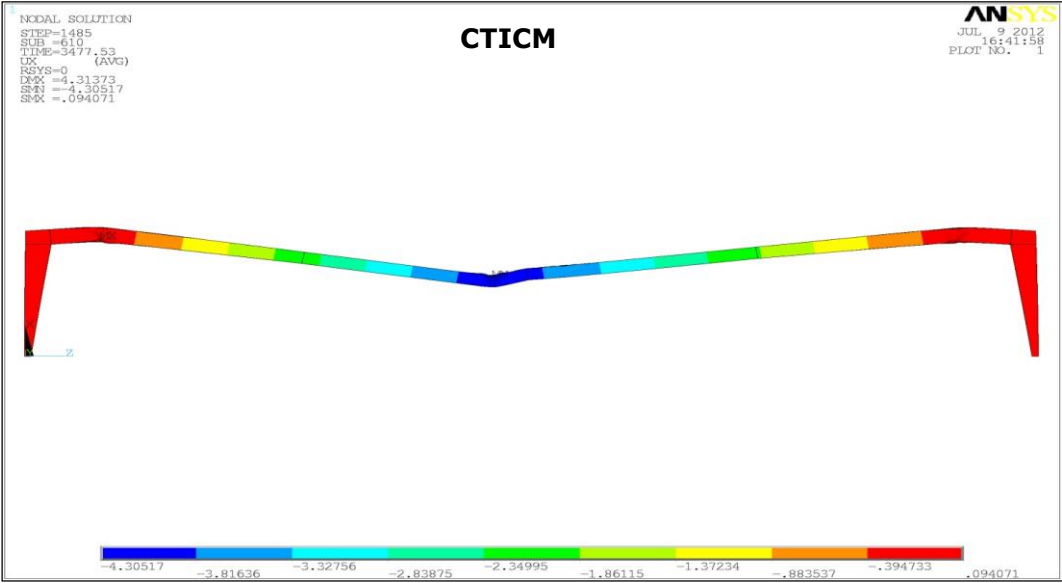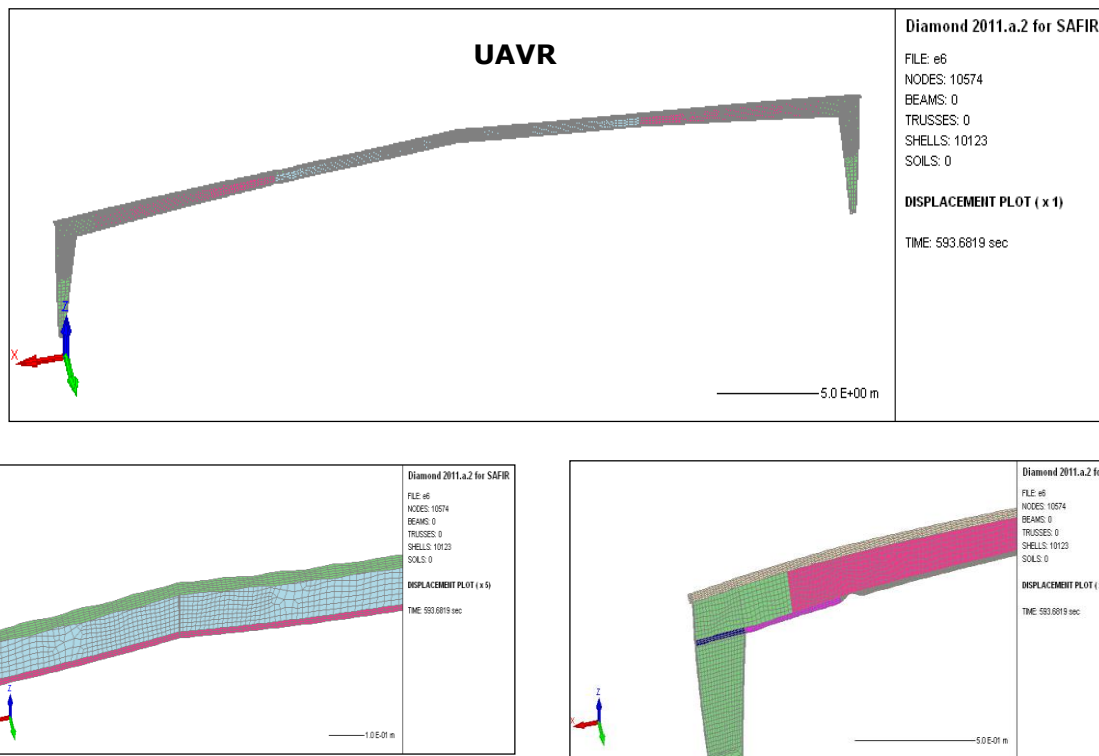
Figure 32: Failure mode of the frame obtained with the different computer codes

In order to ensure result consistency of the studied computer codes (ABAQUS, ANSYS and SAFIR) a numerical benchmark investigation has been carried out among modelling group of the project. Six different examples have been modelled, five of which are tested in other work packages during the project and a single portal frame. In order to reduce possible input differences among the three computer codes, all the examples were defined by partners with the same mesh size, initial imperfections, boundary conditions and others. This helped to ensure a realistic comparison among all the developed models.

The developed models with the help of three different softwares give close results, not only in the studied parameter values, but also in the failure mechanism of the structures.

Regarding Von Mises stresses, in the first stage of the benchmark study, some differences were observed among the stress values provided by all the partners in the chosen nodes. Those differences were analysed, looking into the definition of Von Mises stresses in software. It was then noticed, that the differences were due to the influence of the computational power of each code, which was able to make the simulations finish at different steps when the element had reached failure. For that reason, it was agreed to provide the evolution curve of Von Mises stresses of specified elements of each example, which was more appropriate for the comparison of this parameter. With this change, a good agreement was obtained.

Finally, this study showed that assumptions which seemed not to be important at first sight actually were decisive and must be defined very carefully by engineers in charge of the simulations.

2.2.2   WP2 - Cross-sectional bending resistance of class 4 cross-sections

2.2.2.1   Experimental investigation

Fire tests with I shape beams with slender class 4 cross-sections are conducted in order to have reference results which allows the validation of numerical models. The load capacity of these sections is not directly affected by the yield strength of the steel, but by deformations and buckling of the compressed areas of the cross-section, i.e. the upper wall and the upper flange. To reach this way of deformation of the samples during the planned experiments, it was necessary to choose the appropriate cross-section shape, thickness, beam load form and intensity of the load. Four tests with two types of cross-section loaded by four-point bending are carried out (see Figure 33). Beams incurred a variable load and they are heated with a constant temperature by an electric resistance

mat until exhaustion of the load capacity. Each section is heated up to a temperature of 450 °C or 650 °C:
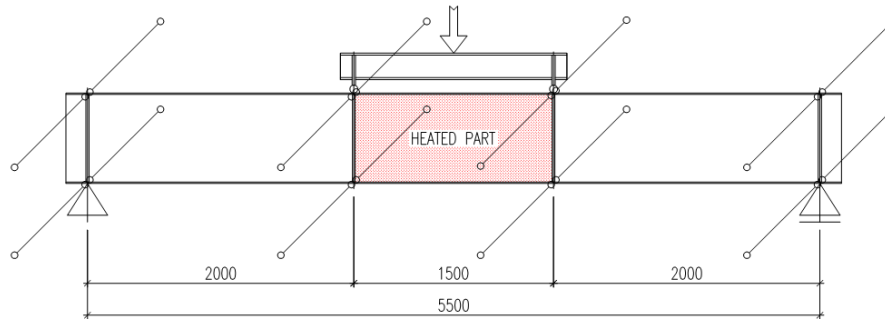
Figure 33: Static scheme of the experiment

For these experiments, two types of welded cross-sections have been chosen. They represent cross-sections of the 4th class and they are sufficiently burdened by the problematic of local stability of the walls:

- The cross-section *A* (IS 680/250/12/4) has a vertical strut in the class 4 ($\bar{\lambda}_p = 1.439$) and the flanges are in class 3 ($\bar{\lambda}_p = 0.661$)
- The cross-section *B* (IS 846/300/8/5) has a vertical strut in the class 4 ($\bar{\lambda}_p = 1.454$) and the flanges are in class 4 ($\bar{\lambda}_p = 1.182$)
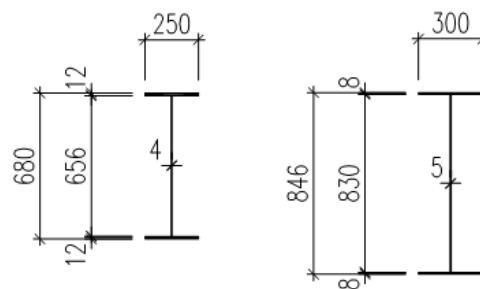
Figure 34: Cross-sections designed for the experiment – *left) Cross-section A, right) Cross-section B*

There were four beams produced for the experiments, with different length of the heated middle part. Due to thermal expansion and to maintain the static scheme (see Figure 33), the middle heated part was shortened depending on the operating temperature. When heated to a prescribed temperature the middle part of the beam will have a length of approximately 1500 mm. The A1 beam (cross-section 680/250/12/4 IS) and B1 beam (cross-section 846/300/8/5 IS) for temperature 450 °C were made with the middle part length of 1492 mm. The beams A2 (cross-section 680/250/12/4 IS) and B2 (cross-section 846/300/8/5 IS) designated for a temperature of 650 °C were made with the middle part length of 1488 mm. For the manufacturers of steel beams (LINDAB - Luxemburg) production documentation in the required range was developed.

The maximum amplitudes of imperfections measured for the tested beam central parts (heated part) are summarized in Table 17:

Beam	Cross-section	Web (mm)	Flange (mm)
A1	680/4+250/12	4.765	0.400
A2		1.340	1.975
B1	846/5+300/8	2.364	1.924
B2		1.595	0.685

Table 17: Comparison between numerical and experimental results

The recorded load-deflection curves of all above beam tests are shown together in Figure 35 and the failure modes of these beams are shown later on. Following observations can be formulated from experimental results:

- Beam A (cross-section: 680/4+250/12) reaches the maximum load-bearing capacity under more important deflection than Beam B (cross-section: 846/5+300/8) due to the fact that Beam A with its smaller cross-section size is much less stiff than Beam B;

- After reaching the maximum strength, the load-bearing capacity decreases slightly for all these beams without any sharp strength fall;

- All the beams failed with local buckling occurred in both upper flange and web. However, the local buckling of Beam A is less developed than Beam B certainly due to the fact that the flanges of Beam B are much slender than Beam A;

- The temperature level of the beam seems to have small influence on the amplitude of its local buckling but the maximum load-bearing capacity of the beams is reached at higher deflection if the heating of the beam is more important.
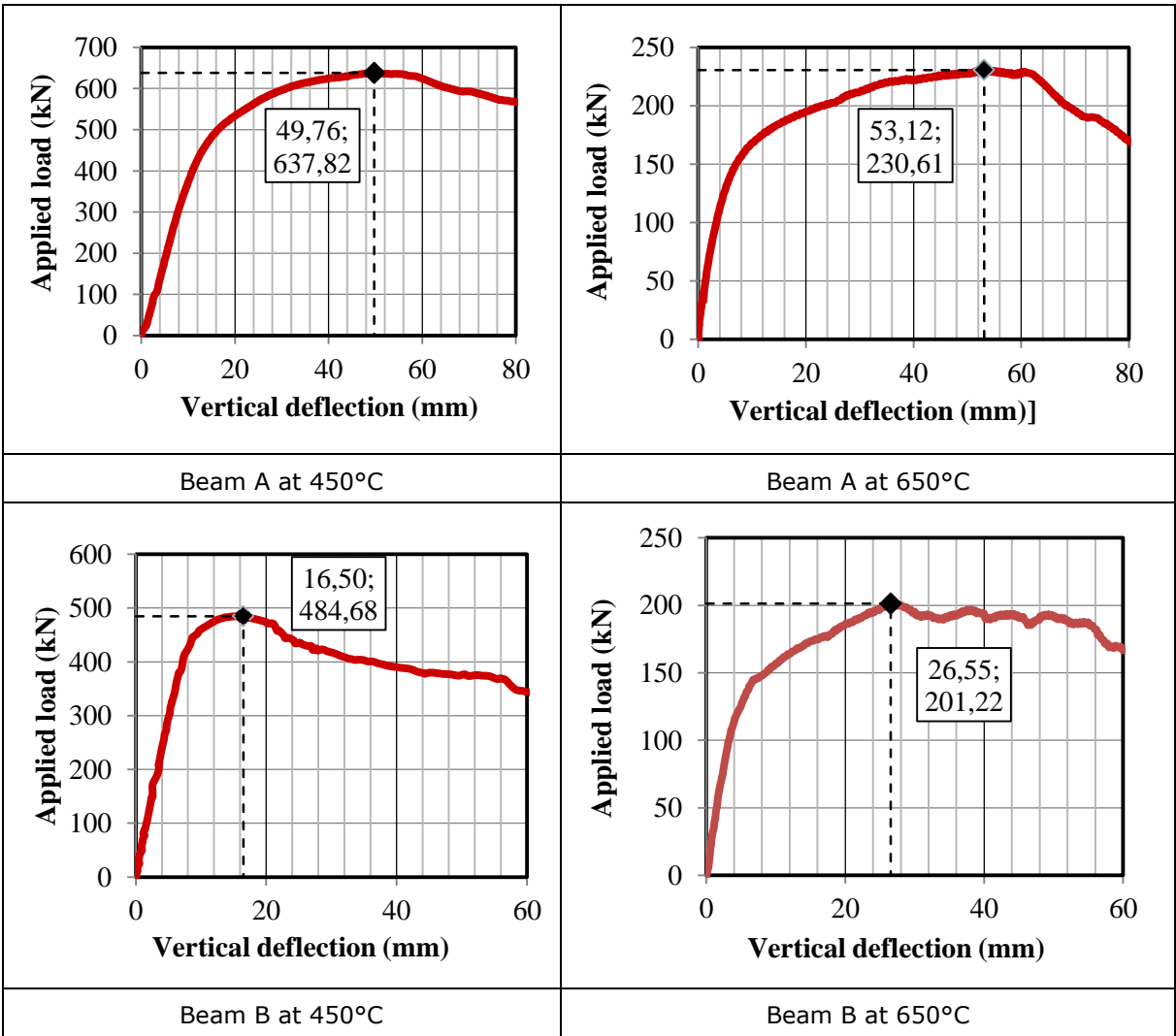
Figure 35: Recorded load-deflection curves of four tested beams

The four tests with class 4 cross-section steel beams subjected to elevated temperatures were conducted with specific test set-up which is quite far from real construction configuration. In fact, the main purpose of these tests is to establish an experimental database from which the relevant numerical models can be created and used thereafter to investigate the fire behaviour of I or H shape class 4 cross-section steel beams under simple bending in extended manner. The numerical models were developed with help of different finite element computer codes, in particular, ABAQUS and ANSYS. In order to deal with the local buckling in case of class 4 cross-section members, these numerical models are specifically based on shell elements capable of taking account of both material and geometric nonlinearities. However, two different types of shell elements are used with the

computer codes ABAQUS and ANSYS which are respectively quadrilateral four nodes linear shell elements and quadrilateral eight nodes (with mid-side nodes) quadratic shell elements. The advantage of eight nodes quadratic shell element of the computer code ANSYS is both its efficiency (larger mesh size and higher accuracy) and numerical robustness (easy convergence under instability behaviour). The other parameters of these numerical models to simulate the tests at elevated temperatures are:

- five integration points through the thickness of the shell elements
- density of mesh used in each model remains constant which leads to about 100 000 degrees of freedom (see Figure 36)
- initial imperfections of the numerical model for tested beam based on eigenvalue analysis with the amplitude measured from the test specimens (see Figure 37)
- average temperature values measured in each part of the beam (flanges and web) affected to numerical model (Figure 37)
- thermal expansion of steel in accordance to EN 1993-1-2 [1]
- stress-strain relationships of steel with its yield stress at room temperature taken from the tensile tests according to EN 1993-1-2

A typical example of the numerical model created to simulate the tests at elevated temperatures is shown in Figure 36 in which the applied boundary and loading conditions are also illustrated. In Figure 37, the initial imperfection and the temperature field used for the same numerical model are provided.
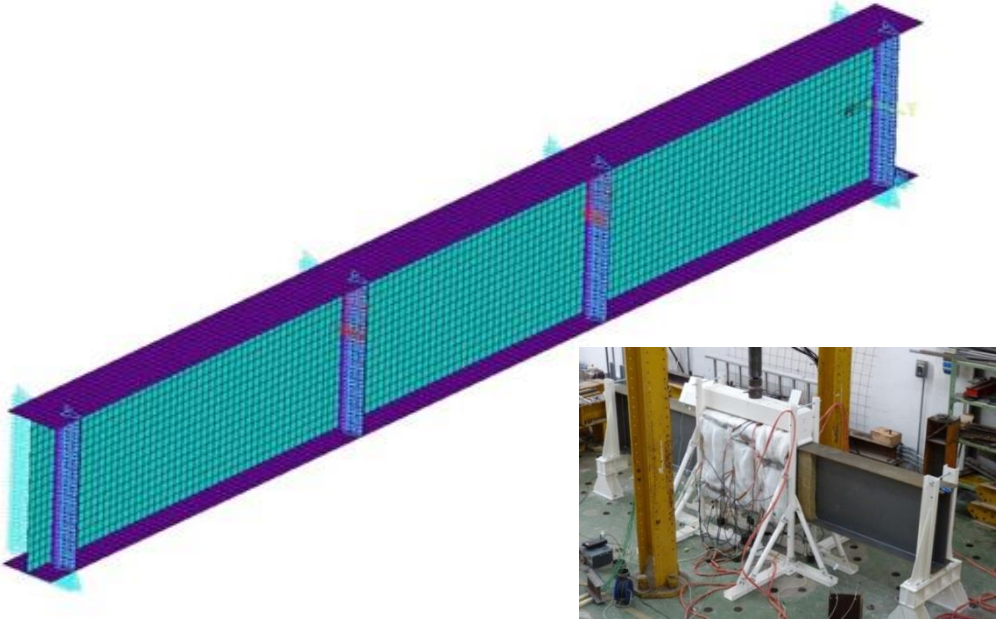
Figure 36: Boundary and loading conditions applied to the numerical model
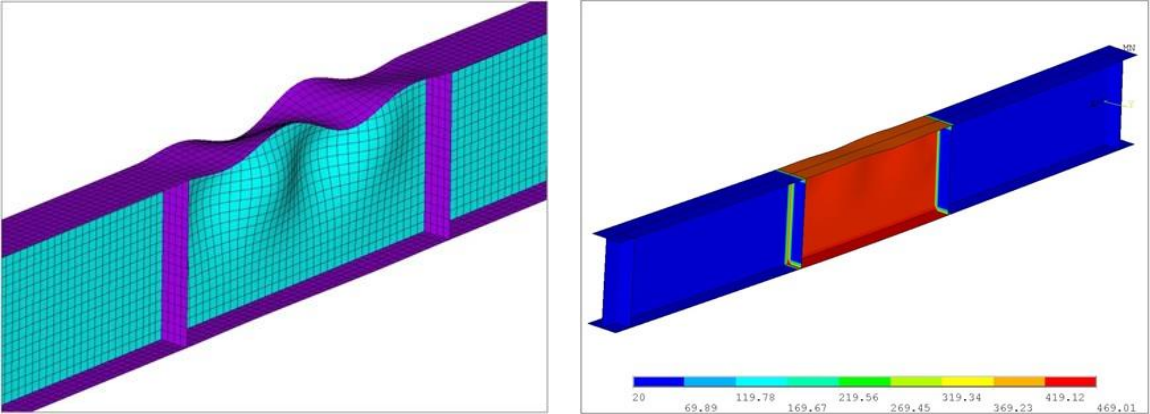
Figure 37: Shape of implemented initial imperfections and temperature field of the beam in the numerical model

For the numerical models in ABAQUS and ANSYS the loads were applied through displacement-controlled method in order to follow the discharging state after buckling. The results from numerical simulations were compared systematically to the experimental ones recorded during the tests (see Figure 38). From these comparisons, one can find that:

- the numerical results from the two computer codes are close to each other up to the ultimate load-bearing capacity of the beams
- the load-bearing capacity predicted by the numerical models is very similar to that obtained by means of the tests
- the numerical initial stiffness of Beam A is slightly lower than the experimental stiffness but the real initial stiffness of Beam B is accurately simulated in the numerical models

The difference between the numerical simulations and tests may be due to the fact that:

- the imperfections are not exactly the same though their amplitude remains the same
- the temperature fields are also slightly different
- initial residual stresses are not taken into account in the numerical model

However, with respect to the key parameter of tested beams, that is the ultimate load-bearing capacity, the numerical models are accurate enough because the scatter between the numerical and experimental results is less than 6% and can be considered as satisfactory (see Table 18).
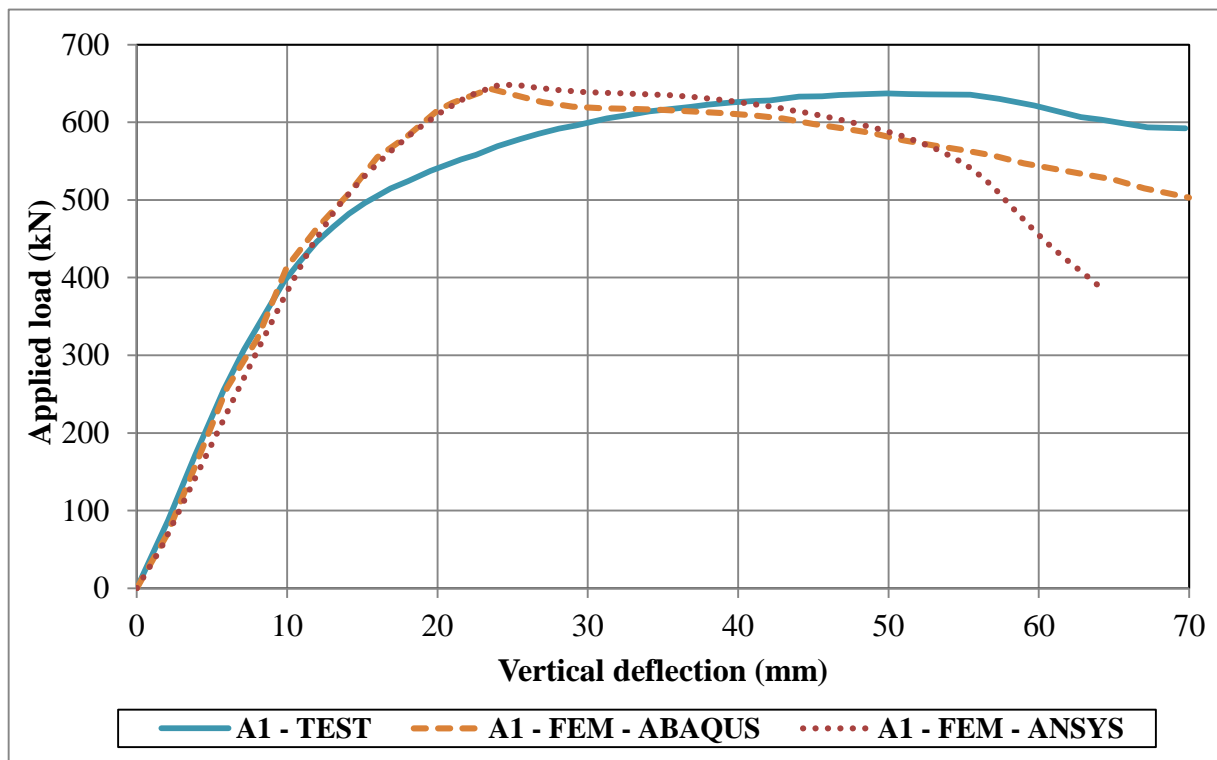
TEST A1: cross-section A – 450 °C
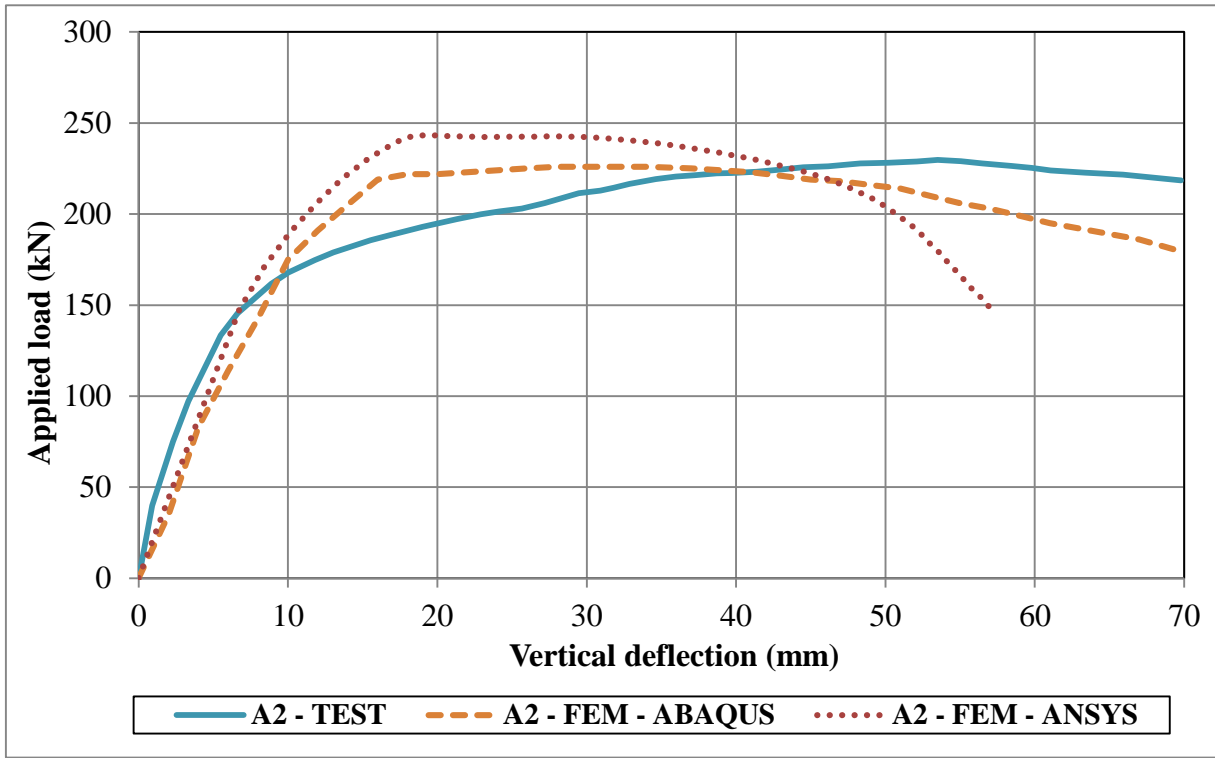
TEST A2: cross-section A – 650 °C
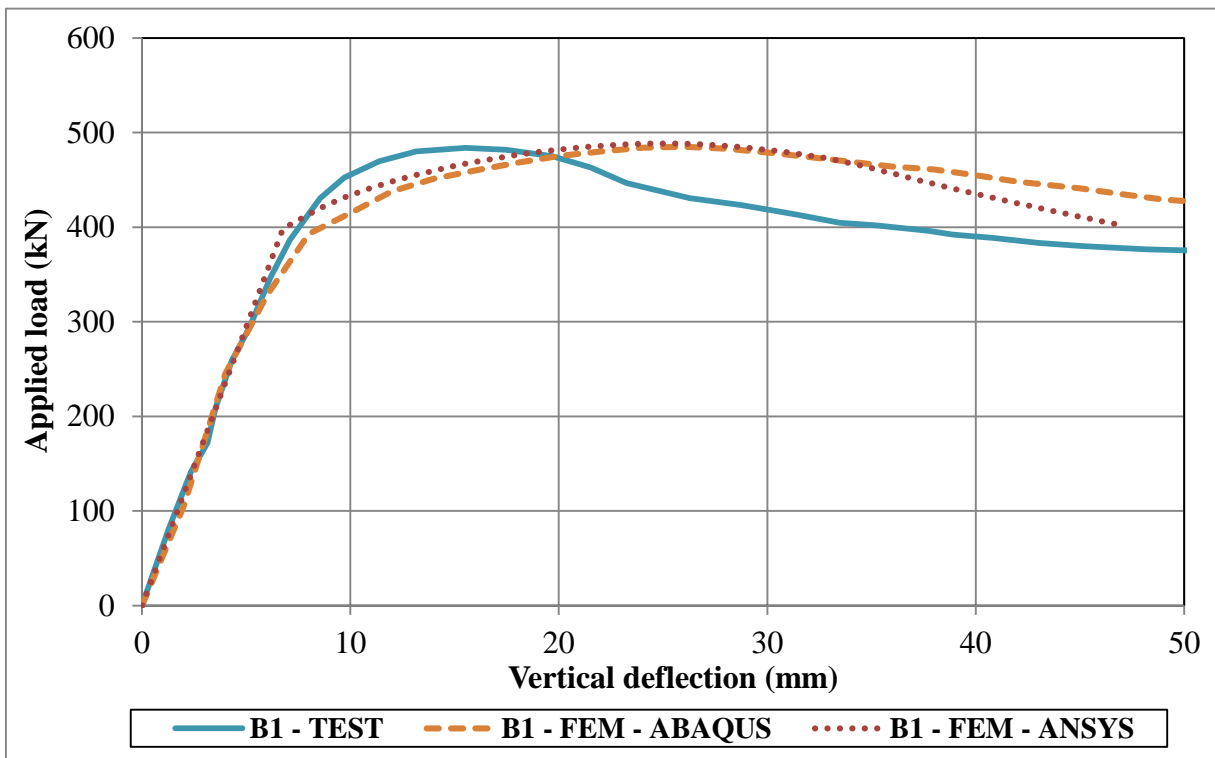
TEST B1: cross-section B – 450 °C
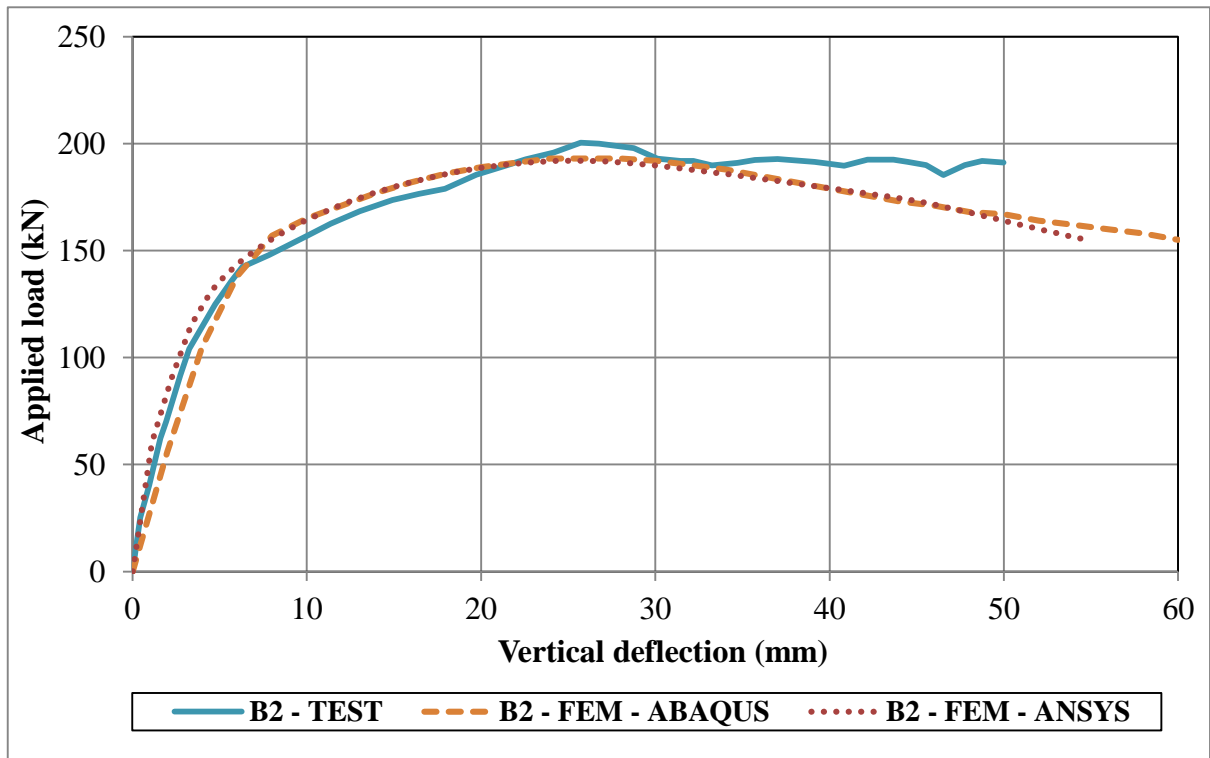
Cross-section B – 650 °C

Figure 38: Applied load (kN) in function of the vertical deflection (mm) for each tested beam – comparison between fire tests and simulations

Test number	Failure load (kN) and relative difference (%)				
	TEST	ABAQUS	Difference	ANSYS	Difference
A1	637.82	643.27	0.85	648.27	1.61
A2	230.61	226.36	1.84	243.32	5.22
B1	484.68	484.58	0.02	488.37	0.76
B2	201.22	193.29	3.94	192.02	4.57

Table 18: Comparison between numerical and experimental results

Another feature to be checked with the numerical models is the failure mode because the validity of the numerical models is also in relation to their capability of predicting correctly the local buckling. In order to do so, the deformed shapes of the four beams from both tests and the numerical simulations are shown together in figures 39 to 42.

Test
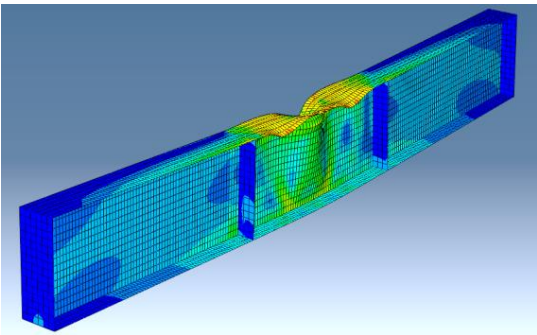
ABAQUS
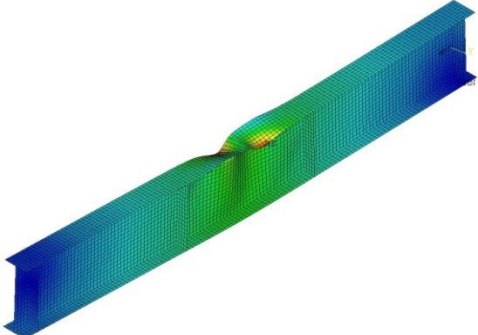
ANSYS

Figure 39: Beam A at 450 °C - deformed shape of beam for both test and simulation
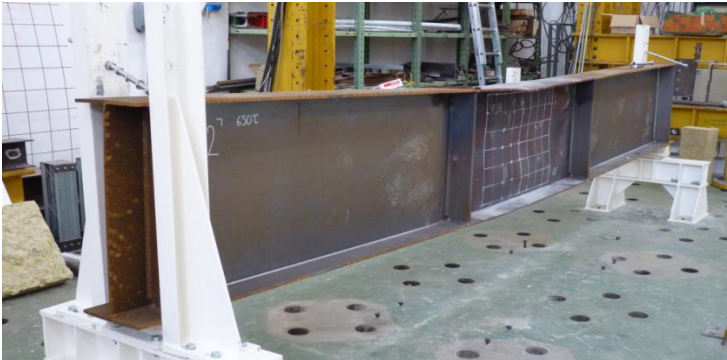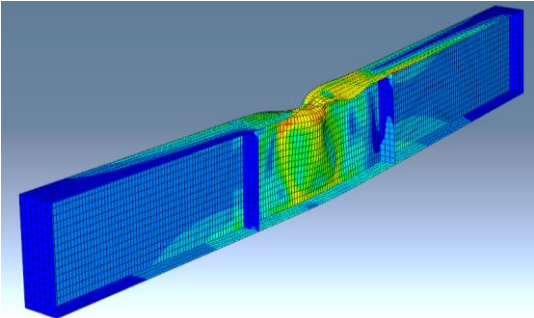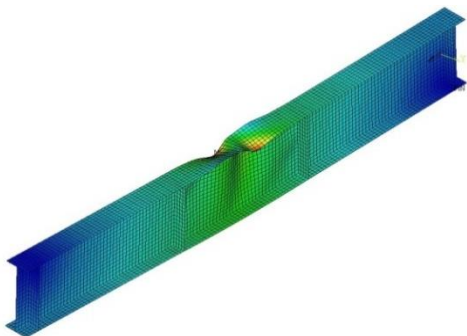
Test

ABAQUS

ANSYS

Figure 40 : Beam A at 650 °C - deformed shape of beam for both test and simulation
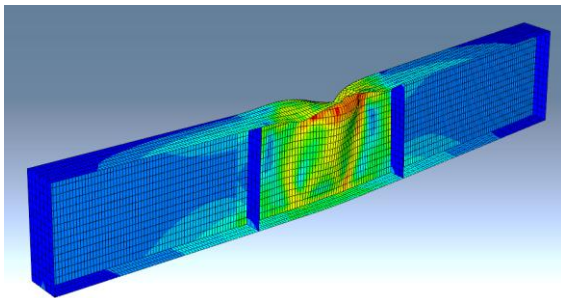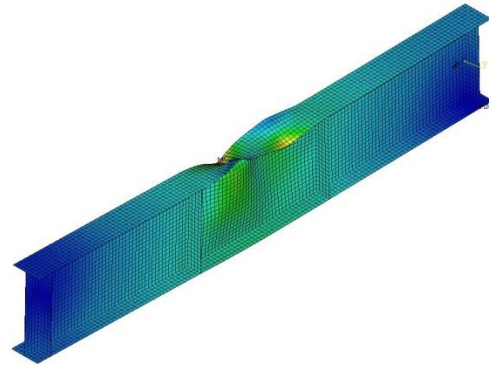
Test

ABAQUS

ANSYS

Figure 41: Beam B at 450 °C - deformed shape of beam for both test and simulation
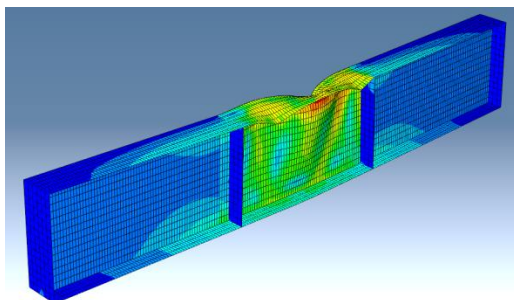
Test

ABAQUS
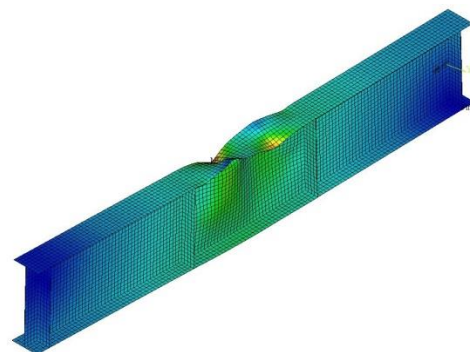
ANSYS

Figure 42: Beam B at 650 °C - deformed shape of beam for both test and simulation

It can be found easily that, for both numerical simulations and fire tests, the collapse of the beams is due to the local buckling of the upper flange and the web, both of them submitted to compression. Furthermore, the buckling modes predicted by means of the numerical models are all close to those of the tested beams. From this point of view, the reliability of the numerical models is convincing.

The comparison between the numerical and experimental results has provided a very good idea about the validity of the numerical models as well as the assumptions adopted for various parameters. In fact, the difference between tests and the numerical simulations remains lower than 6% in terms of load-bearing capacity. Furthermore, the initial stiffness is quite well established by the numerical analysis and the failure modes are precisely predicted. As a conclusion, the developed numerical modelling is validated and can be used with confidence in the numerical parametric studies to enlarge the investigation field of the fire behaviour of I or H shape class 4 cross-section steel beams under simple bending.

2.2.2.2   General principles of simple design rules

According to EN 1993-1-2, the pure bending moment resistance, $M_{fi,\theta,Rd}$ of a steel member with its cross-section in class 1,2 or 3 at a uniform temperature θ can be determined on the basis of the following expression:

$$M_{fi,\theta,Rd} = k_{y,\theta} \left[\frac{\gamma_{M,0}}{\gamma_{M,fi}}\right] M_{Rd} \tag{1}$$

Where $k_{y,\theta}$ is the reduction factor of the yield strength of steel at temperature θ, $\gamma_{M,fi}$ is the partial factor of steel for the fire situation.

In the case of class 4 cross-section steel members, the previous formula becomes:

$$M_{fi,\theta,Rd} = k_{0.2p,\theta} \left[\frac{\gamma_{M,0}}{\gamma_{M,fi}}\right] M_{Rd} \tag{2}$$

The previously cited different reduction factors are illustrated in Figure 43 and are available in EN 1993-1-2 [1]:
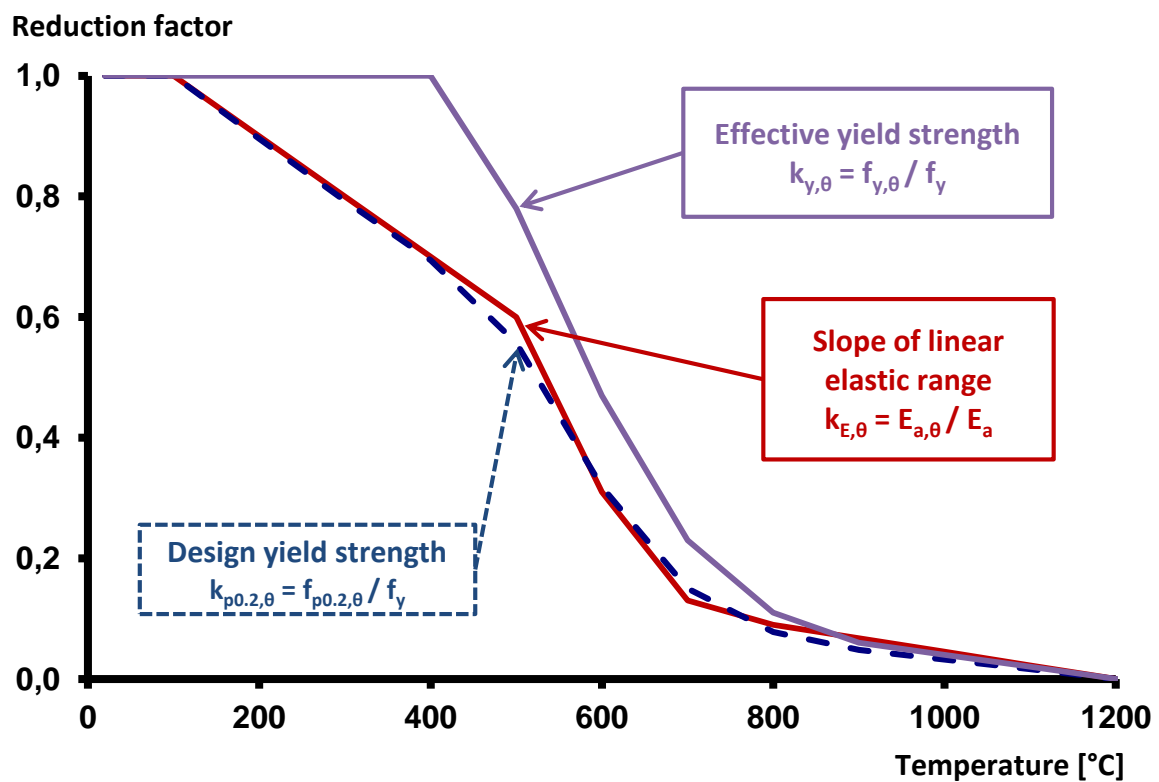
Figure 43: Reduction factors for the stress-strain relationship of hot-rolled class 4 steel sections at elevated temperatures

The bending resistance moment in fire conditions $M_{fi,Rd}$ of a cross-section is determined with the following expressions in function of its class:

$$M_{fi,\theta,Rd} = M_{fi,pl,Rd} = \frac{k_{y,\theta} W_{pl} f_y}{\gamma_{M,0}} \qquad \text{for class 1 or class 2 cross-sections} \qquad (3)$$

$$M_{fi,\theta,Rd} = M_{fi,el,Rd} = \frac{k_{y,\theta} W_{el} f_y}{\gamma_{M,0}} \qquad \text{for class 3 cross-sections} \qquad (4)$$

$$M_{fi,\theta,Rd} = M_{fi,eff,Rd} = \frac{k_{0.2p,\theta} W_{eff} f_y}{\gamma_{M,0}} \qquad \text{for class 4 cross-sections} \qquad (5)$$

With a small simplification and as $\gamma_{M,fi}$ is usually equal to 1 in fire conditions, the following equation is obtained for class 4 cross-sections:

$$M_{fi,\theta,Rd} = k_{0.2p,\theta} W_{eff} f_y \qquad (6)$$

Where W_{eff} is the effective section modulus of the section.

It can be found easily that the design moment resistance in fire conditions for steel members with class 4 cross-sections is determined in different way than other classes with the use of the reduction factor $k_{0.2p,\theta}$ and the effective section modulus W_{eff}.

Figure 44 illustrates the evolution of the design bending resistance of steel members in function of the slenderness of their plates and so the class of these plates:
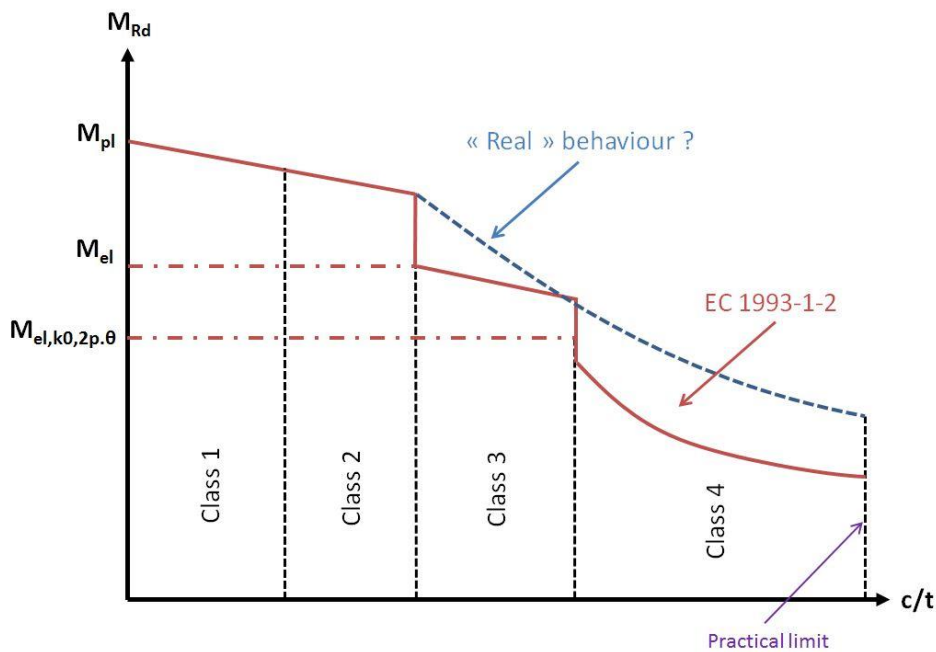
Figure 44: Evolution of the moment resistant in function of the slenderness

One can observe two discontinuities with the design bending resistance. The first noticeable decrease in resistance occurs at the boundary between class 2 and class 3. This is due to the use of the elastic section modulus instead of the plastic section modulus. This issue is not investigated in the context of this project. A second jump in the resistance of the member occurs in the transition from class 3 to class 4 cross-sections. This phenomenon is induced with the use of the reduction factor $k_{0.2p,\theta}$ in case of class 4 cross-sections instead of the reduction factor $k_{y,\theta}$ for lower classes. From a mechanical aspect, the variation of the resistance in function of the slenderness shall be continuous and this discontinuity is purely artificial because of the inappropriateness of current design rules.

2.2.2.3 Comparisons of the numerical results with the current simple method of Eurocode

Each case of the numerical parametric study was compared with the values given by the current simple design rules of Eurocode 3 for fire situation. In figure 45 to 48, M_{Rd} ANSYS represents the moment resistance obtained with the finite elements numerical analysis whereas M_{Rd} EN1993-1-2 represents the moment resistance predicted with current simple design rules of EN 1993-1-2. The points located above the diagonal line mean that the simple design rules lead to more important bending resistance than FEM numerical analysis, so on the unsafe side and the opposite means that the simple design rules predict safe and sometimes really non-economic results compared to FEM numerical analysis.

From the comparison, it can be found that the discrepancy is quite important between the numerical analysis and simple design rules. In fact, simple design rules can give safe results and lead to very conservative design as they can be unsafe with largely overestimated bending moment resistance.

However, these differences depend also on how the cross-sections at the border between class 3 and class 4 are dealt with. In fact, it is possible to design these cross-sections with the rules for either class 3 or class 4 steel members, which is another way to show the problem of the simple design method which provides discontinuity of the bending moment resistance. For room temperature design, new limits were proposed to separate class 3 from class 4 cross-sections. However, these new limits have proven to be inadequate for fire temperature conditions. Furthermore, the explicit boundary values given for these limits won't solve the design problem for cross-sections around this limit (discontinuity between class 3 and class 4). From scientific point of view, the optimal solution for both room temperature and fire temperature designs would be to set a continuous behaviour of cross-sectional resistance in function of the slenderness in order to overcome the problem induced by the current artificial boundaries. For example, Figure 45 shows the comparison results if the steel members are designed as class 3 ones:
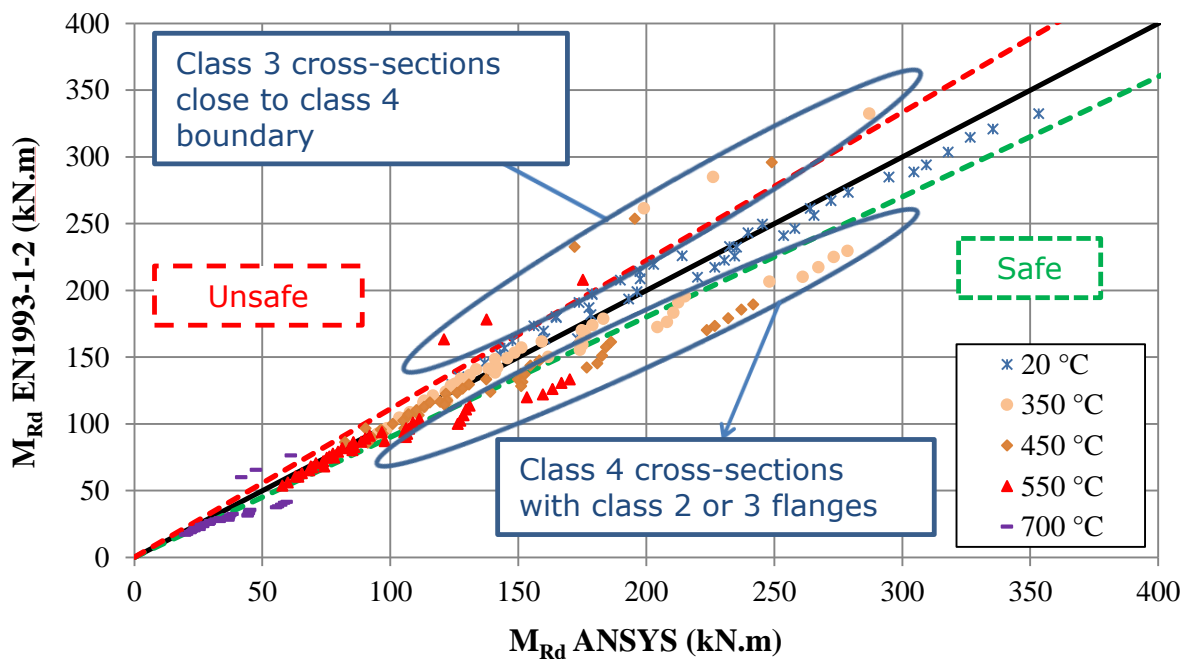
Figure 45: Comparison between numerical analysis and simple design rules for bending moment resistance
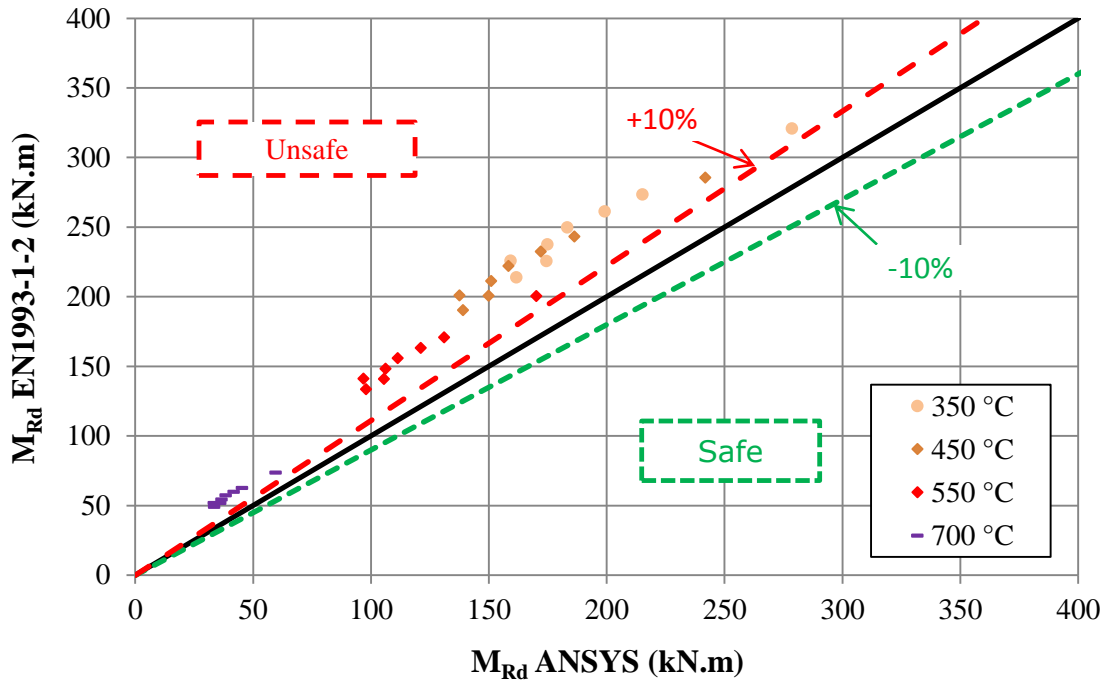
Figure 46: Comparison between numerical analysis and class 3 simple design rules for steel members at the border between class 3 and class 4

This figure shows clearly that with this design assumption, the simple design method overestimates the bending moment resistance of these steel members. On the other hand, these members can also be considered as class 4 members. In this case, Figure 47 shows the comparisons with the numerical results:
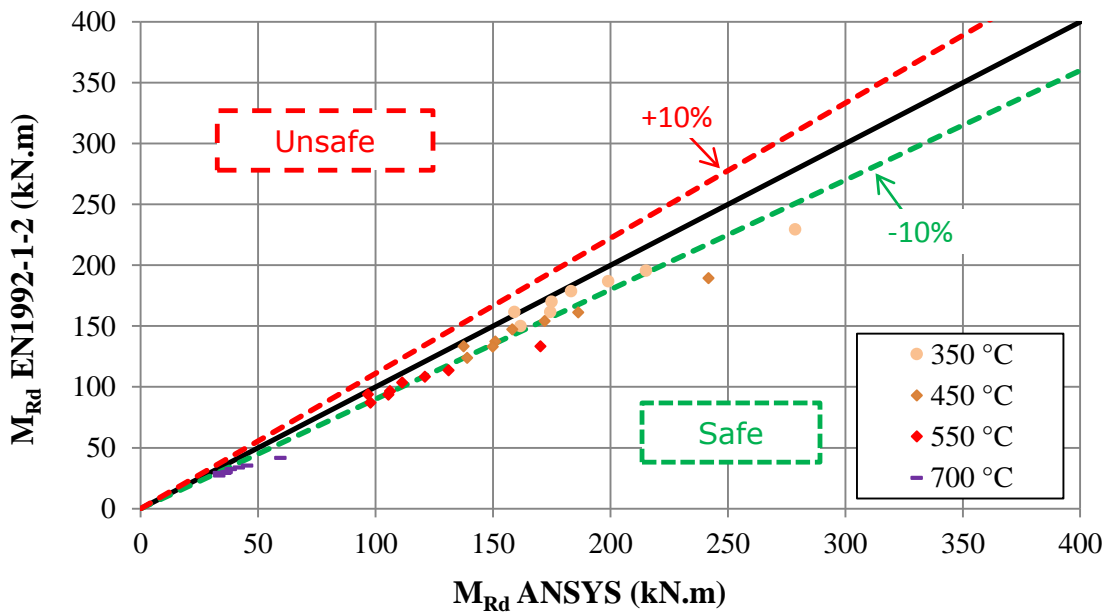
Figure 47: Comparison between numerical analysis and class 4 simple design rules for steel members at the border between class 3 and class 4

Unlike the previous results, this comparison shows less discrepancy but a small underestimation of the bending moment resistance can be observed for some cases. Moreover, both graphs illustrate an important discrepancy between the simple design method and the numerical analysis because the difference is beyond the 10% limit which is considered as the acceptable scatter for the development of simple design rules in fire situation.
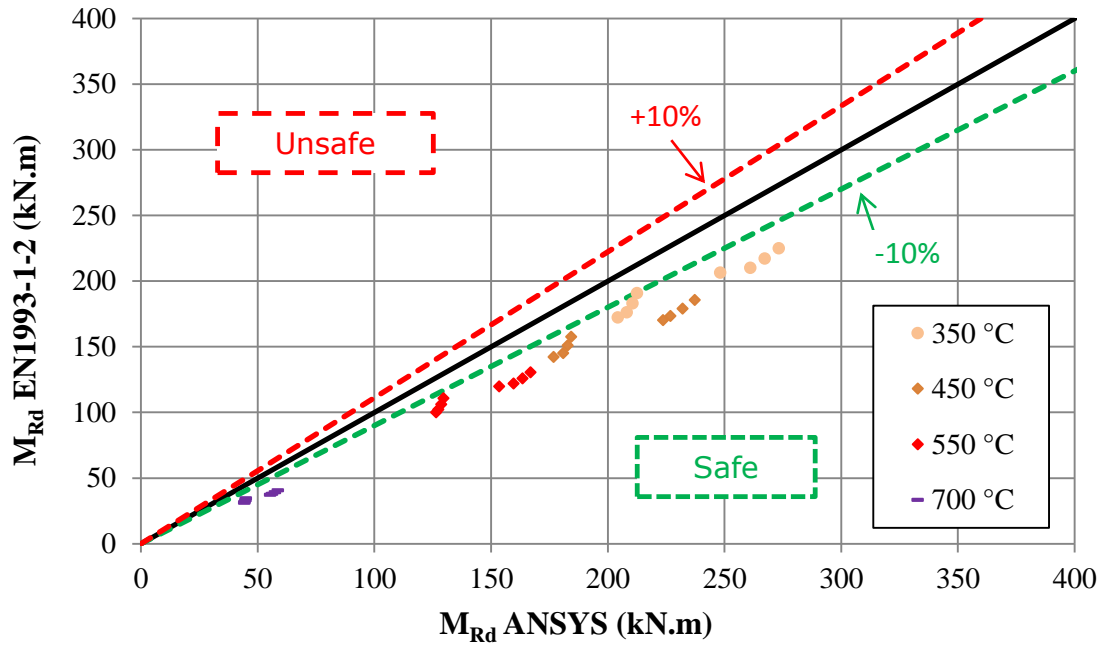
Figure 48: Comparison between numerical analysis and class 4 simple design rules for class 4 steel members with flanges in class 2 or 3

Last but not least, Figure 49 shows more comparisons from which it can be found that the current simple design rules underestimate the bending moment resistance of class 4 beams but with flanges in class 2 or 3.

In fact, if flanges are in class 2 or 3, they can be submitted to a compressive strain more than that corresponding to the strength of $f_{0,2p.\theta}$ without the local buckling. However, since the web is in class 4, the whole cross-section is considered also as class 4 and in this case, its bending moment resistance has to be calculated on the basis of $f_{0,2p.\theta}$ which leads to the underestimated bending moment resistance. The following picture with the deformed shape of a class 4 cross-section with class 2 flanges predicted by the numerical model shows clearly this phenomenon. It can be noted easily that the local buckling occurs only in the web:
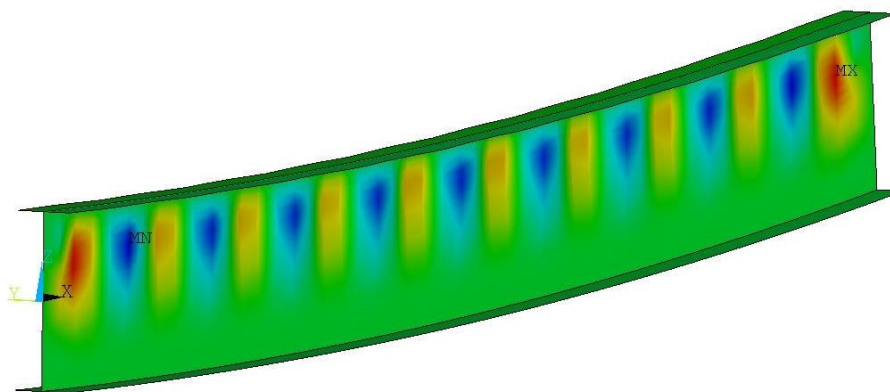
Figure 49: Deformed shape of a class 4 cross-section with class 2 flanges

On the other side, if flanges are in class 4, their local buckling will occur either before or together with that of web, see Figure 50:

Buckling of the flange in compression

Buckling of both flange and web in compression
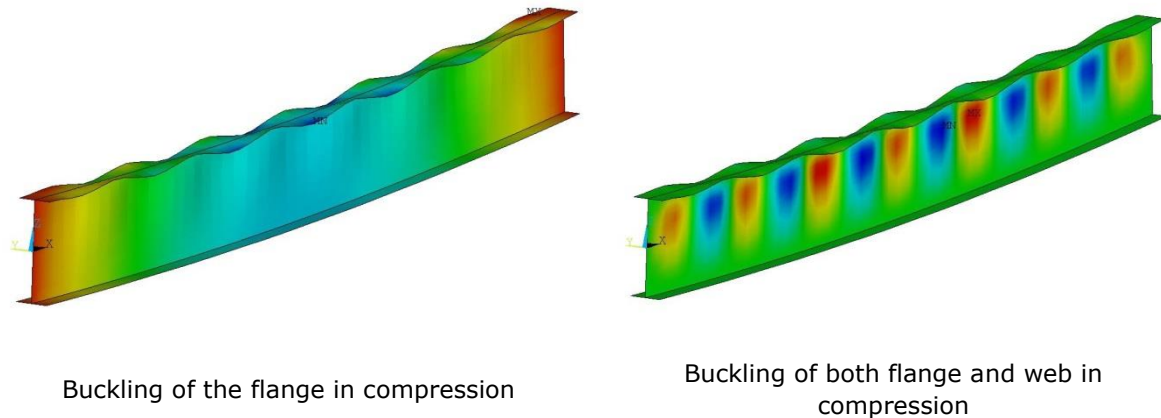
Figure 50: Collapse of a class 4 cross-section with class 4 flanges

It is necessary to point out that all the previously described behaviours remain also valid for all other investigated cross-sections as well as the steel grade S460.

Following general conclusions can be derived from the correlation analysis of current simple design rules of EN1993 with respect to the bending moment resistance of class 4 steel members in fire situation:

- The discrepancy between the simple design rules and the numerical analysis is quite important, regardless of the cross-section size and temperature levels;
- The simple design rules underestimate the bending moment resistance of class 4 steel members with the flanges in class 2 or class 3. In these cases, the design rules are too conservative;
- For steel members at the border between class 3 and class 4, the jump in terms of bending moment resistance according to simple design rules is not physical at all;
- In case of class 4 steel members with both flanges and web in class 4, the results given by the simple design rules and those given by the numerical analysis are close each other.

As a result of above observations, an alternative solution to the current simple design rules of the EN 1993-1-2 for the bending moment resistance of class 4 and also class 3 steel members was developed in order to improve the accuracy of current simple design rules.

2.2.2.4 New proposal for simple design rules and comparisons with numerical results

In the scope of this research project, a new solution for simple design method of class 4 steel members under simple bending in fire condition is developed on the basis of the Winter's formulation for the calculation of the ultimate strength of steel plates under compression. In order to facilitate the design work, in the scope of this project, has been developed a simplified version of the method proposed by the University of Aveiro by P. VILA REAL, N. LOPES and C. COUTO of which the full description is provided in [18] and [24].

The key points of this new method are:

- the design strength of steel at elevated temperatures is $f_{y,\theta}$ whatever the class of the steel member is;
- the effective cross-section of thin wall steel members is determined on the basis of the wall slenderness instead of using the class of cross-sections.

The first point permits to keep the same design strength for steel at elevated temperatures which simplify the design rules and the one will guarantee a continuous resistance evolution with respect to slenderness of cross-section walls. For the latter, following relations are proposed for effective length of walls in compression:

- In the case of internal components (web in bending):

$$\rho = \frac{\left(\bar{\lambda}_p + 0.9 - \frac{0.26}{\varepsilon}\right)^{1.5} - 0.055(3 + \psi)}{\left(\bar{\lambda}_p + 0.9 - \frac{0.26}{\varepsilon}\right)^{3}} \le 1.0 \tag{7}$$

- And in the case of outstand elements (flange under compression):

$$\rho = \frac{\left(\bar{\lambda}_p + 1.1 - \frac{0.52}{\varepsilon}\right)^{1.2} - 0.188}{\left(\bar{\lambda}_p + 1.1 - \frac{0.52}{\varepsilon}\right)^{2.4}} \le 1.0 \tag{8}$$

Above two relations are the simplified version of the full proposal ([18] and [24]) which originally gives the following relations. The simplification consists in setting the temperature parameter θ to a fixed value of 450 °C. This simplification greatly facilitates the use of the design rules with a negligible loss of accuracy:

- In the case of internal components (web in bending):

$$\rho = \frac{\left(\bar{\lambda}_p + \alpha_\theta\right)^{\beta_\theta} - 0.055(3 + \psi)}{\left(\bar{\lambda}_p + \alpha_\theta\right)^{2\beta_\theta}} \le 1.0 \tag{9}$$

In which:

$$\alpha_\theta = 0.9 - 0.315\frac{k_{0.2p,\theta}}{\varepsilon_\theta k_{y,\theta}} \quad and \quad \beta_\theta = 2.3 - 1.1\frac{k_{0.2p,\theta}}{k_{y,\theta}} \tag{10}$$

- And in the case of outstand elements (flange under compression):

$$\rho = \frac{\left(\bar{\lambda}_p + \alpha_\theta\right)^{\beta_\theta} - 0.188}{\left(\bar{\lambda}_p + \alpha_\theta\right)^{2\beta_\theta}} \le 1.0 \tag{11}$$

In which:

$$\alpha_\theta = 1.1 - 0.63\frac{k_{0.2p,\theta}}{\varepsilon_\theta k_{y,\theta}} \quad and \quad \beta_\theta = 2 - 1.1\frac{k_{0.2p,\theta}}{k_{y,\theta}} \tag{12}$$

In previous equations:

$$\varepsilon_\theta = 0.85\varepsilon = 0.85\sqrt{\frac{235}{f_y}} \tag{13}$$

53

Where $\bar{\lambda}_p$ represents the normalised slenderness at room temperature and is given by the following equation:

$$\bar{\lambda}_p = \sqrt{\frac{f_y}{\sigma_{cr}}} = \frac{b}{28.4\varepsilon\sqrt{k_\sigma}} \tag{14}$$

Where f_y is the yield strength and σ_{cr} is the Euler's critical stress and is the width of the plate, t its thickness, ε is the factor depending on f_y and k_σ the buckling factor corresponding to the stress ratio and to the boundary conditions.

$$\varepsilon = \sqrt{\frac{235}{f_y}} \tag{15}$$

Once the effective cross-section is determined with above relations, the bending moment resistance of the concerned steel member can be determined as follows:

$$M_{fi,\theta,Rd} = k_{y,\theta} W_{eff} f_y \tag{16}$$

According to this new design rule, only the relative slenderness $\bar{\lambda}_p$, the coefficient relative to stress distribution state over the length of the wall ψ and ε are necessary to determine the effective width of the wall.

Once again, the results in terms of bending moment resistance obtained with these new relations for effective width of thin walls are systematically compared with the results of numerical analysis in order to show the accuracy of these modified simple design rules:
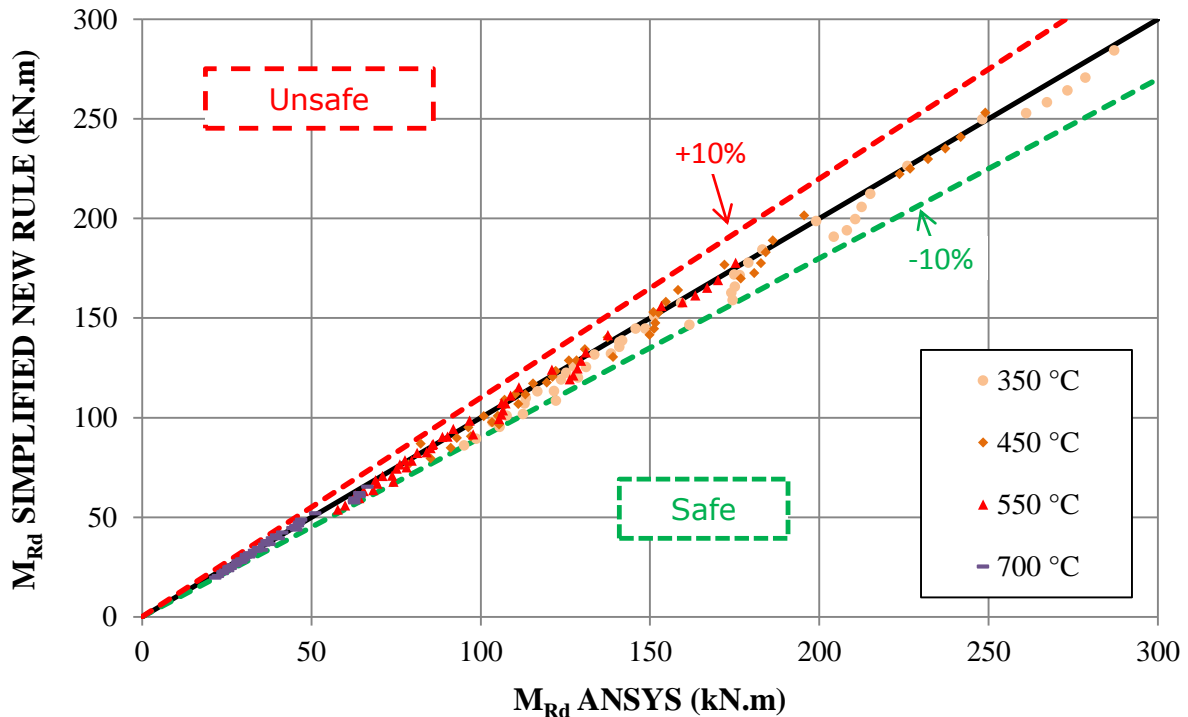
Figure 51: Comparison between numerical analysis and modified new simple design rule for bending moment resistance for steel grade S355
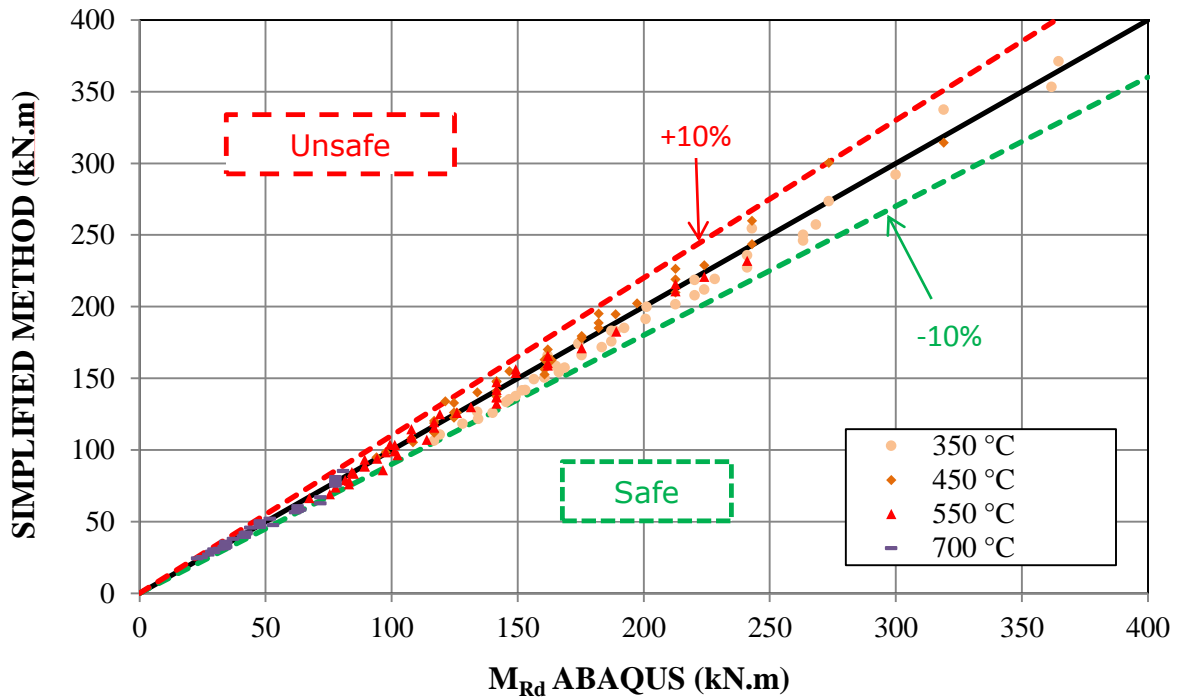
Figure 52: Comparison between numerical analysis and modified new simple design rule for bending moment resistance for steel grade S460

The statistical results derived from the comparisons between the numerical analysis and different design rules, that is EN 1993-1-2 and new proposed design rules in the scope of current project are given in Table 19.

It can be seen that the correlation between the new proposed simple design rules and the numerical analysis is fully satisfactory and the accuracy compared to current design rules of EN1993-1-2 is largely improved. Moreover, the average scatter of these simple design rules tends to be on the safe side compared to the numerical results obtained with advanced calculation models.

	EN 1993-1-2	NEW DESIGN RULES
Average ratio (design rule / FEM)	0.86	0.98
Percentage of unsafe points (%)	16.3	33.6
Maximum unsafe ratio	1.37	1.13
Percentage of safe points by more than 15% (%)	5.1	0
Standard deviation	0.15	0.05
Coefficient of variation	0.17	0.05

Table 19: Statistical results for the simple design rules relative to cross-sectional resistance

2.2.3 WP3 - Lateral torsional buckling of class 4 beams under bending

2.2.3.1 Experimental investigation

The four tests at elevated temperatures differ in the cross-sections and in the adopted heating level. Table 20 describes the main parameters of each test. Three beams with constant cross-section and one with variable cross-section (height of the web varies linearly from one end to another) are considered. The temperature is chosen based on the most significant changes of plate slenderness calculated using the elevated temperature reduction factors. The classification and plate slenderness is done according to EN 1993-1-2 [1].

Test number	Web	Flange	Temperature (°C)
Test 1 / Test 2 **IW460/150/4/5**	Class 4 $\bar{\lambda}_P = 1.33$	Class 4 $\bar{\lambda}_P = 1.13$	450 / 650
Test 3 **IW460/150/4/7**	Class 4 $\bar{\lambda}_P = 1.23$	Class 3 $\bar{\lambda}_P = 0.81$	450
Test 4 **IW585-495/150/4/5**	Class 4 $\bar{\lambda}_P \in [1.45\,;1.76]$	Class 4 $\bar{\lambda}_P = 1.13$	650

Table 20: Tested cross-sections

Figure 53 illustrates the experimentally tested beams:

a)

b)

c)
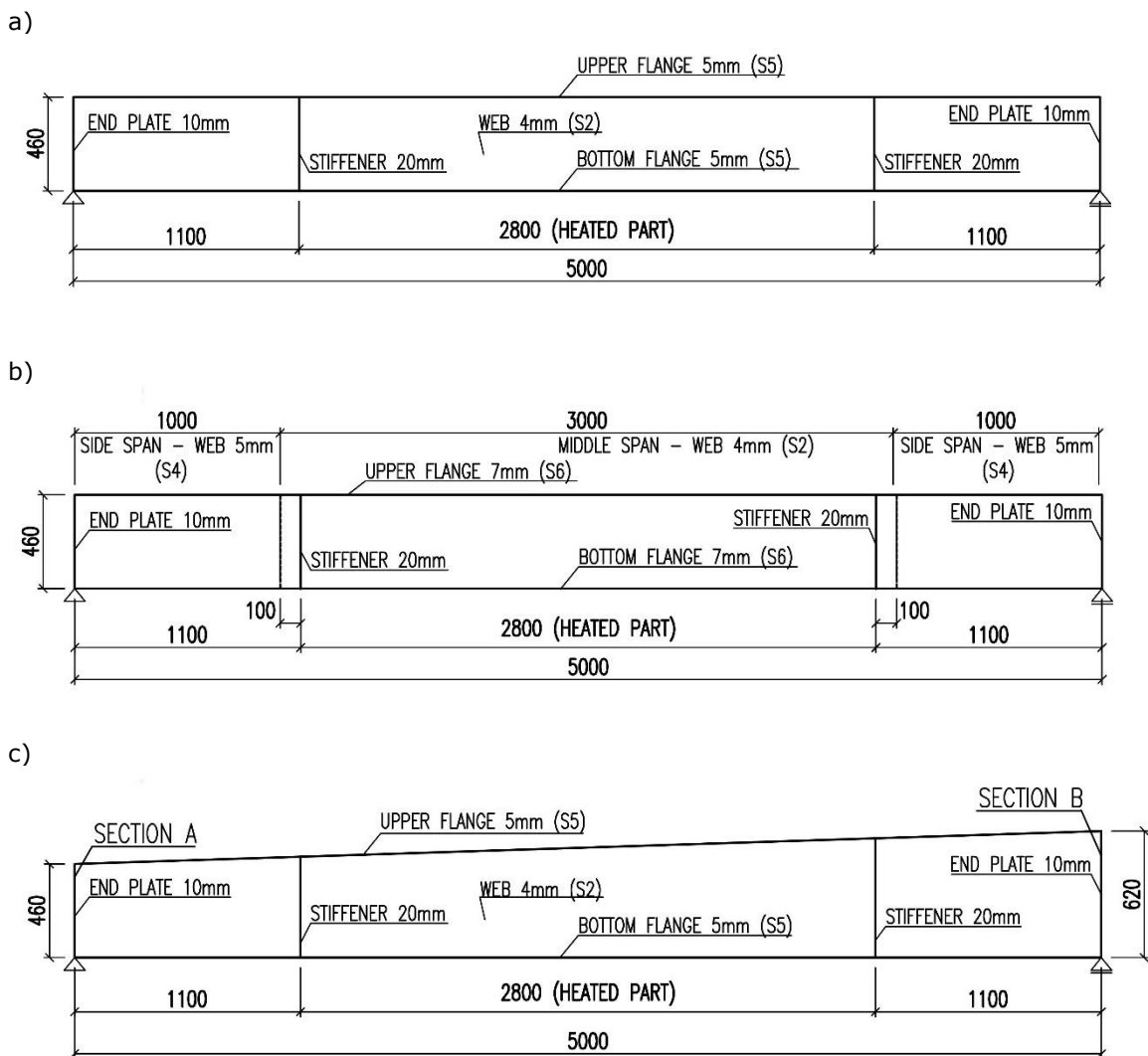
Figure 53: Tested beams: a) tests 1 & 2, b) test 3, c) test 4

The experiment consists of a simply supported beam with two equal concentrated point loads applied symmetrically. The heated central part of the beam where the temperature is aimed to be uniform is therefore subjected to a uniform bending moment. The fire tests are performed on steady state, the beam is heated in a first time and then the loads are applied until failure. The tests are deflection-controlled which is estimated as 3.5 mm per minute. Final deformation at the end of experiments is 50 mm at mid-span of the beam. This procedure is the same for all three beams. Figure 54 shows the scheme of the experiment:
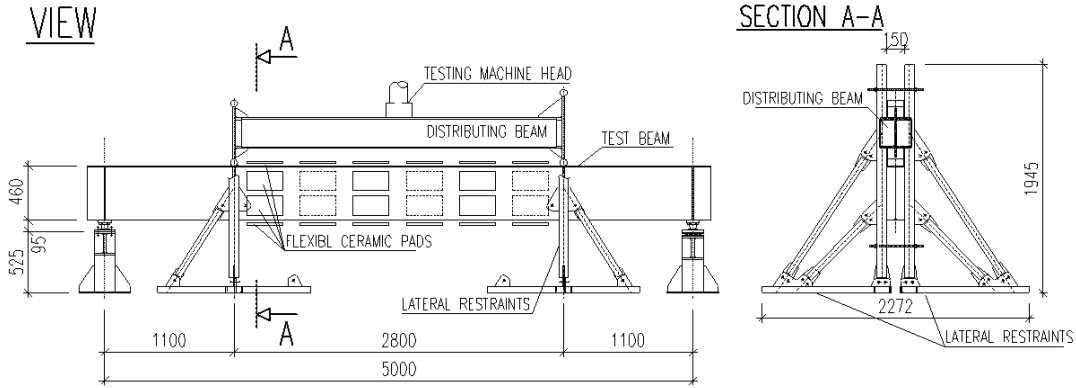
Figure 54: Scheme of the experiment and lateral restraints

The end supports are considered just by one point support. It is made using a high-quality steel sphere bearing placed between two steel plates. Both end supports allow free torsion of the end cross-section. The first one restrains the displacement in all directions. The second allows also free horizontal displacement in the direction along the beam axis.

The load is introduced via a distributing beam at the edges of the heated (central) part. Free rotation and transverse deflection is allowed between these points. The load is applied by means of one hydraulic jack of 650 kN capacity.
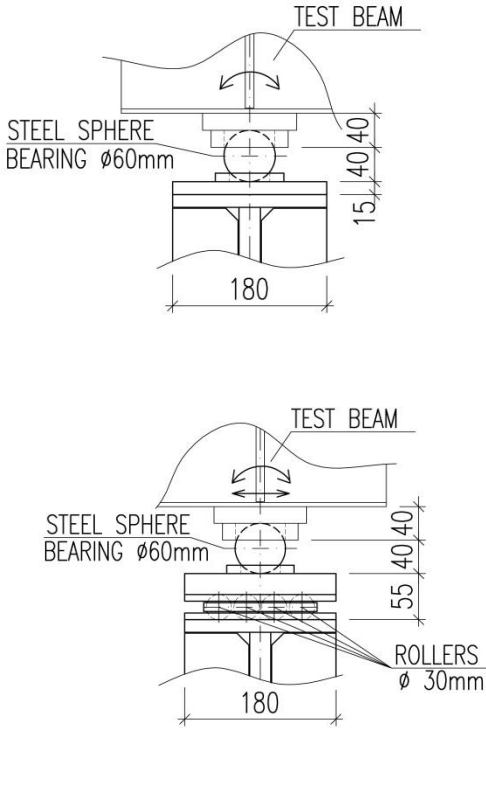
a)
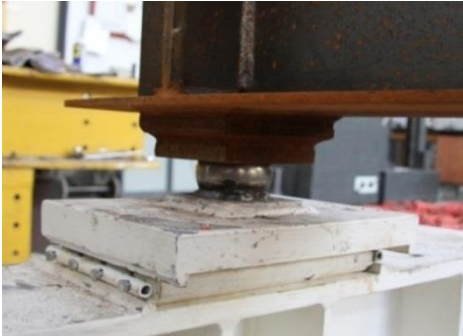
b)

Figure 55: Pinned point supports: a) fixed; b) free

The maximum amplitudes of imperfections of all tested beams are summarized in Table 21:

Test number	Local imperfection (mm)		Global imperfection (mm)
	Web	Flange	
Test 1 IW460/150/4/5	7.36	2.27	2.5
Test 2 IW460/150/4/5	6.24	1.96	1.0
Test 3 IW460/150/4/7	5.80	0.69	1.5
Test 4 IW585-495/150/4/5	7.59	2.13	1.5

Table 21: Amplitude of initial imperfections

The recorded load-deflection curves of all above beam tests are shown together from Figure 56 to Figure 59 and the failure modes of these beams are shown later in the next part. There were some difficulties observed for some of the tests which are described later.
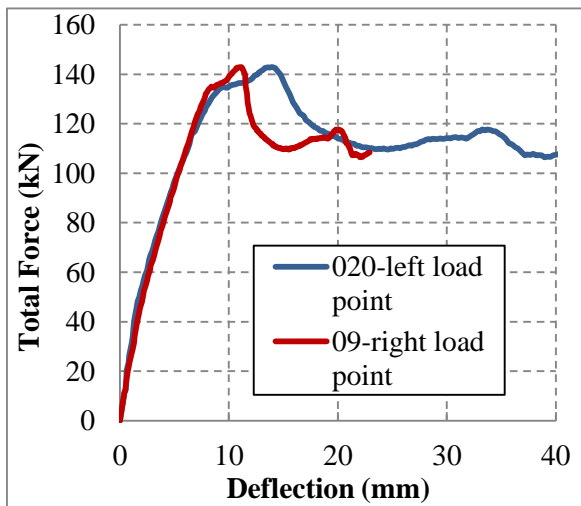
Figure 56: Vertical deflections of bottom flange at the load points (test 1)
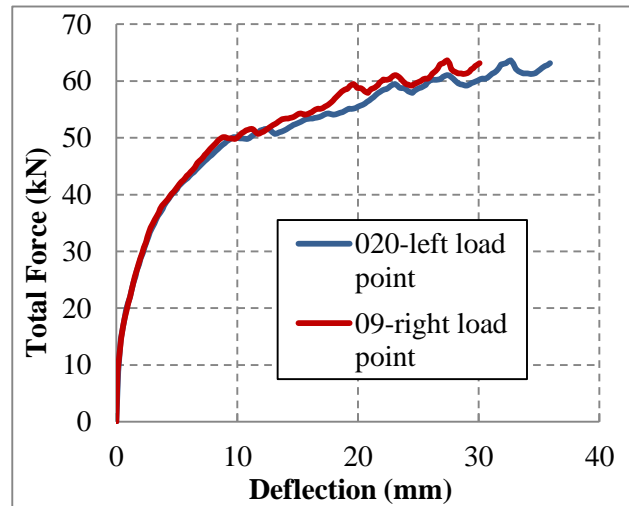
Figure 57: Vertical deflections of bottom flange at the load points (test 2)
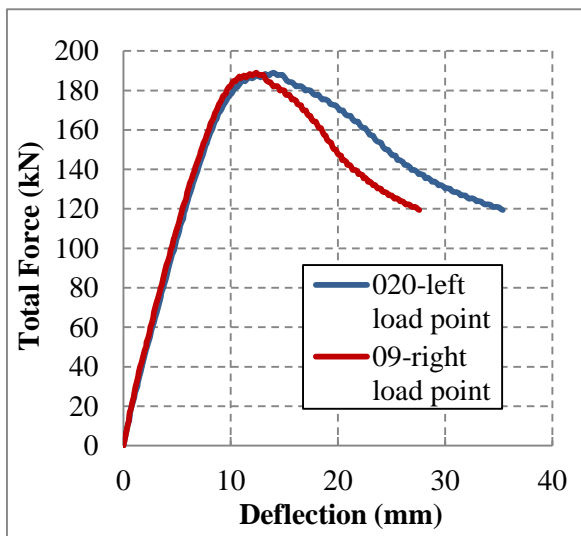
Figure 58: Vertical deflections of bottom flange at the load points (test 3)
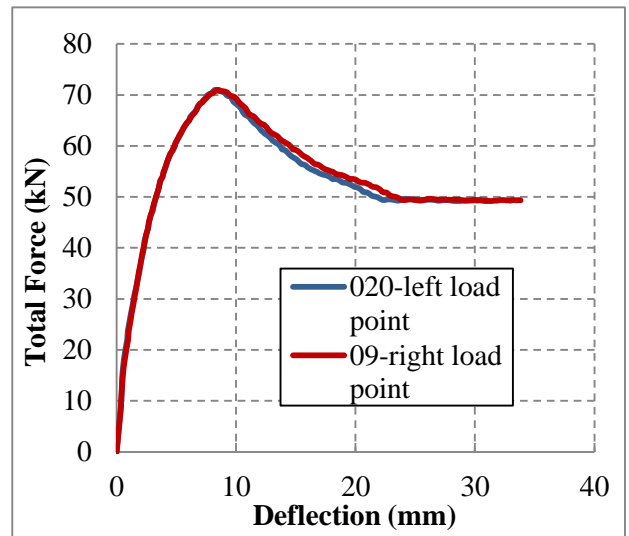
Figure 59: Vertical deflections of bottom flange at the load points (test 4)

The simulations conducted in order to be compared with the experimental fire tests are static simulations. The beam is meshed using quadrilateral conventional shell elements. These shell elements have three displacement and three rotational degrees of freedom at each node. They are fully integrated, general-purpose, finite-membrane-strain shell element. The element has four integration points. For definition of mesh size in ABAQUS model, six elements for flange width and twenty elements for web height are used. Along the beam, four elements are used each 100 mm. All experimental data are used to build the numerical model. The Eigen-modes obtained from a previous elastic buckling analysis are used as the initial geometric imperfection shape for the post-buckling analysis. Two imperfection shapes are considered for the beam: the first local buckling mode and the first global buckling mode (lateral torsional buckling). The imperfection amplitudes are based on the initial geometry measurement of the plates. The material law is defined by elastic-plastic nonlinear stress-strain diagram. The true material stress-strain relationship is calculated from the static engineering strass-strain curves obtained from the coupon tests. The reductions of material properties as well as the material nonlinearity are based on EN 1993-1-2. The average measured temperatures from each heated part of the beams are introduced to the model. Adjacent parts of the beam and stiffeners are considered at room temperature (20 °C).

The applied temperatures on beam of test 1 are listed in Table 22:

Part of beam	Temperature (°C)
Web	444.4
Bottom flange	354.0
Upper flange	456.7

Table 22: Temperatures applied on numerical model of test 1

The amplitudes of the imperfections taken into account are listed in Table 23 and the shapes of buckling modes used are illustrated in Figure 60:

Global imperfection (mm)	Local imperfection of upper flange (mm)	Global imperfection of flange (mm)
2.50	2.27	2.72

Table 23: Amplitude of imperfections
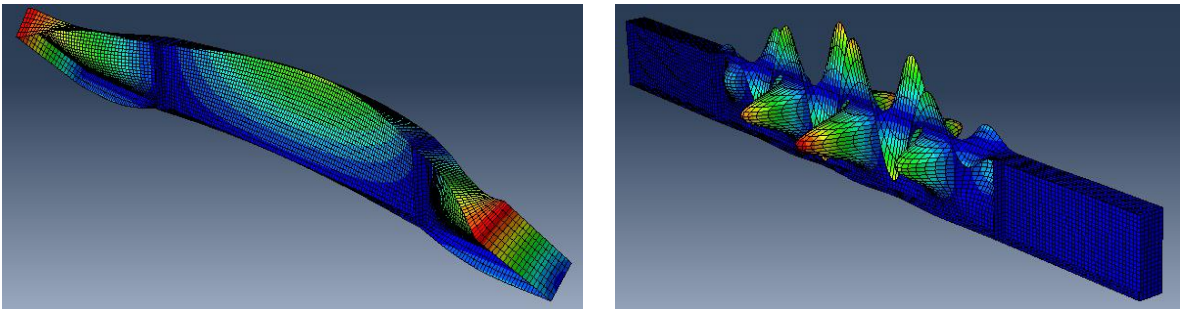
Figure 60: Mode shape from linear buckling analysis: left) lateral torsional buckling failure mode, right) local buckling failure mode

The next diagram of Figure 61 shows the comparison in terms of total applied force in function of deflection for both fire test and numerical analysis:
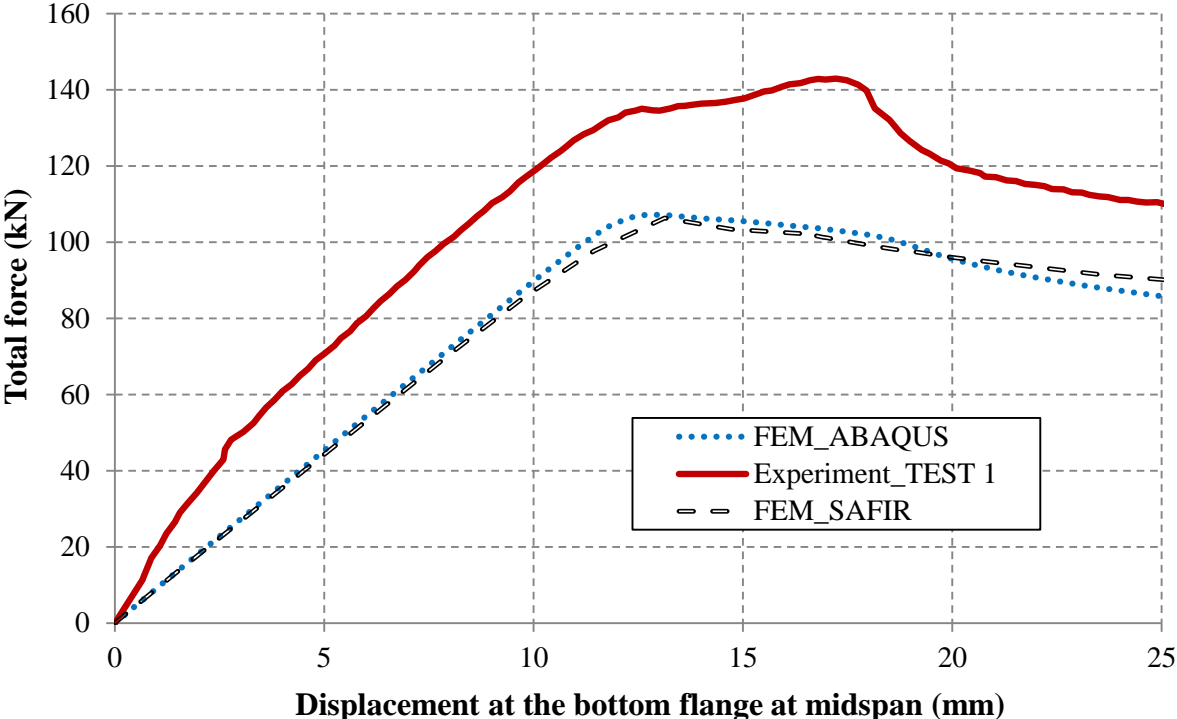
Figure 61: Numerical simulations against experimental fire test

Table 24 illustrates the comparison between the numerical simulation and experimental test in terms of ultimate load:

	Total force (kN)	Half-force (kN)	Ultimate bending moment (kN.m)
ABAQUS	107.2	53.60	58.80
SAFIR	106.3	53.15	58.42
Experiment	142.9	71.50	78.60

Table 24: Numerical simulation against experimental fire test

The Figure 62 illustrates the failure mode for both numerical simulation and experimental test:
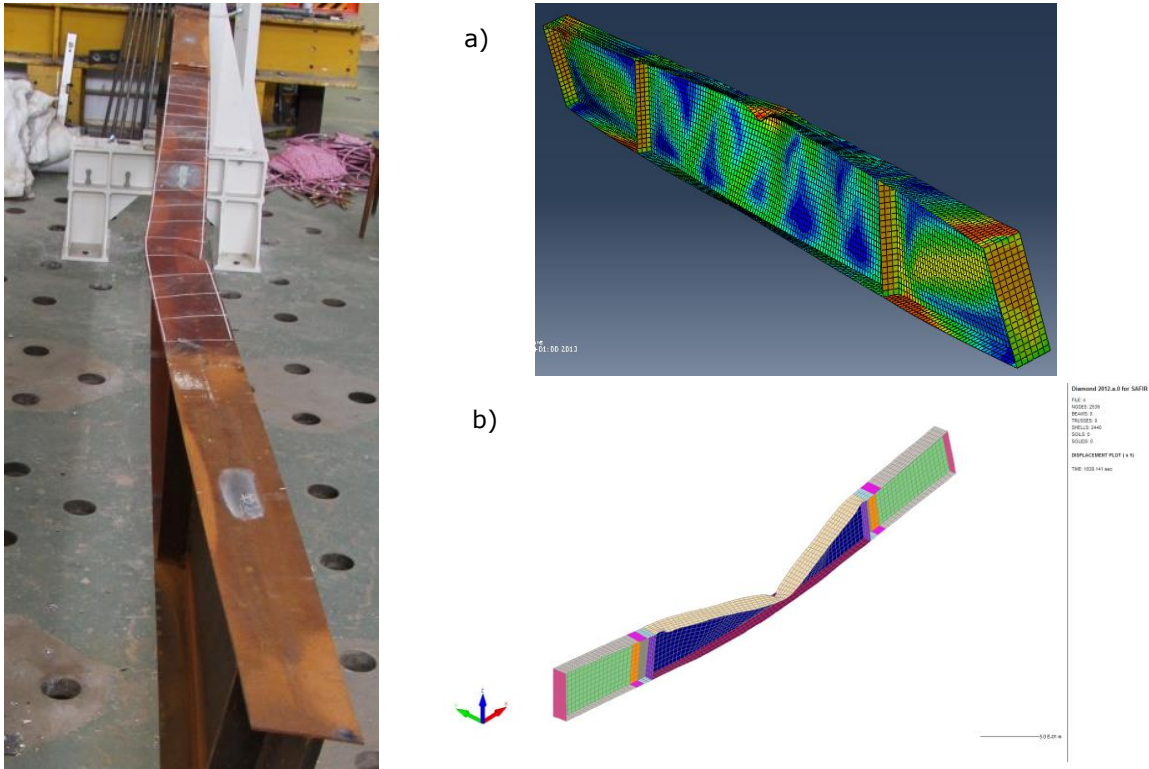
Figure 62: Failure mode shape for fire test and numerical simulation with: a) ABAQUS, b) SAFIR

The applied temperatures on beam of test 2 are listed in Table 25:

Part of beam	Temperature (°C)
Web	613.5
Bottom flange	486.3
Upper flange	651.7

Table 25: Temperatures applied on numerical model of test 2

The amplitudes of the imperfections taken into account are listed in Table 26 and the shapes of buckling modes used are illustrated in Figure 63:

Global imperfection (mm)	Local imperfection of upper flange (mm)	Global imperfection of flange (mm)
1.00	1.96	2.36

Table 26: Amplitude of imperfections
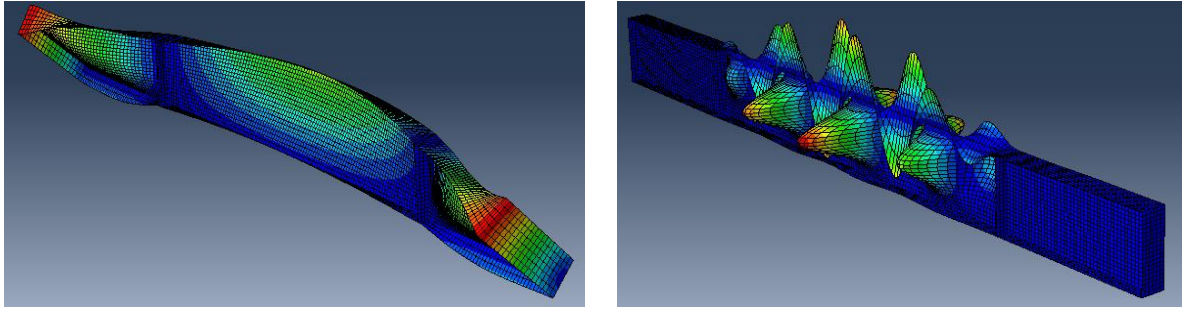
Figure 63: Mode shape from linear buckling analysis: *left) lateral torsional buckling failure mode, right) local buckling failure mode*

The next diagram of Figure 64 shows the comparison in terms of total applied force in function of deflection for both fire test and numerical analysis:
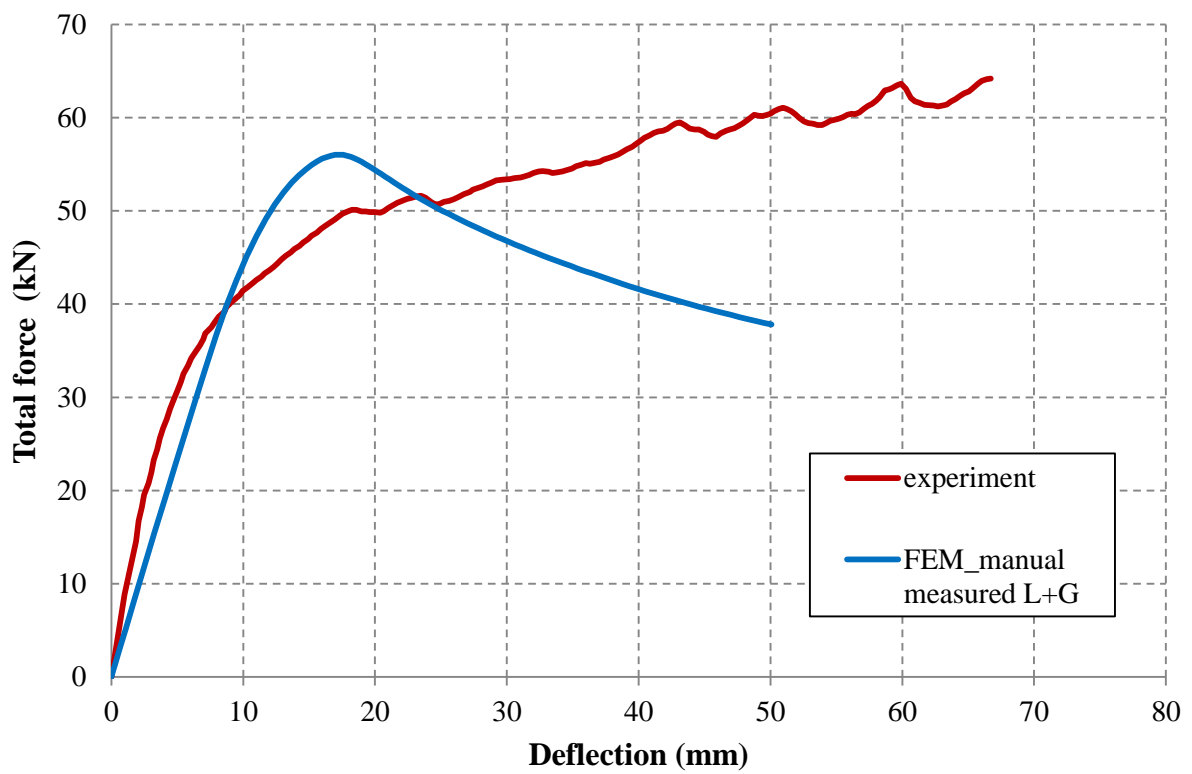
Figure 64: Numerical simulations against experimental fire test

Table 27 illustrates the ultimate load obtained in the numerical simulation (*):

	Total force (kN)	Half-force (kN)	Ultimate bending moment (kN.m)
ABAQUS	56.02	28.01	30.81

Table 27: Numerical simulation against experimental fire test

The Figure 65 illustrates the failure mode obtained with the help of numerical simulations:
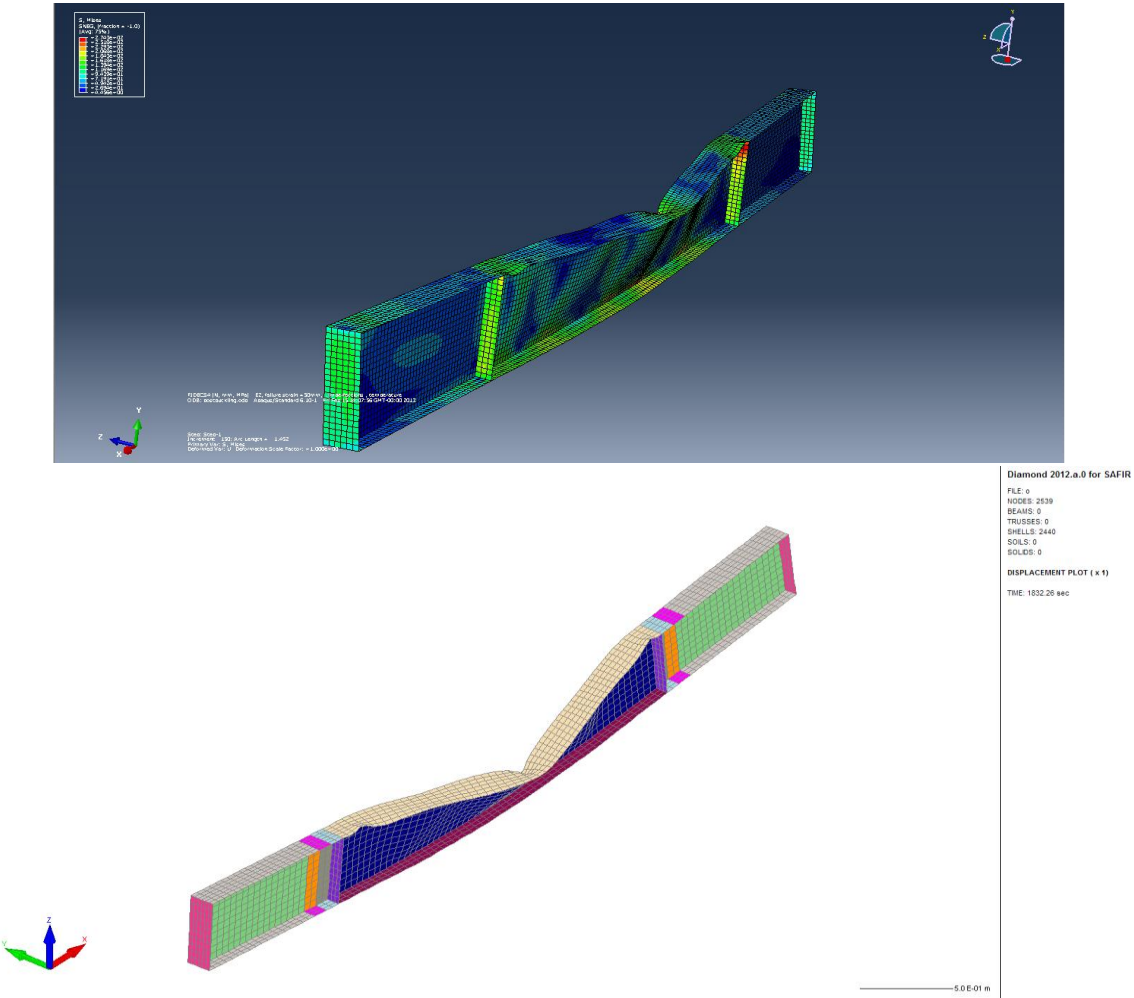
Figure 65: Failure mode obtained numerically with: a) ABAQUS, b) SAFIR

(*) Due to some problems which occurred on the lateral restraints, this test was not successful and the experimental results are not available. Figure 66 illustrates this issue:

Figure 66: Problem with lateral restraints during the second fire test

The applied temperatures on beam of test 3 are listed in Table 28:

Part of beam	Temperature (°C)
Web	443.2
Bottom flange	368.8
Upper flange	481.4

Table 28: Temperatures applied on numerical model of test 3

The amplitudes of the imperfections taken into account are listed in Table 29 and the shapes of buckling modes used are illustrated in Figure 67:

Global imperfection (mm)	Local imperfection of upper flange (mm)	Global imperfection of flange (mm)
1.50	0.69	2.65

Table 29: Amplitude of imperfections
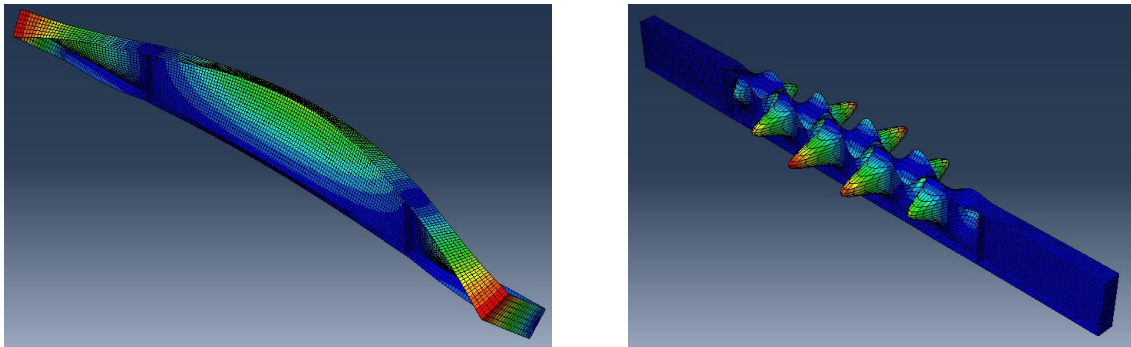
Figure 67: Mode shape from linear buckling analysis: *left) lateral torsional buckling failure mode, right) local buckling failure mode*

The next diagram of Figure 68 shows the comparison in terms of total applied force in function of deflection for both fire test and numerical analysis:
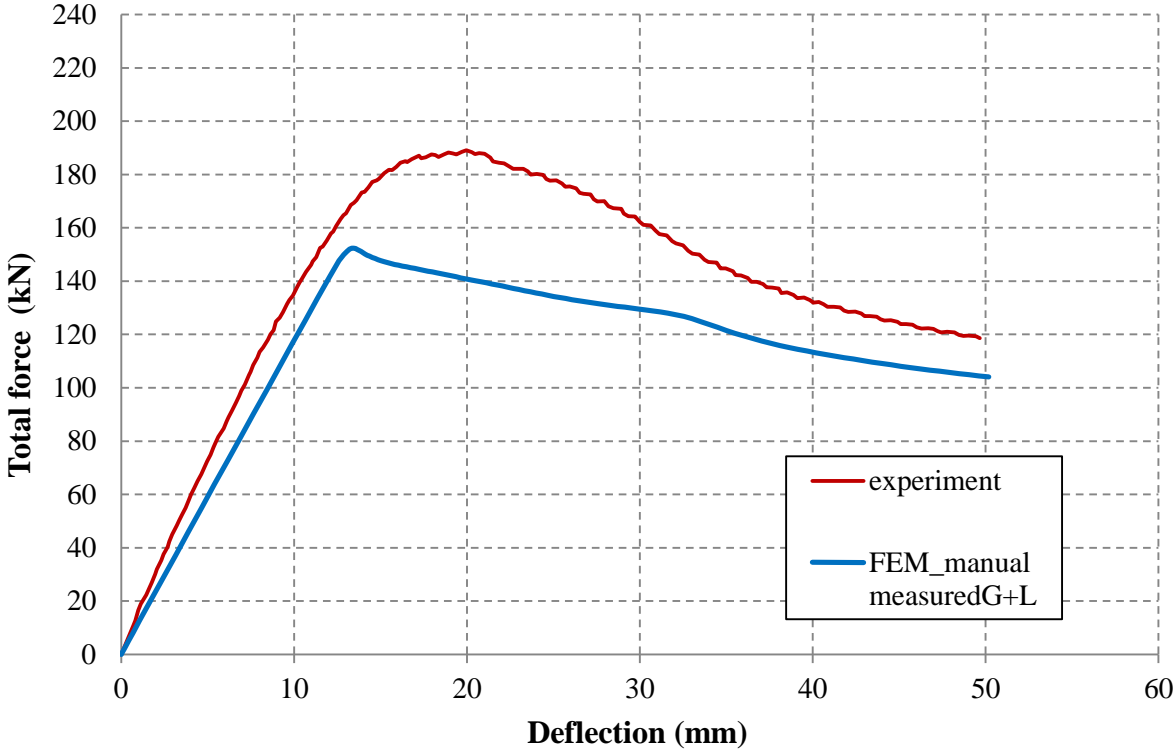
Figure 68: Numerical simulations against experimental fire test

Table 30 illustrates the comparison between the numerical simulation and experimental test in terms of ultimate load:

	Total force (kN)	Half-force (kN)	Ultimate bending moment (kN.m)
ABAQUS	151.80	75.90	83.48
SAFIR	168.50	84.25	92.66
Experiment	189.05	94.23	103.98

Table 30: Numerical simulation against experimental fire test

Figure 69 illustrates the failure mode for both numerical simulation and experimental test:
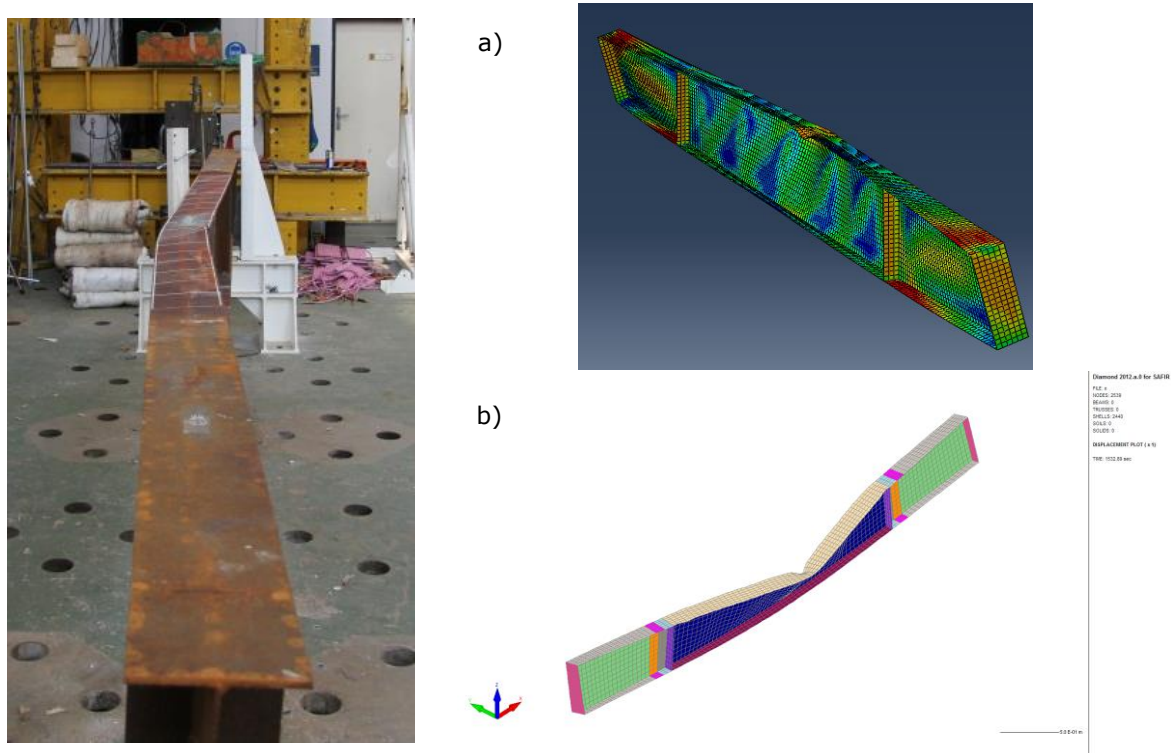
Figure 69: Failure mode shape for fire test and numerical simulation with: a) ABAQUS, b) SAFIR

The applied temperatures on beam of test 4 are listed in Table 31:

Part of beam	Temperature (°C)
Web	567.0
Bottom flange	415.6
Upper flange	623.7

Table 31: Temperatures applied on numerical model of test 4

The amplitudes of the imperfections taken into account are listed in Table 32 and the shapes of buckling modes used are illustrated in Figure 70:

Global imperfection (mm)	Local imperfection of upper flange (mm)	Global imperfection of flange (mm)
1.50	2.13	*

Table 32: Amplitude of imperfections
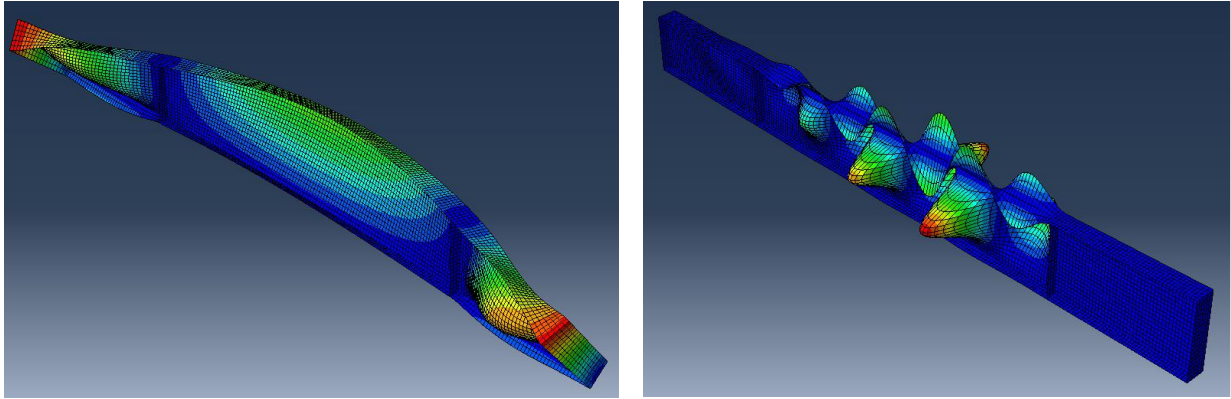
Figure 70: Mode shape from linear buckling analysis: *left) lateral torsional buckling failure mode, right) local buckling failure mode*

The next diagram of Figure 71 shows the comparison in terms of total applied force in function of deflection for both fire test and numerical analysis:
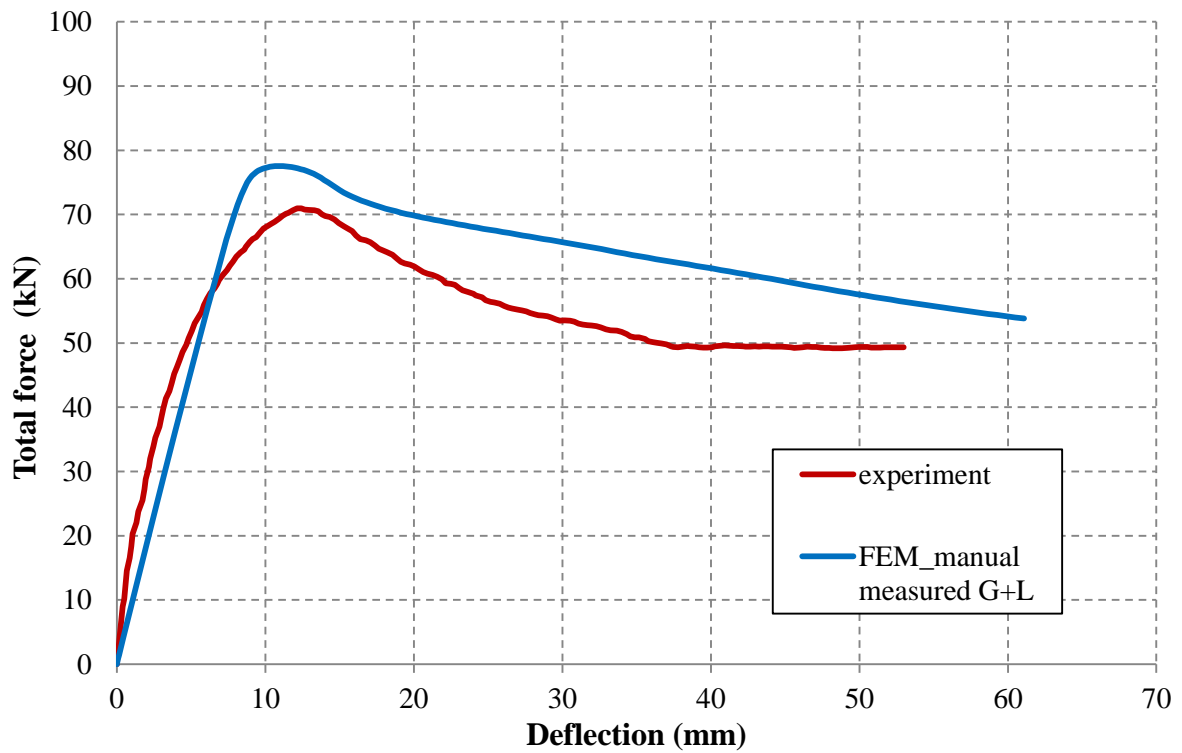
Figure 71: Numerical simulations against experimental fire test

Table 33 illustrates the comparison between the numerical simulation and experimental test in terms of ultimate load:

	Total force (kN)	Half-force (kN)	Ultimate bending moment (kN.m)
ABAQUS	74.10	37.05	40.76
SAFIR	68.20	34.10	37.51
Experiment	70.96	35.48	39.03

Table 33: Numerical simulation against experimental fire test

Figure 72 illustrates the failure mode for both numerical simulation and experimental test:

a)

b)

Figure 72: Failure mode shape for fire test and numerical simulation with: a) ABAQUS, b) SAFIR

The obtained results demonstrate the difficulties of lateral torsional buckling tests, moreover, when high temperature effects are taken into account. The problem of friction at the lateral restraints significantly affected the second test. For the third test, the experimental curve of load displacement relationship is not smooth and the force is suddenly increased for some regions. The obtained experimental initial stiffness is different from the numerical curves mainly in the third test and in the fourth test. The temperatures slightly vary during the tests and are not uniform in the whole section. The temperatures that are employed in the numerical models are considered as the average temperature for each part of the beam (web, upper flange, bottom flange). The maximum loads in the first test and in the third test are higher than the corresponded numerical tests values. Overall, the approximations are reasonable considering the nature of the different parameters involved in the presented tests, as for instance the heating process. The numerical model is capable of predicting with accuracy the behaviour of beams observed in all the tests in terms of mode of failure. However, the numerical models underestimate the loadbearing capacity of first three tested beams due to additional restraints induced by the friction between lateral supports and the specimens. In the fourth test, for which the problem of friction between the beam and the lateral support was minimalised by means of modified test arrangement, the difference between the numerical and experimental loadbearing capacities of the beam is largely reduced, for example only about 4 % between the numerical result of SAFIR and experimental result. From this point of view, the validity of the numerical approach is considered as fully satisfactory.

The model is subsequently simplified and used for the numerical parametric study.

2.2.3.2 General principles of simple design rules

The results of the numerical parametric study were compared with current design rules of EN 1993-1-2. The formulae are presented here after. For the correctness of the comparison it was aimed to eliminate all possible unknown variables in the calculation except the lateral torsional buckling behaviour. Therefore, the resistance of the cross-section for each temperature is numerically determined in ABAQUS and in SAFIR. Non-dimensional slenderness for lateral torsional buckling is given:

$$\lambda_{LT,\theta} = \sqrt{\frac{M_{fi,Rd,\theta}}{M_{Cr}}} \times \sqrt{\frac{1}{k_{E,\theta}}} \tag{17}$$

With:

$M_{fi,Rd,\theta}$ is the resistance of cross-section at temperature θ determined in ABAQUS and in SAFIR, M_{cr} is the elastic critical moment at room temperature obtained from the finite element method with ABAQUS and CASTEM and $k_{E,\theta}$ is the reduction factor (relative to E) for the slope of the linear elastic range.

The value of $\chi_{LT,fi}$ is determined according to the following equations:

$$\chi_{LT,\theta} = \frac{1}{\phi_{LT,\theta} + \sqrt{\left[\phi_{LT,\theta}\right]^2 - \left[\lambda_{LT,\theta}\right]^2}} \tag{18}$$

With

$$\phi_{LT,\theta} = 0.5\left[1 + \alpha \times \bar{\lambda}_{LT,\theta} + (\bar{\lambda}_{LT,\theta})^2\right] \tag{19}$$

And

$$\alpha = 0{,}65 \times \sqrt{235/f_y} \tag{20}$$

The lateral torsional buckling resistance moment in the fire design situation is finally obtained with the following formula:

$$M_{b,fi,Rd,\theta} = \chi_{LT,\theta} \times M_{fi,Rd,\theta} \tag{21}$$

2.2.3.3 Comparisons of the numerical results with the current design rules of EN 1993-1-2

The comparisons between numerical results and current EN 1993-1-2 design rule for all the conducted numerical simulations with SAFIR and ABAQUS are shown in the following diagrams of figures 73 and 74. The numerical parametric study represents a total of about 3700 finite element calculations. In these simulations, the beams are loaded with uniform bending diagram, triangular bending diagram, and bi-triangular bending diagram or with uniform distributed load and both ends of the beams are simply supported. The following diagram of Figure 73 illustrates the results for S355 steel grade:
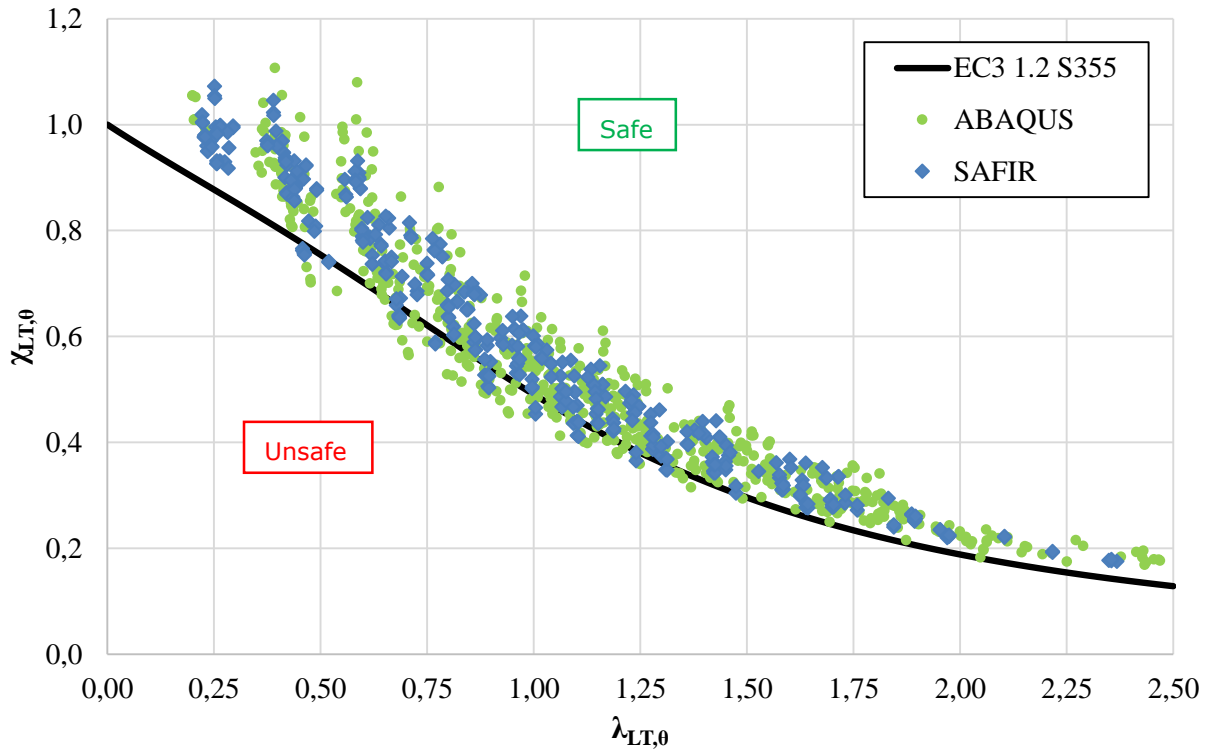
Figure 73: Comparison between FEM LTB curve and LTB curve from EN 1993-1-2 for S355 steel grade

The following diagram of Figure 74 illustrates the results for S460 steel grade:
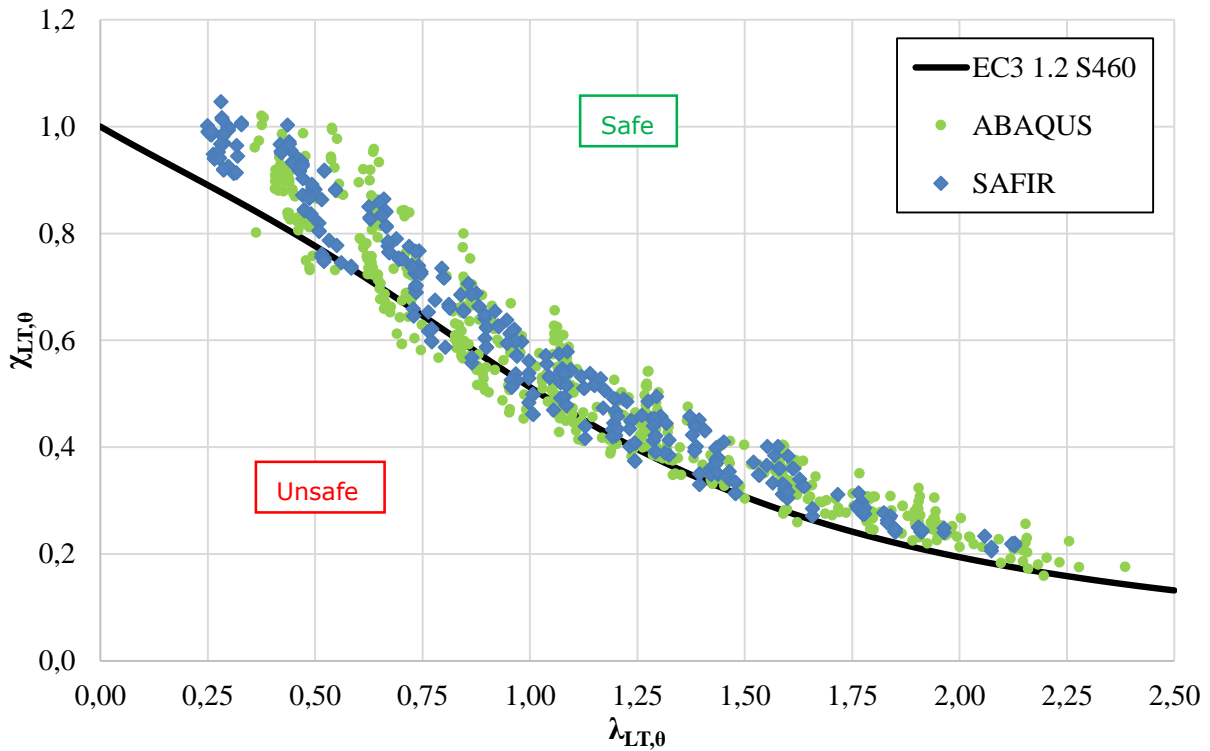
Figure 74: Comparison between FEM LTB curve and LTB curve from EN 1993-1-2 for S460 steel grade

Previous results for both S355 and S460 steel grades are summarized in the following chart. The ratio of the lateral torsional buckling moment resistance, which is obtained from ABAQUS and SAFIR ($M_{b,FEM}$) and lateral torsional buckling moment resistance calculated according to EN 1993-1-2 as described above, is actually illustrated. It appears that the current EN 1993-1-2 design rules for lateral torsional buckling is really safe. But it also shows that it can lead to an un-economical design of beams subjected to this type of loading, regardless of the slenderness:
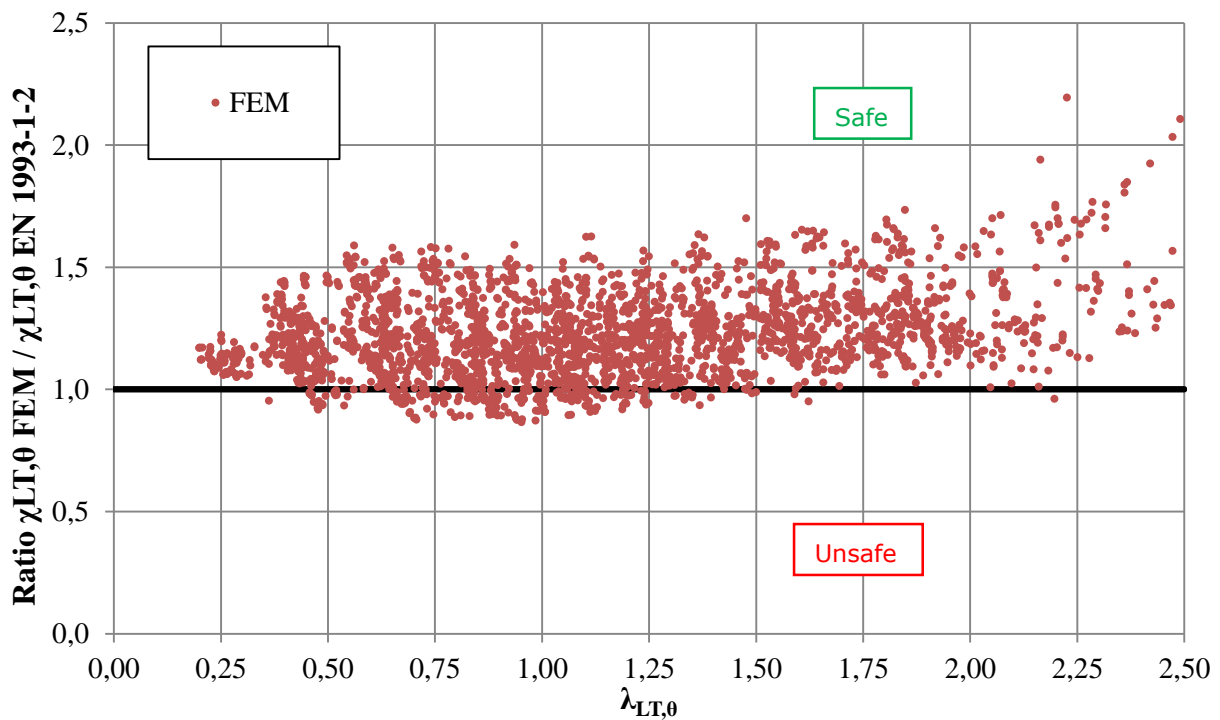
Figure 75: Comparison between results of the parametric study and the current design rules (EN 1993-1-2) for both S355 and S460

About 47% of the 3700 simulations are situated on the safe side by more than 15%. This really shows the non-economical design which can be undertaken by using current EN 1993-1-2 to deal with lateral torsional buckling. That is why it was proposed to improve the design rule mainly in term of accuracy.

The influence of several parameters was checked in the comparisons. The residual stress pattern, the applied temperature and the width to depth ratio (h/b) almost does not influence the lateral torsional buckling response of the beams. However, the cross-section slenderness clearly influences this response. The ratio between the effective section modulus on the elastic section modulus was precisely investigated. It showed a distribution of the results according to the cross-section slenderness. The proposed limits are listed in Table 34:

Curve	Limits (ratio $s=$)
L1	$W_{eff,y}/W_{el,y} > 0.9$
L2	$0.8 < W_{eff,y}/W_{el,y} \leq 0.9$
L3	$W_{eff,y}/W_{el,y} \leq 0.8$

Table 34: Slenderness limits

Figure 76 illustrates for the uniform bending moment distribution load and for S355 steel grade the evolution of $\chi_{LT,\theta}$ in function of the slenderness according to the three defined ranges:
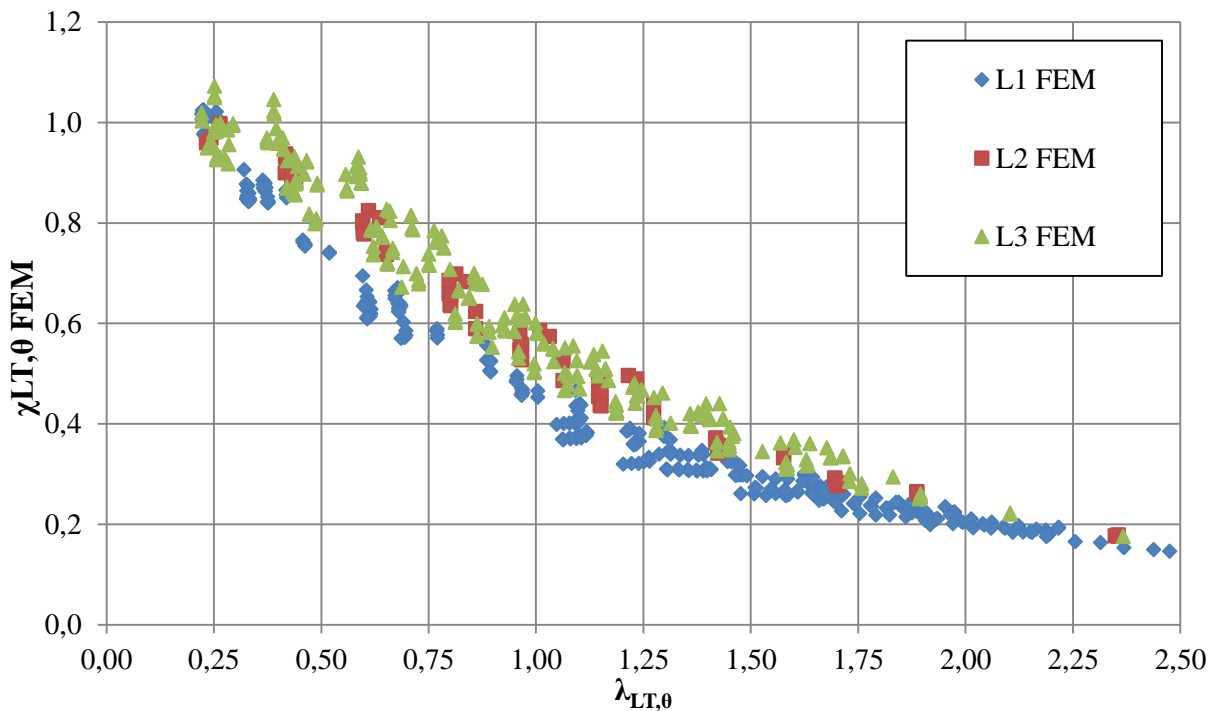
Figure 76: Distribution of χ_{LT} with the separation according to the defined cross-section slenderness ranges

2.2.3.4 *New proposal for lateral torsional buckling of class 4 cross-section beam*

As shown in Table 34 and in Figure 76, a new imperfection factor, which takes into account the influence of cross-section slenderness by means of factor $s = W_{eff,y}/W_{el,y}$ (effective section factor), is proposed. The lateral-torsional buckling resistance moment in the fire design situation is to be determined as proposed in the following equations:

$$M_{b,fi,Rd,\theta,NEW} = \chi_{LT,\theta,NEW} \times W_{eff,y,min} \times f_y \times k_{y,\theta} / \gamma_{M,\theta} \qquad (22)$$

Non-dimensional slenderness for lateral torsional buckling is given by:

$$\bar{\lambda}_{\text{LT},\theta} = \bar{\lambda}_{\text{LT}} \times \sqrt{k_{\text{y},\theta}/k_{\text{E},\theta}} \qquad (23)$$

With

$$\bar{\lambda}_{\text{LT}} = \sqrt{W_{\text{eff,y, min}} \times f_{\text{y}}/M_{\text{cr}}} \qquad (24)$$

The value of $\chi_{LT,\theta,NEW}$ is determined according to the following equation:

$$\chi_{\text{LT},\theta,\text{NEW}} = \frac{1/f}{\phi_{\text{LT},\theta} + \sqrt{\phi_{\text{LT},\theta}^2 - \bar{\lambda}_{\text{LT},\theta}^2}} \qquad (25)$$

With

$$\phi_{\text{LT},\theta} = 0.5 \times \left(1 + \alpha_{\text{LT}} \times \left[\bar{\lambda}_{\text{LT},\theta} - 0.2\right] + \bar{\lambda}_{\text{LT},\theta}^2\right) \qquad (26)$$

The value of the imperfection factor α_{LT} now depends on the limit of cross-sectional slenderness and is taken from Table 35:

Curve	Limits (ratio s=)	α_{LT}
L1	$W_{eff,y}/W_{el,y} > 0.9$	1.25ε
L2	$0.8 < W_{eff,y}/W_{el,y} \leq 0.9$	1.00ε
L3	$W_{eff,y}/W_{el,y} \leq 0.8$	0.75ε

Table 35: Imperfection factor α_{LT}

Factor f should be used in accordance with the approval of the Evolution Group. Therefore, factor f depends on the loading type and is defined for class 4 cross-sections in the following equation:

$$f = 1 - 0.5 \times (1 - k_c) \geq 0.8 \qquad (27)$$

With k_c defined as a correction factor defined in Table 36:
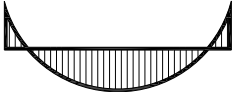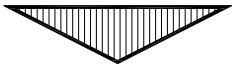
Moment distribution	k_c
M ψM $-1 \leq \psi \leq 1$	$0.6 + 0.3 \times \psi + 0.15 \times \psi^2$ but $k_c \leq 1$
	0.91
	0.90
	0.91
	0.79
	0.73
	0.75

Table 36: Correction factors k_c to be used for factor f

In the following comparisons between finite element results and new proposed simple design rule, the expression $W_{eff,y,min}f_y k_{y,\theta}$ was replaced by $M_{fi,Rd,\theta}$ (resistance of the cross-section determined in ABAQUS and in SAFIR, for each temperature) and to remain consistent the $W_{el,y}$ was replaced by M_{el}.

The following diagrams of figures 77 to 79 show the comparisons between the modified approach and all constant cross-section beam simulations, for all investigated temperatures and for both S355 and S460 steel grades. In these simulations, the beams are loaded with uniform bending diagram and both ends of the beams are simply supported. The choice of only using uniform bending diagram moment allowed the comparison of the new design curve with the numerical simulations. The following chart of Figure 77 illustrates the results for S355 steel grade:
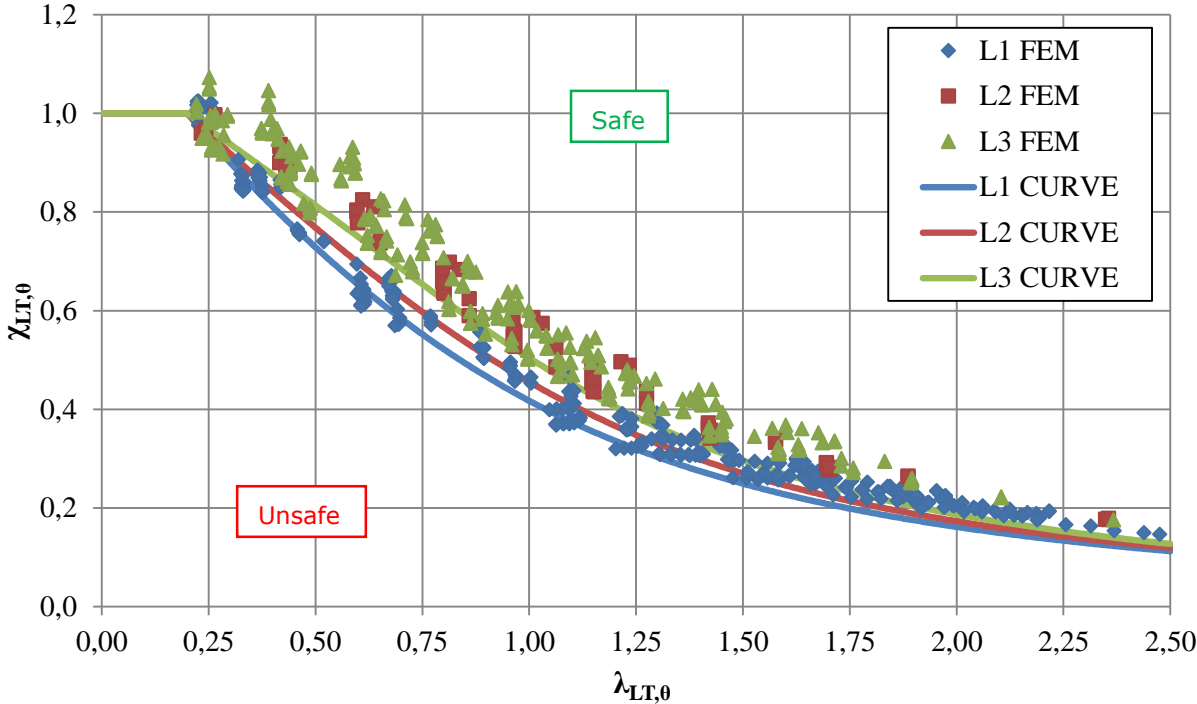
Figure 77: Comparison between the results of the parametric study and the new proposed design procedure for steel S355

The following chart of Figure 78 illustrates the results for S460 steel grade:
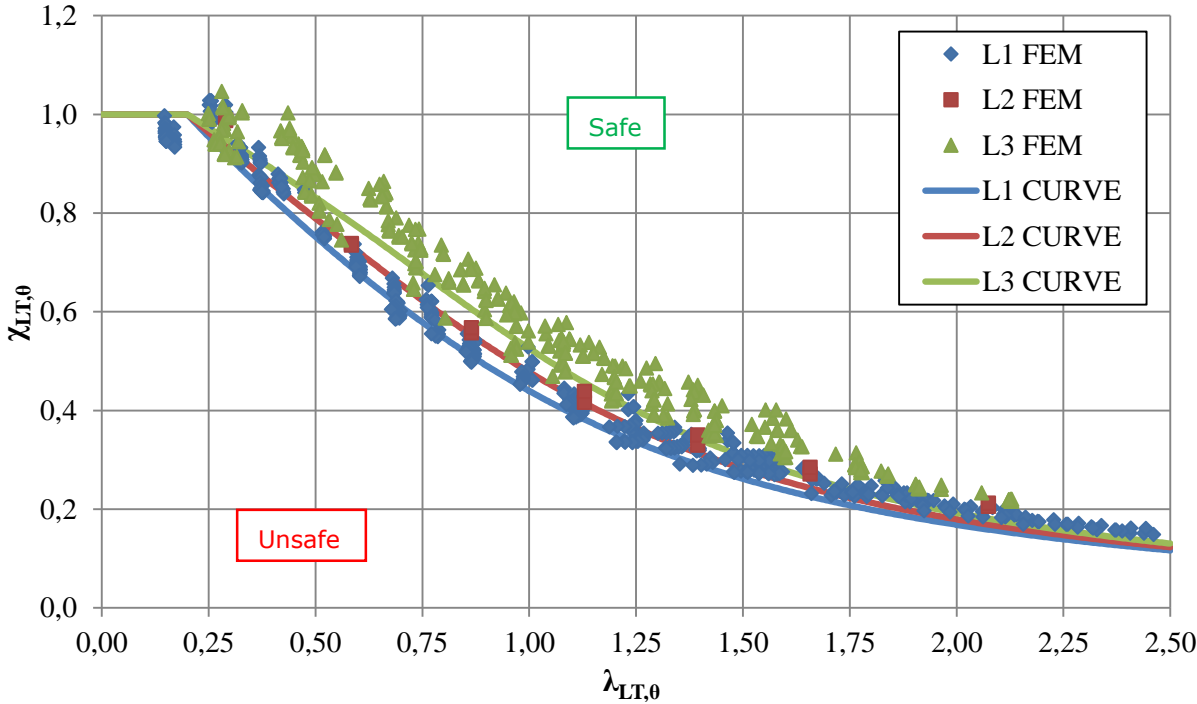
Figure 78: Comparison between the results of the parametric study and the new proposed design procedure for steel S460

All numerical results for both S355 and S460 steel grades are summarized in the following chart. the ratio of the lateral torsional buckling moment resistance, which is obtained from ABAQUS and SAFIR ($M_{b,FEM}$) and lateral torsional buckling moment resistance calculated according to new proposed design rule as described above, is illustrated:
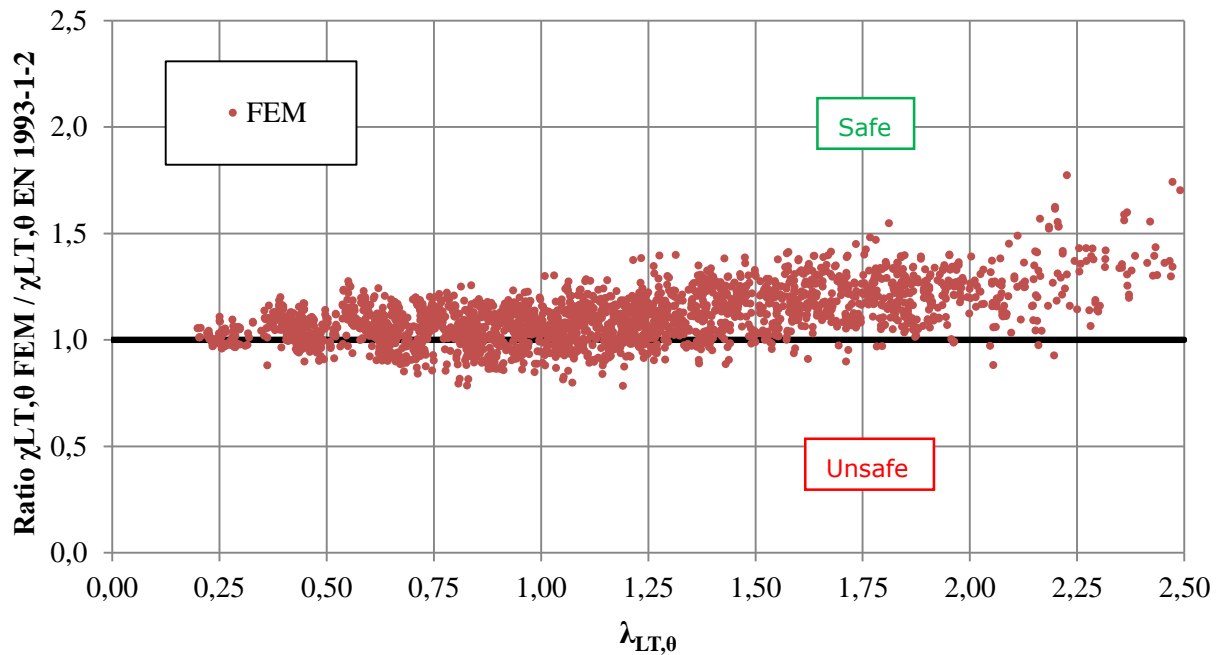
Figure 79: Comparison between the results of the parametric study and the proposed design procedure for both steel grades S355 and S460

The statistical data of the comparisons between the numerical results and the EN 1993-1-2 and between the numerical results and the new proposed design rules are given in Table 37:

	EN 1993-1-2	NEW DESIGN RULES
Average ratio (design rule / FEM)	0.86	0.91
Percentage of unsafe points (%)	15.39	16.65
Maximum unsafe ratio	1.25	1.14
Percentage of safe points by more than 15% (%)	47.31	24.68
Standard deviation	0.13	0.10
Coefficient of variation	0.15	0.11

Table 37: Statistical data for the $M_{b,FEM}/M_{b,NEW}$ ratio

It is noticeable that the average ratio is improved by about 4% in the design rules compared to the current EN 1993-1-2 design curve. The most important change is for points considered as too safe points, i.e. un-economic points. Almost a half of the EN 1993-1-2 design points are lower by more than 15% than the numerical simulations. This number of un-economic points decreases at less than 27% with the new design rules, while remaining in agreement with the safety ratios.

The validity of the new proposal in various cases was checked. The beams were loaded by different moment distributions and both ends of the beams are still simply supported. For these beams, other than uniform moment distribution was considered. The factor f according to the Evolution group for EN 1993-1-2 proposal in fire situation was taken into account (see previous definition). This factor is based on publication of Lopes at al. Numerical analysis of stainless steel beam-columns in case of fire [21]. The lower bound 0.8 of the factor f for Class 4 cross-sections was used.

The following diagrams from figures 80 to 85, show numerical simulations at all defined temperatures compared with updated design method including factor *f*. In these simulations, the beams are loaded by non-uniform bending moment. Figures 80 to 82 illustrate the comparisons between the new simple design rule and the simulations for triangular bending moment and different curves from L1 to L3:
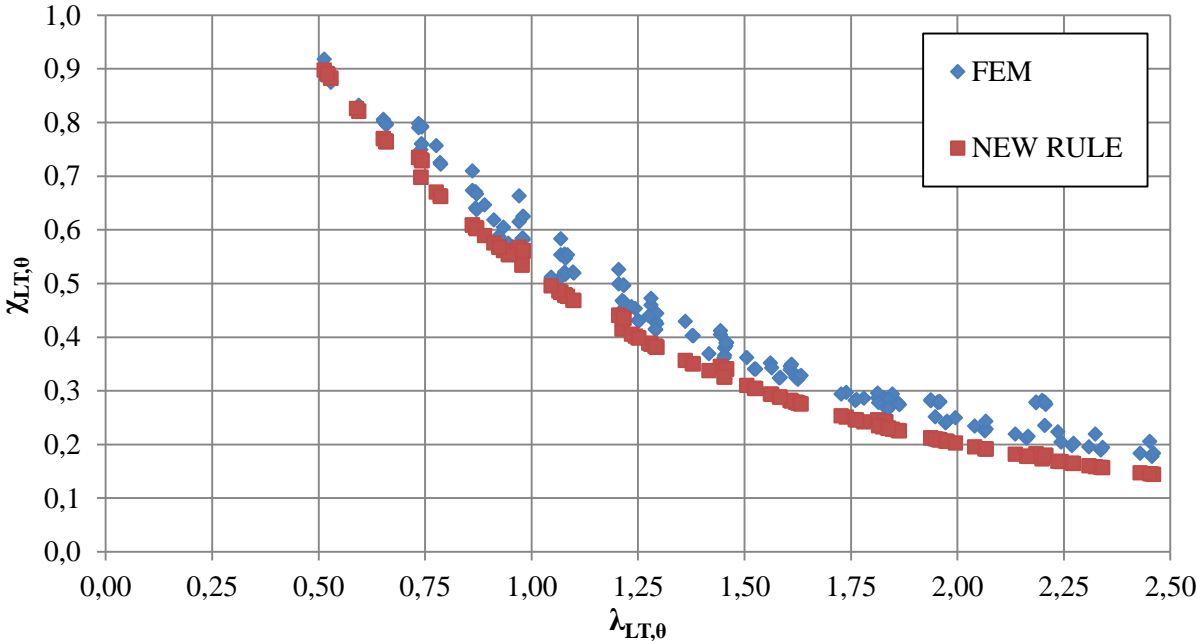
Figure 80: Comparison between the results of the parametric study and the new proposed design procedure for triangular bending moment and curve L1
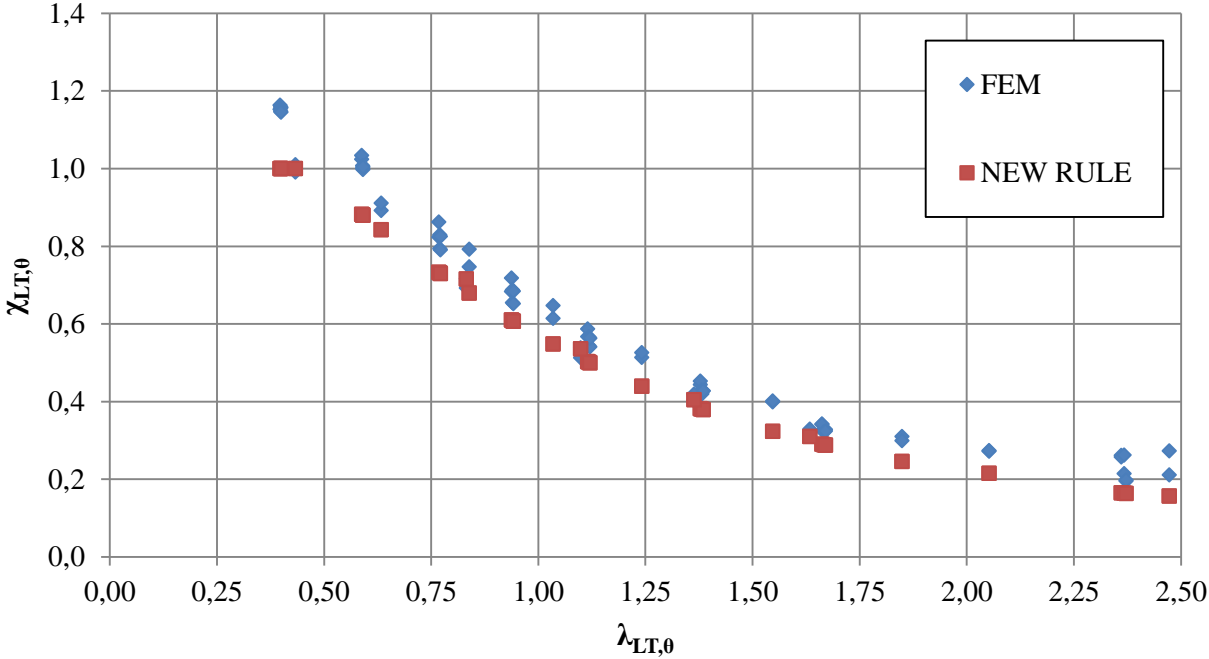
Figure 81: Comparison between the results of the parametric study and the new proposed design procedure for triangular bending moment and curve L2
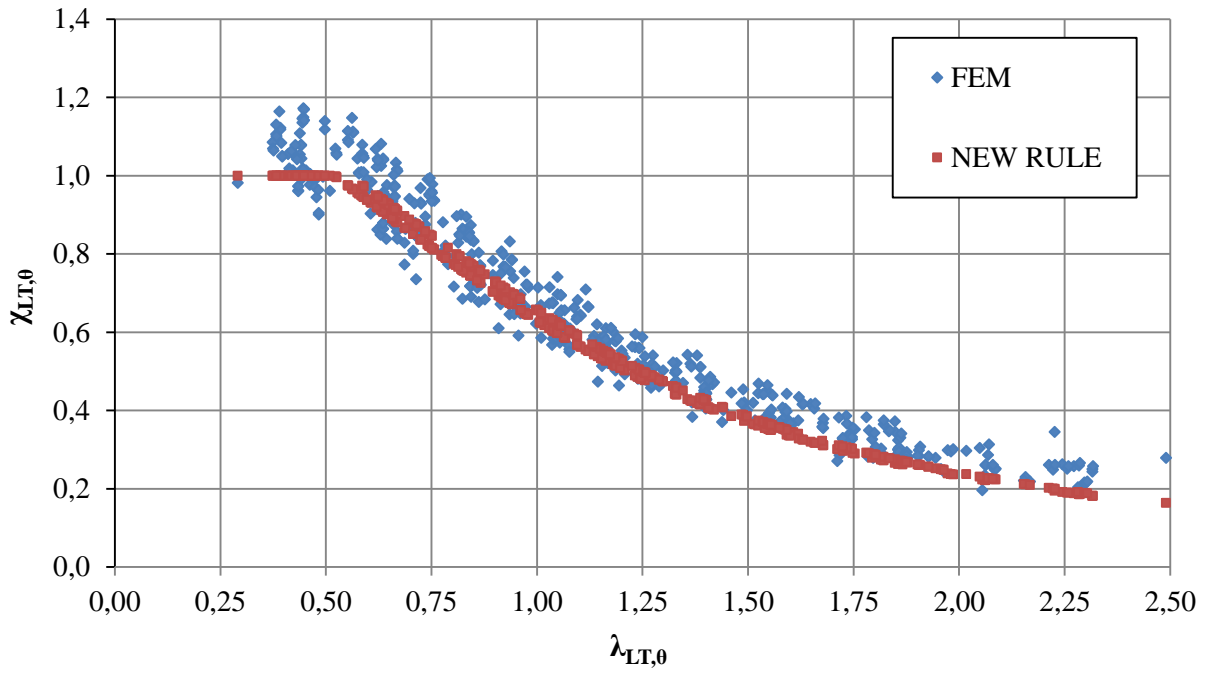
Figure 82: Comparison between the results of the parametric study and the new proposed design procedure for triangular bending moment and curve L3

Figures 83 to 85 illustrate the comparisons between the new simple design rule and the simulations for bi-triangular bending moment and different curves from L1 to L3:
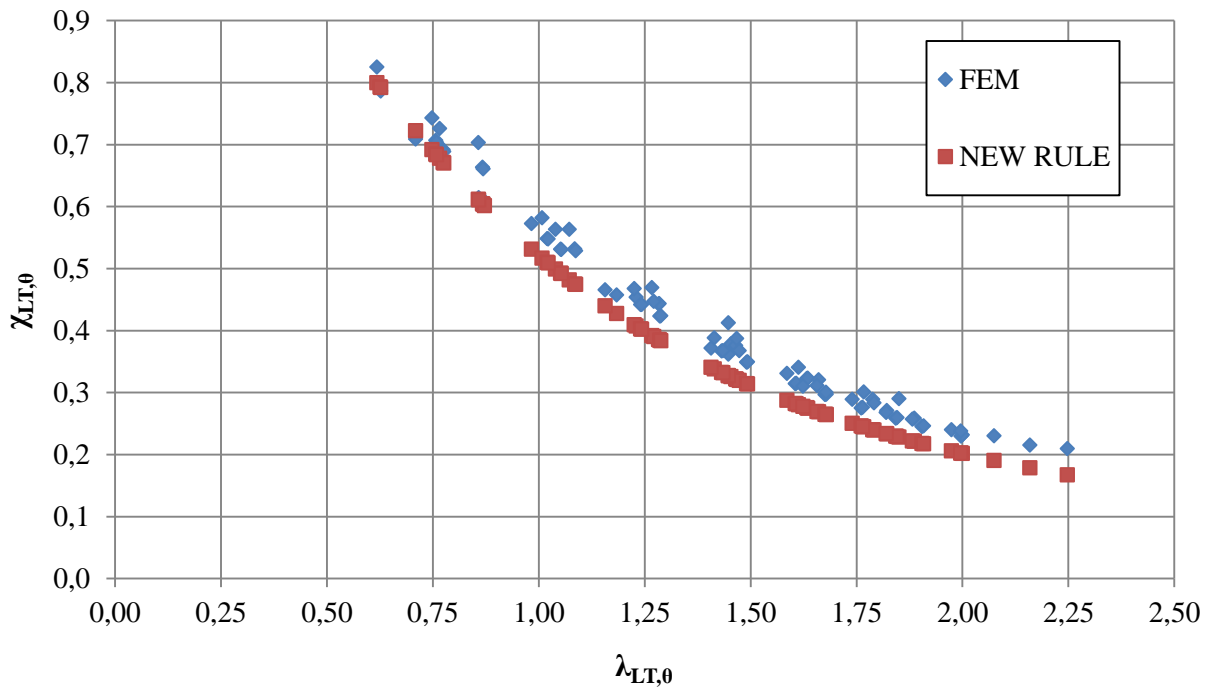
Figure 83: Comparison between the results of the parametric study and the new proposed design procedure for bi-triangular bending moment and curve L1
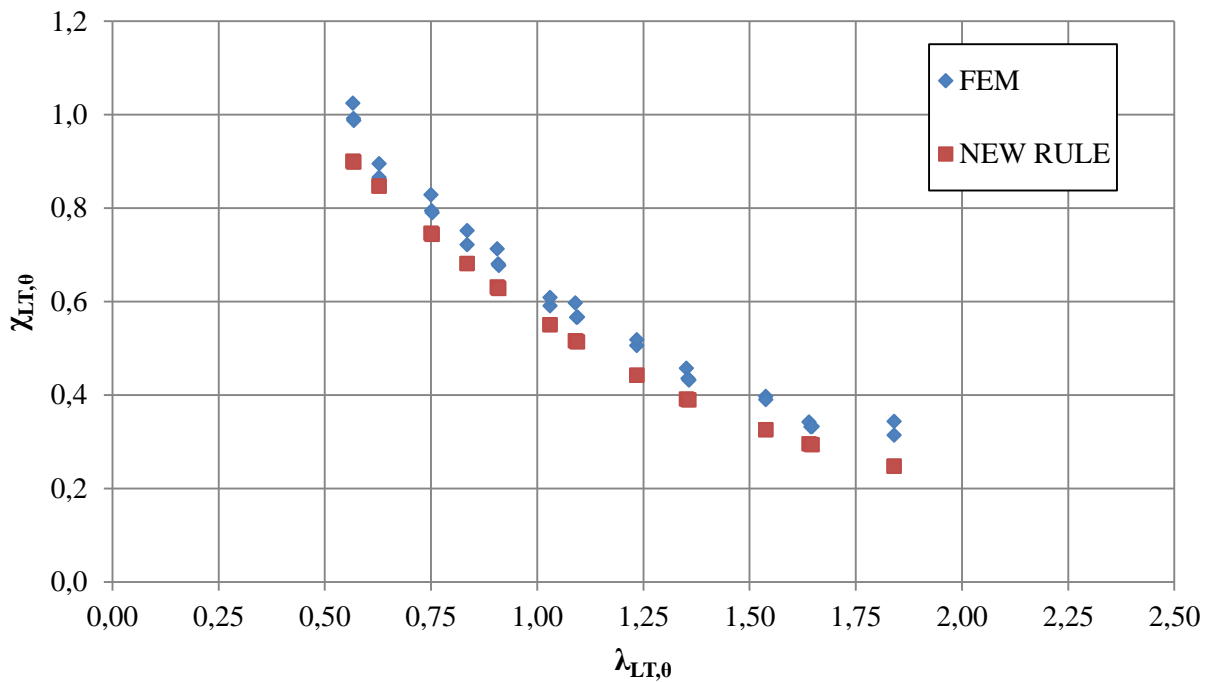
Figure 84: Comparison between the results of the parametric study and the new proposed design procedure for bi-triangular bending moment and curve L2
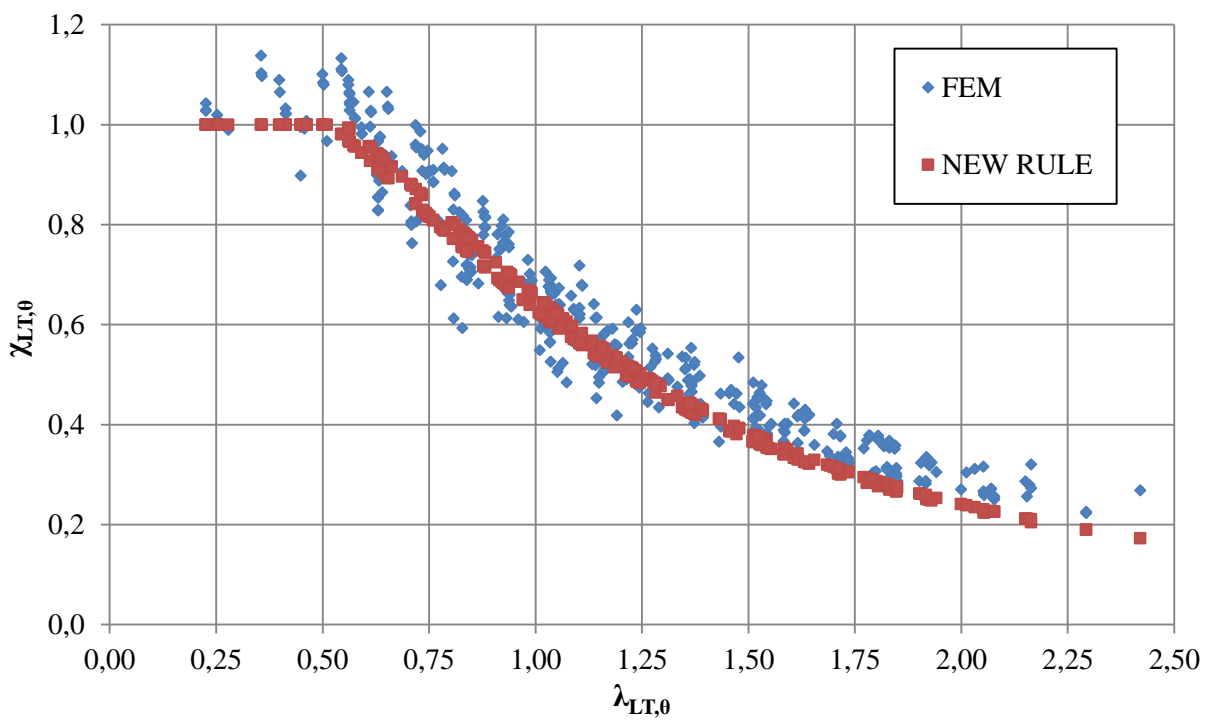
Figure 85: Comparison between the results of the parametric study and the new proposed design procedure for bi-triangular bending moment and curve L3

Tapered members are also investigated and numerical results are confronted with the new design rule taking. In these cases, the used method to evaluate the elastic moment resistant to define the L curve is the following:
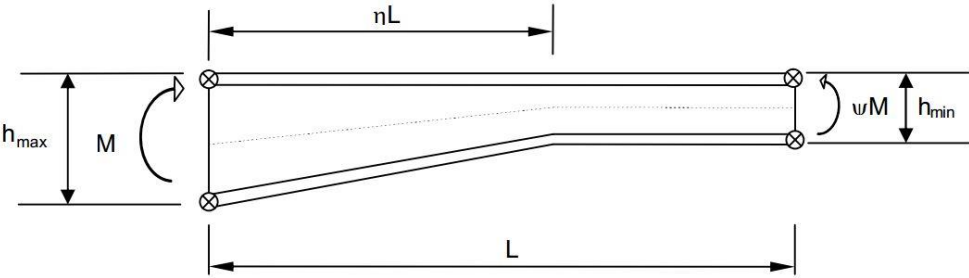
Figure 86: Scheme of general tapered member

The equation to obtain equivalent depth of the web is given with the following equation:

$$h_{eq} = h_{min} \times \left(1 - \eta + \frac{\eta^{\gamma}}{2} \times \left[1 + \frac{h_{max}}{h_{min}}\right]\right) \tag{28}$$

With:

$$\gamma = 1 + 0.25 \times \left(\frac{h_{max}}{h_{min}} - 1\right) \tag{29}$$

This method is based on the simple design method described in the paper: *Déversement des barres à section en I bissymétrique et hauteur d'âme linéairement variable* by Y. GALEA in Revue Construction Métallique – 1986 [23].

Figure 87 illustrates the correlation in terms of lateral torsional buckling resistance of tapered members between the numerical simulations and the current design rule of EN 1993-1-2.
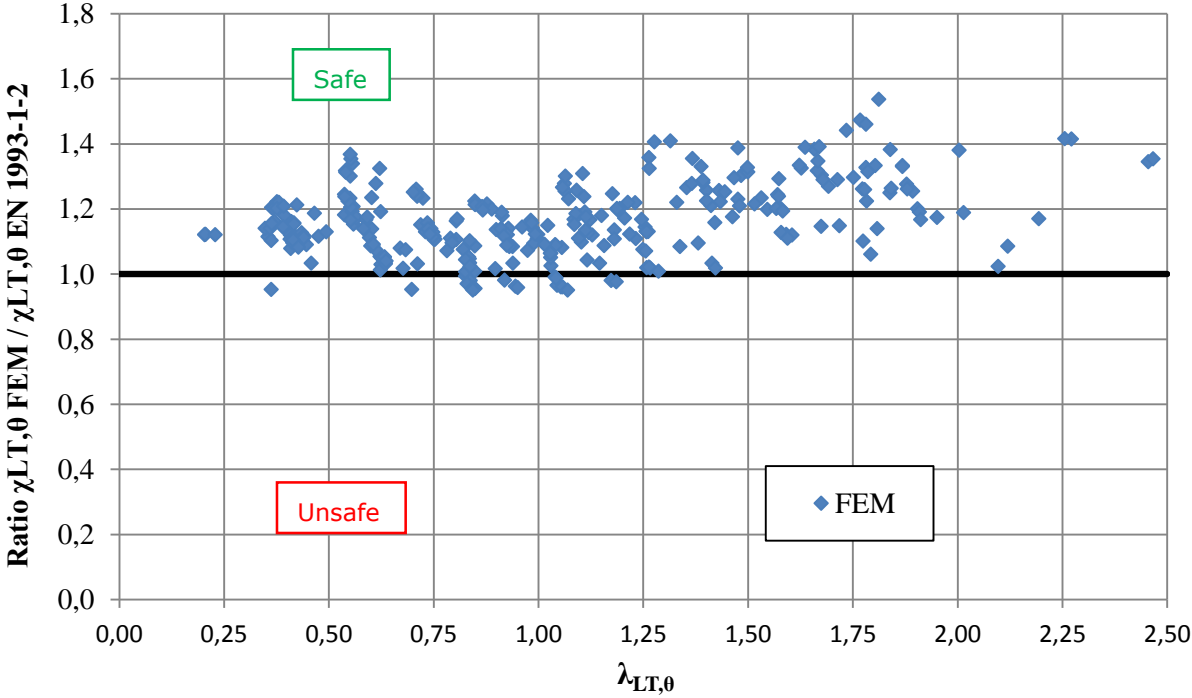
Figure 87: Tapered beams; comparison between numerical results and current EN 1993-1-2 design rules

Figure 88 illustrates the ratio between the numerical lateral torsional buckling resistance of tapered members and the lateral torsional buckling resistance obtained with the new simple design rule:
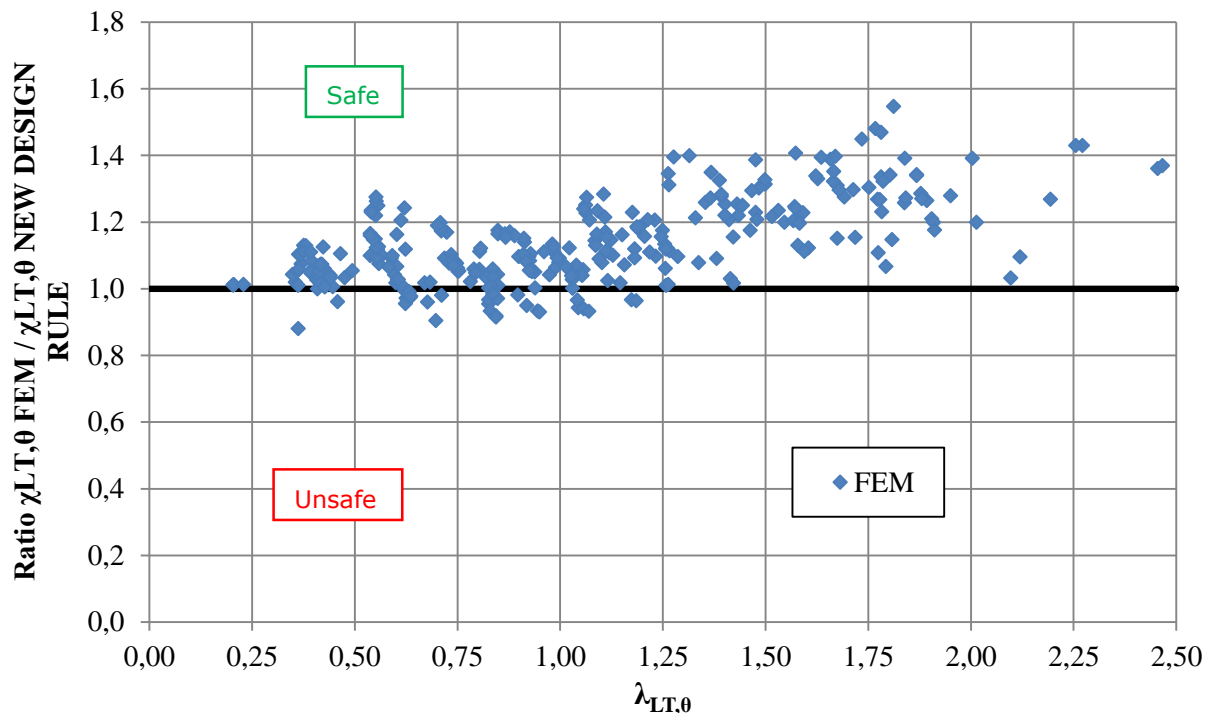
Figure 88: Tapered beams; comparison between numerical results and new design rule

Visually, the differences are not flagrant. Nevertheless, slight improvement is acquired and the new design rule is more satisfactory to deal with tapered cross-sections in terms of both accuracy and cost-effective. Table 38 shows some statistical aspects of the results:

	EN 1993-1-2	NEW DESIGN RULES
Average ratio (design rule / FEM)	0.86	0.90
Percentage of unsafe points by more than 15% (%)	0	0
Percentage of safe points by more than 15% (%)	50.32	39.50

Table 38: Statistical results for the $M_{b,FEM}/M_{b,NEW}$ ratio

The proposed reduction lateral-torsional buckling coefficient for the tapered beam may be used together with the procedure described in EN 1993-1-5 Annex B.

Based on the numerical results, a modified approach for laterally unrestrained beam of Class 4 was proposed and gives more consistent results. Different bending moment distributions were investigated in fire situation as it is described in previous chapters. It was demonstrated that the use of the developed simple design rules for constant cross-section is possible for tapered member as well.

2.2.4   WP4 - Columns under axial compression

2.2.4.1   Experimental investigation

Four I-columns with slender cross-sections were axially loaded in these fire tests. One column was a constant hot-rolled profile. Two out of the four tested columns were constant welded cross-section. The last one was a tapered welded profile. The fire tests consisted in the application of a mechanical load until reaching the load ratio (percentage of the cold failure load) for the steel members and then heating the latter at least until mechanical failure. The columns were heated along their whole length. This procedure was the same for the four tests. These tests were designed so that the failure was induced by a global buckling along weak or strong axis eventually combined with local buckling of sections walls. There was no lateral restraint installed along the weak axis.

The four tested columns which were axially loaded and the different tested cross-sections are given hereafter. One cross-section was an IPE240A. The three other columns were made of welded cross-sections. Table 39 describes the main parameters which were used for these tests:

Test number	Cross-section	Strong axis λ_p	Weak axis λ_p
Test 1	Constant - IPE240A	0.245	1.255
Test 2 & test 3	Constant - 440x4+150x5	0.164	0.995
Test 4	Tapered - 490-290x4.5+150x5	0.267	1.029

Table 39: List of axially loaded columns tested

The tested columns and corresponding cross-sections are illustrated in the following figures from 89 to 91.

An eccentricity of 5 mm was prepared to the applied load in the direction of the weak axis in order to control the failure mode. For this test, the eccentricity of the load and of the support was arranged so that a small uniform bending moment distribution ($\psi = 1$) occured:
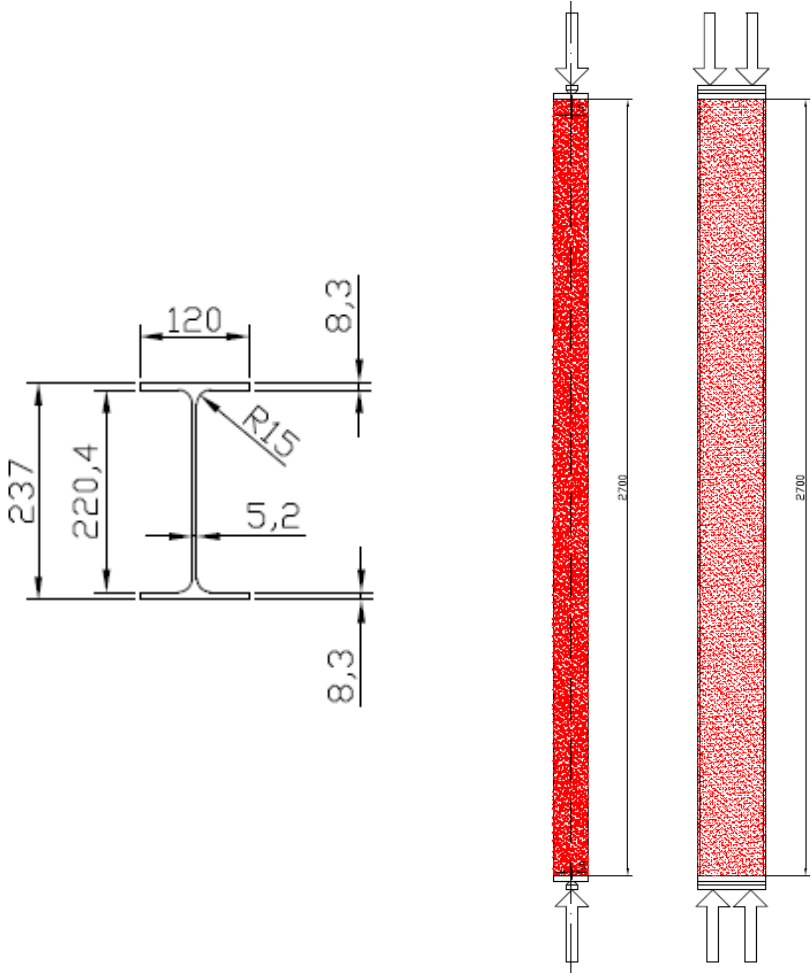
Figure 89: Cross-section design and global design of the test 1

An eccentricity of 5 mm was provided to the applied load in the direction of the weak axis in order to control the failure mode. For this test the eccentricity of the load and of the support were arranged in such a way us to produce a small uniform bending moment distribution ($\psi = 1$):
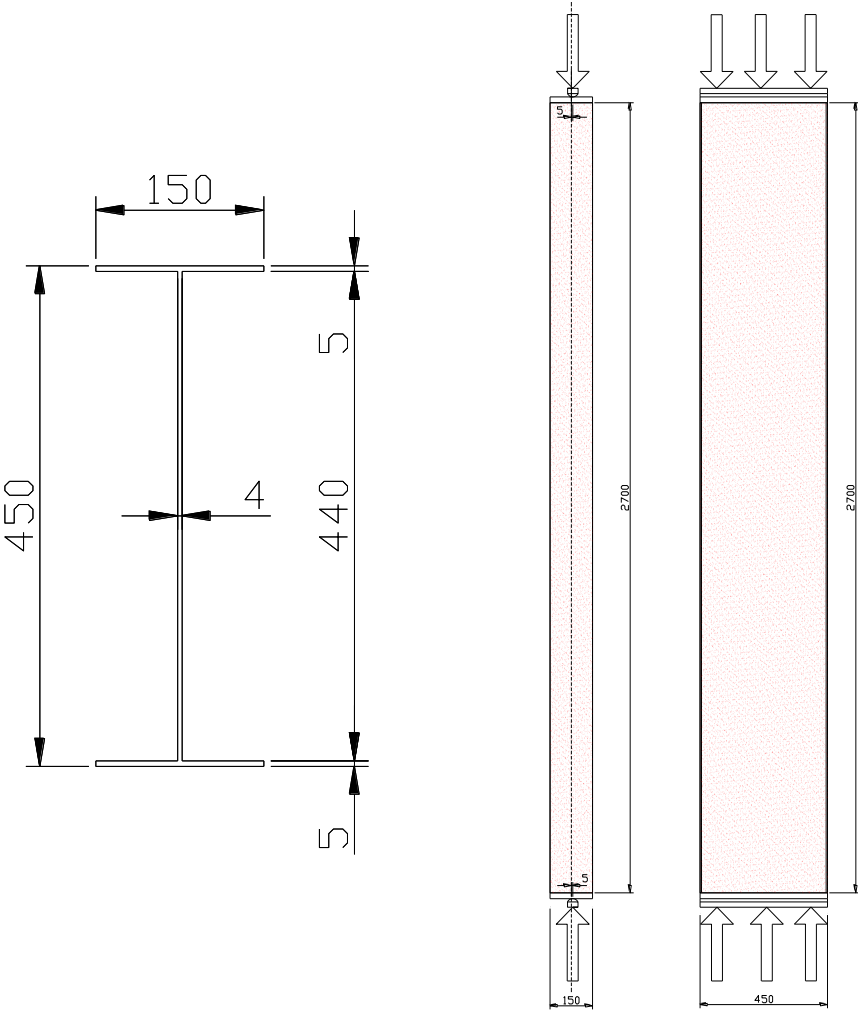
Figure 90: Cross-section design and global design of the tests 2 & 3

The load was applied with an eccentricity of 6 mm in the direction of the strong axis. For this test the eccentricity of the load and of the support were arranged in such a way us to produce a uniform bending moment distribution ($\psi = 1$):
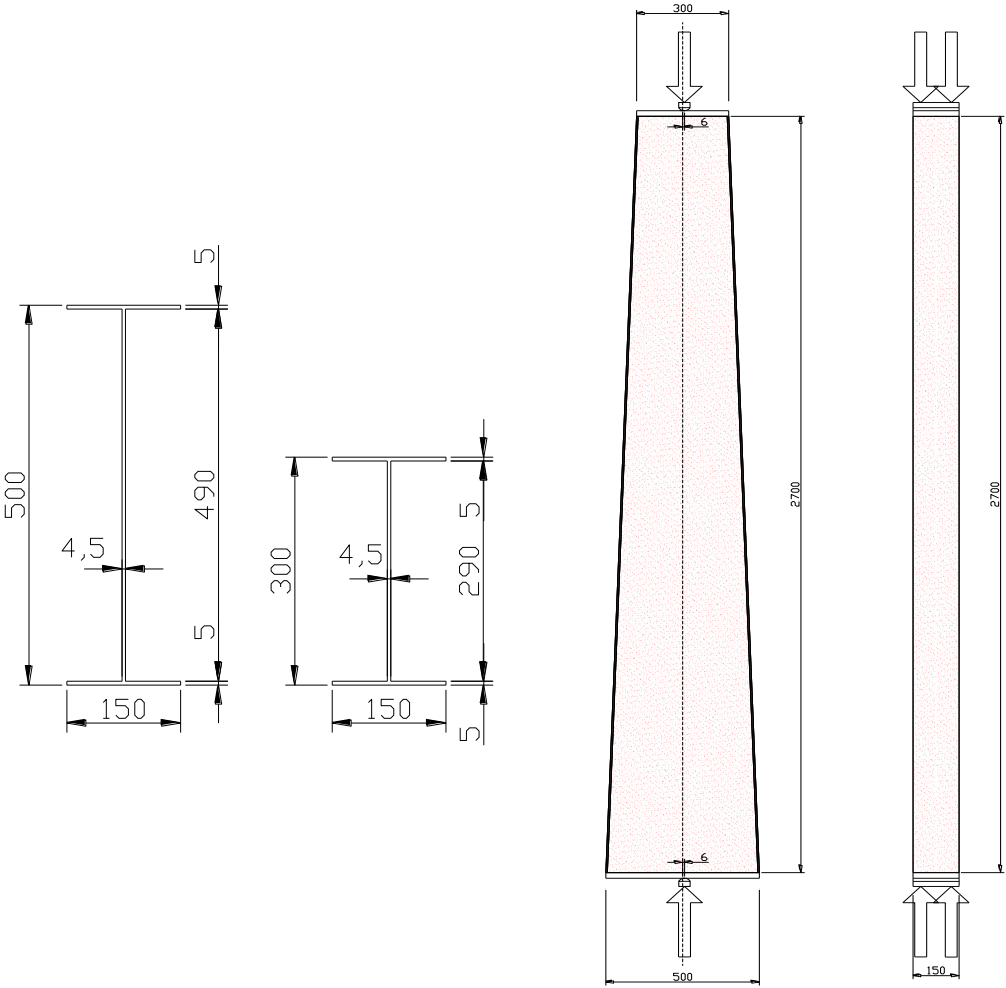
Figure 91: Cross-section design and global design of the test 4

The measurements of the global and local imperfections of the specimens were performed manually. The methodology was to put a straight aluminium bar (with the same length than the specimen) along the web and along the both flanges of each column. Once the rule placed, the distance between the bottom of the ruler and the web (or the flange) of the column was measured each ten centimetres length.

The reference for these profiles was the bottom of the ruler; so by deducing the distance between the ruler and the web (or flange) measured at the two extremities of the specimen from all the other measured distances, the profiles presented in the schemes here below for each column with an imperfection equal to zero at the extremities was drawn. Thus, it was supposed that the two points of reference for the measurements are the two extremities of the column. Thanks to this data providing the profile of the imperfections along the column, the global imperfection of the column and also the local imperfections observed around the global one were deduced. Figure 92 illustrates the profile of imperfection for the first tested column:
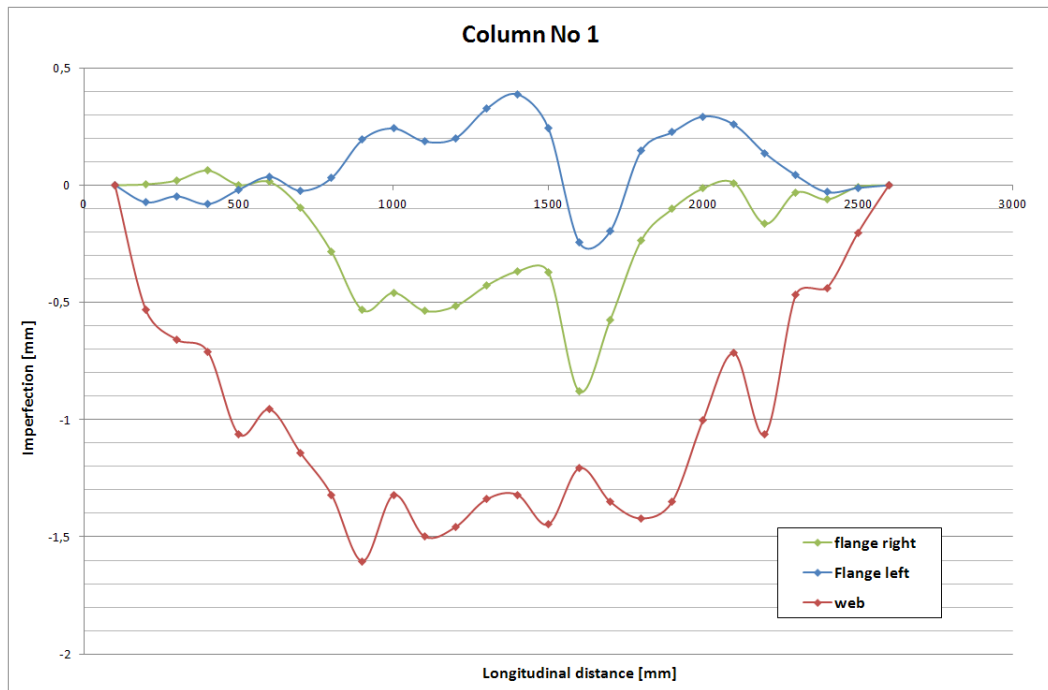
Figure 92: Test 1 – Amplitude of the imperfections along the web and both flanges

The fire tests consisted in applying a mechanical load until reaching the load ratio (percentage of the cold failure load selected to reach a temperature of at least 450°C in the column) for the steel members and then heating the latter at least until mechanical failure. The column was electrically heated along its whole length using flexible ceramic pad heaters.

The tested columns were set in the steel frame of the laboratory which is made with jacks to apply the mechanical load on the tested columns pushing up the lower beam of the frame. Some 20 mm diameter bolts were used to fix the specimen to the pinned support and also to fix the pinned supports to the steel testing frame. The frame is illustrated in Figure 93:

Figure 93: Testing frame for the experimental tests with the equipped column

The extremities of the columns were fixed using pinned supports which enabled the rotation in only one direction, see Figure 94. This kind of supports allowed controlling the failure mode of each tested column:
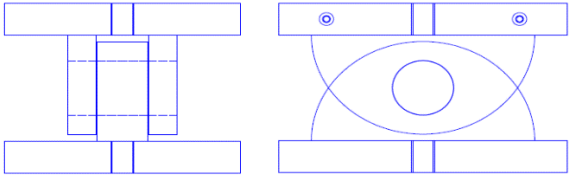
Figure 94: Scheme of pinned supports

In addition, this support could not overreach the temperature of 200 °C. But the columns (and thus its end-plates) were heated up to a maximum of 650 °C. So a thermal disconnection between the steel end-plate of the tested columns and the steel pinned support was installed. A layer of 35 mm of thickness of the material PROMATECT-H that allowed ensuring sufficient compression strength in its heated state for the most critical of our experimental tests and that provided a lambda value at 650 °C of around 0.235 W/m.K measured with hotwire system is placed between the end-plates and the pinned-supports. The description is given in Figure 95:

Figure 95: Pinned support with thermal disconnection

Mannings ceramic pad heating elements were constructed from high grade sintered alumina ceramic beads, Nickel-Chrome core wire and Nickel cold tail wire. The construction allowed the heating element to be flexible and provides high heat transfer efficiency. In order to be able to heat all the eight different columns of the experimental tests, two sizes of the ceramic pad heating elements were used: 610 x 85 mm and 1220 x 45 mm:
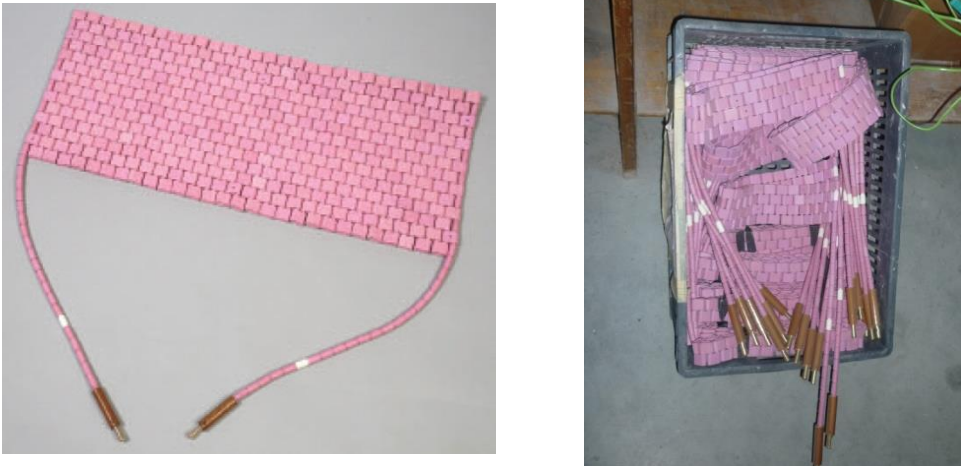
Figure 96: Ceramic pad heating elements

The temperatures were recorded during the whole duration of each test and at several positions along the web and the flanges of the columns by means of several thermocouples:
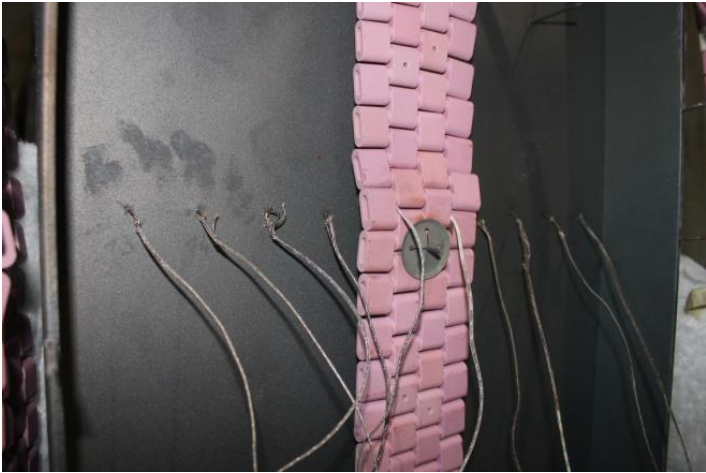
Figure 97: Thermocouples

The temperatures were recorded during the whole duration of each test and at several positions along the web and the flanges of the columns by means of several thermocouples. Calculation of the mean temperature in the steel of the column was possible and the exact temperatures at several positions in order to observe the temperatures distribution and gradients induced along the column by the pad heaters were known. For each test and depending on the geometry of the column, the location of the thermocouple was slightly adapted.

Several displacements were measured by means of displacement transducers. The vertical global extension of the whole column subjected to the fire and to the load was obtained by the mean of the displacements measured by two displacement transducers located at the bottom face of the lower beam of the testing frame. The global deflections at mid-span of the column in the direction of the strong axis and of the weak axis were also measured by means of displacements transducers.

The dimensions of the hot-rolled IPE240A are given in Table 40:

h_w (mm)	t_w (mm)	b (mm)	t_f (mm)	H (mm)
237	5.2	120	8.3	2700

Table 40: Global dimensions of the first tested column

The applied load and the experimental failure temperature for test 1 are given in Table 41:

Cold failure load (kN)	Load applied for the test (kN)	Experimental Failure temperature (°C)
410.3	144.5	610

Table 41: applied load and failure temperature for test 1

With the mean temperature information, the evolution of the transversal displacements as a function of the temperature of the column was obtained and is displayed in the next graph:
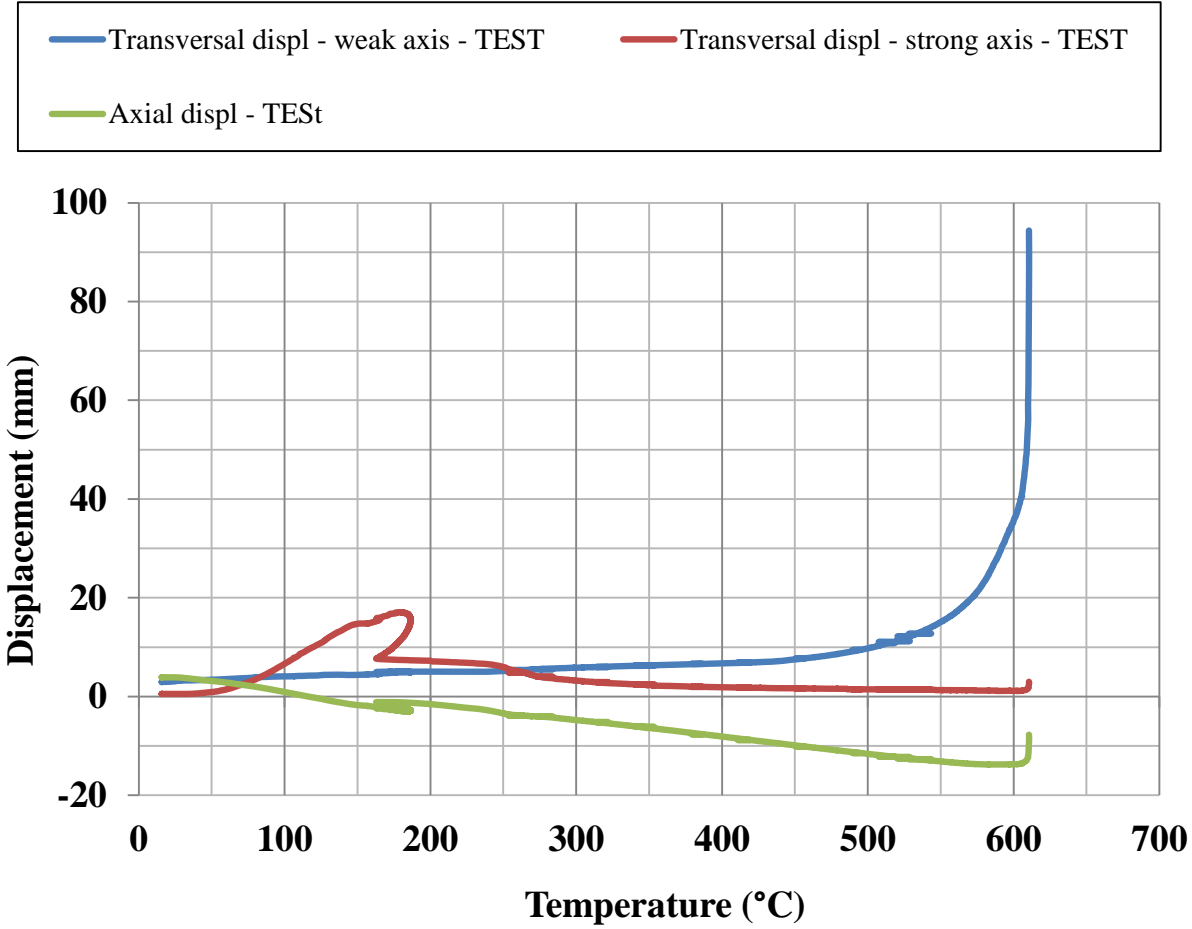
Figure 98: Displacements (mm) in function of the mean temperature (°C)

The deformed shape of the column of test 1 after failure is shown in the following pictures of Figure 99:

Figure 99: Deformed shape after test 1

The dimensions of the welded 450x4+150x5 are given in Table 42:

h_w (mm)	t_w (mm)	b (mm)	t_f (mm)	H (mm)
450	4	150	5	2700

Table 42: Global dimensions of second tested column

The applied load for the test and the experimental temperature are given in Table 43:

Cold failure load (kN)	Load applied for the test (kN)	Experimental Failure temperature (°C)
408	122.4	608

Table 43: applied load and failure temperature for test 2

With the mean temperature information, the evolution of the transversal displacements as a function of the temperature of the column was obtained and is displayed in Figure 100:
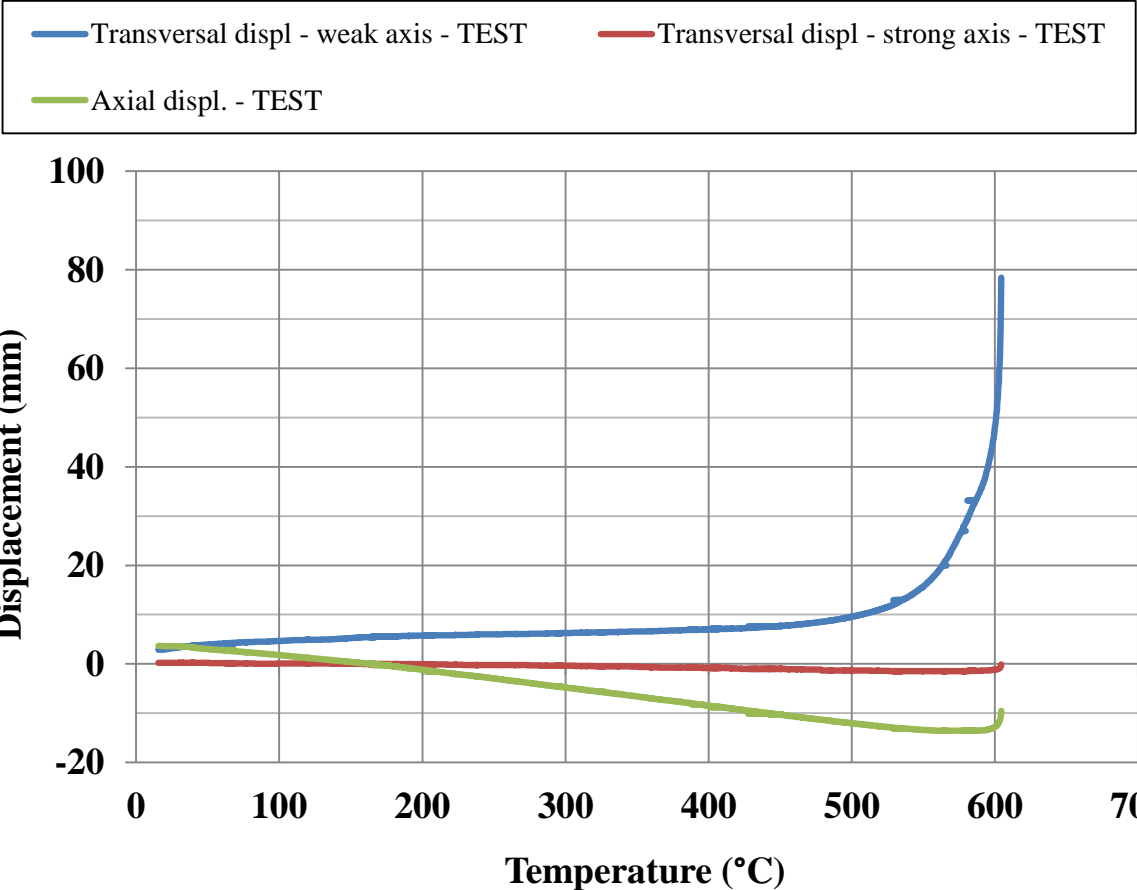
Figure 100: Displacements (mm) in function of the mean temperature (°C)

The deformed shape of column of test 2 after failure is shown in the following pictures of Figure 101:

Figure 101: Deformed shape after test 2

The dimensions of the welded 450x4+150x5 are given in Table 44:

h_w (mm)	t_w (mm)	b (mm)	t_f (mm)	H (mm)
450	4	150	5	2700

Table 44: Global dimensions of the third tested column

The applied load for the test and the experimental failure temperature are given in Table 45:

Cold failure load (kN)	Load applied for the test (kN)	Experimental Failure temperature (°C)
408	204	452

Table 45: applied load and failure temperature for test 3

With the mean temperature information, the evolution of the transversal displacements as a function of the temperature of the column was obtained and is displayed in Figure 102:
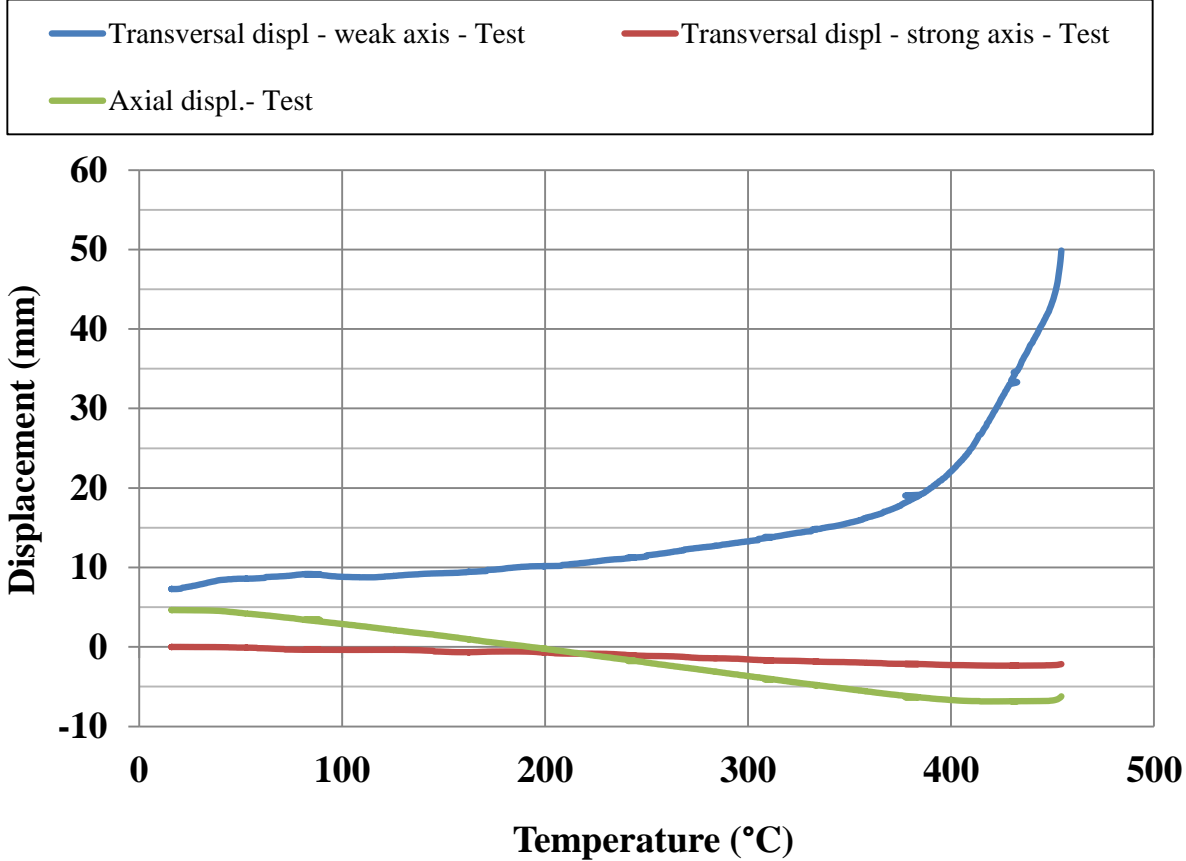
Figure 102: Displacements (mm) in function of the mean temperature (°C)

The deformed shape of column of test 3 after failure is shown in the following pictures of Figure 103:

Figure 103: Deformed shape after test 3

The dimensions of the welded 500-300x4+150x5 are given in Table 46:

h_w (mm)	t_w (mm)	b (mm)	t_f (mm)	H (mm)
300 (small base)	4	150	5	2700
500 (large base)				

Table 46: Global dimensions of the fourth tested column

The applied load for the test and experimental failure temperature are given in Table 47:

Cold failure load (kN)	Load applied for the test (kN)	Experimental Failure temperature (°C)
696	348	520

Table 47: applied load and failure temperature for test 4

With the mean temperature information, the evolution of the transversal displacements as a function of the temperature of the column was obtained and is displayed in Figure 104:
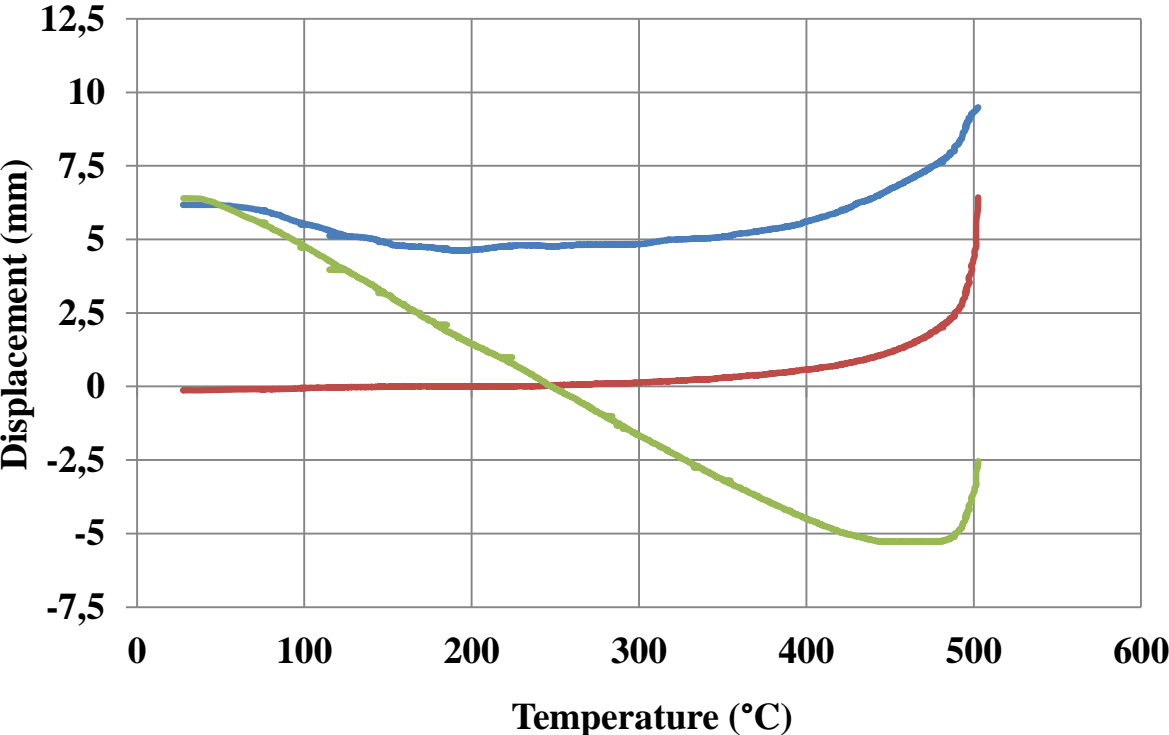
Figure 104: Displacements (mm) in function of the mean temperature (°C)

The deformed shape of column of test 4 after failure is shown in the following pictures of Figure 105:

Figure 105: Deformed shape after test 4

Several numerical simulations were conducted in order to catch with the experimental results obtained with the fire tests. The objective was to simulate the tests using the measured properties of the steel of the columns, the measured global and local imperfections, the measured temperature distribution along the column, the measured value of the load and the measured eccentricities of the load applied with the testing frame.

Table 48 illustrates the results obtained in the first fire test compared with the results obtained with both computer codes ABAQUS and SAFIR:

Failure temperature (°C)					
Test	**ABAQUS**	**ε (%)**	**Test**	**SAFIR**	**ε (%)**
610	587.3	-3.7	610	572.1	-6.2

Table 48: Failure temperature of simulations compared with experimental test

The following diagram of Figure 106 illustrates the displacements of the column in function of the mean temperature for both experimental test and SAFIR simulation:
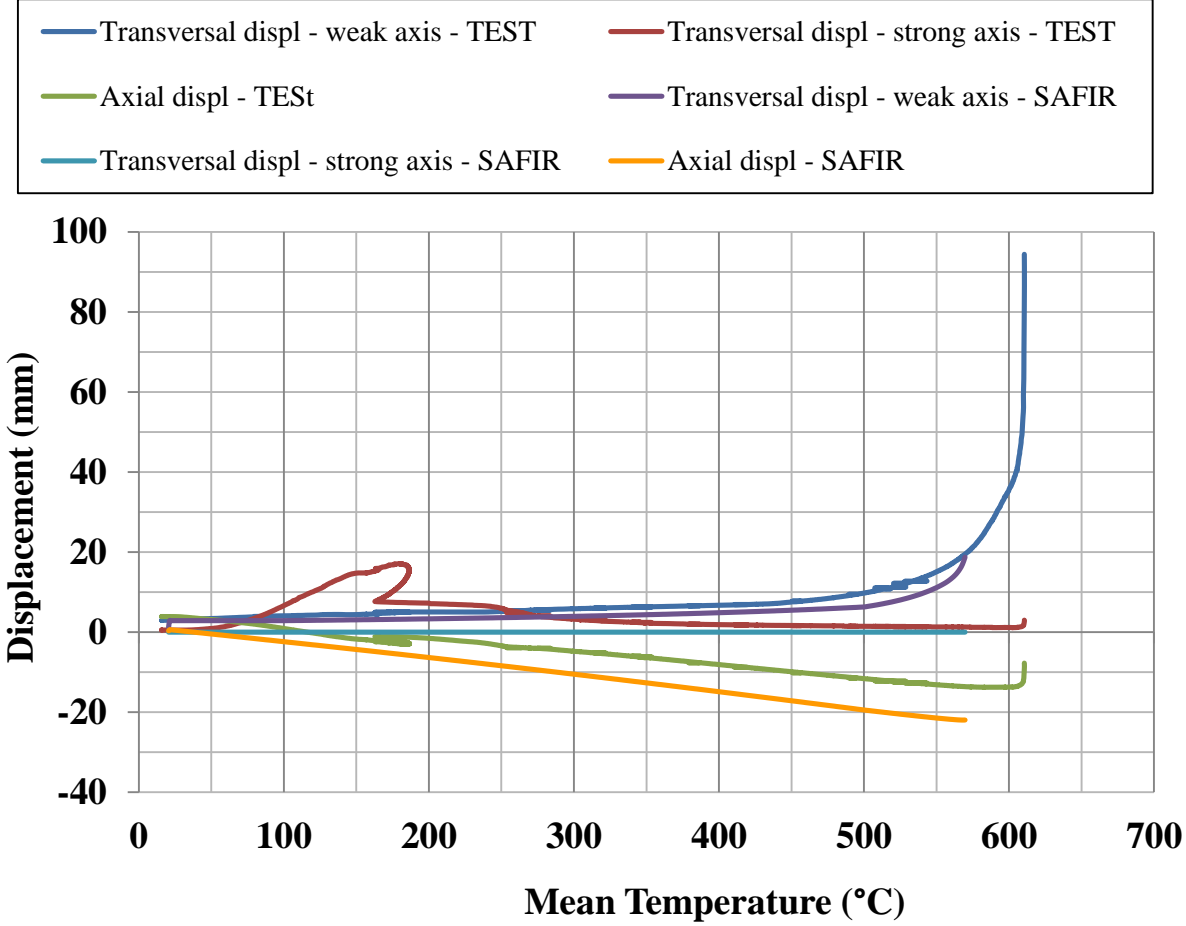
Figure 106: Displacements (mm) in function of temperature (°C) – SAFIR comparison

The following chart of Figure 107 illustrates the displacements of the column in function of the mean temperature for both experimental test and ABAQUS simulation:
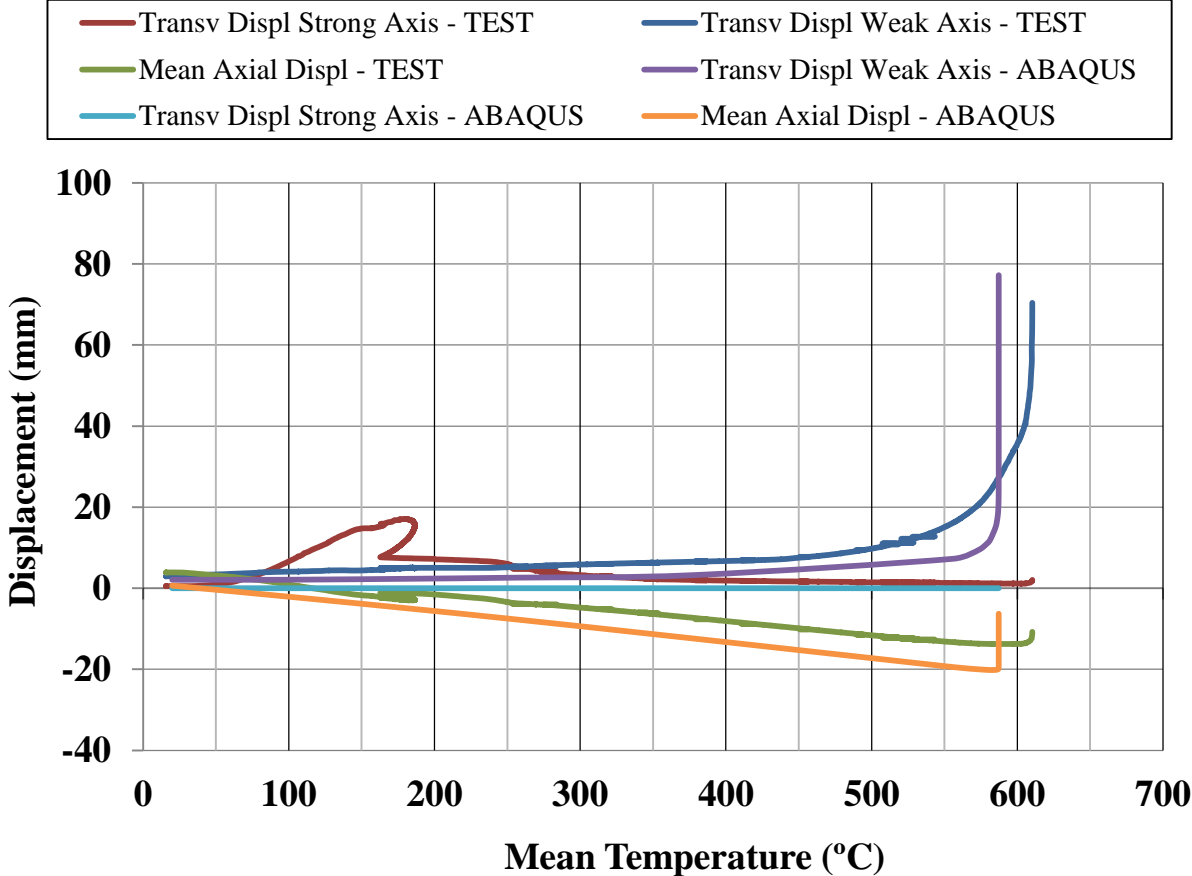
Figure 107: Displacements (mm) in function of temperature (°C) – ABAQUS comparison

The failure mode obtained numerically with SAFIR was a global buckling along the weak axis as the experimental failure mode, as illustrated in Figure 108:
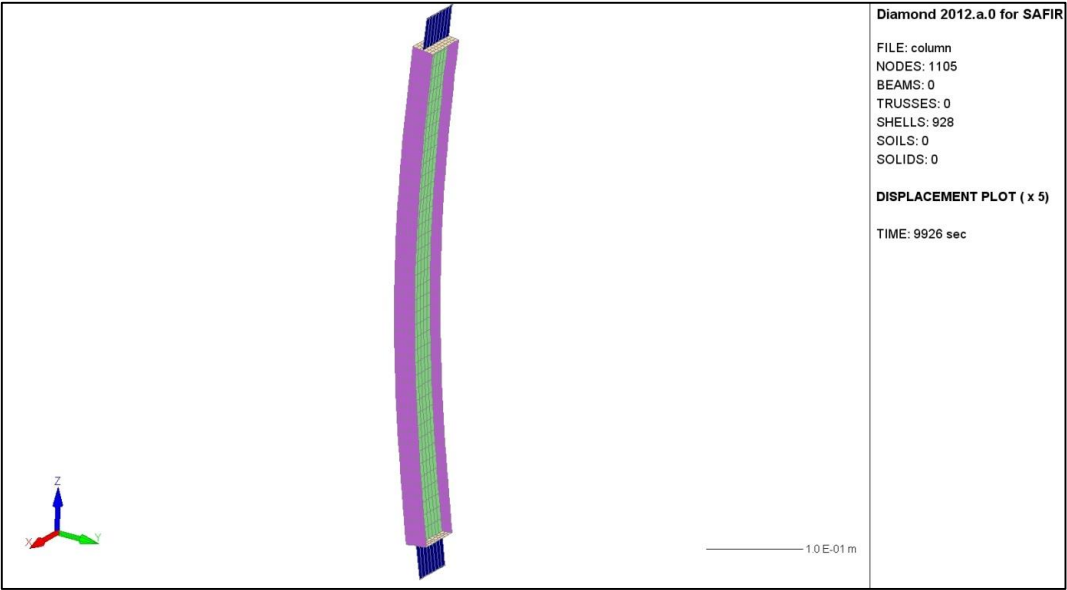
Figure 108: Numerical failure mode obtained with SAFIR

The failure mode obtained numerically with ABAQUS was a global buckling along the weak axis as the experimental failure mode:
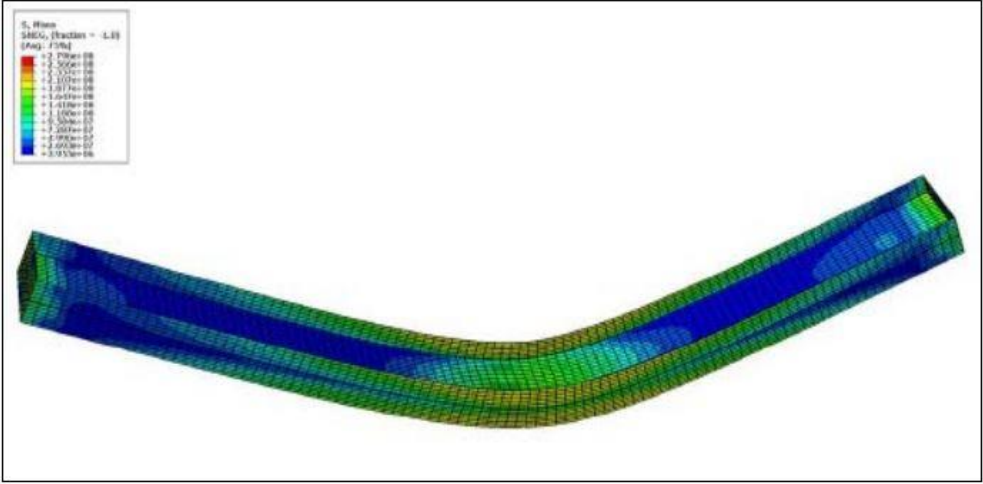
Figure 109: Numerical failure mode obtained with ABAQUS

Table 49 illustrates the results obtained in the second fire test compared with the results obtained with both computer codes ABAQUS and SAFIR:

Failure temperature (°C)					
Test	ABAQUS	ε (%)	Test	SAFIR	ε (%)
608	597.3	-1.8	608	594.7	-2.2

Table 49: Failure temperature of simulations compared with experimental test

The following diagram of Figure 110 illustrates the displacements of the column in function of the mean temperature for both experimental test and SAFIR simulation:
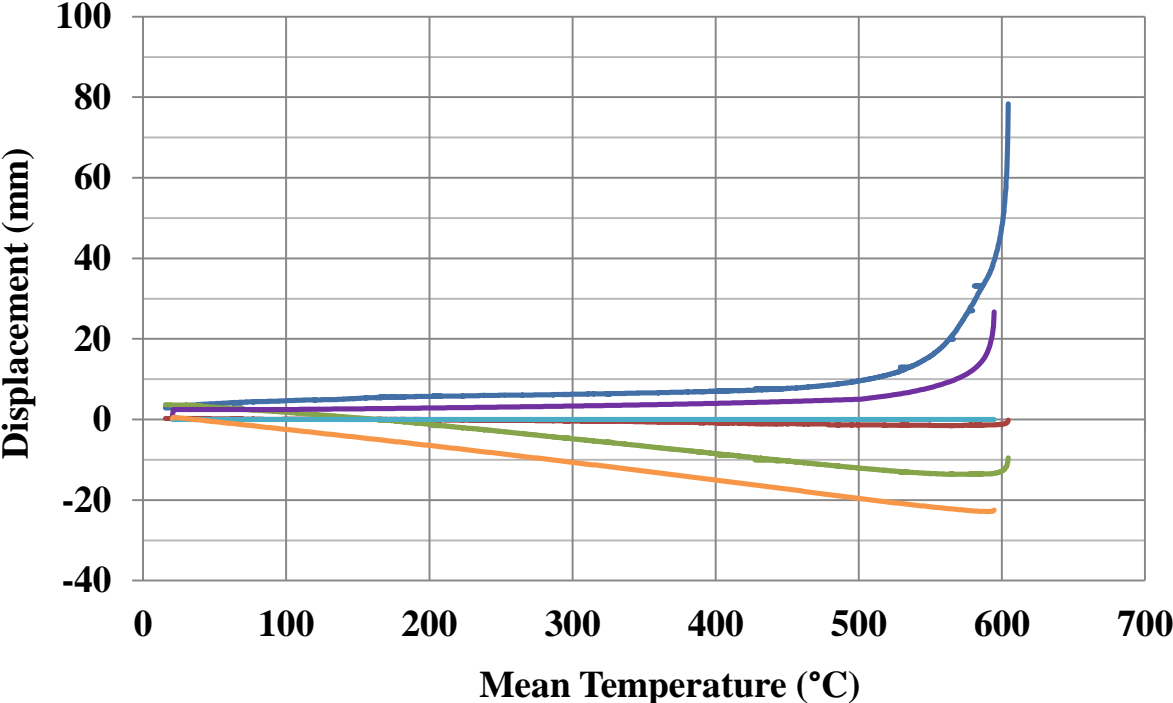
Figure 110: Displacements (mm) in function of temperature (°C) – SAFIR comparison

Figure 111 illustrates the displacements of the column in function of the mean temperature for both experimental test and ABAQUS simulation:
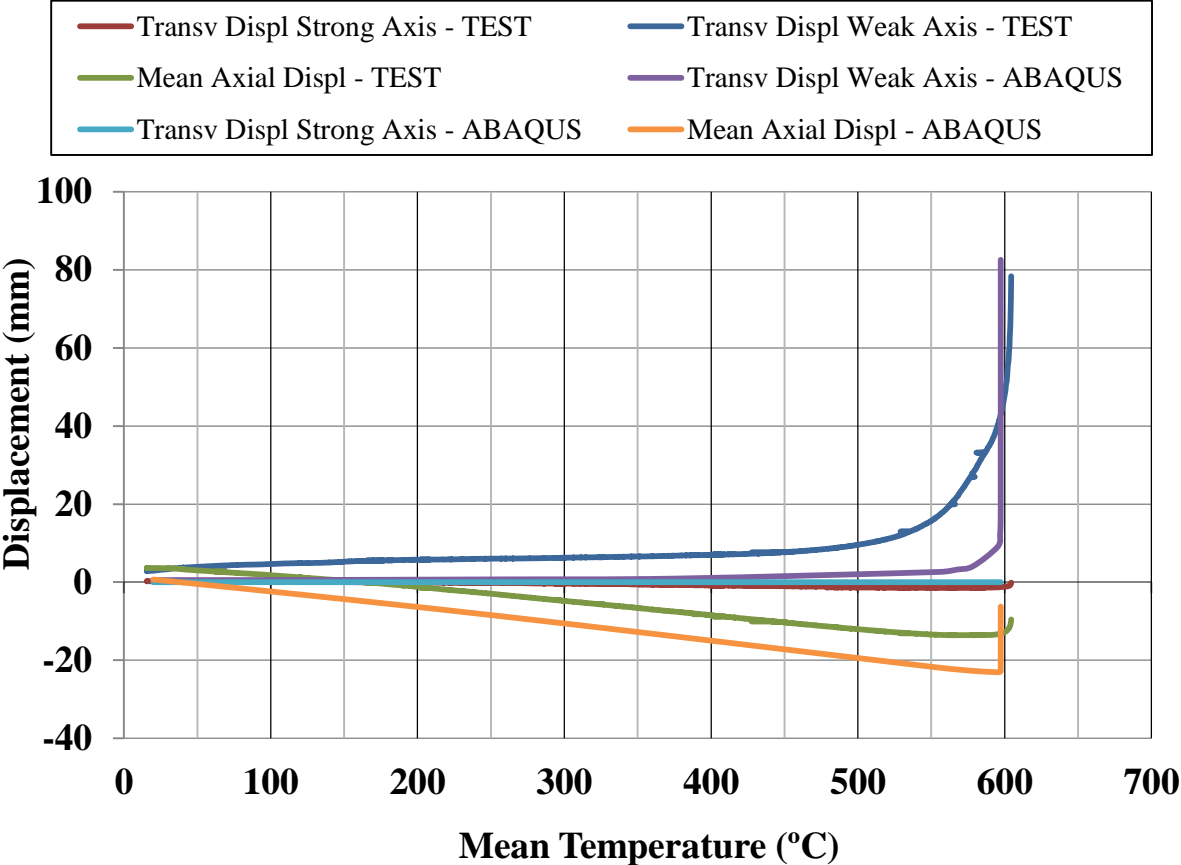
Figure 111: Displacements (mm) in function of temperature (°C) – ABAQUS comparison

The failure mode obtained numerically with SAFIR was a global buckling along the weak axis with a local buckling of the flange at mid-high of the column, as illustrated in Figure 112:
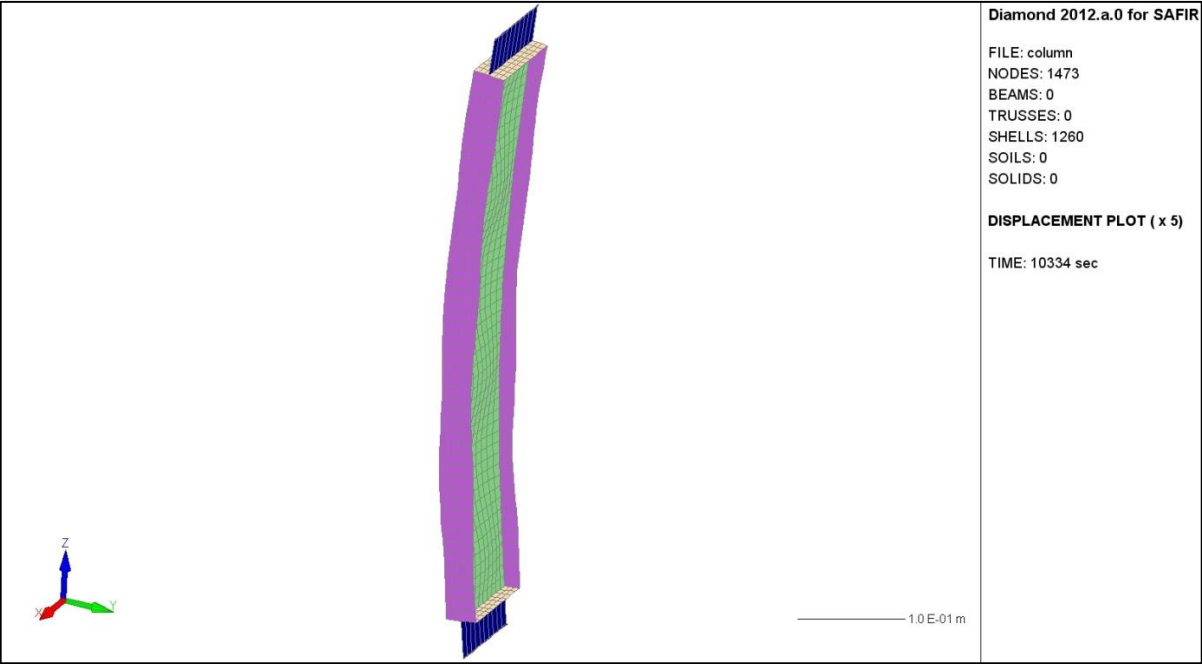
Figure 112: Numerical failure mode obtained with SAFIR

The failure mode obtained numerically with ABAQUS was a global buckling along the weak axis as the experimental failure mode:
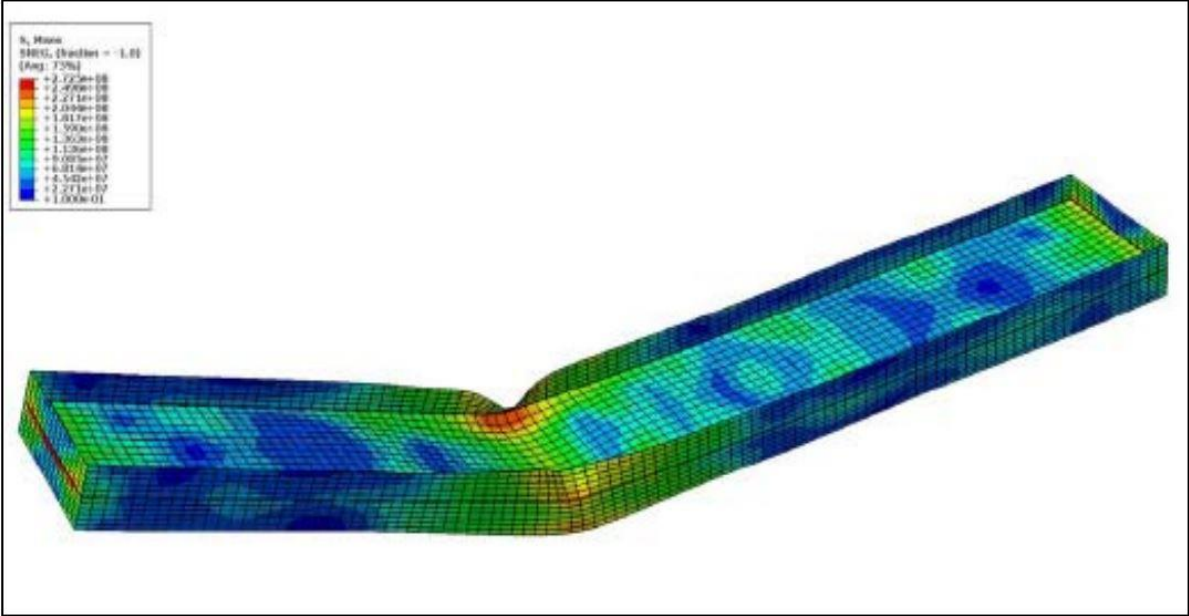
Figure 113: Numerical failure mode obtained with ABAQUS

Table 50 illustrates the results obtained in the third fire test compared with the results obtained with both computer codes ABAQUS and SAFIR:

Failure temperature (°C)					
Test	ABAQUS	ε (%)	Test	SAFIR	ε (%)
452	445.6	-1.4	452	459	1.5

Table 50: Failure temperature of simulations compared with experimental test

The following chart of Figure 114 illustrates the displacements of the column in function of the mean temperature for both experimental test and SAFIR simulation:
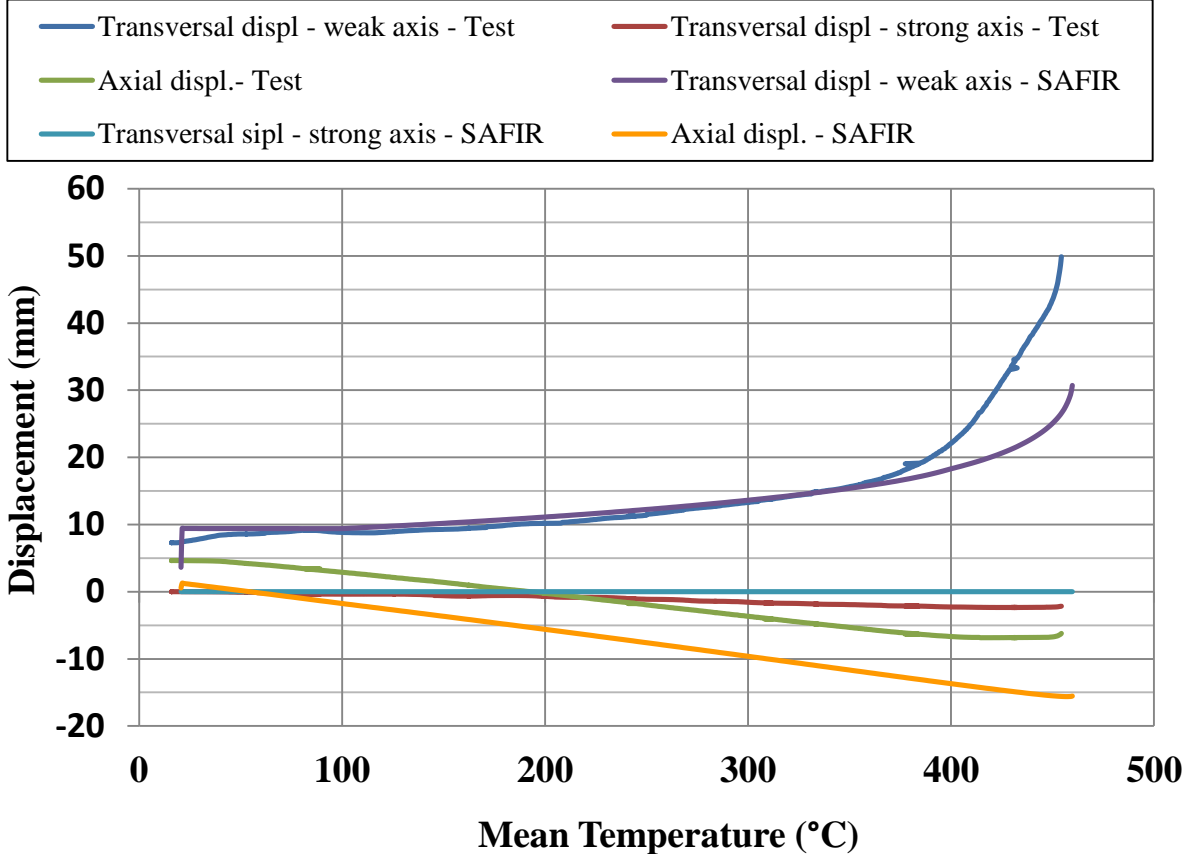
Figure 114: Displacements (mm) in function of temperature (°C) – SAFIR comparison

The following diagram of Figure 115 illustrates the displacements of the column in function of the mean temperature for both experimental test and ABAQUS simulation:
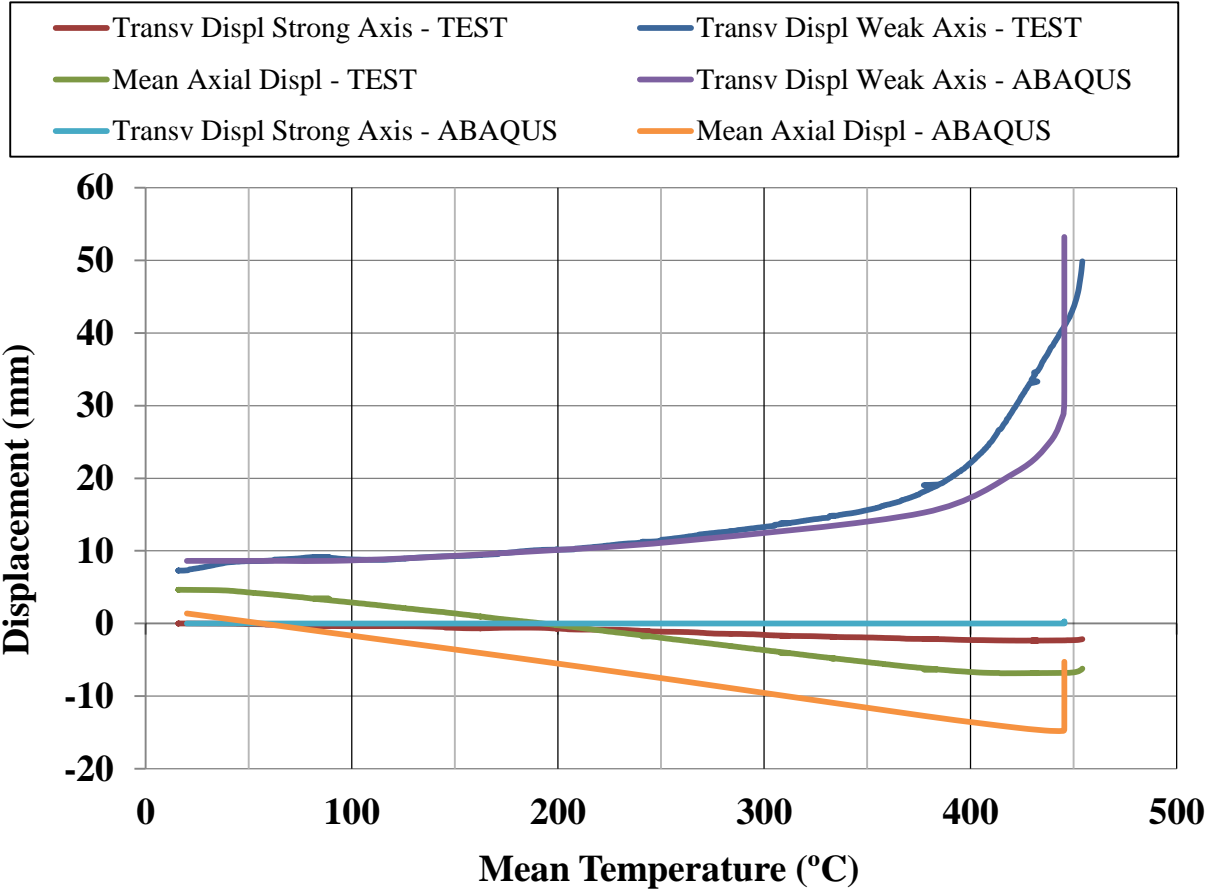
Figure 115: Displacements (mm) in function of temperature (°C) – ABAQUS comparison

The failure mode obtained numerically in SAFIR was a global buckling along the weak axis with a local buckling of the flange at mid-high of the column:
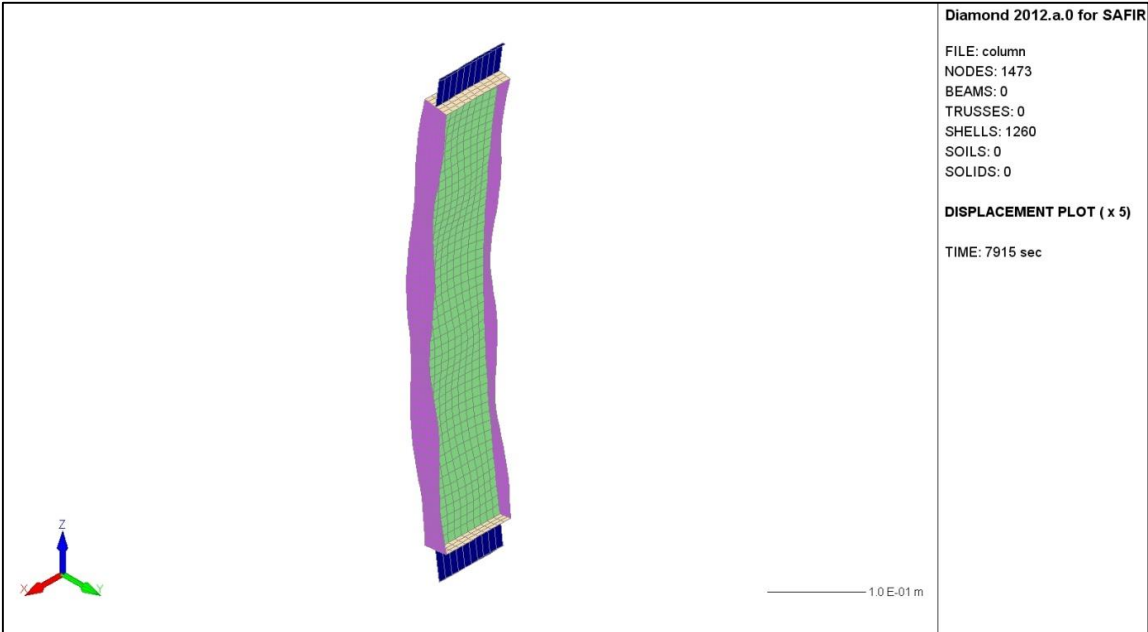
Figure 116: Numerical failure mode obtained with SAFIR

The failure mode obtained numerically with ABAQUS was a global buckling along the weak axis as the experimental failure mode:
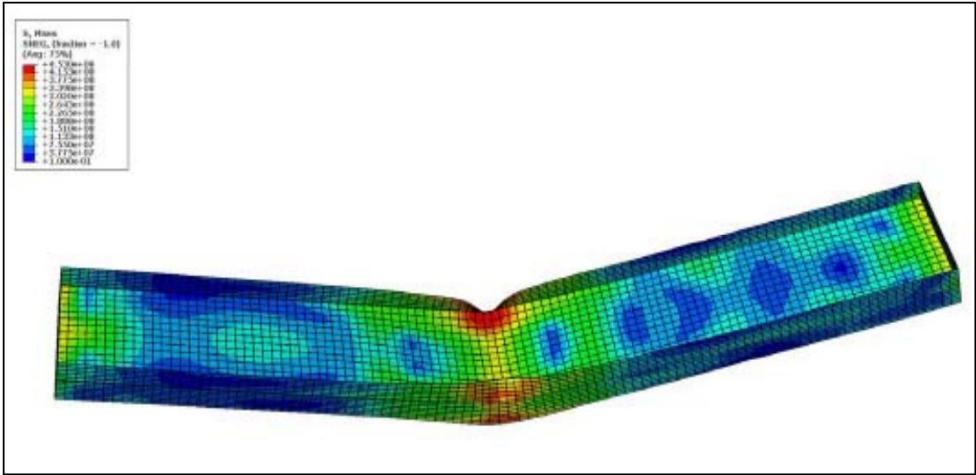
Figure 117: Numerical failure mode obtained with ABAQUS

Table 51 illustrates the results obtained in the fourth fire test compared with the results obtained with both computer codes ABAQUS and SAFIR:

Failure temperature (°C)					
Test	ABAQUS	ε (%)	Test	SAFIR	ε (%)
519.5	533.9	2.8	519.5	535	2.9

Table 51: Failure temperature of simulations compared with experimental test

The following diagram illustrates the displacements of the column in function of the mean temperature for both experimental test and SAFIR simulation:
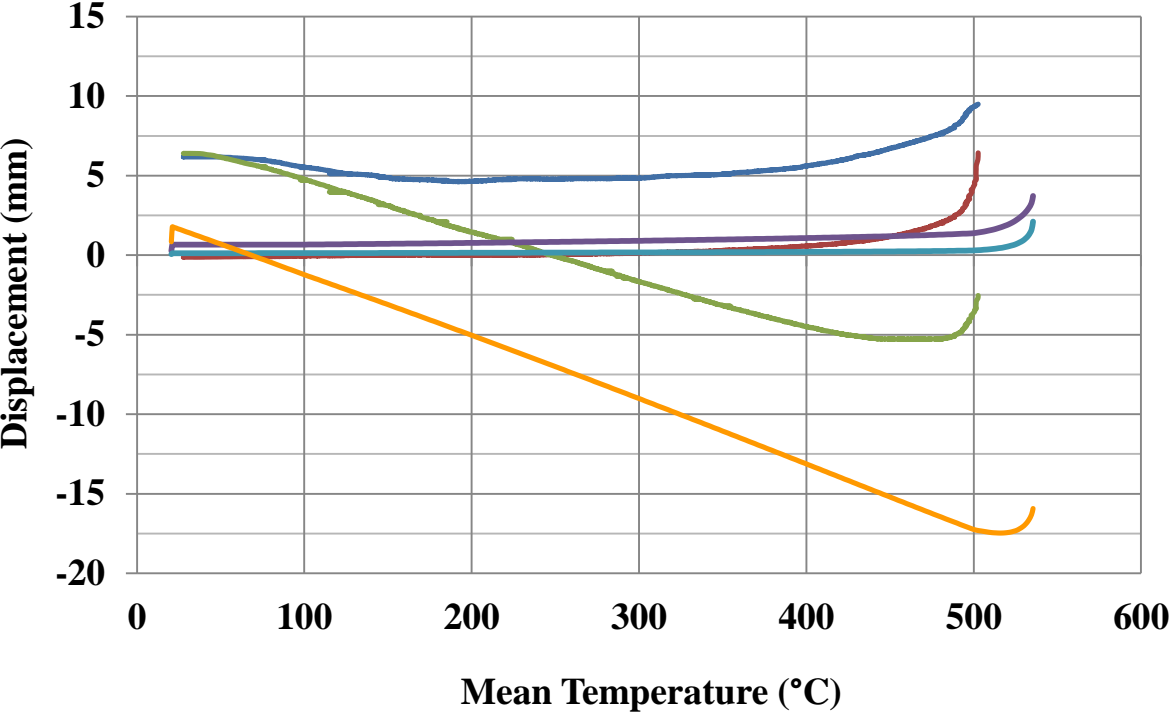
Figure 118: Displacements (mm) in function of temperature (°C) – SAFIR comparison

The following diagram illustrates the displacements of the column in function of the mean temperature for both experimental test and ABAQUS simulation:
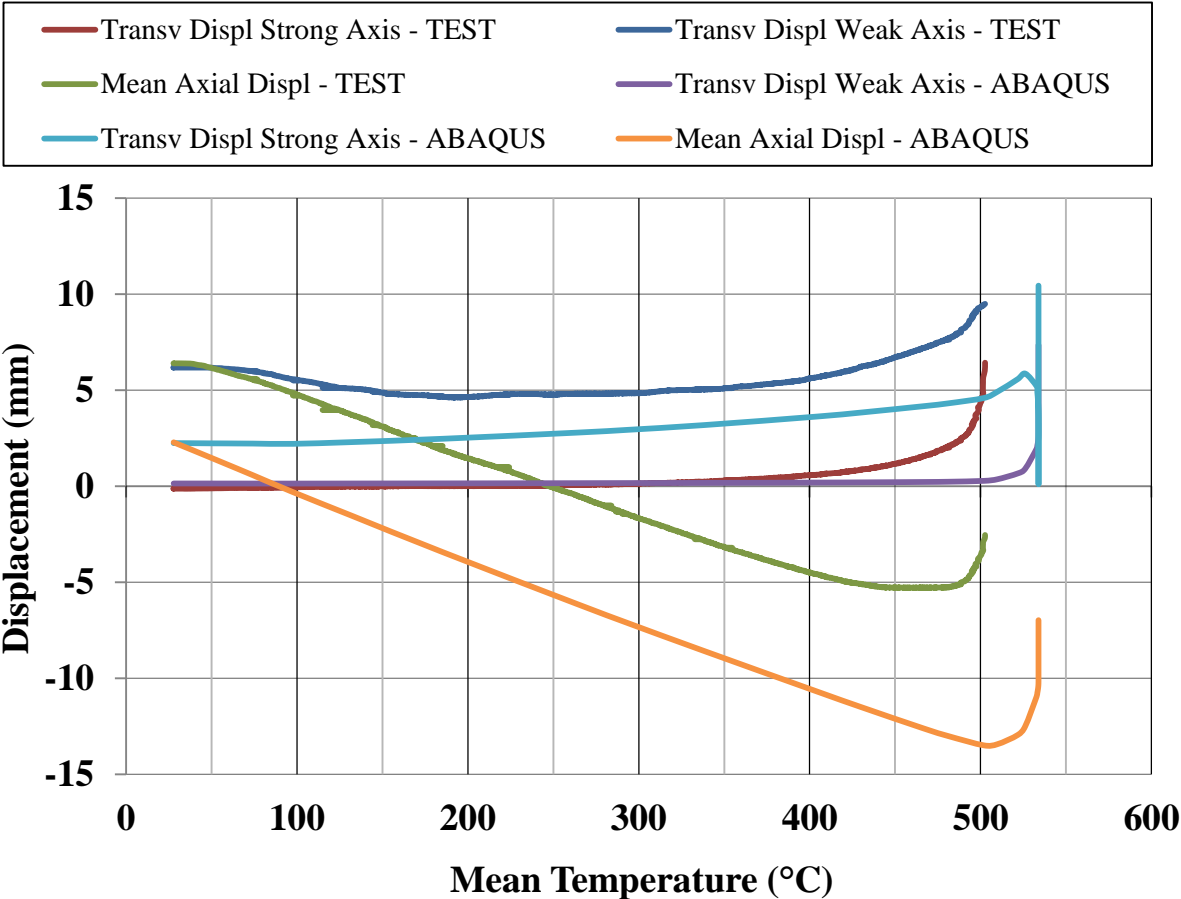
Figure 119: Displacements (mm) in function of temperature (°C) – ABAQUS comparison

The failure mode obtained numerically in SAFIR was a global buckling along the weak axis with a local buckling of the flange at mid-high of the column:
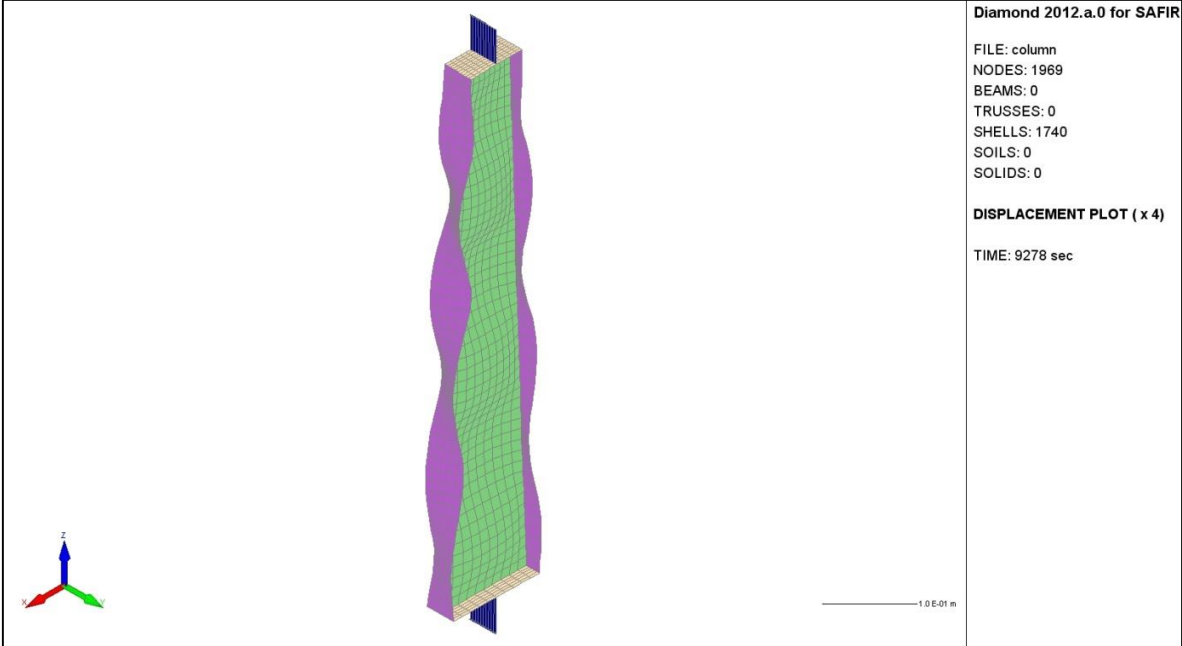
Figure 120: Numerical failure mode obtained with SAFIR

The failure mode obtained numerically with ABAQUS was a global buckling along the weak axis as the experimental failure mode:
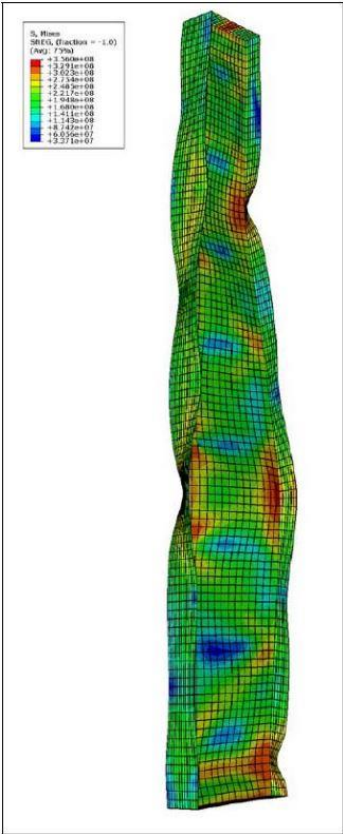
Figure 121: Numerical failure mode obtained with ABAQUS

2.2.4.2 General principles of simple design rules

As a first step in this part, the load bearing capacity of the columns is calculated with the simple design rules recommended by EN 1993-1-2. The formulae are presented here after. Both strong axis buckling and weak axis buckling are treated. The first step is the evaluation of the critical compressive load defined for strong axis buckling as:

$$N_{cr-strong} = \frac{\pi^2 \, E \, I}{(L_{strong})^2}$$

(30)

With I representing the inertia along the strong axis, E the Young modulus and L_{strong} is the buckling length along strong axis. For weak axis buckling the critical compressive load is defined as follow:

$$N_{cr-weak} = \frac{\pi^2 \, E \, I}{(L_{weak})^2}$$

(31)

With L_{weak} representing the buckling length along the weak axis of the column.

The following step is the evaluation of the non-dimensional slenderness of the column along strong axis:

$$\lambda_{strong} = \sqrt{A_{eff} \, f_y \Big/ N_{cr-strong}}$$

(32)

And weak axis:

$$\lambda_{weak} = \sqrt{A_{eff} \, f_y \Big/ N_{cr-weak}}$$

(33)

105

With A_{eff} representing the effective area of the class 4 cross-section in pure compression. f_y is the Yield strength of steel at room temperature.

The effective non-dimensional slenderness to take account for is defined as the maximum of non-dimensional slenderness:

$$\lambda = \max(\lambda_{strong}; \lambda_{weak}) \tag{34}$$

At high temperature the non-dimension slenderness becomes:

$$\bar{\lambda}_\theta = \lambda \sqrt{k_{0.2,\theta}/k_{E,\theta}} \tag{35}$$

The value of reduction factor is determined according to the following equations:

$$\chi_{fi} = \frac{1}{\varphi_\theta + \sqrt{\varphi_\theta^2 - \lambda_\theta^2}} \tag{36}$$

With:

$$\varphi_\theta = 0.5 \times (1 + \alpha \times \lambda_\theta + \lambda_\theta^2) \tag{37}$$

And α is an imperfection factor corresponding to the cross-sections dimensions. The values are given from the following equation:

$$\alpha = 0.65 \times \sqrt{235/f_y} \tag{38}$$

Finally, the compressive buckling resistance in the fire design situation is finally obtained with the following formula:

$$N_{b,fi,Rd} = \chi_{fi} \times A_{eff} \times k_{0.2,\theta} \times f_y \tag{39}$$

2.2.4.3 Comparison of the numerical results with current simple design rules of EN 1993-1-2

The ratio between the failure load obtained through the numerical analysis and the failure load obtained with the simple design rules provided by EN 1993-1-2 [1] was calculated for each column, and then, the mean, the standard deviation and the covariance are calculated for all of them:

	EN 1993-1-2
Average ratio (design rule / FEM)	0.92
Percentage of unsafe points (%)	6.35
Maximum unsafe ratio	1.15
Percentage of safe points by more than 15% (%)	23.14
Standard deviation	6.3
Coefficient of variation	6.8

Table 52: Statistical data of comparison with EN 1993-1-2

The comparisons between the numerical simulations and the design points of EN 1993-1-2 for investigated cross-sections are given in the following chart of Figure 122 :
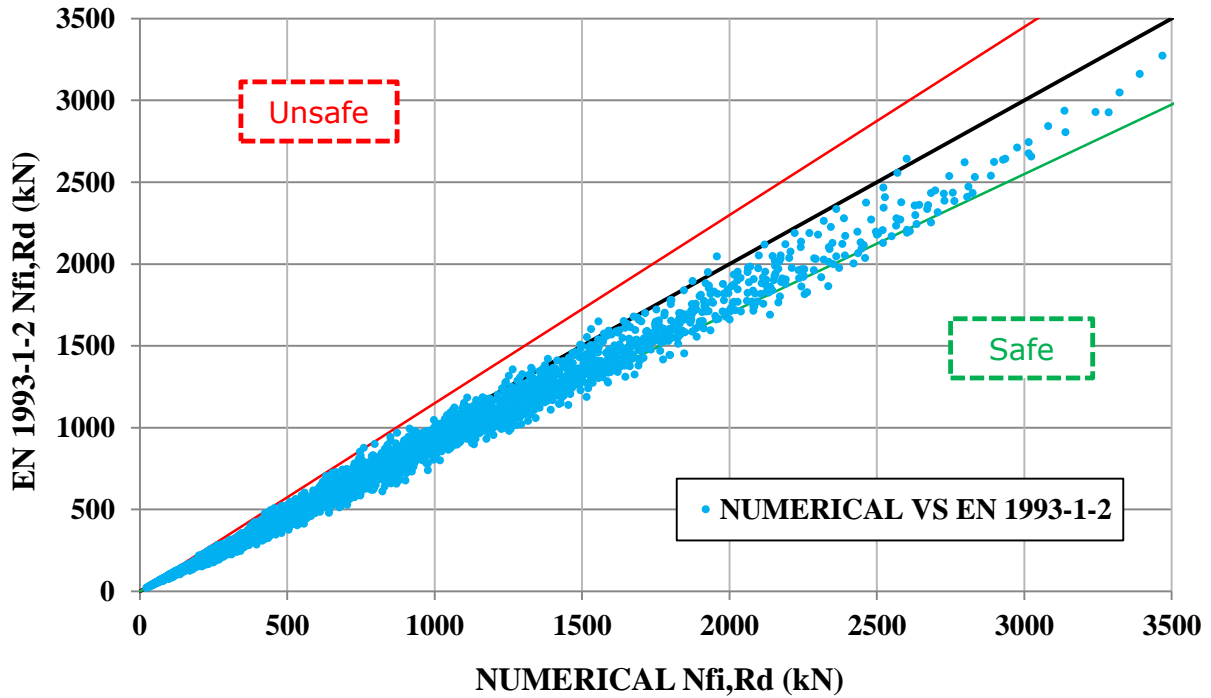
Figure 122: Comparison between EN 1993-1-2 design rules and numerical results for investigated cross-sections

The values presented in Figure 122 show that the current method recommended by EN 1993-1-2 is safe. This method is even too safe and un-economical in numerous cases, and the load bearing capacity calculated with formula from EN 1993-1-2 could be increased to obtain a more economical design. Therefore, new simple design rules are proposed with the objective of improving those results and the competitiveness of class 4 steel columns. The comparisons between the new design rules and the numerical simulations are described in the following part.

2.2.4.4 *New design rules for axial compression buckling and confrontation with the numerical results*

The key point of this new proposed design rule was the use of the new effective cross-section calculation method defined for cross-sectional resistance and described in 2.2.2.4. With this method, the effective area of the cross-section in compression was evaluated. Then, it was proposed to replace current $k_{0.2p,\theta}$ by $k_{y,\theta}$ as it was done for effective cross-section calculation too. The new method is described in the equations below:

$$N_{cr-strong} = \frac{\pi^2 \, E \, I}{(L_{strong})^2}$$

(40)

With I representing the inertia along the strong axis, E the Young modulus and L_{strong} is the buckling length along strong axis. For weak axis buckling the critical compressive load is defined as follow:

$$N_{cr-weak} = \frac{\pi^2 \, E \, I}{(L_{weak})^2}$$

(41)

With L_{weak} represents the buckling length along the weak axis of the column.

The following step is the evaluation of the non-dimensional slenderness of the column along strong axis:

$$\lambda_{strong} = \sqrt{\frac{A_{eff} \, f_y}{N_{cr-strong}}}$$

(42)

And weak axis:

$$\lambda_{weak} = \sqrt{\frac{A_{eff}\ f_y}{N_{cr-weak}}} \qquad (43)$$

With A_{eff} representing the effective area of the class 4 cross-section in pure compression calculated with the new design method of this project. f_y is the Yield strength of steel at room temperature.

The effective non-dimensional slenderness to take account for is defined as the maximum of non-dimensional slenderness:

$$\lambda = \max(\lambda_{strong}; \lambda_{weak}) \qquad (44)$$

At high temperature the non-dimension slenderness becomes:

$$\bar{\lambda}_\theta = \lambda \sqrt{k_{y,\theta}\big/k_{E,\theta}} \qquad (45)$$

The value of reduction factor is determined according to the following equations:

$$\chi_{fi} = \frac{1}{\varphi_\theta + \sqrt{\varphi_\theta^2 - \lambda_\theta^2}} \qquad (46)$$

With:

$$\varphi_\theta = 0.5 \times (1 + \alpha \times \lambda_\theta + \lambda_\theta^2) \qquad (47)$$

And α is an imperfection factor corresponding to the cross-sections dimensions. The values are given from the following equation:

$$\alpha = 0.65 \times \sqrt{235\big/f_y} \qquad (48)$$

The compressive buckling resistance in the fire design situation is finally obtained with the following formula:

$$N_{b,fi,Rd} = \chi_{fi} \times A_{eff} \times k_{y,\theta} \times f_y \qquad (49)$$

The ratio between the failure load obtained through the numerical analysis and the failure load obtained with new proposed simple design rules was calculated for each column, and then, the mean, the standard deviation and the covariance were calculated for all of them:

	NEW DESIGN RULES
Average ratio (design rule / FEM)	0.94
Percentage of unsafe points (%)	15.7
Maximum unsafe ratio	1.11
Percentage of safe points by more than 15% (%)	10.6
Standard deviation	0.58
Coefficient of variation	0.61

Table 53: Statistical data of comparison with new design rule

The comparisons between the numerical simulations and the design points of the new proposed design rules for investigated cross-sections are given in the following chart of Figure 123:
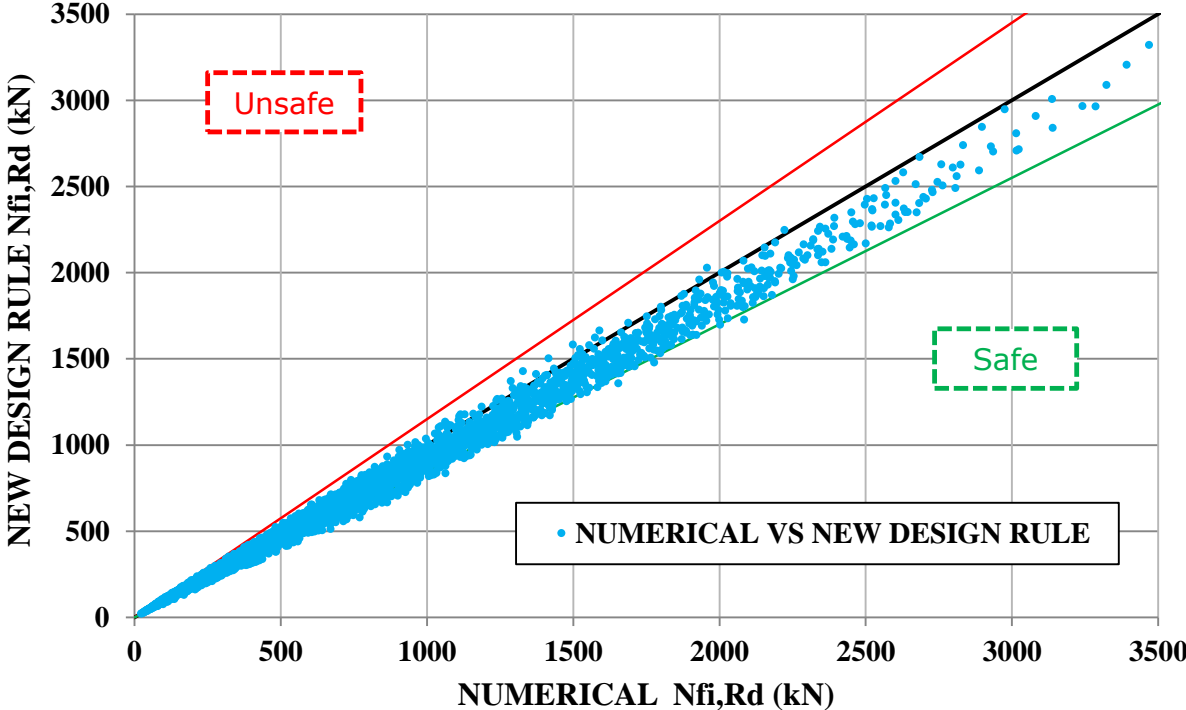
Figure 123: Comparison between new design rules and numerical results for investigated cross-sections

The new proposed design rules rely on the new definition of the effective cross-section area calculation defined in 2.2.2.4. The form of the rule remains very close to the current one of the EN 1993-1-2 except the use of $k_{y,\theta}$ reduction factor instead of $k_{0.2p,\theta}$ factor, which is in accordance with previous defined design rules. Theses design rules remain safe enough, propose a more accurate comparison and decrease the number of uneconomical cases which do not propose an economic design of class 4 steel columns.

Another formulation is proposed to get a more economical new design rule. The change occurs in the following definition:

$$\alpha = 0.55 \times \sqrt{235/f_y} \tag{50}$$

This new definitions offsets the reduction factor toward a more economical value. Using this new design equation, the statistical data are given in Table 54:

	NEW DESIGN RULES
Average ratio (design rule / FEM)	0.96
Percentage of unsafe points (%)	26.3
Maximum unsafe ratio	1.15
Percentage of safe points by more than 15% (%)	6.3
Standard deviation	0.61
Coefficient of variation	0.64

Table 54: Statistical data of comparison with new design rule

The comparisons between the numerical simulations and the design points of the new proposed design rules for investigated cross-sections are given in the following chart of Figure 124:
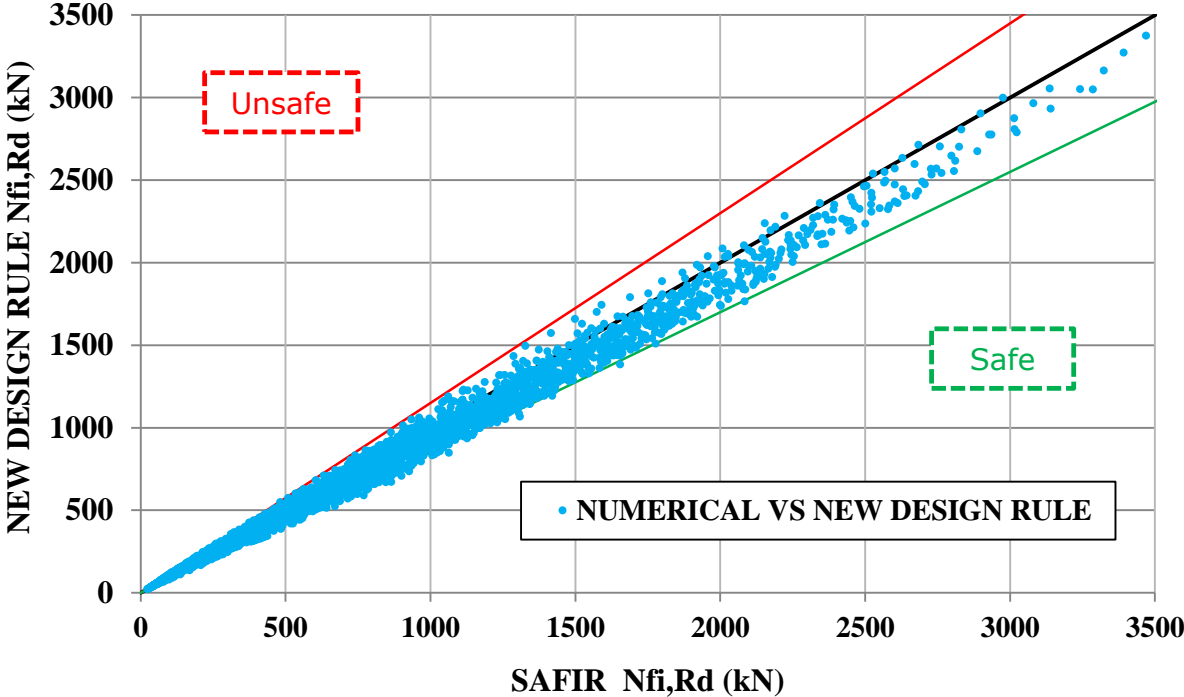
Figure 124: Comparison between adapted new design rules and numerical results for investigated cross-sections

However, with this formulation, about 30% of the design resistances are situated on the unsafe side which remains acceptable knowing that only one case on to the more than 4000 simulations is unsafe by more than 15%. This proposition can be debated in the future project teams to approve or not its inclusion in a revised version of the EN 1993-1-2.

2.2.5 WP5 - Combined bending and compression for class 4 beam-columns

2.2.5.1 Experimental investigation

The four tested columns which were subjected to combined compression and bending and the different tested cross-sections are given hereafter. One cross-section was a hot-rolled HE340AA. The three other columns were made of welded cross-sections. Table 55 describes the main parameters taken into account for these tests:

Test number	Cross-section	Strong axis λ_p	Weak axis λ_p
Test 5 & 6	Constant – 350x4+150x5	0.212	0.991
Test 7	Constant – HE340AA	0.256	0.478
Test 8	Tapered – 440-340x4+150x5	0.164	0.995

Table 55: List of columns subjected to combined compression and bending

The tested columns and corresponding cross-sections are illustrated in Figure 125, Figure 126, Figure 127 and Figure 128.

The load was applied with an eccentricity of 71 mm in the direction of the strong axis. For this test the eccentricity of the load and of the support were arranged in such a way us to produce a uniform bending moment distribution ($\psi = 1$):
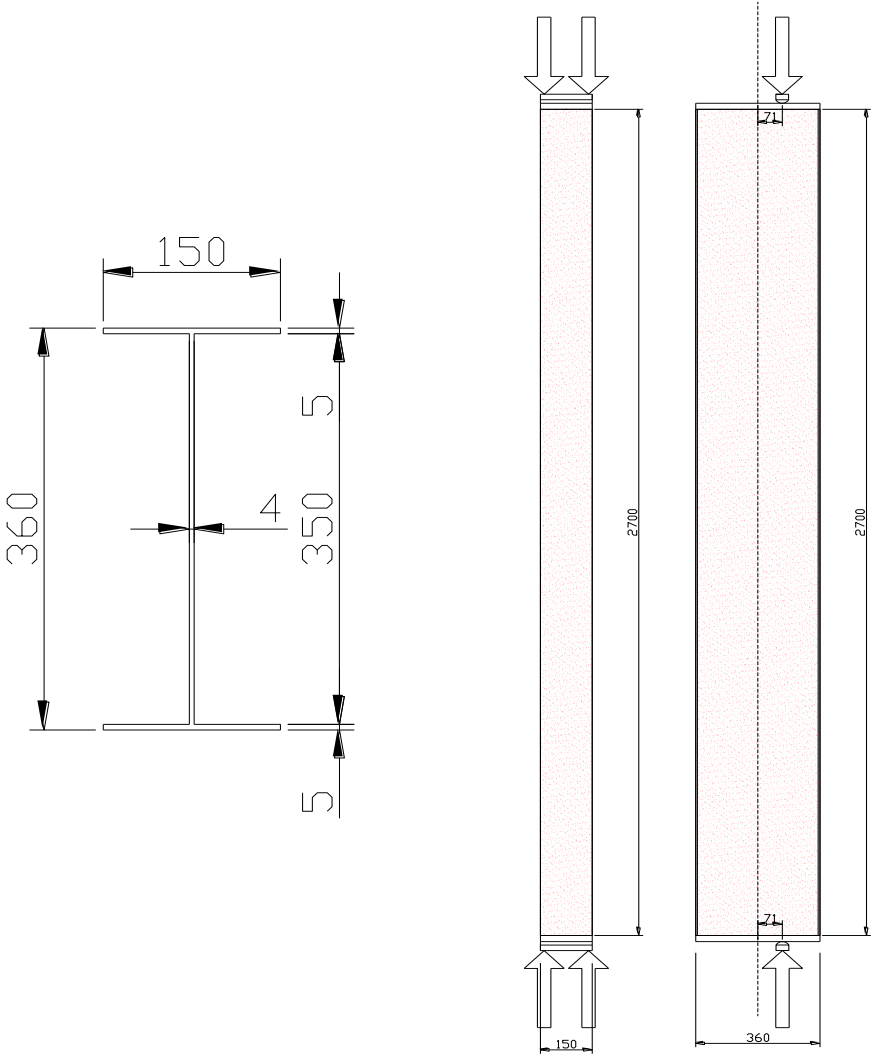
Figure 125: Cross-section design and global design of the tests 5

The same column geometry and test set-up as the fifth test was used. However, the eccentricity of the applied load was larger. Indeed the load was applied with an eccentricity of 177.5 mm. in the direction of the strong axis:
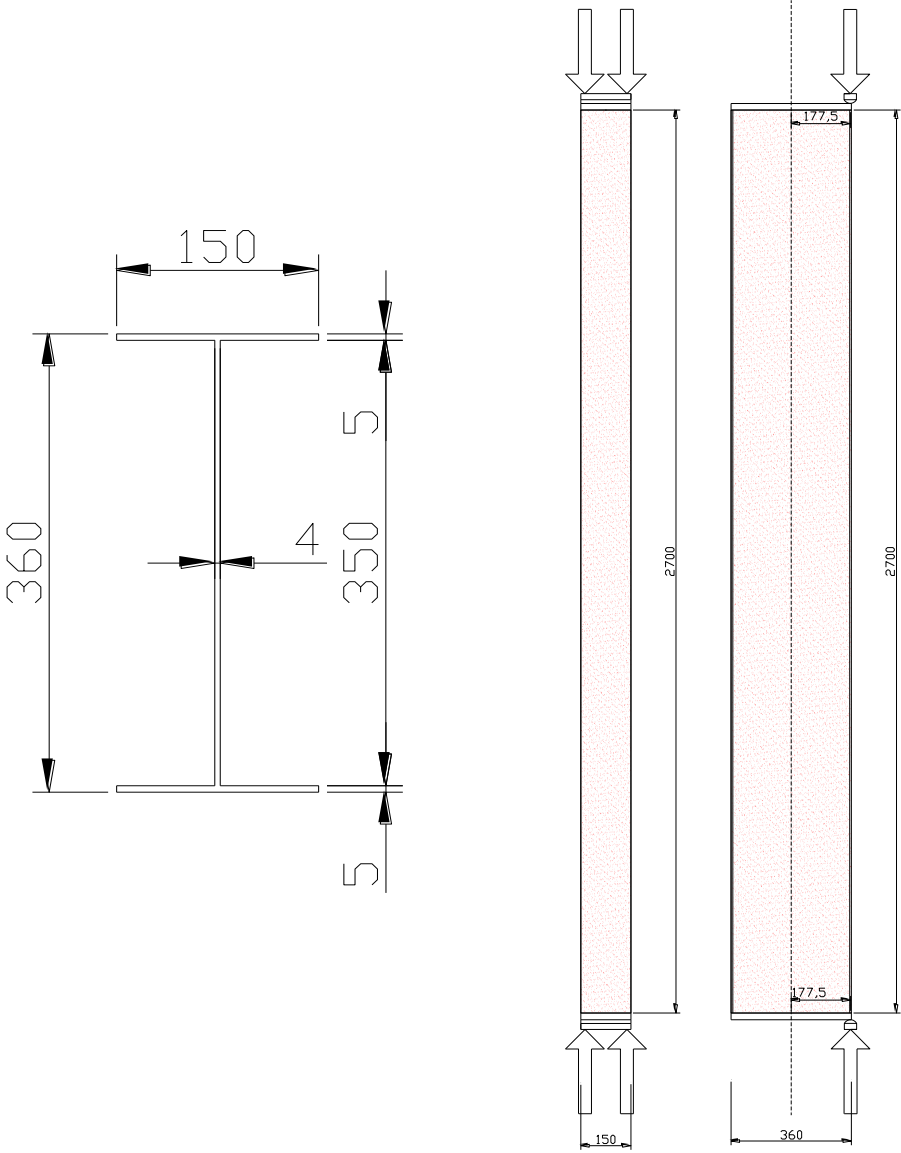
Figure 126: Cross-section design and global design of the tests 6

The load was applied with an eccentricity of 100 mm. in the direction of the strong axis at the top of the column and without eccentricity at the other extremity. For this test the eccentricity of the load and of the support were arranged in such a way us to produce a triangular bending moment distribution ($\psi = 0$):
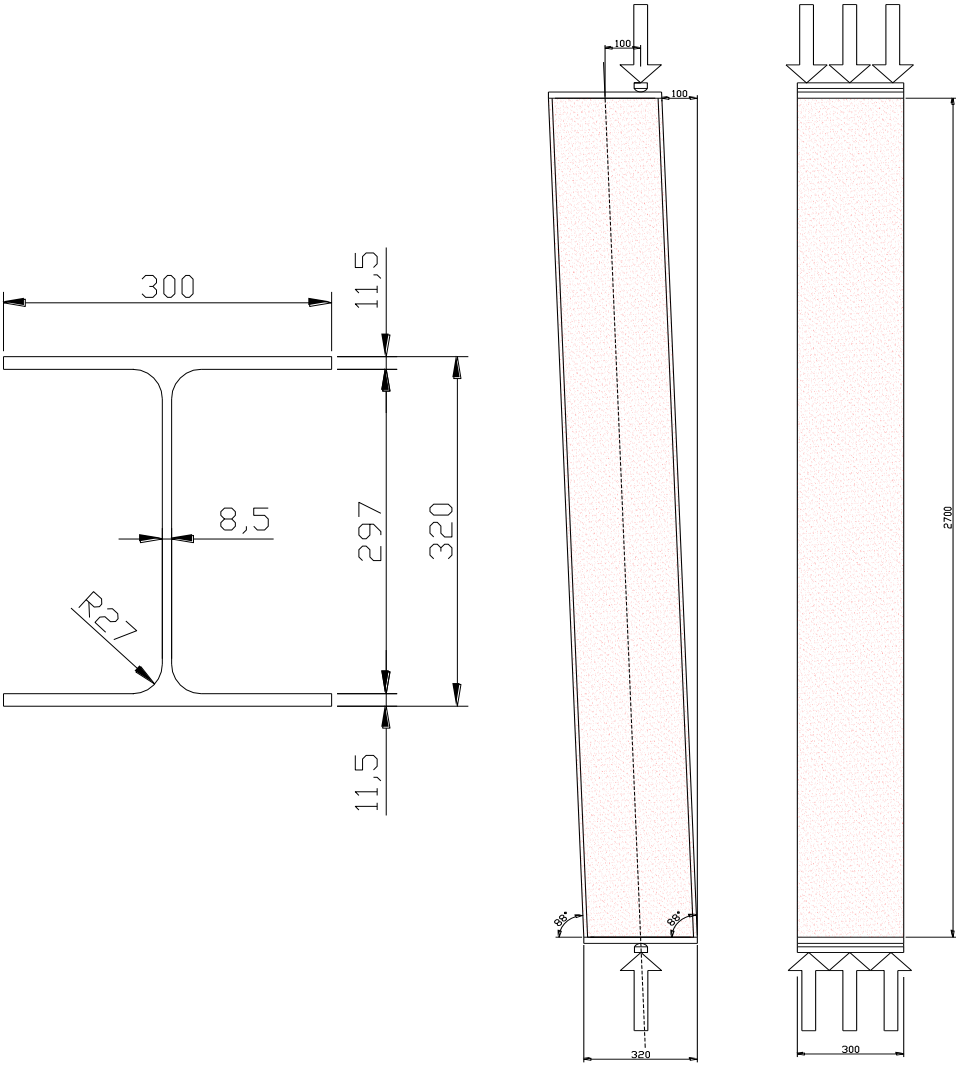
Figure 127: Cross-section design and global design of the test 7

113

The load was applied with an eccentricity of 150 mm in the direction of the strong axis at the larger base of the steel member and without eccentricity at the other base. For this test the eccentricity of the load and of the support are arranged in such a way us to produce a triangular bending moment distribution ($\psi = 0$):
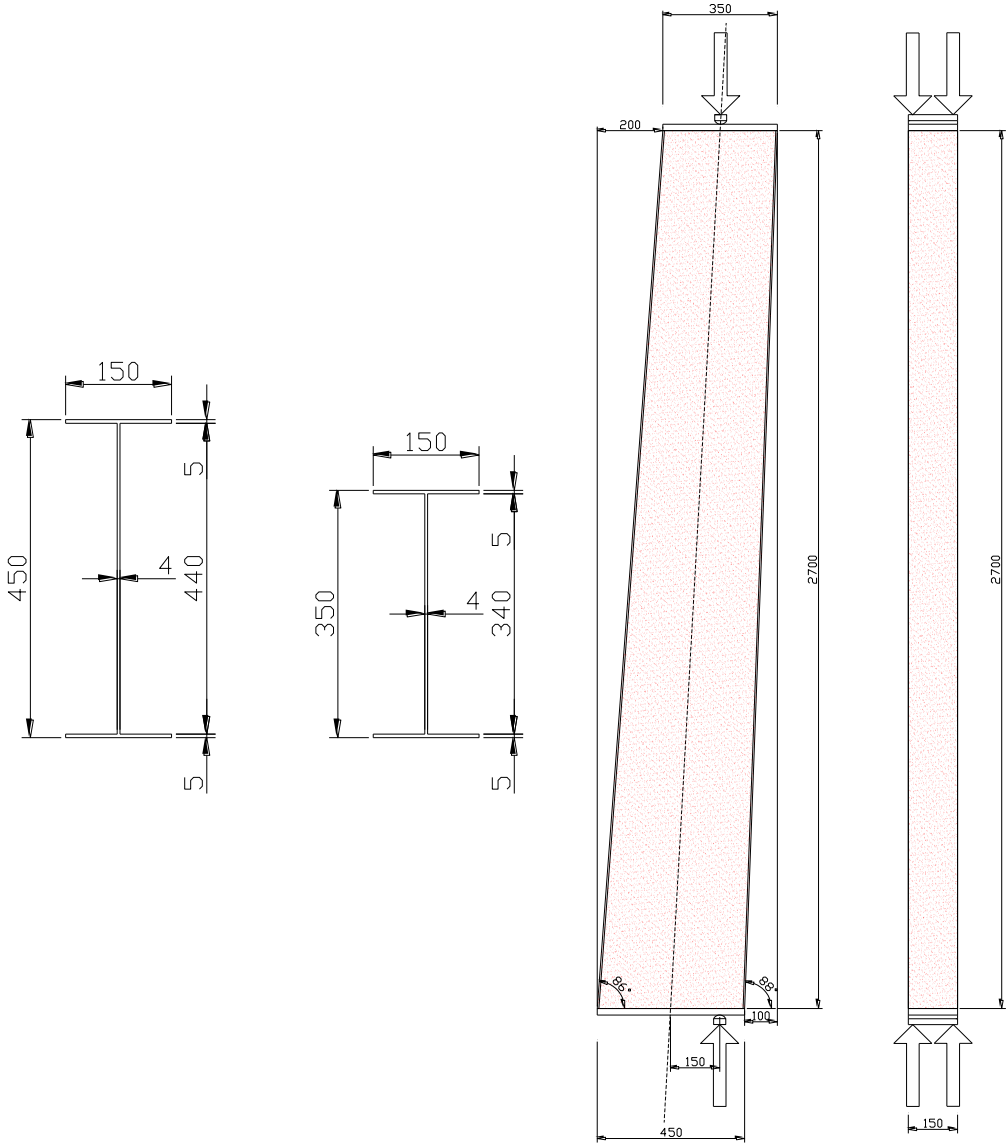
Figure 128: section design and global design of the test 8

All other parameters and set-up used for these experimental fire tests are identical than the ones of the axially loaded columns. The details are available in part 2.2.4.1 and more precisely in the third deliverable.

2.2.5.2 General principles of simple design rules

According to EN 1993-1-2, the design buckling resistance R$_{fi,d}$ for a member without lateral restraints and with a class 4 cross section subject to combined bending and axial compression in fire situation should be verified by satisfying the interaction curve defined by the two following equations for doubly symmetric cross-sections. These are the equations (4.21c) and (4.21d) respectively of EN 1993-1-2 adapted for Class 4, i.e., considering the effective cross-sectional properties:

$$\frac{N_{fi,Ed}}{\chi_{min,fi}A_{eff}k_{0.2p,\theta}\dfrac{f_y}{\gamma_{M,fi}}} + \frac{k_yM_{y,fi,Ed}}{W_{eff,y,min}k_{0.2p,\theta}\dfrac{f_y}{\gamma_{M,fi}}} + \frac{k_zM_{z,fi,Ed}}{W_{eff,z,min}k_{0.2p,\theta}\dfrac{f_y}{\gamma_{M,fi}}} \leq 1 \tag{51}$$

$$\frac{N_{fi,Ed}}{\chi_{z,fi}A_{eff}k_{0.2p,\theta}\dfrac{f_y}{\gamma_{M,fi}}} + \frac{k_{LT}M_{y,fi,Ed}}{\chi_{LT,fi}W_{eff,y,min}k_{0.2p,\theta}\dfrac{f_y}{\gamma_{M,fi}}} + \frac{k_zM_{z,fi,Ed}}{W_{eff,z,min}k_{0.2p,\theta}\dfrac{f_y}{\gamma_{M,fi}}} \leq 1 \tag{52}$$

All symbols are those defined in EN1993-1-2. k$_y$ is defined with the following equation:

$$k_y = 1 - \frac{\mu_y N_{fi,Ed}}{\chi_{y,fi}A_{eff}k_{0.2p,\theta}\dfrac{f_y}{\gamma_{M,fi}}} \leq 3 \tag{53}$$

And:

$$\mu_y = \left(2\beta_{M,y} - 5\right)\bar{\lambda}_{y,\theta} + 0.44\beta_{M,y} + 0.29 \leq 0.8 \ but \ \bar{\lambda}_{y,20°\,C} \leq 1.1 \tag{54}$$

For equation (52), k$_{LT}$ is defined with the following equation:

$$k_{LT} = 1 - \frac{\mu_{LT} N_{fi,Ed}}{\chi_{z,fi}A_{eff}k_{0.2p,\theta}\dfrac{f_y}{\gamma_{M,fi}}} \leq 1 \tag{55}$$

And:

$$\mu_{LT} = 0.15\bar{\lambda}_{z,\theta}\beta_{M,LT} - 0.15 \leq 0.9 \tag{56}$$

The equivalent uniform moment factors $\beta_{M,LT}$ and $\beta_{M,y}$ are evaluated using the bending diagram corresponding to the major axis: M$_{y,fi,Ed}$. Only uniaxial bending (about the major axis) was considered in this numerical investigation. Furthermore, in fire situation $\gamma_{M,fi}$ = 1. As a consequence, the terms related to the minor axis (z) are not taken into account. Equations (51) and (52) respectively lead to a value, named κ$_{in}$ for in-plane buckling and κ$_{out}$ for out-of-plane buckling which are compared to 1. κ < 1 means that the result given by the simple design rules can lead to unsafe design. In fact, when the beam-column reaches its numerical collapse, the simple rules would permit a higher load level, which is not safe. On the other side, κ > 1 means that the numerical results lead to a higher resistance than the one admitted in the simple design rules. Thus, equations (51) and (52) respectively become:

$$\frac{N_{fi,Ed}}{\chi_{min,fi}A_{eff}k_{0.2p,\theta}f_y} + \frac{k_yM_{y,fi,Ed}}{W_{eff,y,min}k_{0.2p,\theta}f_y} = \kappa_{in}(\leq 1) \tag{57}$$

$$\frac{N_{fi,Ed}}{\chi_{z,fi}A_{eff}k_{0.2p,\theta}f_y} + \frac{k_{LT}M_{y,fi,Ed}}{\chi_{LT,fi}W_{eff,y,min}k_{0.2p,\theta}f_y} = \kappa_{out}(\leq 1) \tag{58}$$

The in-plane behaviour of the beam-columns is numerically investigated with the help of lateral restraints (preventing out-of-plane buckling) in the flanges as it is depicted in Figure 129:
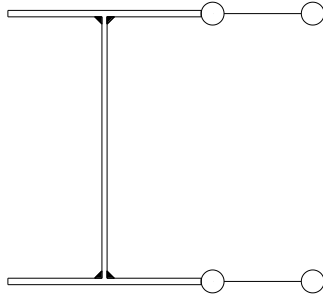
Figure 129: Additional restraints added to the model to prevent the out-of-plane displacements

2.2.5.3 *Comparison of current EN 1993-1-2 design rules with the numerical results*

For in-plane behaviour, the coefficient κ_{in} given by equation (57) was employed considering the ultimate axial force and uniform bending moment given by numerical simulations as the design loads. Buckling reduction factors, effective width properties and cross-sectional resistance are determined using current design rules of EN 1993-1-2. The interaction curve is determined according to the current EN 1993-1-2 equations too. The obtained results are plotted in Figure 130 against the non-dimensional slenderness $\lambda_{y,\theta}$ and in Figure 131 against the ratio between the applied bending moment and the cross-sectional bending resistance $M_{y,fi,Ed}/M_{y,fi,Rd}$. In these figures, the line corresponding to the value 1 in the vertical axis defines the interaction curve. If the points, which represent the numerical results, are below the line it means the resistances obtained numerically are lower than those predicted by equation (57) and therefore are unsafe and safe otherwise:
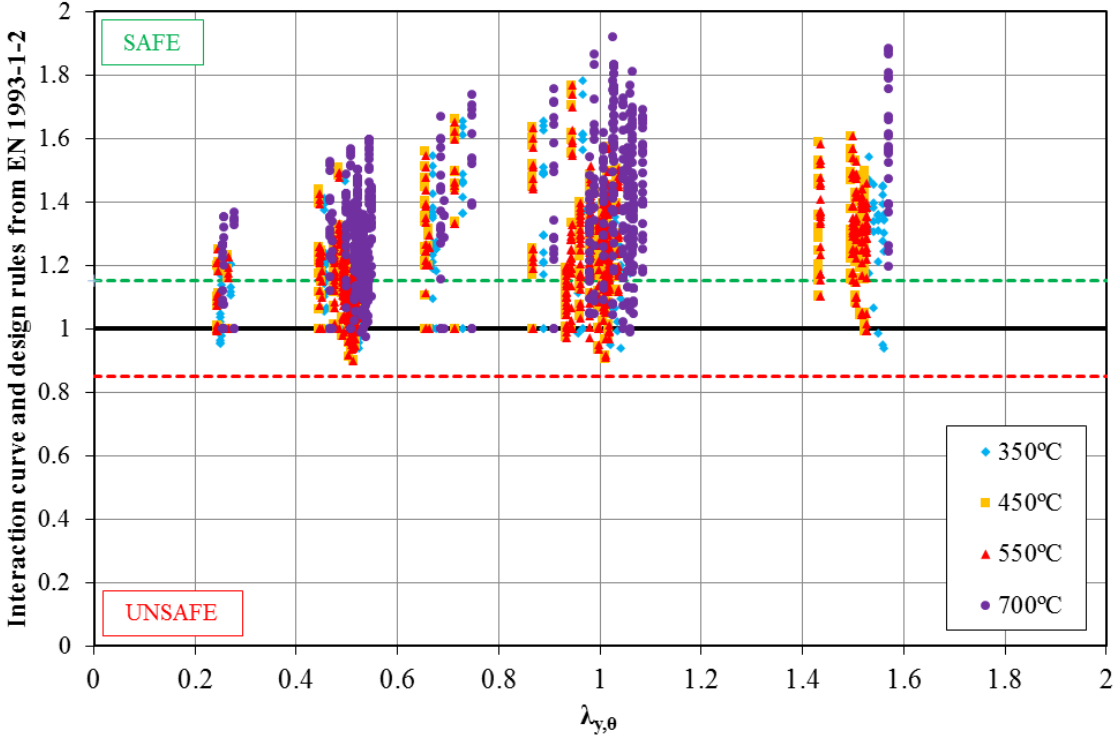
Figure 130: Comparison of the numerical analysis results with the design rules of EN 1993-1-2 in case of in-plane interaction curve at various temperature levels as a function of the beam-column slenderness
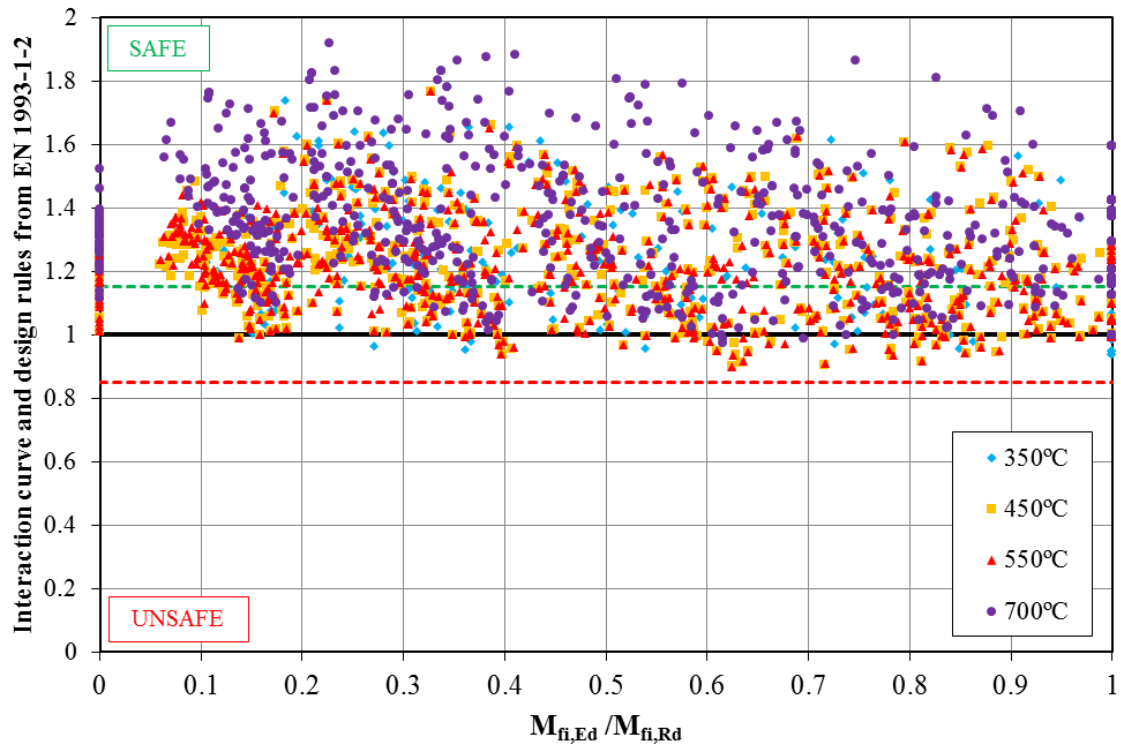
Figure 131: Comparison of the numerical analysis with the design rules of EN 1993-1-2 in case of in-plane interaction curve at various temperature levels as a function of the applied bending moment

The out-of-plane behaviour of beam-columns was also investigated. Coefficient κ_{out} given by equation (58) was used considering ultimate axial load and bending moment given by the numerical simulations as the design loads. Results are plotted in Figure 132 against the non-dimensional slenderness $\lambda_{z,\theta}$ and in Figure 133 against the ratio between the applied bending moment and the cross-sectional bending resistance $M_{y,fi,Ed}/M_{y,fi,Rd}$. In these figures, the horizontal line at the value 1 in the vertical axis defines the interaction curve. If the points that represent the numerical results are below the line it means the ultimate loads obtained numerically are below those predicted by equation (58) and therefore are unsafe or safe otherwise.
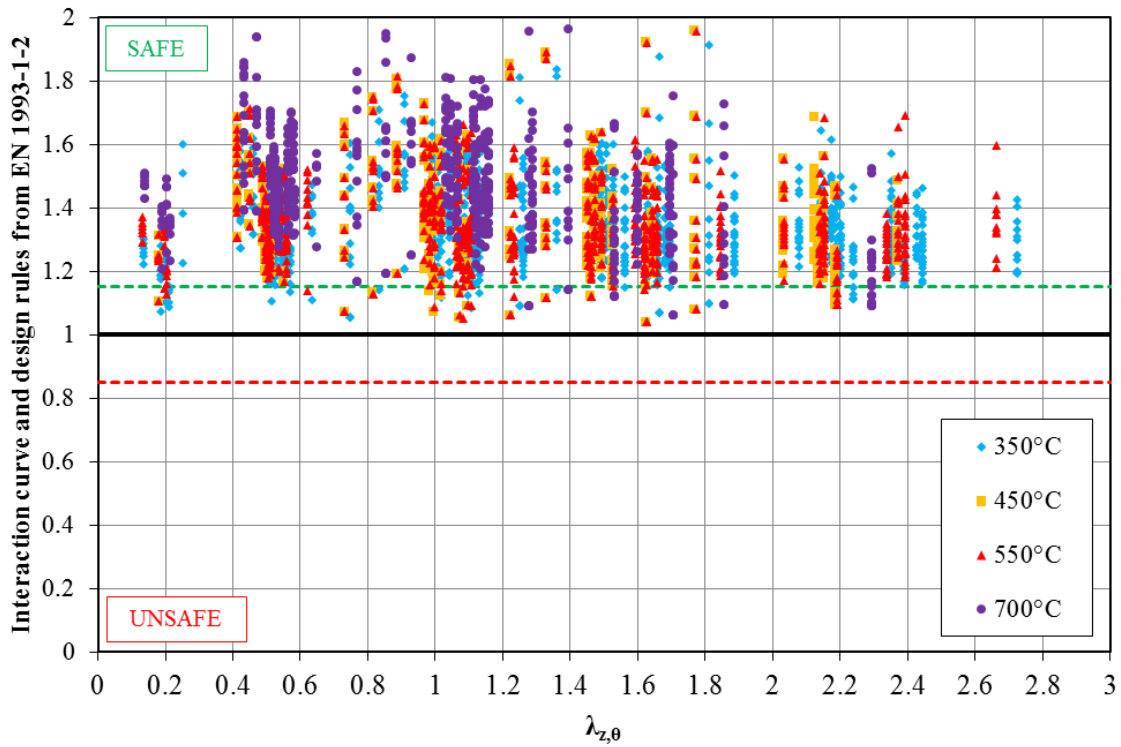
Figure 132: Comparison of the numerical analysis with the design rules of EN 1993-1-2 in case of out-of-plane interaction curve at various temperature levels as a function of the beam-column slenderness
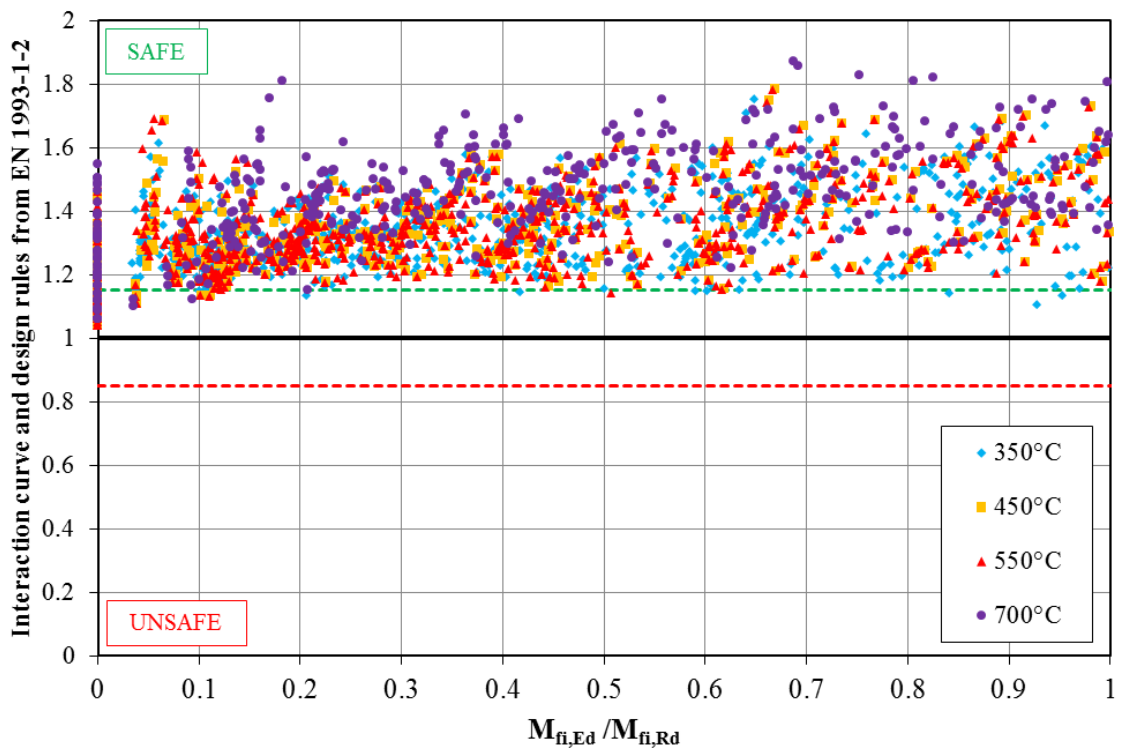
Figure 133: Comparison of the numerical analysis with the design rules of EN 1993-1-2 in case of out-of-plane interaction curve at various temperature levels as a function of the applied bending moment

Table 56 summarises the statistical data for both in-plane and out-of-plane cases of the conducted simulations compared to EN 1993-1-2 design rules and interaction curve:

Type of behaviour	EN 1993-1-2	
	In-plane	Out-of-plane
Average ratio (design rule / FEM)	0.81	0.73
Percentage of unsafe points (%)	7.42	0
Maximum unsafe ratio	1.15	N/A
Percentage of safe points by more than 15% (%)	65.94	95.51
Standard Deviation	0.18	0.16
Coefficient of variation	0.22	0.21

Table 56: Statistical results based on about 5900 simulations

When using the full design rules available in EN 1993-1-2 it is noticeable that the design resistance of class 4 cross-sections submitted to combined bending and compression is really not cost-effective. This is the case for both in-plane and out-of-plane behaviours. Furthermore, for beam-columns without lateral restraints, almost all cases (95%) are situated on the safe side by more than 15%.

2.2.5.4 Comparison of previously defined new design rules combined with EN 1993-1-2 interaction curve

The following paragraph shows the same comparison but using the new design rules previously proposed for resistance of class 4 cross-section steel members subjected to single action. Only the interaction curve is still that defined with the EN 1993-1-2 equation. This comparison allows to understand the influence of the proposed new design rules for resistance of class 4 steel members under single action, that is buckling and lateral torsional buckling resistance. In this case, equations (57) and (58) respectively become equations (59) and (60):

$$\frac{N_{fi,Ed}}{\chi_{min,fi}A_{eff}k_{y,\theta}f_y} + \frac{k_y M_{y,fi,Ed}}{W_{eff,y,min}k_{y,\theta}f_y} = \kappa_{in}(\leq 1) \tag{59}$$

$$\frac{N_{fi,Ed}}{\chi_{z,fi}A_{eff}k_{y,\theta}f_y} + \frac{k_{LT} M_{y,fi,Ed}}{\chi_{LT,fi}W_{eff,y,min}k_{y,\theta}f_y} = \kappa_{out}(\leq 1) \tag{60}$$

The accuracy of simple design rules can be investigated by replacing in Equations (59) and (60) the design loads $N_{fi,Ed}$ and $M_{y,fi,Ed}$ with the ultimate axial force and corresponding bending moment derived from numerical simulations. On the contrary, other parameters such as the buckling reduction factors, effective width properties and cross-sectional resistance are determined with help of simple design rules previously defined in the scope of this project. For this comparison, the interaction curve of current EN 1993-1-2 remains unchanged. In case of in-plane bending, the obtained comparison results are plotted respectively in Figure 134 against the non-dimensional slenderness $\lambda_{y,\theta}$ and in Figure 135 against the ratio between the applied bending moment and the cross-sectional bending resistance $M_{y,fi,Ed}/M_{y,fi,Rd}$. In these figures, the line corresponding to the value $\kappa_{in} = 1$ on the ordinate axis defines the interaction curve. If the points are below this line, it means that the resistance obtained numerically are smaller than those predicted with simple design rules and therefore are unsafe. Otherwise, the simple design rules are on the safe side:
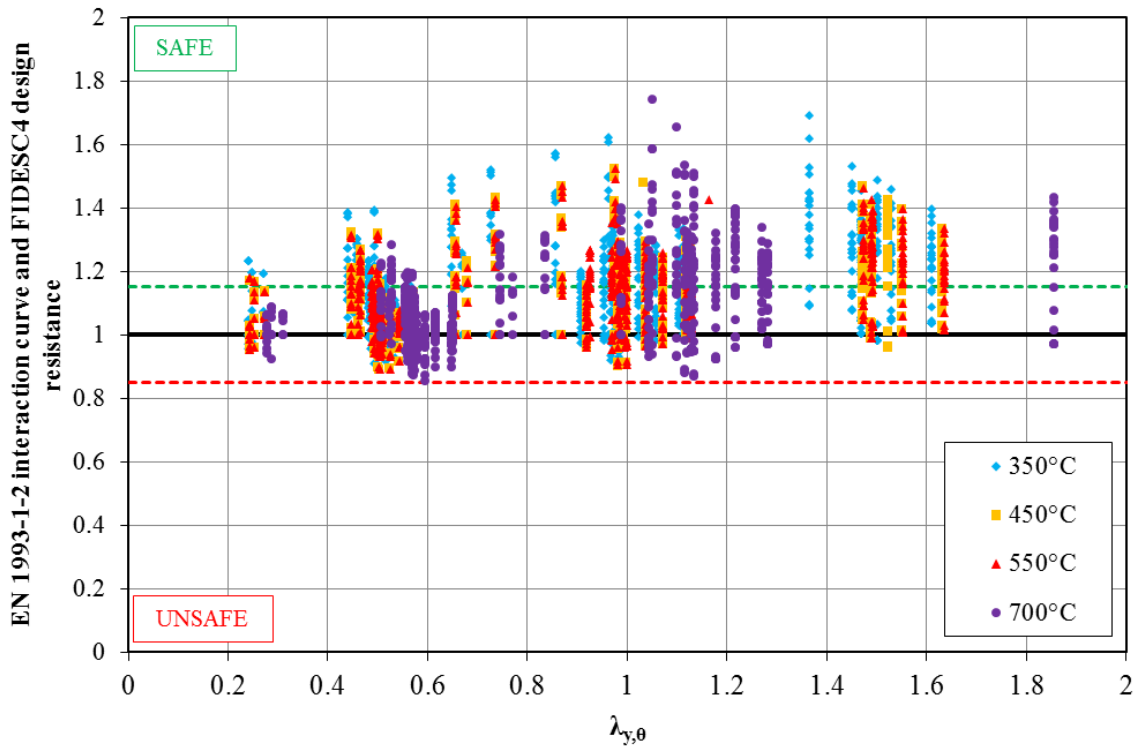
Figure 134: Comparison of the numerical analysis with the simple design rules of FIDESC4 relative to single loading condition combined with in-plane interaction curve of EN 1993-1-2 at various temperature levels as a function of the beam-column slenderness
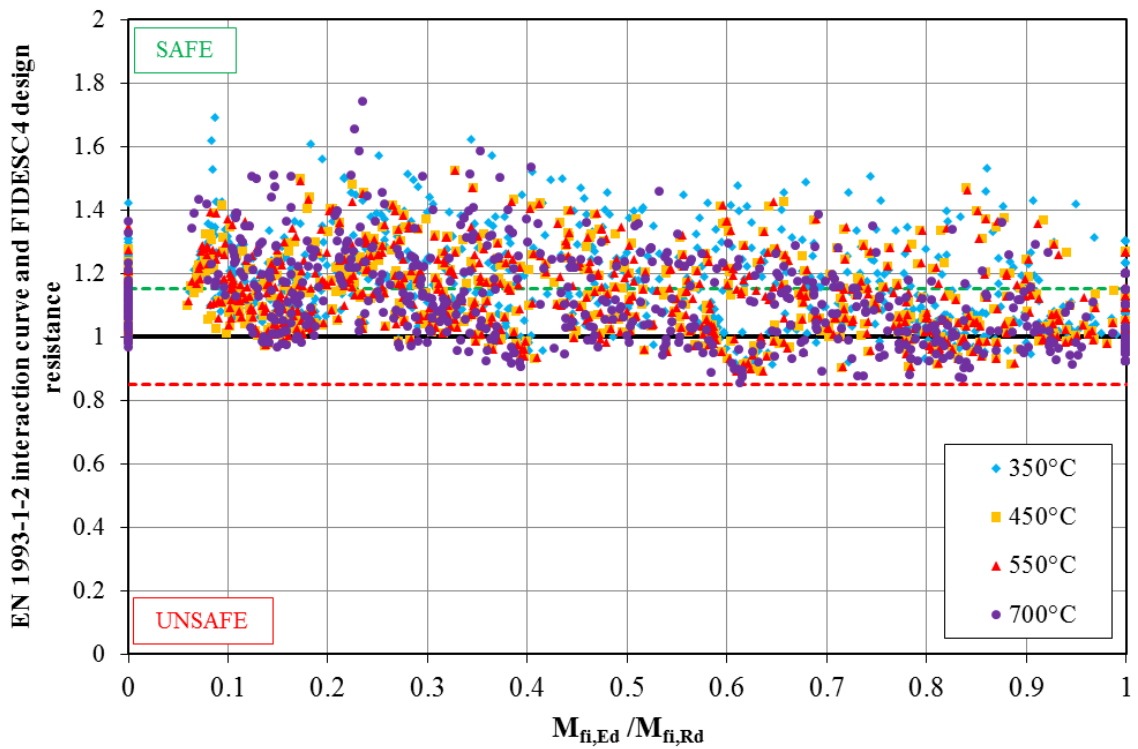
Figure 135: Comparison of the numerical analysis with simple design rules of FIDESC4 relative to single loading condition combined with in-plane interaction curve of EN 1993-1-2 at various temperature levels as a function of the applied bending moment

The accuracy of the simple design rules relative to out-of-plane behaviour of beam-columns was also investigated. In this case, the obtained results are plotted in Figure 136 against the non-dimensional slenderness $\lambda_{z,\theta}$ and in Figure 137 against the ratio between the applied bending moment and the cross-sectional bending resistance $M_{y,fi,Ed}/M_{y,fi,Rd}$. In these figures, the horizontal line at the value $\kappa_{out} = 1$ on the ordinate axis defines the interaction curve on the basis of numerical results. If the points are below this line, it means the ultimate loads obtained numerically are lower than those predicted with help of simple design rules and therefore are unsafe. Otherwise, the simple design rules are on the safe side.
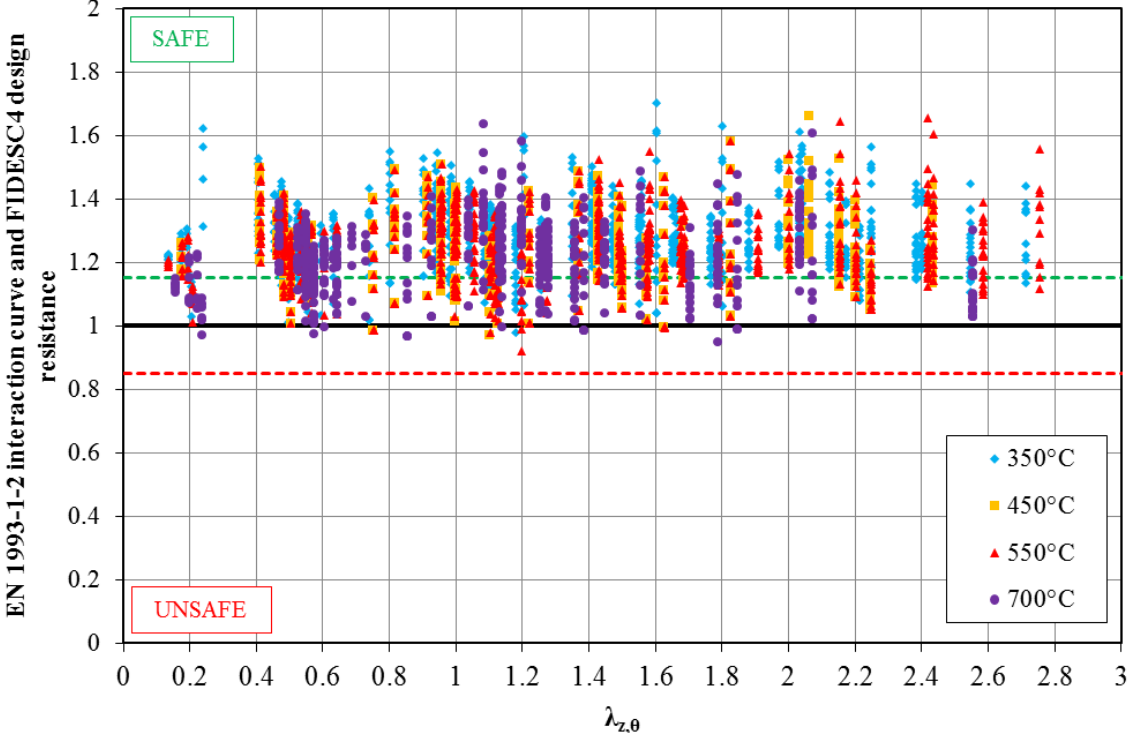
Figure 136: Comparison of the numerical analysis with simple design rules of FIDESC4 relative to single loading condition combined with out-of-plane interaction curve of EN 1993-1-2 at various temperature levels as a function of the beam-column slenderness
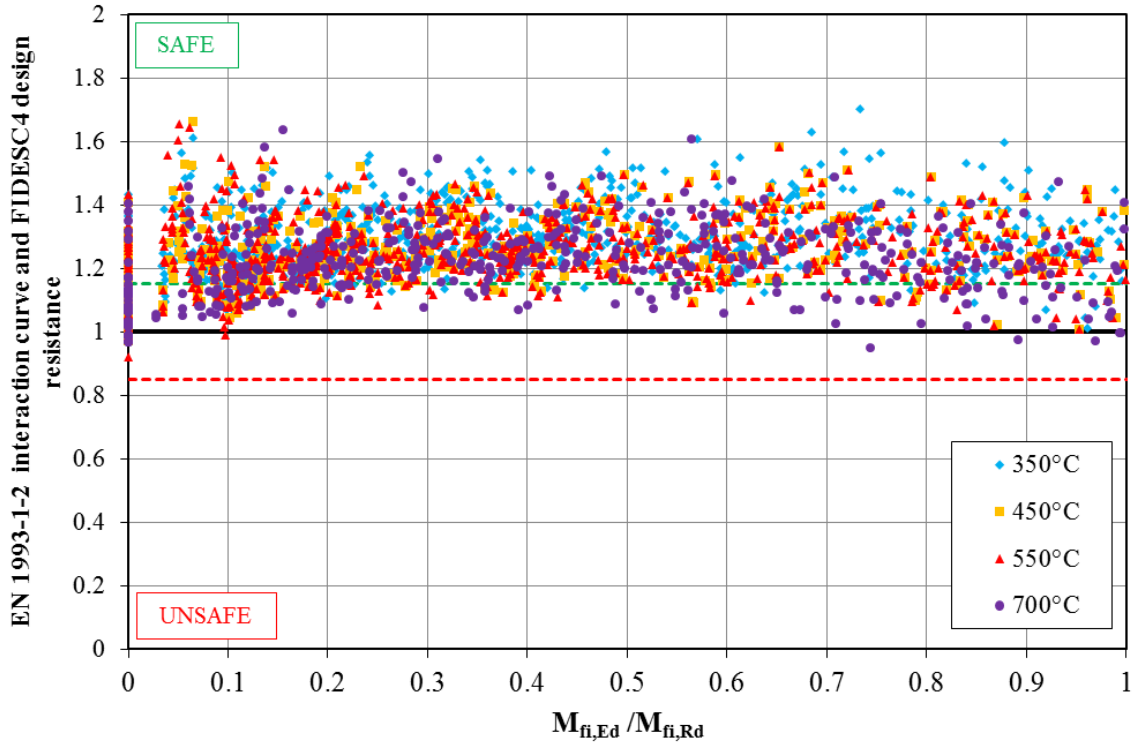
Figure 137: Comparison of the numerical analysis with simple design rules of FIDESC4 relative to single loading condition and out-of-plane interaction curve from EN 1993-1-2 at various temperature levels as a function of the applied bending moment

Table 57 summarises the statistical analysis results in case of both in-plane and out-of-plane bending interactions.

Type of behaviour	FIDESC4 + EN 1993-1-2	
	In-plane	Out-of-plane
Average ratio (design rule / FEM)	0.89	0.80
Percentage of unsafe points (%)	15.29	1.10
Maximum unsafe ratio	1.17	1.09
Percentage of safe points by more than 15% (%)	38.84	82.94
Standard Deviation	0.12	0.11
Coefficient of variation	0.13	0.14

Table 57: Statistical results on to about 5900 simulations

It can be found that the use of new proposed design rules relative to single loading condition significantly improves the accuracy and cost-effective aspect of the beam-column design. However, the interaction rule for out-of-plane behaviour is still too conservative while the in-plane behaviour could be considered as satisfactory. In consequence, a new proposal was provided to improve the interaction curves for both in-plane and out-of-plane behaviours which are described in the following paragraph.

2.2.5.5 New proposal for interaction curve and corresponding accuracy investigation

In order to obtain a more cost-effective design, the μ_y and μ_{LT} factor were calibrated following the same methodology adopted by Talamona in [22]. According to this procedure the following expression was used to extract from each numerical simulation the value of μ_y factor, which fulfils equation (54):

$$\mu_y = \frac{M_{y,fi,Rd} \times N_{FEM} - \chi_{y,fi} \times N_{c,fi,Rd} \times M_{y,fi,Rd} + \chi_{y,fi} \times N_{c,fi,Rd} \times M_{FEM}}{N_{FEM} \times M_{FEM}} \qquad (61)$$

Moreover, the next equation was used to extract from each numerical simulation the μ_{LT} factor, which fulfils equation (56):

$$\mu_{LT} = \frac{\chi_{LT} \times M_{y,fi,Rd} \times N_{FEM} + \chi_{z,fi} \times N_{c,fi,Rd} \times M_{FEM} - \chi_{z,fi} \times \chi_{LT} \times N_{c,fi,Rd} \times M_{y,fi,Rd}}{N_{FEM} \times M_{FEM}} \qquad (62)$$

Where $N_{c,fi,Rd}$ and $M_{y,fi,Rd}$ are respectively the axial and moment cross-sectional resistance obtained with the new design rules previously proposed in the scope of this project, and N_{FEM} and M_{FEM} are the ultimate axial load and bending moment given by finite element analysis.

When in-plane behaviour is concerned, Figure 138 shows the evolution of μ_y factor as a function of the non-dimensional slenderness $\lambda_{y,\theta}$ with the proposed modification given with equation (63), denoted as "proposal". The "Linear (FEA)" term denotes the linear trend line of the numerical results:

$$\mu_y = \left(2 \times \beta_{M,y1} - 5\right) \times \bar{\lambda}_{y,\theta} + 0.44 \times \beta_{M,y2} + 0.7 \leq 0.6 \; but \; \bar{\lambda}_{y,20^\circ \, C} \leq 1.1 \qquad (63)$$

When out-of-plane behaviour is concerned, Figure 139 shows the evolution of μ_{LT} factor as a function of the non-dimensional slenderness $\lambda_{z,\theta}$ with the proposed modification given with the equation (64), denoted as "proposal". The "Linear (FEA)" term denotes the linear trend line of the numerical results:

$$\mu_{LT} = 0.45 \times \bar{\lambda}_{z,\theta} \times \beta_{M,LT} + 0.2 \leq 0.9 \qquad (64)$$

With:
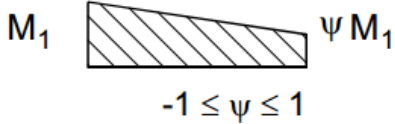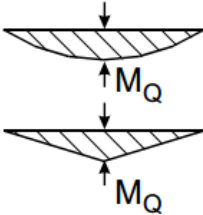
End moments	
M_1 ⬓ ψM_1 $-1 \leq \psi \leq 1$	$\beta_{M,y1} = \beta_{M,\psi} = 1.8 - 0.9\psi$ $\beta_{M,y2} = \beta_{M,y1}$ $\beta_{M,LT} = \beta_{M,\psi} = 1.8 - 0.9\,\psi$
Moments due to in-plane lateral loads	
M_Q M_Q	$\beta_{M,y1} = \beta_{M,Q} = 1.6$ $\beta_{M,y2} = 0$ $\beta_{M,LT} = \beta_{M,Q} = 1.6$

Table 58: Equivalent uniform moment factor
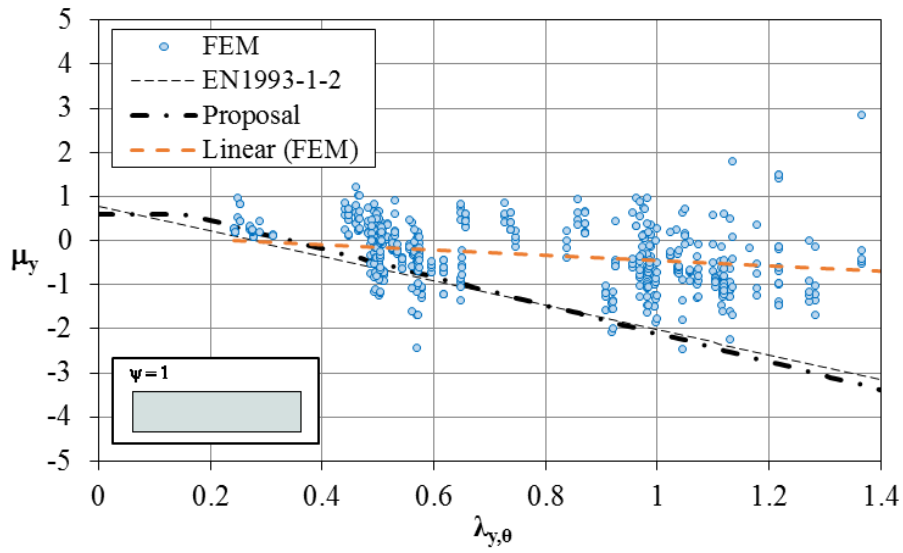
a) Uniform bending moment
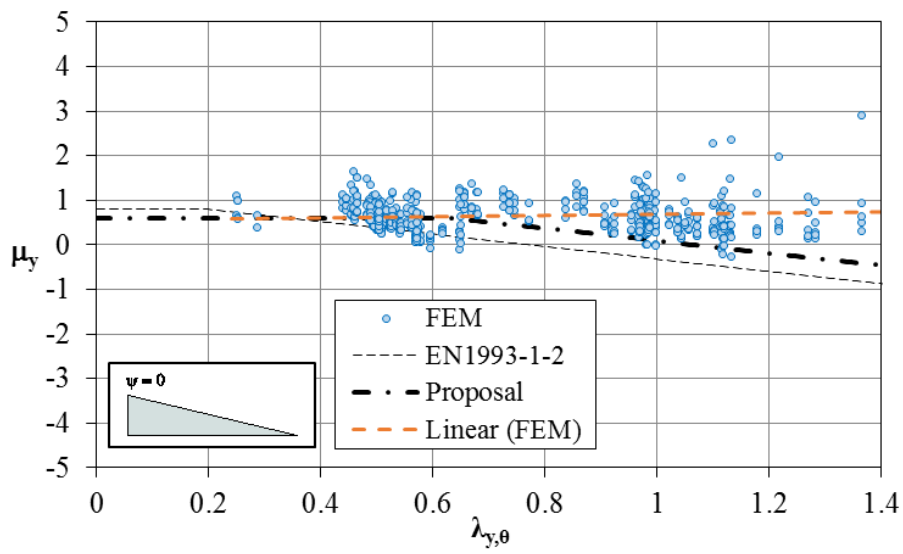
b) Triangular bending moment

c) Bi-triangular bending moment

124

d) Distributed load

Figure 138: Calibration of μ_y factor for the in-plane behaviour of beam-columns considering different loading cases

a) Uniform bending moment

b) Triangular bending moment

125
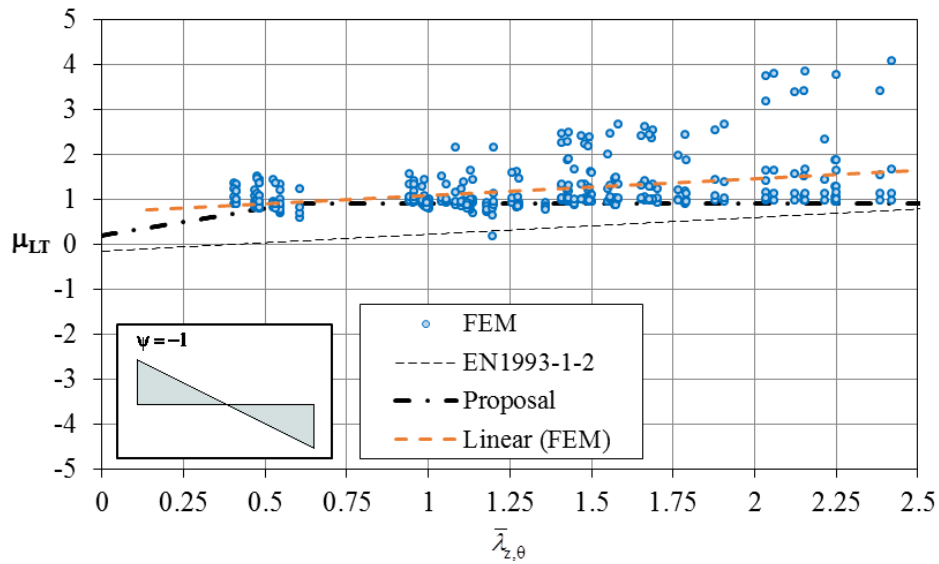
c) Bi-triangular bending moment
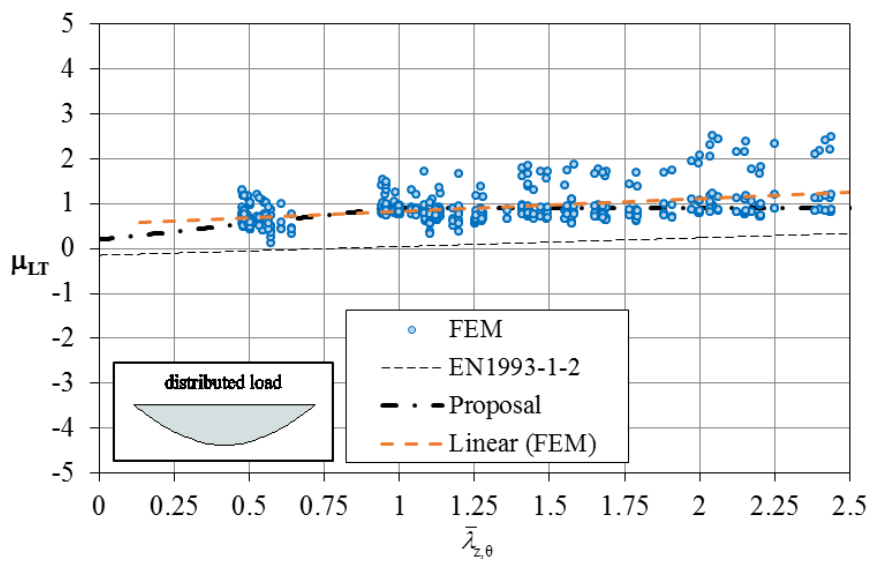
d) Distributed load

Figure 139: Calibration of μ_{LT} factor for the out-of-plane behaviour of beam-columns considering different loading cases

Table 59 summarises the statistical analysis results on the basis of new proposed interaction curve in case of both in-plane and out-of-plane behaviour of class 4 steel members.

	NEW DESIGN RULES	
Type of behaviour	**In-plane**	**Out-of-plane**
Average ratio (design rule / FEM)	0.90	0.91
Percentage of unsafe points (%)	15.29	19.25
Maximum unsafe ratio	1.15	1.14
Percentage of safe points by more than 15% (%)	32.30	28.75
Standard Deviation	0.12	0.11
Coefficient of variation	0.13	0.12

Table 59: Statistical results on about 5900 simulations

126

It can be found that the new proposed interaction curves now allow a far more cost-effective design of class 4 beam-columns subjected to combined loadings and at different temperature levels for both in-plane and out-of-plane behaviours. Furthermore, the maximum unsafe ratio remains always lower than or equal to 1.15.

However, these interaction curves differ from current design rules of EN1993-1-2 for classes 1, 2 and 3 steel members. This difference will make the design work of engineers more complex, which can be easily dealt with thanks to user-friendly design software.

2.2.6 WP6 - User-friendly software to apply simple design rules

The "FIDESC4" software has been developed for the evaluation of the critical temperature and the verification of the fire resistance of cross-sections or structural elements, following the simple calculation models of Part 1.2 of Eurocode 3. For the case of class 4 cross-sections the software has been developed in accordance with Annex E of Part 1.2 of the same Eurocode. Additionally, the effective properties of class 4 cross-sections can be evaluated according to new approaches developed and listed previously, as well as the calculation of the resistance of class 4 members subjected to different type of loading conditions. For the cases not covered by Part 1.2 of the Eurocode 3, Part 1.1 and 1.5 have been used.

The software was developed using Visual Basic and is fully compatible with Windows standards."

"FIDESC4" software was optimized to run on the following Operating Systems:

- Windows XP (with the appropriate Microsoft .NET framework installed);
- Windows Vista;
- Windows 7.

Installation will require 25Mb of free disk space.

2.2.6.1 Brief description of the software

FIDESC4 calculates the critical temperature or checks the fire resistance of cross-sections and steel members loaded about the strong axis or about the weak axis for the case of doubly symmetric cross-sections.

The software has two modules: one dealing with the fire resistance of the cross-sections and the other with fire resistance of members (columns, beams and beam-columns), as shown in Figure 140:
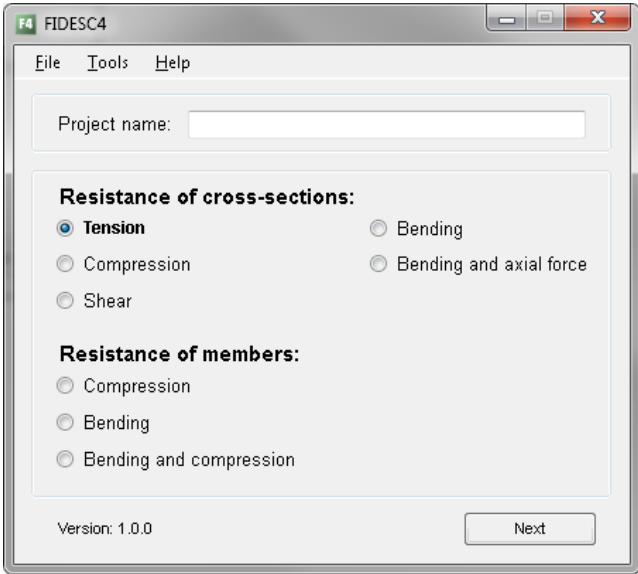
Figure 140: Main menu

The software evaluates the critical temperature considering the resistance of cross-sections subjected to:

i) Axial force (tension or compression);

ii) Shear;

iii) Bending (Bi-axial bending);

iv) Bending and axial force (tension or compression);

Regarding the fire resistance of structural members, the software verifies the buckling resistance of the members submitted to:

i) Compression;

ii) Bending;

iii) Bending and compression.

The user can choose the section type of the profile. Typical cross-sectional shapes include: HD, HE, HL, HP, IPE, UB, UC, W, L, RHS, CHS from a database. User-defined dimensions can be included (hot rolled, welded (see Figure 141).
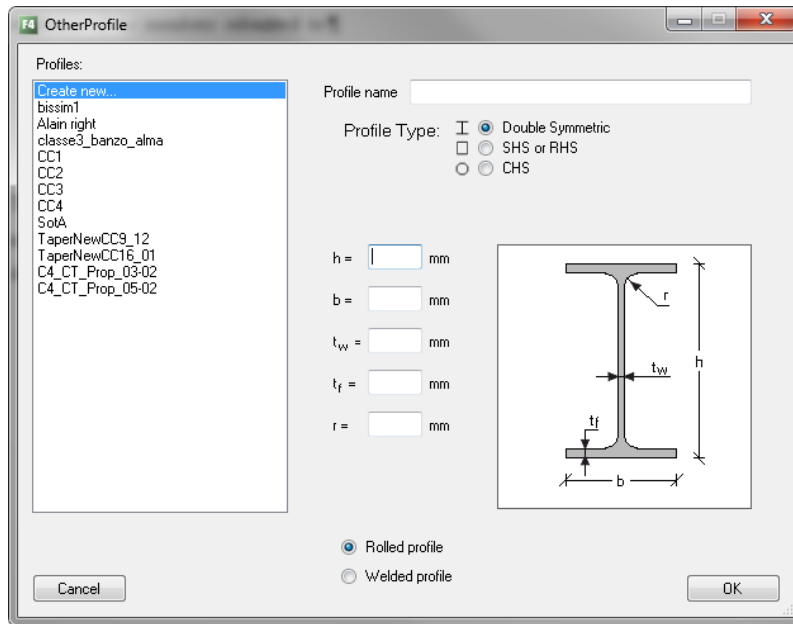
Figure 141: Dialog box for user-defined double symmetric section

If the cross-section is class 4, the software evaluates its effective cross-section, as shown in Figure 142, according the new method developed and described in 2.2.2.4.
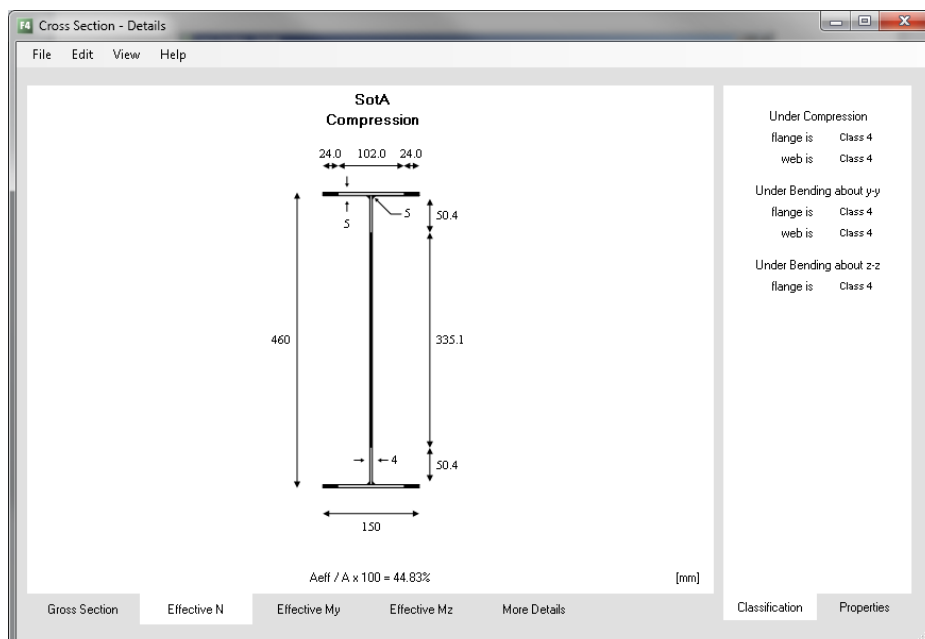
a)
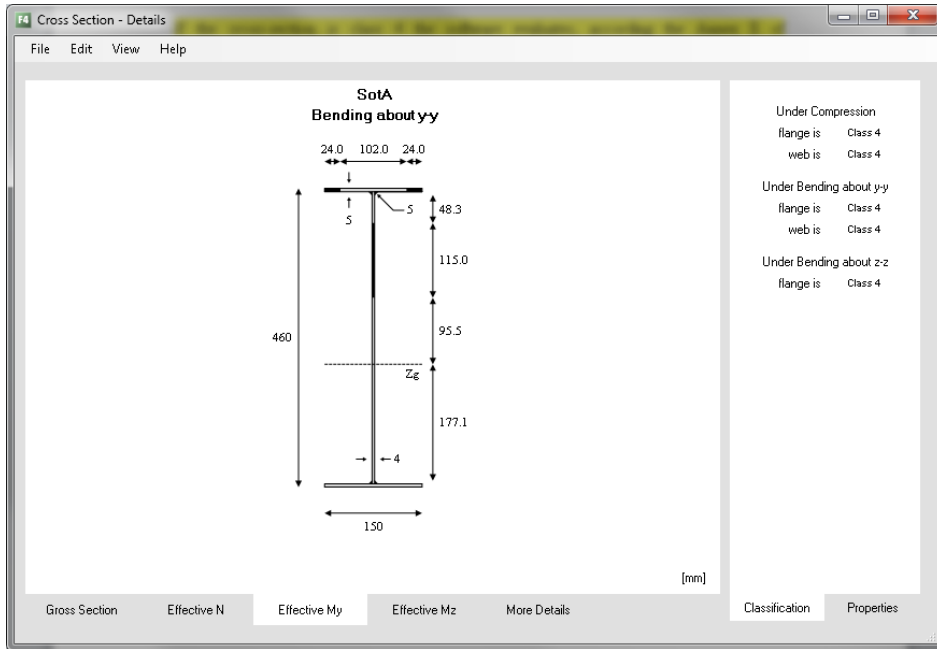
b)

Figure 142: Effective cross-section: a) under axial compression, b) under bending about major axis

2.2.6.2 Adopted methodologies

For the evaluation of the critical temperature, the software uses an incremental procedure starting with a temperature of 20 ºC and using a increment of $\Delta\theta = 0.1$ ºC until the design value of the fire resistance, $R_{fi,d,t}$ is equal to the design value of the effect of the actions in fire situation, $E_{fi,d}$, see Figure 143:
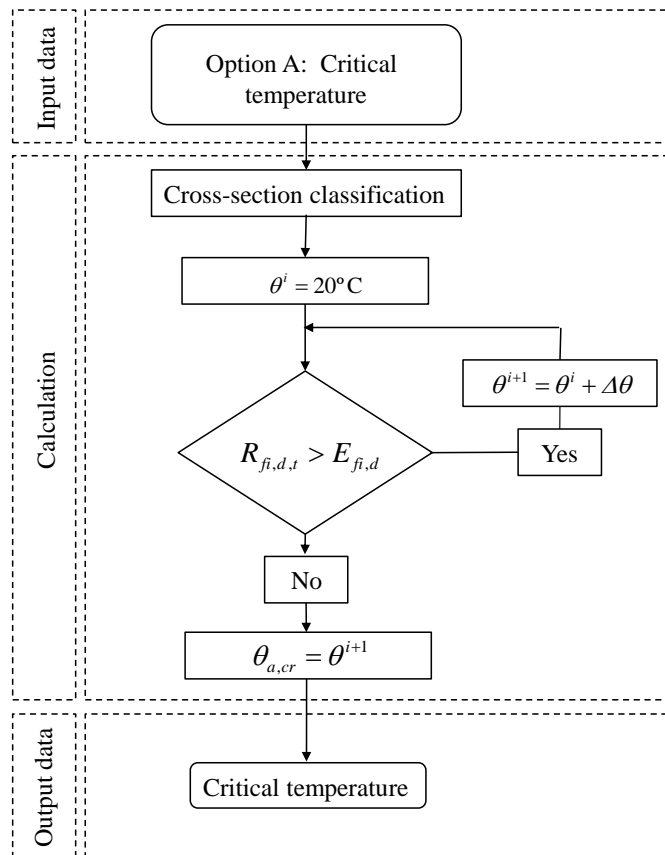
Figure 143: Option A: Calculation flowchart for evaluating the critical temperature

For the evaluation of the design value of the fire resistance or for the verification of the fire resistance at a given temperature, the user introduces a temperature and the software checks the fire resistance of the cross-section or the structural element; see Figure 144:
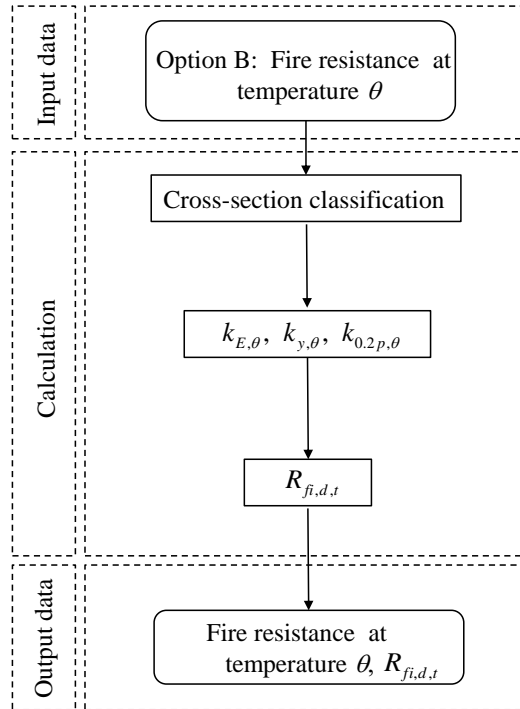
Figure 144: Option B: Calculation flowchart for checking the fire resistance

The calculation of class 4 effective cross-sections is based on the new approach developed in the framework of the project FIDESC4.

According to this methodology, new expressions for the plate reduction factor (ρ) were developed in order to replace the use of the design yield strength corresponding to the 0.2% proof strength ($f_{0.2p,\theta}$) with the stress for 2% total strain ($f_{y,\theta}$).

For internal compression elements, the following expression is used:

$$\rho = \frac{\left(\overline{\lambda}_p + 0.9 - \dfrac{0.26}{\varepsilon}\right)^{1.5} - 0.055(3+\psi)}{\left(\overline{\lambda}_p + 0.9 - \dfrac{0.26}{\varepsilon}\right)^{3}} \le 1.0$$

And for outstand compression elements:

$$\rho = \frac{\left(\overline{\lambda}_p + 1.1 - \dfrac{0.52}{\varepsilon}\right)^{1.2} - 0.188}{\left(\overline{\lambda}_p + 1.1 - \dfrac{0.52}{\varepsilon}\right)^{2.4}} \le 1.0$$

Where

$$\varepsilon = \sqrt{235/f_y}$$

The detailed description of the software is made in the deliverable n°6. Different loading conditions for the resistance are illustrated and an application example is provided.

2.2.7 WP7 - Global structural analysis using beam-column finite element with class 4 cross-section steel members

The aim of this task was to develop and calibrate a new beam-column finite element able to take account of local buckling of class 4 cross-section. In order to achieve this calibration, a numerical parametric study on single elements and frames taking into account different heating conditions was conducted. The comparisons were made between the shell models and the beam model using a new material law definition.

2.2.7.1 New carbon steel material law

The used new carbon steel material law was taken from a research carried out by Prof. J.M. Franssen from the University of Liege in the scope of this project. This method proposed to take into account the local instabilities by the means of an effective constitutive law of steel. The effective law was based on the following assumption: the plastic capacity obtained with the effective law in the full section is equal to the capacity of the slender plate with the real material under local buckling. The Figure 145 illustrates this approach:
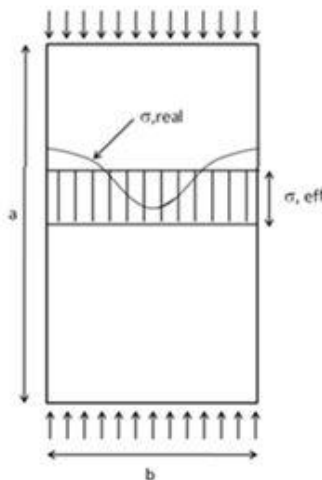
Figure 145: effective stress method

Local buckling occurs only for compressive plates. As a consequence, the stress-strain relationship was modified only in compression and remains unchanged in tension. This led to a non-symmetrical law with respect to compression-tension.

The tangent modulus at the origin of the law was not modified (which comes from the fact that low compression stresses do not produce local instabilities), but the development of local instabilities was reflected by a reduction of the limit of proportionality, of the effective yield strength and of the characteristic strain corresponding to the relationship beginning of the horizontal plateau in the stress-strain.

The effective stress-strain relationship in compression depends on the slenderness and on the boundary conditions of the plates, either supported on four sides (as in a web) or supported on three sides (as in half flanges), and possibly also on the steel grade, but these conditions were known at the time of creating the model and could easily be entered by the user as new material properties. The material law also depends on the temperature, but this was already the case for the real law considered up to now and this could be easily accommodated by the numerical code.

The method used in this research to determine the effective stress-strain relationship was based on the simulation of isolated plates modelled in SAFIR computer code with shell elements, simply supported on three or four sides and subjected to progressive imposed shortening in one direction. The simulations were performed first at ambient temperature and then at various elevated temperatures. From each simulation of a plate, the effective strain at any time was considered as the shortening of the plate divided by initial length of the plate, whereas the effective stress was considered as the reaction force applied on the edge of the plate divided by the sectional area of the plate:
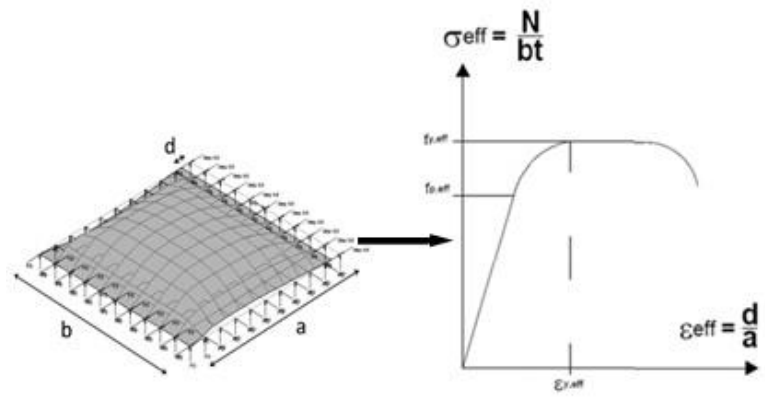
Figure 146: Illustration of the applied method to get the new material law

If the obtained curves were be very different in shape from these currently used for the virgin material, new effective stress-strain relationship should be developed. It has been decided here to keep the relationship proposed by the Eurocode.

From the effective stress-effective strain curve obtained each plate, the effective yield strength, the effective proportionality limit and the effective strain corresponding to the beginning of the plateau were determined, depending on the relevant conditions of the plate. Additional illustrations and explanations are exposed in figures 147 and 148:
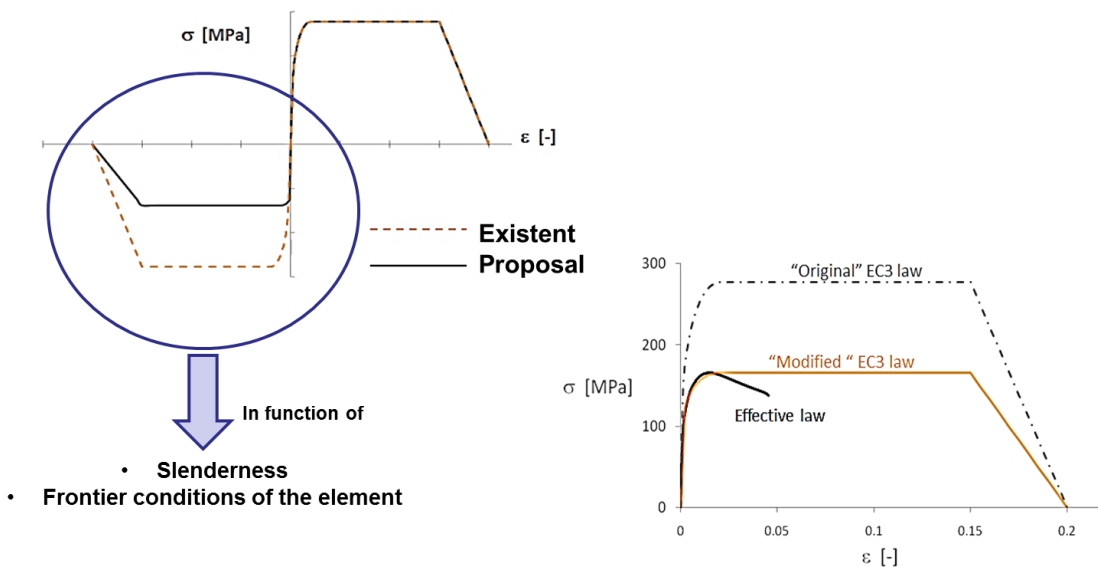
Figure 147: Differences between the material laws
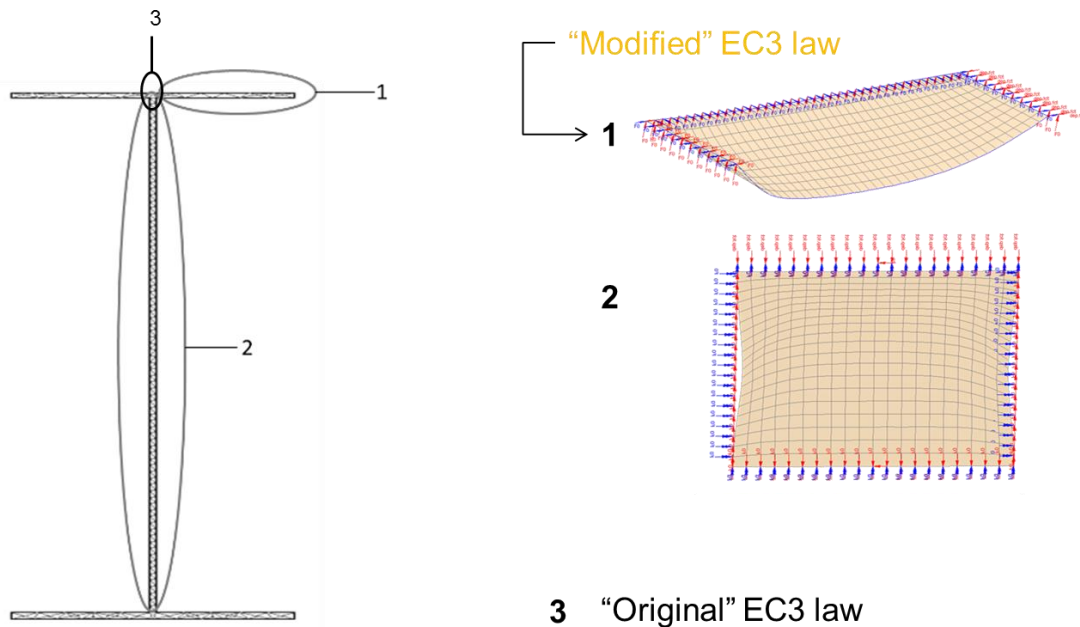
Figure 148: Illustration of buckling with "modified" EC3 law

The tables that give the values of the parameters of the effective law (limit of proportionality, effective yield strength and characteristic strains) at various values of the temperature and slenderness are established for both boundary conditions.

It has to be noticed that a simple adaptation of the subroutine at the material level can be made and easily introduced in any computer code. The user only has to introduce a different material model for the web and for the flanges, to give the slenderness of each plate as a new material property, and the software automatically takes care of the temperature, of the stress level and of the direction of the stress, tension or compression in each integration point. This procedure can be used also for analyses of structures at room temperature. It has to be underlined that, compared to existing methods, there is no stepwise variation of the behaviour at the interface between the four classes; in fact, there is no need to define the class because the adaptation of the material model is a continuous function of the slenderness.

The limit of this approach is that it cannot capture local buckling produced by shear forces, but this is also the case for the effective width approach.

This constitutive material model was already applied in case of single steel member under uniform heating and the obtained results are satisfactory. However, as it is very common that the temperature is not uniform in particular along the length of steel members under real fire condition, it was necessary to check whether this constitutive model remains available or not. In consequence, another parametric study was carried out to check the validity of this constitutive model through its comparison with shell element models under real heating condition in case of both single class 4 steel member and global structures.

2.2.7.2 Description of the parametric study

In order to run the simulation with non-uniform heating conditions in the elements, a real fire scenario was established.

The design fire is defined with a heat release rate of 750 kW/m², a fire area of 36 m² (diameter of about 6.77 m) and a flame height of 7 m. The heat transfer to the structural sections is calculated as the maximum of different methods (Cfast, Hasemi and Heskestad) depending on the distance from fire (radiation and or hot layer).
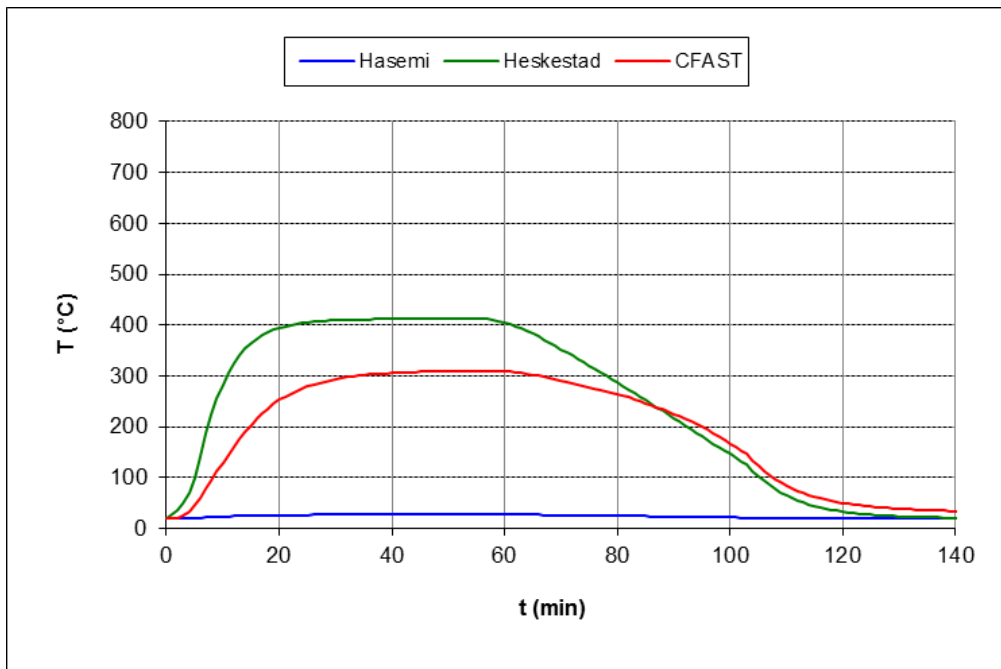
Figure 149: Evolution of temperature in function of time in the selected real fire scenario

For this task it was proposed to study 10 single steel members from the previously developed parametric studies. As the chosen dimension of the fire is 6x6 m, studied beam elements should be longer than 6 m, in order to have non-uniform heating conditions along the member length. In that way, natural fire conditions can be taken into account.

In the cases of beam analysis ten out of the cases of beams under pure bending were chosen as well as ten out of the beams subjected to lateral torsional buckling. The load and boundary conditions applied on the beams were the same as for their respective original parametric study. The difference was that a load ratio compared to room temperature resistance was applied when the temperature was gradually increased. The variable temperature distribution along the element length was a linear interpolation between every two cross-sections, separated every 1 meter long, which their steel temperature values in function of time have been extracted previously from fire development analysis. The steel temperature distribution was symmetric and the maximum temperature was in the mid-span of the beam, considering that the fire location is just in the centre of the span:
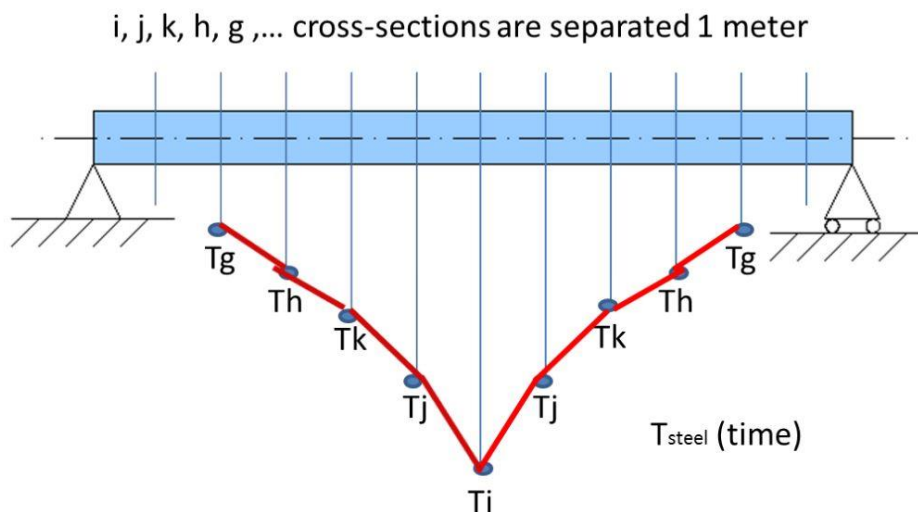
Figure 150: Temperature distribution in different sections of a beam

134

In the cases of columns, seven were chosen for the parametric study for axially loaded columns and ten were chosen from the parametric study for beam-columns. The load and boundary conditions in these analyses were the same as in their respective original parametric study. The difference was that a load ratio compared to room temperature resistance was applied when the temperature was gradually increased. The variable temperature distribution along the element height was a linear interpolation between every two cross-sections, separated every 1 meter long, which their steel temperature values in function of time have been extracted previously from fire development analysis. In case of columns analysis, the steel temperature distribution was not symmetric and the maximum temperature was located at the bottom of the column that decrease along the height of the column, considering that the fire location is close to the base of column:
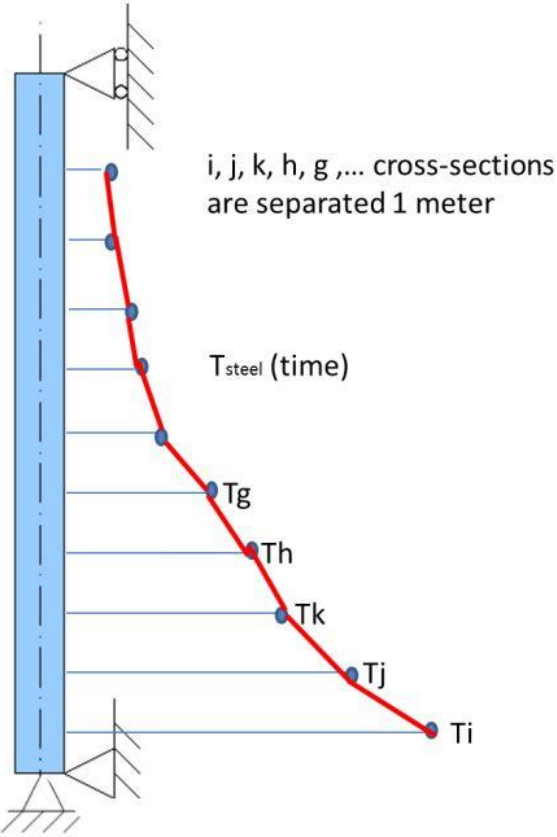
Figure 151: Temperature distribution in different sections of a column

It must be mentioned that some fire parameters were updated in order to study short columns. Actually, in these cases the HRR was decreased in order to prevent the columns from having an almost uniform temperature in their whole height.

The exhaustive list of investigated beams and columns is given in deliverable 5.

Two portal frames were investigated for this parametric study with both shell and new beam-column finite elements. Two different heating conditions were considered for each portal frame, first one with a fire located near a column, and the second one with a fire located under a beam. The first proposed portal frame was the following: 6th example from the numerical benchmark study. This model was already calibrated by all partners of the modelling group for the shell elements. The load and boundary conditions in this analysis were the same as in the benchmark study. The second investigated portal frame was a two span frame. The total length is about 80 m which means 40 m length by single frame. Columns are 7.5 m high and the mid-span of each frame is about 9.5 m high. Figure 152 illustrates this portal frame:
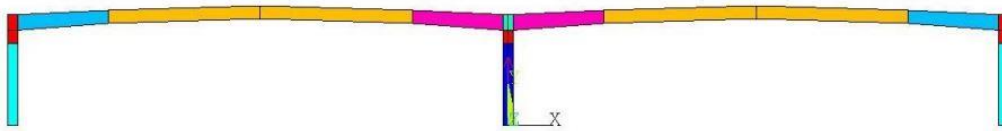
Figure 152: two-span portal frame for the parametric study

The variable temperature distribution along the element length was a linear interpolation between every two cross-sections, separated following a scheme, which their steel temperature values in function of time have been extracted previously from fire development analysis.

2.2.7.3 Results of the parametric study

The comparisons of the numerical simulations between the shell models and the new beam finite element models are illustrated in the following charts. The comparisons are made in terms of ratio for the critical temperature for both modelling type. Figures 150 to 153 illustrate the ratio of the critical temperature of new beam element model on shell model for beams and columns for both load ratio 0.3 and 0.5 compared to room temperature failure load:
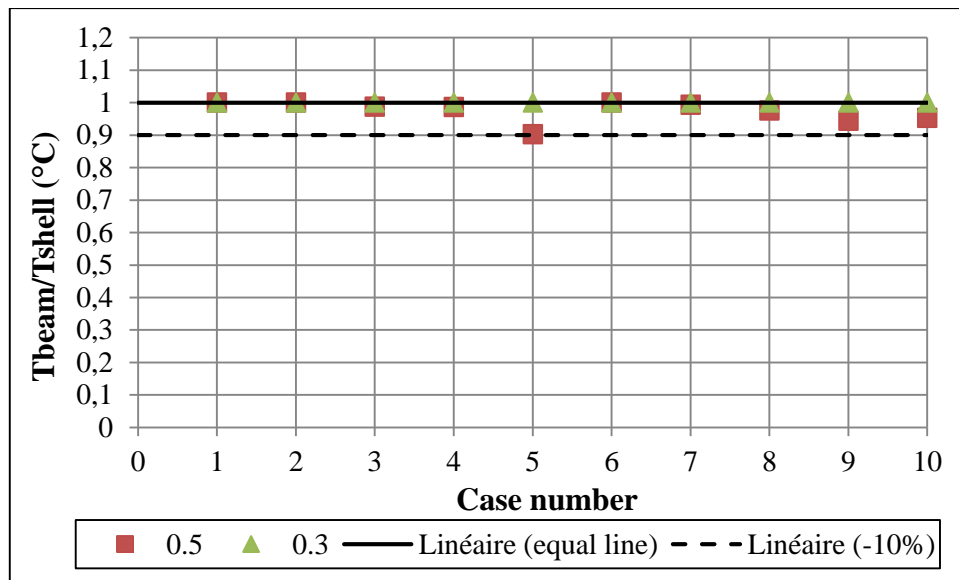
Figure 153: Comparisons between shell and new beam element models for pure bending
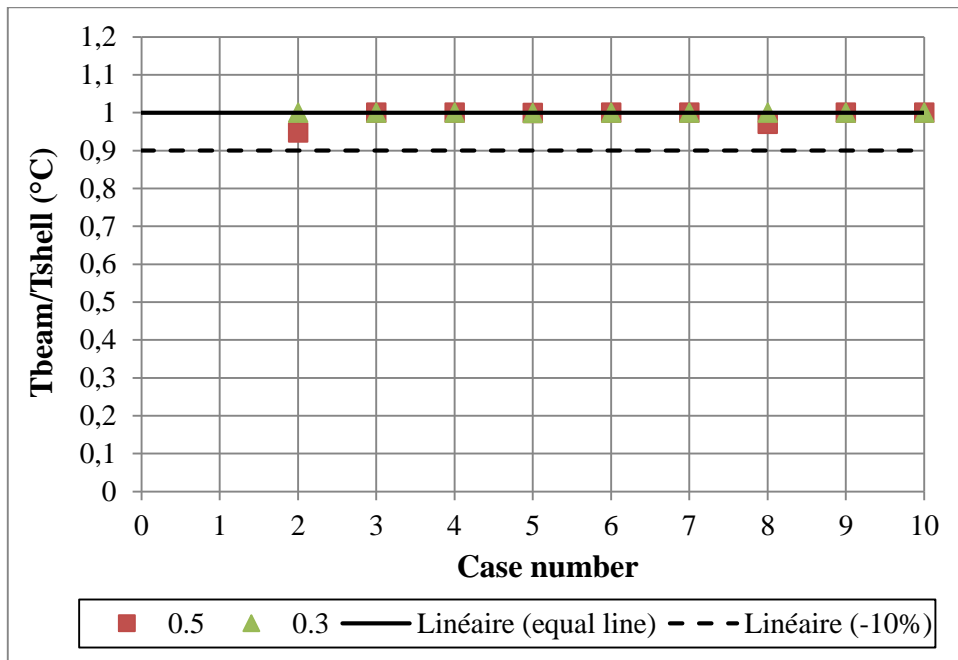
Figure 154: Comparisons between shell and new beam element models for lateral torsional buckling
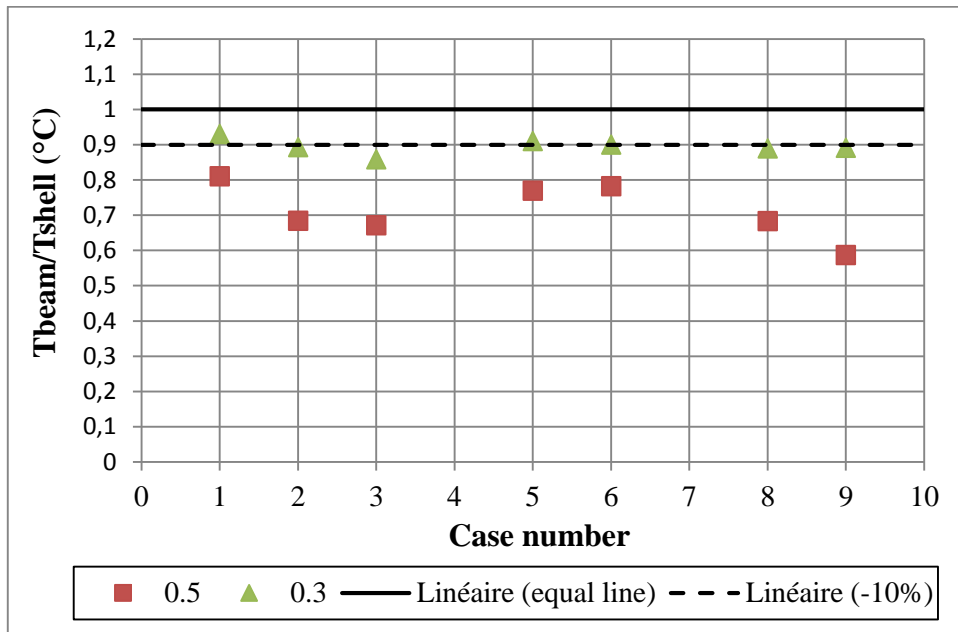
Figure 155: Comparisons between shell and new beam element models for axially loaded columns

137
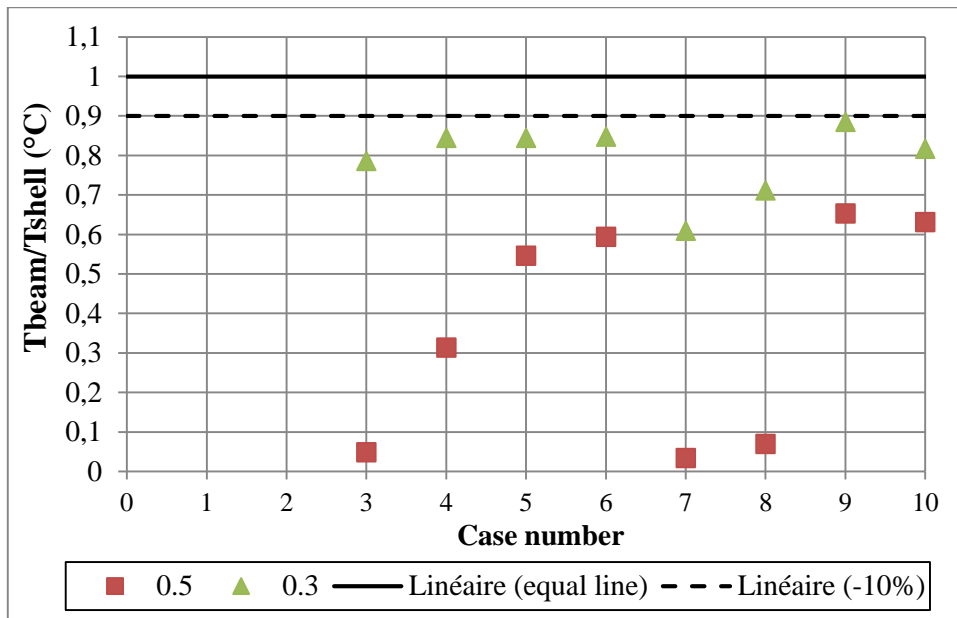
Figure 156: Comparisons between shell and new beam element models for columns subjected to combined axial load and bending moment

The previously detailed results show that the beam-column models always provide safe compared to the shell elements models. For both beams under pure bending or beams subjected to lateral torsional buckling, whatever the load ratio, the safe character is at a maximum of 10%. When columns are concerned, some numerical issues were encountered. 0.3 load ratio remains safe and economically reasonable whereas 0.5 load ratio show uneconomical results due to numerical issues in the cases of columns subjected to combined compression load and bending.

The failure mode shape of the two-span portal frame is illustrated for both mid-span fire and internal column fire:
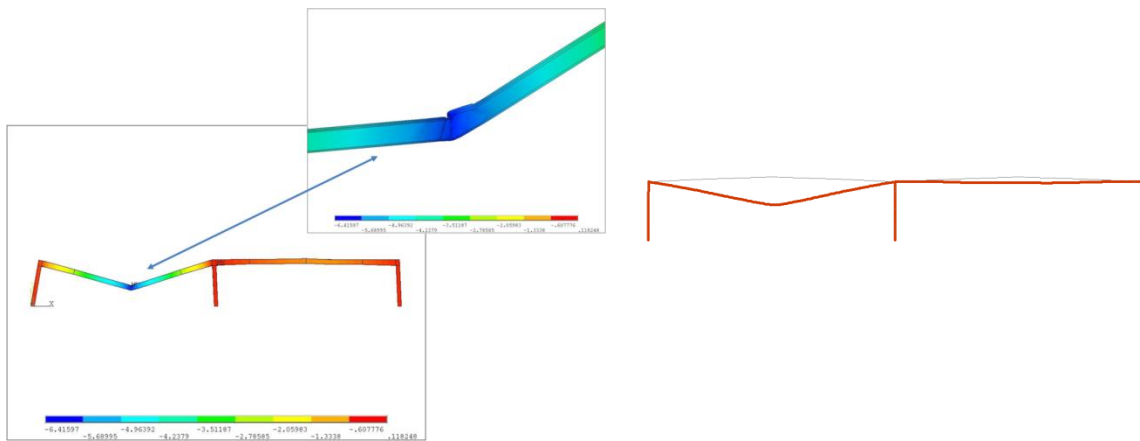
Figure 157: Failure mode for mid-span fire: *left) shell model, right) new beam element model*

Figure 158: Failure mode for internal column fire: *left) shell model, right) new beam element model*

138

The new beam-column finite element is able to predict the failure mode of a portal frame submitted to real fire conditions.

Figure 159 illustrates the vertical displacement in function of temperature at mid span for both models:
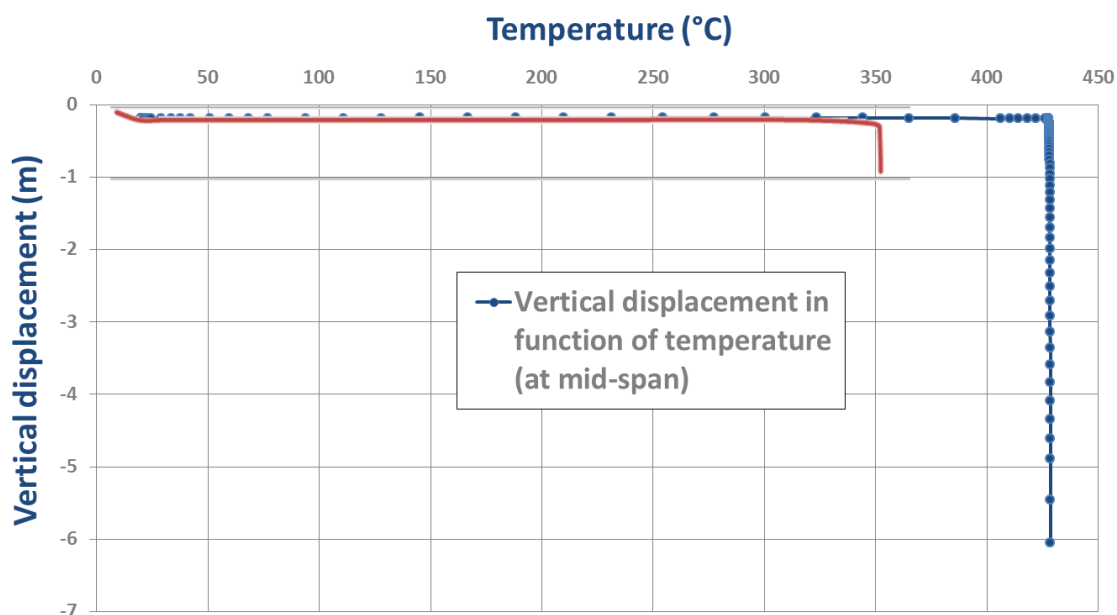
Figure 159: Vertical displacement (m) in function of temperature (°C) at mid span (red is beam model, blue is shell model)

In all the developed analysis, errors up to 60% in the calculation of failure times have been reported in the scope of this study due to the influence of non-uniform variation of temperature in beam sections, always on the safe side. This influence appears to be highly dependent of heating rate and the way the geometrical discretization is made to the implementation of variable temperatures. The more beams sections are defined to define the temperature variation in the portal frame length, the more the result is accurate. On the other side, it considerably increases the complexity of the modelling.

2.3   General conclusions

In the scope of this research project, the improvement of simple design rules for fire resistance assessment of class 4 cross-section steel members is done on the basis of both experimental and numerical studies. More precisely, the proposed simple design rules for the cross-sectional fire resistance give much better agreement compared with the results derived from the extensive parametric study using numerical models based on shell finite elements. Concerning the lateral torsional buckling behaviour of beams under bending, the proposed simple design rules lead to a less conservative fire resistance assessment. Furthermore, these simple design rules also allow the lateral torsional buckling resistance of beams with tapered cross-sections to be evaluated in fire situation, which constitutes an important advancement for future revision of EN1993-1-2 because no research work has been conducted for such type of development in the past. Though the developed simple design rules for fire resistance assessment of axially loaded columns give only slightly improved economic results compared with current rules of EN1993-1-2, they are much more consistent with those proposed for beams under bending, which will lead to significant ease of use of all these design rules. Finally, as far as the interaction curves for beam-columns are concerned, the unsafe design in case of in-plane buckling has been improved. However, it is necessary to point out here that further improvements can still be achieved for more economical design of class 4 cross-section steel members under combined bending and compression.

The sixteen fire tests conducted on beams and columns within the scope of the current project have provided a solid experimental basis about the fire behaviour of class 4 cross-section steel members. In addition, the adopted test set-up, as well as the testing experience acquired during the tests, will be very instructive for other researchers in the preparation of future fire tests in the similar field. The experimental results derived from above fire tests have allowed the validation of various numerical models which are used afterwards for extensive numerical investigation of the fire behaviour of class 4 cross-section steel members.

Numerous numerical results of class 4 cross-section beams and columns are now available in the databases created within the scope of this project. The details of the adopted hypothesis in the numerical finite element analysis and the scientific reasons of their choice are all described, particularly in the deliverable relative to benchmark study and in the reports of parametric studies. This database can be easily used, on the one hand, by any other design engineers to ensure consistent finite element models that they have to create in case of using advanced calculation models and on the other hand, by the researchers in their future scientific investigation of the fire resistance of steel members.

The developed numerical approach on the basis of beam-column finite element using a specific material model for global structural analysis in fire situation of steel structures comprising class 4 cross-section steel members, as well as the corresponding numerical guidance, provide to all fire safety engineers a safe and cost-effective way to assess the global fire behaviour of steel structures, where the local buckling of class 4 cross-sections is involved.

Newly developed simple design rules within the scope of this project are definitely more accurate and lead to much more economic fire resistance design than current simple design rules of EN 1993-1-2. Moreover, as these simple design rules are based on the same reduction factor used for the fire resistance design of lower class cross-section steel members (class 1 to class 3), consequently, they simplify significantly current design rules of EN1993-1-2 and facilitate the ease of use of Eurocodes which is one of major concern in the next revision of these European standards.

2.4   *Exploitation and impact of the research project*

The most important potential exploitation of the results derived from this project is to incorporate the simple design rules developed within the scope of this project into the next version of Eurocodes. As CEN/TC250 has obtained the mandate from the European Commission to start officially the revision of current Eurocodes, the time schedule will be excellent to take the necessary actions which can be composed of following two steps: presentation of these simple design rules firstly to the Working Group of EN1993-1-2 and secondly to the Project Team of EN1993-1-2 in the future. In fact, this work may be easily achieved with three partners of this project being already the active members of above-mentioned Working Group.

Currently, thanks to the provided software, it is possible for design engineers to apply easily current simple design rules of EN1993-1-2 for fire resistance assessment of class 4 cross-section steel members. In the future, if the developed simple design rules are accepted for next version of EN1993-1-2, the engineers will have a cost-effective design tool available very quickly. Nevertheless, if these rules are accepted at any national level, the software will become exploitable even earlier.

The numerical guidance for global structural analysis in fire situation of steel structures comprising class 4 cross-section steel members can help any engineers to use the recommended numerical approach for cost-effective fire engineering safety analysis so that the design cost can be largely reduced.

Within the context of this research work, a number of papers were proposed by different partners, either for scientific journals or during international conferences. All these scientific papers are on the basis of the research works conducted by the different partners of this report.

The following papers are directly linked to FIDESC4 project:

- Hricák, J. - Prachař, M. - Jandera, M. - Wald, F.: *Experiments of Class 4 section beams at elevated temperature*. In Sborník 51. celostátní konference o ocelových konstrukcích Hustopeče 2013. Brno: Česká společnost pro ocelové konstrukce, 2013, s. 3-9. ISBN 978-80-02-02413-2.

- Prachař, M. - Jandera, M. - Wald, F. - Zhao, B.: *Fire Resistance of Slender Section Beams. Steel Construction*. 2014, vol. 7, no. 3, art. no. 188, p. 188-192. ISSN 1867-0520.

- Prachař, M. - Jandera, M. - Wald, F. - Zhao, B.: *Lateral torsional buckling of class 4 steel welded beams at elevated temperature*. In Progress on Safety of Structures in Fire. Shanghai: Tongji University Press, 2014, p. 113-120. ISBN 978-7-5608-5494-6.

- Prachař, M. - Jandera, M. - Wald, F. - *Fire Tests on Beam with Class 4 Cross-section Subjected to Lateral Torsional Buckling*. In Proceedings of International Conference Applications of Structural Fire Engineering. Praha: Česká technika - nakladatelství ČVUT, ČVUT v Praze, 2013, p. 173-178. ISBN 978-80-01-05204-4.

- Prachař, M. - Jandera, M. - Wald, F. - *Lateral torsional buckling of class 4 steel plate beams at elevated temperature: experimental and numerical comparisons*. Journal of Structural Fire Engineering. 2015, no. 3, ISSN 2040-2317.

- Zhao, B. - Sanzel, A. - Wald, F. - Vila Real, P. - Hricák, J. - et al.: *development of simple fire design method for I shape thin wall steel members under simple bending*. Revue Construction Métallique. 2014, vol. 50, no. 2, p. 2-23. ISSN 0045-8198.

- Couto, C. - *Fire design of steel members with class 4 cross-section*, PhD Thesis in Civil Engineering, University of Aveiro, defense in 2015.

- Couto, C.; Vila Real, P.; Lopes, N.; Zhao B. - *Resistance of steel cross-sections with local buckling at elevated temperatures*, Journal of Constructional Steel Research, DOI: 10.1016/j.jcsr.2015.03.005, Elsevier, June 2015.

- Couto, C.; Vila Real, P.; Lopes, N.; Zhao B. - *Effective width method to account for the local buckling of steel thin plates at elevated temperatures*, Thin-walled Structures, DOI: 10.1016/j.tws.2014.06.003, Elsevier, November 2014.

- Couto, C.; Vila Real, P.; Lopes, N.; Zhao B. - *Fire design of steel beams with slender cross-section – the influence of loading*, submitted to ASFE 2015 - Applications of structural fire engineering, 15-16 October 2015, Dubrovnik, Croatia.

- Couto, C.; Vila Real, P.; Lopes, N.; Zhao B. - *Fire design of tapered steel beams with class 4 cross-sections*, submitted to Eighth International Conference on Advances in Steel Structures, Lisbon, Portugal, July 22-24, 2015.

- Couto, C.; Vila Real, P.; Ferreira, P.; Lopes, N. - *Verification of web tapered beam-columns in case of fire using the general method of Eurocode 3*, submitted to International Fire Safety Symposium. Coimbra, Portugal, 20th-23rd April 2015.

- Couto, C.; Vila Real, P.; Lopes, N.; Zhao B. - *Steel beam-columns with class 4 cross-sections at elevated temperatures*, proceedings of the EUROSTEEL 2014 - 7th European Conference on Steel and Composite Structures, pp. 771-772, ISBN 978-92-9147-121-8, Napoli, Italy, 10 to 12 of September of 2014.

- Couto, C.; Vila Real, P.; Ferreira, J.; Lopes, N. - *Numerical validation of the general method for structural fire design of single members*, proceedings of the EUROSTEEL 2014 - 7th European Conference on Steel and Composite Structures, pp. 857-858, ISBN 978-92-9147-121-8, Napoli, Italy, 10 to 12 of September of 2014.

- Couto, C.; Vila Real, P.; Lopes, N.; Zhao B. - *A new design method to take into account the local buckling of steel cross-sections at elevated temperatures*, proceedings of the 8th International Conference on Structures in Fire SiF'14, pp. 49-56, ISBN 978-7-5608-5494-6, Tongji University, Shanghai, China, 11 to 13 of June of 2014.

- Couto, C.; Vila Real, P.; Lopes, N.; Zhao B. - *Fire design of steel beams with welded class 4 cross-section*, International Conference on Applications of Structural Fire Engineering ASFE'13, pp. 232-237, ISBN 978-80-01-05204-4, Prague, Czech Republic 19-20, April 2013.

- Prachar, M.; Lopes, N.; Couto, C.; Jandera, M.; Vila Real, P.; Wald, F. - *Lateral torsional buckling of class 4 steel plate girders under fire conditions: experimental and numerical comparison*, COST Action TU0904 – Benchmarks studies, Experimental validation of numerical models in fire engineering", pp. 21-33, ISBN 978-80-01-05443-7, CTU Publishing House, Czech Technical University in Prague, January of 2014.

- Prachar, M.; Couto, C.; Lopes, N.; Jandera M.; Vila Real, P.; Wald, F. - *Benchmark study of lateral torsional buckling of Class 4 steel plate girders under fire conditions: Numerical Comparison*, COST Action TU0904 – Benchmarks studies, Experimental validation of numerical models in fire engineering", pp. 72-83, ISBN 978-80-01-05442-0, CTU Publishing House, Czech Technical University in Prague, January of 2014.

- Couto, C.; Vila Real, P.; Lopes, N.; Zhao B. - *Steel beam-columns with Class 4 cross-sections in case of fire*, Thin-walled structures, under review.

- Couto, C.; Vila Real, P.; Lopes, N.; Zhao B. - *Numerical investigation on the lateral torsional buckling of beams with slender cross-sections at elevated temperatures*, in preparation.

- Franssen JM; Zhao B. and Gernay T. - *Experimental tests and numerical modelling on eight slender steel columns under increasing temperatures,* proceedings of the 8th International Conference on Structures in Fire SiF'14, Tongji University, Shanghai, China, 11 to 13 of June of 2014

Finally, it is important to point out that this project did not solve all the problems relative to fire behaviour of class 4 cross-section steel members. For example, the mono-symmetrical class 4 cross-section steel members, which were not investigated within the scope of this project. This could be another interesting research work to be undertaken for the development of new simple design rules for this type of class 4 cross-section members.

3   List of figures and tables

3.1.1   Figures

3.1.2 Tables

4   List of references

[1] EN 1993–1–2, Eurocode 3, Design of Steel Structures – Part 1–2: General rules Structural fire design, 2005

[2] Renaud C., Zhao B., "Investigation of Simple Calculation Method in EN 1993-1-2 for Buckling of Hot Rolled Class 4 Steel Members Exposed to Fire," in Structures in Fire: Proceedings of the Fourth International Conference, Aveiro, Portugal, 2006, pp. 199-211

[3] Marques L., Taras A., Simões da Silva L., Greiner R., Rebelo C., "Development of a consistent buckling design procedure for tapered columns", Journal of Constructional Steel Research, 2011

[4] Raftoyiannis I., Ermopoulos J., "Stability of tapered and stepped steel columns with initial imperfections", Engineering Structures, vol. 27, pp. 1248-1257, 2005

[5] Bazeos N., Karabalis D., "Efficient computation of buckling loads for plane steel frames with tapered members", Engineering Structures, vol. 28, pp. 771-775, 2006

[6] Saffari H., Rahgozar R., Jahanshahi R., "An efficient method for computation of effective length factor of columns in a steel gabled frame with tapered members", Journal of Constructional Steel Research, vol. 64, pp. 400-406, 2008

[7] Salem a. H., El Aghoury M., Fayed M. N., El Aghoury I. M., "Ultimate capacity of axially loaded thin-walled tapered columns with doubly symmetric sections", Thin-Walled Structures, vol. 47, pp. 931-941, 2009

[8] Braham, M., "Elastic Lateral-Torsional buckling of web tapered I-Beams subjected to end moments", 18th Czecho-Slovak International Conference on Steel Structures and Bridges '97, Brno, Czech Republic, pp. 37-42, May 28-30, 1997

[9] EN 1993–1–1, Eurocode 3, Design of Steel Structures – Part 1–1: General rules and rules for buildings, 2005

[10] Simões da Silva L., Marque L., Rebelo C., Numerical validation of the general method in EC3-1-1 for prismatic members, Journal of Constructional Steel Research 66 (2010) 575590, 2010

[11] EN 1993–1–5, Eurocode 3, Design of Steel Structures – Part 1–5: Plated structural elements, 2006

[12] Braun, B., Kuhlmann, U., "Reduced stress design of plates under biaxial compression", Steel Construction 5, No. 1, pp. 33-40, 2012

[13] European Commission, "Fire safety of industrial halls and low-rise industrial buildings, C.E.C. 7210 PR378", ed, June 2005

[14] Fontana M., Knobloch M., "Local buckling behaviour under fire conditions," in Proceedings of the IABSE Symposium on "Structures and Extreme Events", 2005

[15] Fontana M., Knobloch M., "Elements with nonlinear stress-strain relationships subjected to local buckling," in Proceedings of ICMS 2006 Conference, 2006

[16] Knobloch, M., Fontana, M., "Strain-based approach to local buckling of steel sections subjected to fire", Journal of Constructional Steel Research, 62: pp. 44-67, 2006

[17] Lopes N., Real P. V., da Silva L. S., Franssen J. M., "Numerical Modelling of Thin Walled Stainless Steel Structural Elements in Case of Fire", Fire Technology, vol. 46, pp. 91-108, Jan 2010

[18] Couto C, Vila Real P, Lopes N, Zhao B, "Effective width method to account for the local buckling of steel thin plates at elevated temperatures. Thin-Walled Struct 2014;84:134-49. Doi:10.1016/j.tws.2014.06.003.

[19] HGF-130-accuracy of assessment methods.pdf

[20] Franssen, J.-M.; Cowez, B. (2012). *Consideration of local instabilities in beam finite elements by means of effective constitutive law"*, 7th International Conference on Structures in Fire, Zurich, Switzerland.

[21] Lopes at al. Numerical analysis of stainless steel beam-columns in case of fire, Fire Safety Journal, 2012

[22] Talamona D. "Flambement de poteaux métalliques sous charges excentrées à haute temperature", 1995

[23] Galéa Y.; *Déversement des barres à section en I bissymétrique et hauteur d'âme linéairement variable*, Revue Construction Métallique, 1986

[24] Couto C, Vila Real P, Lopes N, Zhao B, "Resistance of steel cross-sections with local buckling at elevated temperatures. J Constr Steel Res 2015;109:101-14. Doi:10.1016/j.csr.2015.03.005

The main aim of the current project was to develop accurate, practical and economic simple design rules for fire resistance assessment of class 4 cross-section steel members through enhanced scientific findings on the basis of both experimental and numerical investigations.

In the scope of this project, have been acquired the following main outcomes:

• Experimental investigation of class 4 cross-section steel members under various loading conditions, such as simple bending, bending subject to lateral torsional buckling, axial compression subjected to buckling and combined compression and bending

• Development and validation investigation of numerical models against fire tests and conduct of extensive numerical parametric studies

• Development of new simple design rules to assess the fire resistance of class 4 cross-section steel members under different loading conditions on the basis of the results derived from both experimental investigation and numerical parametric studies as well as the detailed correlation investigation of these design rules

• Development of a user-friendly software so that all above simple design rules can be applied cost-effectively by design engineers

• Elaboration of a numerical guidance dealing with the global structural analysis under fire situation of steel structures composed of class 4 cross-section steel members on the basis of cost-effective numerical approach

• Establishment of a common database comprising all the necessary information relative to the experimental investigation and numerical parametric studies for future exploitation by any other researchers

The principal information of above outcomes is provided in the main part of this report and all the important details are explained in several separate deliverables.